THE PERCUTANEOUS ABSORPTION OF IONISABLE COMPOUNDS

JULIAN CRAIG SMITH

A THESIS SUBMITTED FOR THE DEGREE OF DOCTOR OF PHILOSOPHY

ASTON UNIVERSITY

April 1997

ASTON UNIVERSITY

THE PERCUTANEOUS ABSORPTION OF IONISABLE COMPOUNDS

JULIAN CRAIG SMITH

Submitted for the degree of Doctor of Philosophy, 1997

SUMMARY

The effects of ionisation on transdermal drug delivery using excised human epidermis (HS) and silastic rubber (SR) as model permeation barriers was investigated *in vitro* using Franz-type absorption cells. Suspensions and solutions of salicylic acid (SA), the model ionogenic permeant, were used as donors and the variables studied were vehicle pH and trans-membrane pH-gradients . For solutions, the pH effect was related to the level of ionisation of the drug and the degree of saturation of the solution. With suspensions, the observed permeation rate was unaffected by pH. The penetration profiles through HS and SR were similar, although the overall flux through HS was about 70% of that observed through SR. Pretreatment of the membranes with various enhancer regimens, including oleic acid, Azone and N,N-dimethylamides in propylene glycol (PG) and isopropyl myristate (IPM) promoted the penetration of SA. SR was not a suitable model for enhancer pretreatment using IPM as a vehicle as the membrane was significantly disrupted by this vehicle. The results from comparable experiments with and without a trans-membrane pH-gradient did not have a significant effect upon flux or flux enhancement after pretreatment with the above enhancers.

A theoretical model for the extraction coefficients of weak acids was derived using the partition coefficients of the ionised and unionised species, pH and pK_a. This model was shown to account for the variation in overall partition of salicylic acid dependent upon pH and pK_a. The distribution of this solute between aqueous and oily phases, with and without added enhancer was measured as a function of pH. The extraction coefficients determined were consistent with the model and showed that the behaviour of the system can be explained without referral to ion-pair mechanisms.

Phosphonoacetate is an effective antiviral agent. However, as it is charged at physiological pH, its permeation across cell membranes is limited. To assess the improvement of the transport properties of this molecule, mono-, di- and tri-ester prodrugs were examined. These were assessed for stability and subsequent breakdown with respect to pH by HPLC. *In vitro* percutaneous absorption was observed using the triester, but not the ionic mono- or di-esters. The triester absorption could be potentiated using a range of enhancers with oleic acid being the most effective.

Cyclodextrins (CD) have a role as absorption enhancers for peptide compounds across nasal epithelium. One potential mode of action is that CDs include these compounds, protect them from enzymic attack and thereby increase their residence time in the nasal epithelium. This study investigated the potential of CDs to protect ester prodrugs from enzymatic breakdown and prevent production of poorly transportable ionic species. Using a range of CD to ester molar ratios (10:1 to 2500:1) a small, but measurable, protection for the model esters (parabens) against esterase attack was observed. Possible mechanisms for this phenomenon are that CDs include the ester, making it unavailable for hydrolysis, the CDs may also affect the esterase in some way preventing access for the ester into the active site.

Key words: Salicylic acid, percutaneous absorption, ionisation, absorption enhancers, partition coefficients, phosphonoacetate, prodrug, cyclodextrin, esterase.

DEDICATION

To my family, especially my daughter, without whose help this thesis would have been written more quickly!

"I am in blood
Stepp'd in so far that, should I wade no more,
Returning were as tedious as to go o'er:"

(Macbeth, W Shakespeare)

ACKNOWLEDGEMENTS

I am indebted to Professor William Irwin for his supervision, guidance, endurance and ceaseless confidence throughout the period of this research. My thanks also to Dr Helen Nelson for representing my interests at the Queen's Hospital, Burton on Trent, the West Midlands Regional Health Authority and the Queen's Hospital for their financial support for this work.

I must also thank my staff for relinquishing much of the laboratory's equipment for what must have seemed an interminable length of time. Also, for coming to my aid, forsaking all else, when my two hands could not perform sufficient tasks simultaneously.

I am grateful to Ian Pickering and his staff of the mortuary at the Queen's Hospital, Burton, who have endeavoured to supply my perpetual demand for cadaver and amputation samples.

I must express my adoration to my wife for her patience, support and fortitude, especially during the frequent late nights, and by no means least for her help in typing this manuscript.

LIST OF CONTENTS

ABBREVIATIONS

A	Area
a	Thermodynamic activity
AIDS	Acquired immune deficiency syndrome
Aufs	Absorbance units full scale
C	Concentration
CD	Cyclodextrin
CDA	Caproic acid N,N-dimethylamide
CI	Confidence interval
CNS	Central nervous system
D	Diffusion coefficient
DCA	Dodecylamine
DMSO	Dimethyl sulphoxide
DNA	Deoxyribonucleic acid
DPPC	Dipalmitoyl phosphatidylcholine
DSC	Differential scanning calorimetry
E	Enzyme
ER	Extraction ratio
ES	Enzyme substrate
FS	Fraction saturated
FTIR	Fourier transform infra-red
HIV	Human immuno-deficiency virus
HPLC	High-performance liquid chromatography
HS	Human epidermis
HSV	Herpes simplex virus
id	Internal diameter
IPM	Isopropyl myristate
IU	International units
J	Flux
J	Joule
k	Rate constant

K	Kelvin
K_m	Michaelis constant
k_{obs}	Observed Permeability coefficient
K_{sp}	Solubility product
LDA	Lauric acid N,N-dimethylamide
M	Molar
M_t	Mass of permeant transported at time t
N	Normal
OA	Oleic acid
ODS	Octadecylsilane
P	Probability
P_{oct}	Partition coefficient (Octanol)
PG	Propylene glycol
P_{obs}	Observed Partition coefficient
PVC	Polyvinyl chloride
r	Correlation coefficient
S	Substrate
S	Solubility of compound
S_o	Solubility of unionised species
s	Seconds
SA	Salicylic acid
SE	Standard error
SEM	Standard error of the mean
SR	Silastic rubber
t	Time
TBH	Tetrabutyl ammonium hydroxide
TC	Transcutol
t_L	Lag time
UV	Ultra-violet
V	Volume
VIS	Visible
V_{max}	Maximum reaction velocity
V_o	Initial reaction velocity

w/w	Weight by weight
α	Fraction ionised
γ	Activity coefficient
μ	Chemical potential
η	Viscosity
Δ	Difference in
δ	Membrane thickness

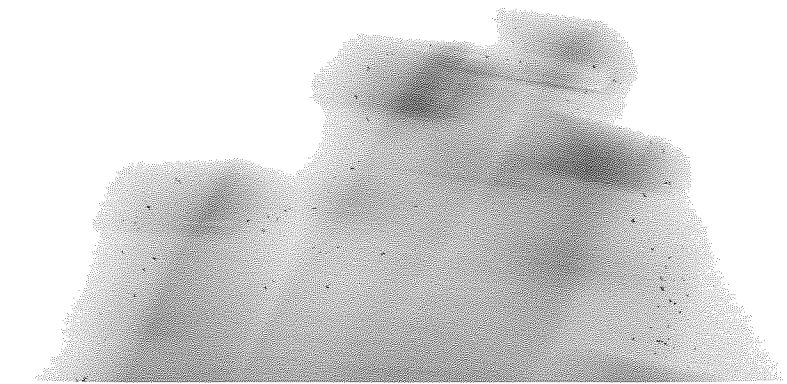

LIST OF FIGURES

LIST OF TABLES

CHAPTER ONE

INTRODUCTION

THEORY AND METHODS OF INVESTIGATING TOPICAL DRUG DELIVERY

1.1 Anatomy of the Skin

The skin is divided anatomically into three layers; the epidermis, dermis and subcutaneous tissue. (Figure 1.1A) The epidermis is a cellular avascular tissue, consisting of four layers; the basal or germinative layer, the "prickle cell" or malpighian layer, the stratum granulosum or granular layer and the outermost layer called the stratum corneum (Figure 1.1B). Differing cell types found within these layers denote stages in the conversion of epithelial cells into horn-cells (Matoltsy, 1976). A function of the epidermis is the constant replacement of the stratum corneum, that is being continuously shed (Roxburgh, 1986). The thickness of the epidermis varies, depending upon the anatomical site and ranges from about 0.8 mm on the palms of the hands and soles of the feet to 0.06 mm on the eyelids.

The basement membrane of the basal layer is responsible for the adhesion of the epidermis to the dermis. Mitosis within the basal layer provides cells which migrate and differentiate towards the outer layer of the epidermis and eventually desquamate from the stratum corneum. The time taken for this process is normally about 28 days, of which half is spent in the living layers and half in the stratum corneum. Cell division is rapid in the basal layer and daughter cells, keratinocytes, are pushed upwards as other cells are produced beneath them. The first stage of differentiation is the appearance of prickles or spines on the cell surface. These cells are nearly round in shape and are connected together by specialised areas of contact called desmosomes. These intercellular connecting bridges give the epidermis its strength, enabling it to resist mechanical stress.

As keratinocytes migrate towards the outer layers of the epidermis, they reach the granular layer. This area of intense biochemical activity and morphological change is where the keratinocytes rapidly die, losing their nuclei and cytoplasmic organelle. The process commences with the appearance of granules, hence the origin of this layer's name. During the transition, these granules develop to fill the interior space of the keratinocyte with keratin filaments surrounded by an amorphous matrix of sulphur-rich proteins. These filaments and proteins are probably responsible for maintaining the characteristic flat hexagonal shape. As the keratohyalin granule forms, another much smaller granule appears, described by various others as Odland bodies (Odland, 1960), cementosomes, membrane-coating granules and

A

B

Figure 1.1 Schematic cross-sections of the skin. (From Barry, 1983)

(A) Full-thickness skin.

(B) An expansion of the epidermis.

lamellar granules (Frei and Sheldon 1961; Elias *et al.*, 1977a; Hayward, 1979; Landmann, 1980). In the final stages of differentiation, these smaller granules migrate to the cell's surface disgorging their contents into the extracellular space (Matoltsy, 1986). There is a concurrent destruction of the nucleus and other remaining cell organelles. The cell plasma membrane becomes thickened with protein deposited on its inner surface to form the horny cell envelope (Farbman, 1966). The resulting stratum corneum formed from these fully differentiated corneocytes comprises an anucleated flat cell filled mainly with protein and keratin and surrounded by a thick cell envelope. In humans, this layer generally comprises 10-15 layers of these flattened keratinised dead cells, stacked in highly organised units of vertical columns. These cells are often described as the bricks and the multilaminer lipid/aqueous extracellular space as the mortar in the frequently referred to "bricks and mortar" theory of the stratum corneum composition (Elias, 1981; Wertz *et al.*, 1989; Chandrasekaran and Shaw, 1978).

As this differentiation proceeds, changes occur in the amount and composition of the lipids associated with the keratinocyte. In the basal layer, cells contain the arrangement of phospholipids and cholesterol found in many cell types. With differentiation, the mass of lipid per cell increases as ceramides and glucosylceramides are synthesised. On completion, the phospholipids are completely catabolised and the sugar units are removed from the glucosylceramides (Yardley and Summerly, 1981; Yardley, 1983; Long *et al.*, 1985). This makes the lipids of the stratum corneum unusual, because unlike all other biological membranes, phospholipids are absent (Wertz and Downing, 1989). Instead, they comprise ceramides, cholesterol, fatty acids (Imokawa *et al.*, 1991) and cholesterol esters (table 1.1; figure 1.2). Although this composition is readily ascertained, the precise arrangement of the lipid components within the stratum corneum is extremely difficult to determine. There is also considerable inter- and intra-species variation (table 1.1). It is widely accepted that the intercellular lipids are present in distinct structured bilayer lamellae (Reviewed in Elias, 1983; Williams and Elias, 1987). This structure depends upon the cooperative interactions between the polar head groups and the hydrophobic alkyl chain interactions of the ceramides. (Figure 1.3) Into this basic bilayer structure, cholesterol molecules will align themselves so that they immobilise the hydrocarbon region near the polar head groups, but permit the remainder of the chain more mobility. The cholesterol sulphate may have a critical role

Table 1.1 Composition of stratum corneum lipids (Source: Wertz and Downing, 1989)

Figure 1.2 Major lipids of the intercellular regions of the human stratum corneum (Brain and Walters, 1993).

stabilising the lipid bilayer, due to the absence of phospholipids (Williams and Elias 1987). It is possible that these cholesterol sulphate moieties may be bridged through divalent counter ions and the cholesterol esters span adjacent bilayers. The adjacent lipid lamellae may also be cohesively linked by the long chain Ceramide 1, by bifunctional glucosylceramides, or by protein bridges. Although the exact alignments of these components is still a subject of great conjecture, it is unlikely that they are randomly arranged within the bilayer structure, and in all probability there is a biological order with distinct lipid domains (Klausner *et al.*, 1980).

Figure 1.3 Proposed model detailing the structure of the lipid bilayers throughout the intercellular domains of human stratum corneum. (From Barry, 1991a)

The dermis or corium is 3-5 mm thick and consists of a matrix of connective tissue woven from fibrous proteins (collagen, elastin and reticulin) which are embedded in an amorphous ground substance of mucopolysaccharide. The dermis has a rich blood supply which reaches

to within 0.2 mm of the skin surface and acts as a "sink" for diffusing molecules reaching the capillaries. Thus, concentrations of penetrants in the dermis are low, maximising epidermal concentration gradients. Nerves, blood vessels and lymphatics traverse the dermis and skin appendages (eccrine sweat glands, apocrine glands and pilosebaceous units) cross the epidermis and penetrate the dermis.

The pilosebaceous unit is a complex structure comprising the hair follicle, one or more sebaceous glands and the erector pili muscle. The hair follicles are sebum filled openings from which keratinous hair filaments protrude. These follicles occupy about 0.1% of the skin surface area, but are absent from plantar and palmar surfaces, the red areas of the lips, and parts of the genitalia. The sebaceous glands secrete sebum by a holocrine mechanism *via* ducts to the hair follicle. There are about 100 sebaceous glands per square centimetre of normal skin, which increases to between 400 and 900 per square centimetre on the more hairy regions. Breakdown of cells from the sebaceous glands yields sebum which consists of 95% lipids, principally triglycerides, wax esters, squalene cholesterol esters and cholesterol.

Eccrine sweat glands are important in thermoregulation and are distributed over the entire body surface. There are about two million eccrine sweat glands on the average human body, where they predominate on the hairless surfaces of the hands and feet. The deepest secretory portion of the gland is a coiled structure situated in the reticular dermis and the excretory portion spirals through the papillary dermis and the epidermis to open onto the surface at the pore. The latter is covered by a loose meshwork of horn cells. Sweat secreted by eccrine glands varies in composition with the stimulus, the rate of sweating and the site. It is a clear watery liquid of acid pH containing electrolytes, trace elements and organic substances.

Apocrine sweat glands are larger than eccrine ones, but are fewer in number. They are vestigial remnants of the odoriferous glands of the lower animals and are found in the axillae, the areola of the nipples, umbilical, anal and genital regions. Apocrine sweat differs in composition from eccrine and may be cloudy and coloured.

The dermis rests on a thick pad of subcutaneous tissue consisting of loose connective tissue or adipose cells. The layer serves as an energy source and has insulative properties. It also acts as a cushion to reduce trauma injury to the upper dermal layers.

1.2 Routes of Percutaneous Absorption

The potential routes of percutaneous absorption broadly fall into two categories; transappendageal (hair follicles and sweat glands) and across intact skin. The latter pathway can be further subdivided into the intercellular route, which follows the tortuous "mortar" and the transcellular route, directly across both bricks and mortar (Hadgraft 1983).

As dermal appendages arise in the dermis and traverse the epidermis, it has been suggested that they could be exploited to bypass the stratum corneum barrier. This transappendageal or "shunt" route (Barry 1986; Guy and Hadgraft, 1992) may have a role in the diffusion of large polar molecules with very low diffusion coefficients through the stratum corneum and low partition coefficients from water (Barry, 1983; Williams and Barry, 1992). There is evidence that inorganic ions (Sugibayashi *et al.*, 1992) and some steroids are absorbed *via* this route, especially at the early stages of penetration (Scheuplein and Blank, 1971). A rapid absorption immediately upon application of the drug to the skin surface, *ie* having a minimal lag time, is characteristic of a shunt-route (Scheuplein, 1967; Shelley and Melton, 1949; Barry, 1988a). The transdermal permeation of cortisone shows significant absorption followed by a long lag time and a relatively small steady state slope. This is indicative of transport *via* a shunt route (Scheuplein, 1972). Generally, it is believed that dermal appendages do not provide a significant route of entry from the skin surface (Blank, 1964; Kligman, 1964; Malkinson, 1964; Scheuplein and Blank, 1971), because the relative cross-sectional area of the pores is only a small fraction of the total skin area: approximately 0.1% (Scheuplein, 1967). Furthermore, penetration of the drug would have to diffuse against the outward movement of sweat or sebum. More recent studies have questioned this notion and suggest that follicles have a significant function in percutaneous absorption (Illel *et al.*, 1991). The shunt-route or porous pathway has also been identified as a significant route of transdermal permeation for compounds that are iontophoretically delivered across the skin (Burnette, 1989; Green, *et al.*, 1993).

Figure 1.4 The brick and mortar model of the stratum corneum showing possible micro routes of drug penetration through human skin - (Barry, 1991, Elias, 1981)

The unbroken epidermis constitutes the larger surface for absorption and is widely regarded as the major pathway for the percutaneous absorption of many compounds. As mentioned, there are two possible routes for the transepidermal absorption of drugs (figure 1.4). The first involves the intercellular route, a tortuous course between the cells of the stratum corneum and the second, the intra- or transcellular route, is the direct diffusion of drugs through the cells. Due to the difficulty in designing experiments to demonstrate which of these two routes is predominant, there is still much argument as to their relative influences.

The preferential route taken by a transdermal penetrant is controlled by a number of factors, including chemical potentials, the partition coefficients of the penetrant for adjacent phases (Barry, 1987a), and the diffusion coefficients within the relative intra- or inter-cellular regions (Barry, 1987b). Although these routes are described as separate entities, it is important to realise that the majority of permeants will diffuse by both courses, but their physical and chemical characteristics determine which is favoured (Wiechers, 1989). Work studying the absorption kinetics of some esters of nicotinic acid showed that these molecules penetrated the epidermis *via* the intercellular channels (Albery and Hadgraft, 1979). Although there are arguments for and against each individual route, the belief that the intercellular route is the principal absorption pathway and the major barrier to most drug permeation (Elias *et al.*, 1977b; Potts, 1989; Curatolo, 1987; Stoughton, 1989, Guy and Hadgraft, 1988 and Houk and Guy, 1988) has directed considerable research into the precise composition of the lipid lamellae. The barrier properties have been studied using thermal analysis, including differential thermal analysis and differential scanning calorimetry, infra-red spectroscopic and X-ray diffraction techniques. These are well established methods of elucidating the structure and function of proteins, lipids and water in a variety of biological barriers (Bach, 1984; Amey and Chapman, 1984; Makowski and Li, 1984).

For a molecule to traverse unmodified stratum corneum, it will have to cross successive aqueous and hydrophilic layers. The rate limiting step for a polar or hydrophilic compound could well be the hydrophobic alkyl chain regions. One means of promoting transdermal penetration, would be to increase the aqueous regions or decrease the resistance of the hydrophobic lamellae. This may be achieved by absorbing chemicals into the intercellular lipids that have the capability of increasing the partition coefficient or disrupting the ordered bilayers, increasing the fluidity of the absorption barriers and "enhancing" the rate of transdermal drug absorption.

1.3 Absorption of Drugs

The logical approach to the treatment of skin disease is the topical application of medicaments. The occurrence of systemic side effects from these treatments inevitably led to investigations utilising the skin as an administration route for systemic treatment regimes. (Shaw & Urquhart 1981). Drugs are administered by various oral, parenteral and rectal routes and these regimens involve the systemic administration of often potent drugs. The treatment of a localised ailment such as pain or inflammation by systemic administration subjects the entire individual to potent drug concentrations. The potential for unwanted side-effects is considerable. Practitioners desire a "magic bullet" to target a drug to the disease and local application may be a small step in this direction. The requirement of systemic administration avoiding potential gastro-intestinal and first-pass metabolic effects, may also be achieved by topical formulations.

There are only a limited range of drugs that are suitable for transdermal absorption. These are highly active substances with the appropriate physicochemical properties to cross the stratum corneum, a total daily dose of a few milligrams (Guy and Hadgraft, 1985) and a therapeutic plasma concentration in the range of nanograms per millilitre (Guy and Hadgraft, 1989). An important consideration limiting the use of percutaneous drug administration *in vivo* is irritation and sensitisation of the skin (Vermeer, 1991; Benezra, 1991; Kurihara-Bergstrom *et al.*, 1991). If a pharmacologically active material is held in contact with the skin under an occlusive patch system for extended periods of time, the likelihood of an irritant or allergic response is increased. The reports of allergic contact dermatitis with patients using transdermal delivery patches become more prevalent as these delivery devices become increasingly popular (Lynch *et al.*, 1987; Fisher, 1984; Holdiness, 1989; Maibach, 1987; McBurney *et al.*, 1987)

Percutaneous absorption, whether *via* the intercellular or intracellular route, is essentially a passive diffusion process. Very few compounds are absorbed transdermally *via* specialised transport systems or transdermal shunts, such as trans-epidermal appendages. Passive diffusion is a process where matter moves down a concentration gradient from one region to an other and there is no competition between structurally related compounds for transport. The physicochemical properties of a drug that determines its ability to permeate skin are expressed in Fick's first law of diffusion. This defines the flow rate of matter from one region

of a system to another. This flow rate, or flux, is the amount of drug passing through a unit area in unit time. For percutaneous absorption of drugs, this is normally expressed in mole $cm^{-2} min^{-1}$. In mechanical systems, the direction of spontaneous change can be predicted by examining the relative-chemical potentials. The relative-chemical potentials or Gibbs' Functions can be expressed as :-

$$\mu_i = \mu_i^{\circ} + R.T.\ln a_i \qquad \text{(Eq 1.1)}$$

Where μ_i^0 is the chemical potential of solute i in a standard state(J mol^{-1}), a_i is the activity of solute i in a solution at a given concentration, R is the Gas Constant (8.3 J $K^{-1}mol^{-1}$)and T is the absolute temperature (K). It is the difference in potentials due to the relative activity gradient that provides the driving force for transport; the skin provides the proportionality factor or diffusion coefficient between flux and this activity gradient. Experimentally, flux is calculated by measuring the amount of drug permeating through a membrane with relation to time. Provided the solute or solvent does not damage the stratum corneum, the source of permeant remains constant and sink conditions remain throughout. A plot of the amount transported versus time has the form shown in Figure 1.5. After an initial non-linear period, the profile establishes a linear relationship. During this period there is, to an experimental approximation, a steady-state equilibrium in which the concentration gradient remains constant at all points within the absorption barrier. The kinetics represent a simple zero-order flux case. The gradient of the linear section of the graph is the steady state flux, *J*.

The simplest way of modelling the process of skin absorption is to apply Fick's first law of diffusion to this steady-state phase. This states that the rate of absorption is proportional to the concentration difference across the membranes.

$$J \propto \frac{-dc}{dx} \qquad \text{(Eq 1.2)}$$

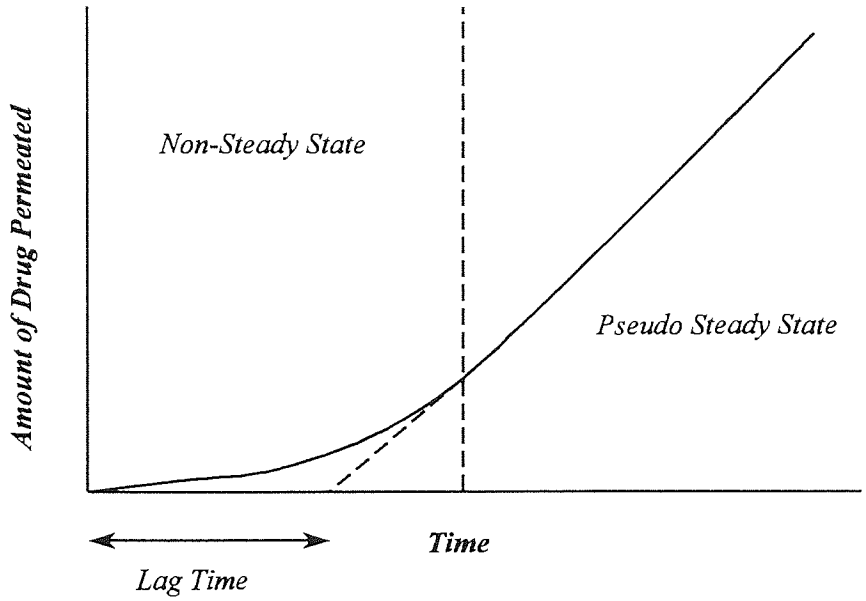

Figure 1.5 Typical profile of amount transported versus time for drug diffusion through the epidermis

The rate of absorption or flux J (μmol cm^{-2} hr^{-1}) is by convention a vector flowing from left to right and hence has a positive sign. Mass flows down a concentration gradient, *i.e.* decreasing concentration to the right, therefore, the constant of proportionality or diffusion coefficient (D).

$$J = -D \frac{dc}{dx} \qquad \text{(Eq 1.3)}$$

From Figure 1.5 the concentration gradient across the membrane $dC = C_1 - C_2$ and the membrane thickness $\delta = X_1 - X_2$. Therefore

$$J = -D \left(\frac{C_1 - C_2}{X_1 - X_2} \right) \qquad \text{(Eq 1.4)}$$

Figure 1.6 Concentration profile across ideal membrane at steady state : simple zero order case. (From Barry 1983)

If sink conditions apply, then C_2 approximates to zero and the concentration gradient C_1-C_2 tends to C_1, the membrane thickness X_1-X_2 is represented by δ, hence:

$$J = D.\frac{C_1}{\delta} \qquad \text{(Eq. 1.5)}$$

If absorption from a vehicle is considered, the drug concentration at the skin surface will not be the same as in the formulation. This is due to partitioning of the drug between the skin barrier and the vehicle. Therefore the effective partition coefficient, P, of the drug between these two regions must be considered.

As:

$$P = \frac{C_1}{Cd} \qquad \text{and} \qquad C_1 = P.Cd$$

Hence, the flux across membranes such as the stratum corneum in percutaneous absorption is described as (Cooper and Berner, 1985):

$$J = \frac{D.P.Cd}{\delta} \qquad \text{(Eq 1.6)}$$

If the drug is presented to the skin surface as a suspension, concentration C_s, the maximal flux (J_{max}) is obtained:

$$J_{max} = \frac{D.P.Cs}{\delta} \qquad \text{(Eq 1.7)}$$

From the linear section of an experimental profile of the amount transported versus time, J is defined as the mass of permeant (M_t) per unit of area (A) per unit of time (t).

$$J = \frac{dM_t/dt}{A} \qquad \text{(Eq 1.8)}$$

therefore

$$\frac{dM_t/dt}{A} = \frac{D.P.Cs}{\delta} \qquad \text{(Eq 1.9)}$$

and

$$\frac{dM_t}{dt} = \frac{D.A.P.Cs}{\delta} \qquad \text{(Eq 1.10)}$$

and

$$M_t = \frac{D.A.P.Cs.t}{\delta} \qquad \text{(Eq 1.11)}$$

Taking into consideration the lag time of absorption from the permeation profile Figure 1.5 the total mass of permeant transported after a time period t is, where t_L is the lag time :

$$M_t = \frac{D.A.P.Cs.(t - t_L)}{\delta} \qquad \text{(Eq 1.12)}$$

The parameters which are difficult to individually measure with precision are often collected into a single variable defined as:

$$k_p = \frac{D.P}{\delta} = \frac{J}{Cs} \qquad \text{(Eq 1.13)}$$

Where k_p is the permeability coefficient. Significant characteristics of the permeant that influence the transfer rate are the partition coefficient (P) and the diffusion coefficient (D) in the stratum corneum. It is difficult to measure skin/vehicle partition coefficients experimentally and these two components are sometimes multiplied together to give an apparent or observed permeability coefficient (k_{obs}).

If the drug molecule is roughly spherical and the molecules of the surrounding solvent are smaller or comparable in size, the diffusion coefficient can be expressed by the Stokes - Einstein equation (Loftsson, 1982):

$$D = \frac{k.T}{6\pi.r.\eta} \qquad \text{(Eq 1.14)}$$

Where k is the Boltzmann's Constant (J K^{-1}), T is the absolute temperature (K), r is the hydrodynamic radius of the diffusing molecule (m) and η is the viscosity of the barrier (kg m^{-1} s^{-1}). The dependence on molecular weight is minimal since relatively large changes are

required to affect significantly the mean radius, although the diffusion coefficient is dependent upon the polarity of the diffusant which controls the hydration shell and hence the effective size of the molecule. The important variable in the permeability coefficient (k_p) is therefore the effective partition coefficient (P), which is an extremely sensitive function of molecular structure and size (Loftsson, 1982). It is this factor that can be significantly affected by the modification of vehicles for drugs designed for transdermal absorption. This index of mutual affinity between the drug and vehicle is important in determining the rate at which drugs will be delivered through the skin. A high partition coefficient value indicates that the vehicle has a poor affinity for the drug. A low partition coefficient value indicates a high degree of mutual interaction, reflecting the tendency of the drug to remain in the vehicle. This relationship is usually parabolic as very lipophilic compounds cannot escape in aqueous vehicle compartments. Hence, the release of a substance will be favoured by the selection of vehicles having a low affinity for the penetrant or those in which the drug is least soluble. Optimal release of drug will be obtained from vehicles containing the minimum concentration of solvent required for complete solubilisation of the drug (Poulsen, 1972). This implies that topical formulations should be at the limit of the drug's solubility and that different concentrations of active ingredient may require different formulations. Each formulation should maximise the thermodynamic activity of the drug in the preparation (Higuchi, 1960, 1977 and 1987). Thermodynamic activity has been described as the "escaping" tendency of a molecule from a vehicle (Barry, 1985) and the following equation has been derived to quantify activity (Higuchi, 1960):

$$J = \frac{a.D}{\gamma.\delta} \qquad \text{(Eq 1.15)}$$

Where J is the penetrant flux, D is the drug diffusivity, a is the thermodynamic activity, δ is the membrane thickness and γ is the activity coefficient of the drug in the skin. This equation predicts that under ideal conditions of an intact homogeneous membrane providing the rate limiting step and non-interacting non-ionic diffusing permeant, the drug flux through the skin should be directly proportional to the drug activity in the vehicle, provided D, γ and δ remain constant. Evidence of this effect has been shown studying the *in vivo* release rates of fluocinolone acetonide and its acetate ester from aqueous solutions using propylene glycol as

a co-solvent. Maximum release was achieved with propylene glycol concentrations just sufficient to solubilise the steroid. Excess co-solvent lowered the thermodynamic activity of the steroid and therefore the release rate (Poulsen *et al.*, 1968). Similar trends were observed with skin penetration experiments studying fluocinolone acetonide and fluocinonide (Ostrenga *et al.*, 1971) and hydrocortisone (Shahi and Zatz, 1978). Suspensions do not increase the rate of absorption, as a drug must first dissolve before it can be absorbed and dissolution of drugs in suspension may be the rate-limiting step to absorption.

J is the most important parameter determined in a skin permeation experiment. To determine J accurately, the permeation experiment should be continued for at least 6 - 10 t_L. An accurate determination of t_L is best obtained if the linear region is taken from times greater than $2t_L$ (Cooper and Berner, 1985). Lag time is important because it allows a simple estimation of the diffusion coefficient provided the drug does not bind to the membrane (Katz and Poulsen, 1971). Lag time is given by (Flynn *et al.*, 1974) :

$$t_L = \frac{\delta^2}{6D} \qquad \text{(Eq 1.16)}$$

Diffusion related to Fick's first law relates to flux under the influence of a concentration gradient. It is therefore a time-independent process, or one where the donor solution remains constant without significant loss and the receiver phase concentration does not increase significantly, providing constant sink conditions. Obviously with transdermal situations *in vitro*, this situation is maintained as closely as possible using a saturated donor phase and either a "flow through" or a relatively large volume receiver phase. This situation is an approximation and is further exaggerated *in vivo* where absorption through skin is not necessarily a steady-state process. This is because the stratum corneum is a relatively impermeable barrier and it takes a long time to establish steady-state conditions. This length of time is not likely to be attained within normal therapeutic or cosmetic applications (Guy and Hadgraft, 1989b). Application of drugs to the skin is a time-dependent process in which there is some distribution of concentration without replenishment. This phenomenon is mathematically modelled by Fick's second law of diffusion (Scheuplein, 1967).

$$\frac{dc}{dt} = D.\frac{d^2C}{dx^2} \qquad \text{(Eq 1.17)}$$

This partial differential diffusion equation states that the rate of change in concentration at a point within a diffusional field is proportional to the change in concentration gradient at that point. The assessment of diffusion coefficients within the non steady-state (see Figure 1.3) period become increasingly more complex (Edwards and Langer, 1994). The mathematics require the correct boundary conditions for proper solution and sometimes the model includes events other than transport, for example metabolism, when the diffusion equations become even more complicated. The determination of diffusion coefficients within the non steady-state period, or as it is frequently entitled, short time approximations, become attractive when using thick membranes or solutes with low diffusivities where potential analytical instrument instability, membrane degeneration and problems with maintaining sink conditions make it experimentally impossible to wait for steady-state conditions.

Short time permeation profiles have been modelled by (Hadgraft, 1979; Rodgers *et al.*, 1954 and Short *et al.*, 1970):

$$\log\left(\frac{M_t}{t^{3/2}}\right) = \log\left(\frac{8Cv}{\delta^2\pi^{1/2}}\right) + \frac{3}{2}\log D - \frac{\delta^2}{9.2Dt} \qquad \text{(Eq 1.18)}$$

Where M_t is the cumulative amount of drug in the receptor phase.

1.4 pH-Partition Hypothesis

Many drugs are weak organic acids or bases and in aqueous solutions they are ionised to different degrees depending upon pH. It is generally accepted that most drugs of this type are absorbed across biological membranes by the passive diffusion of the neutral molecule. The rate of absorption is influenced by the drug's lipophilicity and this is directly related to its degree of ionisation. Unionised forms of electrolytes are considered capable of crossing biological membranes as opposed to their corresponding hydrophilic ionised species. This assumption is used to effect in the treatment of aspirin (pKa = 3.5) or phenobarbitone (pKa = 7.4) drug poisoning. Increasing the urinary pH from 5 to 8 with sodium bicarbonate or lactate can have significant effects upon the resorption of these ionic compounds from the renal tubule (Laurance, 1973).

This phenomenon is described as the pH-partition hypothesis, which states that unionised molecules partition into lipid membranes, whereas ionised molecules do not. Hence, transdermal absorption of weak electrolytes is favoured by the unionised form. Therefore, ideal aqueous vehicles for ionogenic compounds are where the compound is predominantly associated and at the limit of its solubility.

The fraction ionised and unionised of a weak acid or base can be calculated from the Henderson-Hasselbalch equation:

$$pH = pK_a + \log\frac{[base]}{[acid]} \qquad \text{(Eq 1.19)}$$

Hence, for weak acids where

$$pH = pK_a + \log\frac{[A^-]}{[HA]} \qquad \text{(Eq 1.20)}$$

The fraction ionised (α) and unionised ($1-\alpha$) equals :

$$\alpha = \frac{K_a}{K_a + [H_3O^+]} \qquad 1 - \alpha = \frac{[H_3O^+]}{K_a + [H_3O^+]} \qquad \text{(Eq 1.21)}$$

and for weak bases where

$$pH = pK_a + \log \frac{[B:]}{[BH^+]} \qquad \text{(Eq 1.22)}$$

The fractions ionised (α) and unionised ($1 - \alpha$) equal :

$$\alpha = \frac{[H_30^+]}{K_a + [H_30^+]} \qquad 1 - \alpha = \frac{K_a}{K_a + [H_3O^+]} \qquad \text{(Eq 1.23)}$$

The release rate of drugs from topical preparations depends directly upon the physical and chemical properties of the vehicle and the drug employed. The physiological availability of topically applied drugs is dependent on both the release rate from the vehicle and the permeability through the skin. If the pH-hypothesis applies to topically applied preparations the pH of the vehicle will have a significant influence upon the rate of absorption.

1.5 *In Vitro* Absorption Evaluation

The object of *in vitro* investigation is to create an experimental method that can predict the penetration kinetics of drugs into the human body *in vivo*. The advantage of *in vitro* investigation is that it allows the control of the environment and the simplification of the complex variables that characterise *in vivo* experimentation. These controls must not diverge so far from biological reality as to make the results meaningless. The best use of *in vitro* experimentation is to compare and contrast relative drugs and vehicles to optimise formulation, determine absorption mechanisms and the role of enhancing mechanisms, such as chemical, physical, iontophoresis and phonophoresis, as far as possible before subjecting living subjects to potentially noxious chemicals.

In vitro diffusion cells can not exactly duplicate the *in vivo* scenario. Enzymatic metabolism may be compromised within excised skin and the absence of dermal vascularisation may modify the clearance and therefore the flux of the permeant. Good correlation between *in vitro* and *in vivo* data is possible provided diffusant clearance from the distal surface of the barrier is not the rate limiting step to diffusion (Franz, 1975;78 and Marzulli *et al.*, 1969) and a well defined methodology is employed.

The centre piece to *in vitro* transdermal absorption measurements is the diffusion cell. Basic variations include orientation (vertical and horizontal) and receptor compartments (static or flow-through). An early vertical diffusion cell was proposed by Coldman *et al.* (1969). This basic design has been used and modified by many workers (Chowhan and Prichard, 1978 and Ostrenga *et al.*, 1971). Traditionally, the vertical cell is named after Franz (1975,1978) who tested a design based upon a dumbbell-shaped receiver compartment. There have been many criticisms of this design directed at the inadequate stirring and poor temperature control of the receiver compartment (Chien *et al.*, 1983; Keshary and Chien, 1984; Chien and Valia, 1984 and Gummer *et al.*, 1987). The Keshary-Chien cell was designed as an alternative based upon these criticisms using a cylindrical receptor compartment that is completely enclosed by the water jacket. A star-head magnet replaced the bar magnet and a stopper closed off the sampling port to reduce evaporation during long experimental permeation profiles.

In the standard vertical static glass cell, the top compartment holds the formulation under investigation and in the bottom a buffer solution is kept in direct contact with the absorption barrier (Figure 1.7).

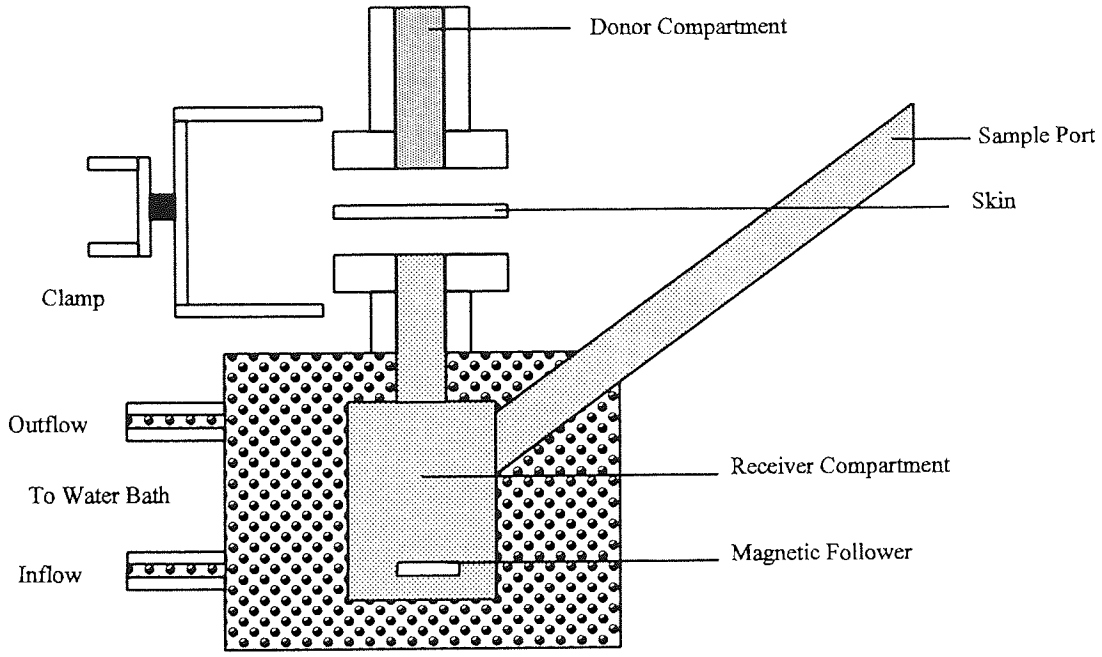

Figure 1.7 The Franz-type, vertical *in vitro* absorption cell

Samples are taken from the sampling port for analysis. The receiver cell is continually agitated, using a magnetic follower and is maintained at a constant temperature *via* a water jacket. As the donor compartment cannot be agitated in this type of cell, chemicals must diffuse to the absorption surface. Although it lends itself well in the assessment of delivery devices such as patches, problems such as air bubbles collecting in the lower compartments reducing the contact surface with the absorption barrier are difficult to eliminate.

Using the vertical cell, a range of *in vitro* techniques can be performed. Most investigations utilise an infinite dose technique (Smith and Haigh, 1989) where sufficient permeant is applied to the donor membrane surface to assume the concentration remains constant during the

experiment. The donor surface is usually covered with a suspension or solution of the donor. Provided the receiver is of sufficient volume to approximate sink conditions, a profile, as discussed in section 1.3, can be achieved. This technique approximates a steady-state technique and permeation data can be mathematically extrapolated from the linear section of the permeation profile. A criticism levelled at this experimental set-up is that the absorption barrier is fully hydrated throughout the experiment and that the rate of penetration may be influenced by the continued occlusion of the barrier surface. For this reason, comparisons between *in vitro* and *in vivo* determinations may be unreliable.

In vivo topically applied drugs cannot practically be applied to the entire skin surface in an infinite dose. In an attempt to mimic this *in vivo* situation, a finite-dose technique has been utilised by many authors (Foreman *et al.*, 1977,1978; Franz, 1978, Akhter and Barry, 1985;Southwell and Barry, 1984; Watkinson *et al.*, 1991). Here, a known dose of drug is applied to the skin surface, usually in a volatile solvent. This solvent can then be evaporated off, leaving a thin film of drug of finite dose upon the surface. This also enables the control of donor compartment variables, such as humidity and exposure to atmospheric conditions, thereby simulating occluded and non-occluded clinical situations. It is this technique that gives the vertical cell the alternative name of "*in vitro* mimic cells".

Horizontal diffusion cells have similar sized receptor and donor compartments positioned either side of the absorption barrier under assessment (Langguth *et al.*, 1986). This barrier is placed in the vertical plane (Figure 1.8). With this system, it is relatively easy to remove air bubbles and agitation of the vehicle ensures homogeneity of the formulation under investigation. A disadvantage is that a large volume of donor solution is required to completely cover the barrier surface. This is exaggerated when investigating expensive diffusants, or diffusants that are not readily available in large quantities. This is especially so if designing infinite dose experiments with saturated suspensions of a solute readily soluble in aqueous vehicles.

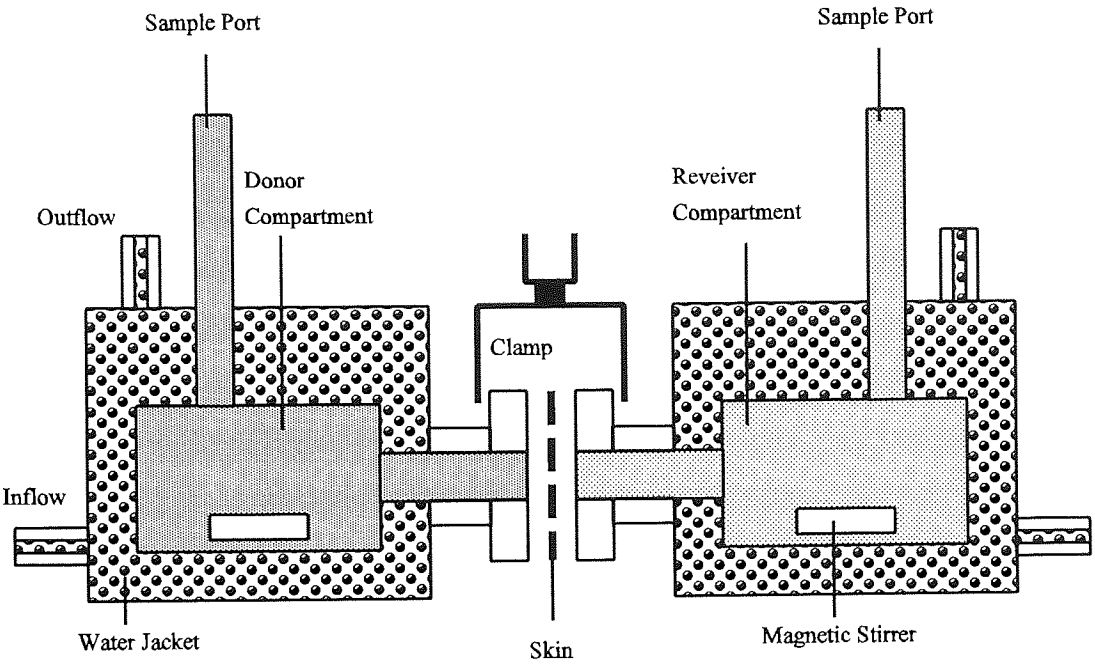

Figure 1.8 The horizontal-type *in vitro* absorption cell

There are many variations upon the basic design (Durrhein *et al.*, 1980; Harper Bellantone *et al.*, 1986; Galey *et al.*, 1976; Flynn and Smith, 1971; Southwell and Barry, 1981,1984; Chien and Valia, 1984 and Valia and Chien, 1984a,b), each group claiming advantages and disadvantages based mainly upon agitation and temperature control. The majority of horizontal cells require large sections of membrane making them impractical for human skin investigations where the availability of membrane is not only limited, but it is relatively difficult to produce large sheets of intact membrane.

Pretreatment of membrane surfaces is unrealistic using horizontal cells, but they are especially useful for assessing the intrinsic diffusivity of a molecule through a membrane, or the effect of partition coefficient, pH, or boundary layers on diffusion. The use of identical donor and receptor solvents within these cells enables the study of drug diffusion through a medium, in the absence of any factors that may enhance penetration. These cells are also frequently referred to as zero-order steady-state diffusion cells, because they are ideal for infinite dose experiments with the steady-state region of the permeation profile. They enable the monitoring of a number of kinetic events simultaneously, including the degree of binding or

reservoir formation within the absorption barrier. This is achieved by analysing the loss of drug from the donor compartment at the same time as its appearance in the receptor compartment. The total mass loss is due to partitioning or binding of the permeant with the membrane (Scheuplein, 1978).

One of the most important design aspects of *in vitro* absorption cells is the degree of agitation within the compartments. Agitation must be sufficient to minimise diffusion boundary layers at the interfaces between the donor and receiver phases and the absorption barrier. The trans-barrier permeation of compounds may be exaggerated by the existence of large static diffusion boundaries at the membrane surfaces. The depth of boundary layers decreases as compartment agitation increases, which results in a relative increase in drug permeation (Lovering and Black, 1974 and Stehle and Higuchi, 1972). In comparative work, the rate of agitation should be carefully monitored and maintained at a uniform rate to annul boundary layer effects (Ackerman and Flynn, 1987; Ackerman *et al.*, 1985;87 and Sato and Win Kim, 1984), failure to maintain uniform rates will produce unreliable results.

The composition of the donor and receiver phases must be carefully considered when designing an experimental protocol for *in vitro* transdermal investigation. The receiver phase should ideally mimic biological fluids. It must be carefully selected not to affect the function of the barrier. Receiver solutions containing solvents such as alcohols, may extract lipids from skin membranes, potentially enhancing the permeation rate of many donor compounds. A buffered aqueous receiver phase is the most straightforward, as the potential for barrier effects are minimal and the analysis of compounds from these solutions is uncomplicated. However, the receiver must also possess favourable partitioning characteristics for the penetrant. The effect of poor solute solubility in the receptor phase may be the reason for discrepancies between some *in vivo* and *in vitro* results. The poor partition into aqueous receivers *in vitro* may not compare favourably with partition into biological fluids and the continuous sink conditions created by the vasculature. Compounds with a water solubility of less than 10 mg l^{-1} may exhibit reduced permeation characteristics (Bronaugh and Stewart, 1984). The use of a receiver with the properties simply to solubilise the diffusant without damaging the membrane, may not be enough to overcome the diffusion anomalies of highly lipophilic compounds. The receiver must maintain a greater overall lipid solubility to enable the penetrant to overcome the lipophilic properties of the skin and partition adequately into the receiver.

The chemical potential of the donor phase is equally important. If the diffusant is very soluble in the donor vehicle, and is at a relatively low concentration, it will have little affinity for the barrier membrane and will not readily partition into it (Smith and Haigh, 1989).

Franz-type and horizontal *in vitro* absorption cells have the advantage that temperature can be easily maintained *via* water-jackets, but sampling usually requires someone to take aliquots at various time intervals and this is labour intensive. With traditional flow-through diffusion cells, the collection of receptor phase can be automated. Samples can be taken for analysis *via* a scintillation counter. This system is a best approximation of the receptor sink that occurs *in vitro*. It can suffer from lack of convenient temperature control, but for comparative transport, maintenance of the absorption barrier at body temperature (32°C) is not always essential.

Design of these cells is becoming ever more complex and can enable agitation of the receptor phase by stirring or modification of the flow through solution (Hawkins and Reifenrath, 1986;Guy, *et al.*, 1986; Bronaugh and Stewart, 1985a,b; 1986; Bronaugh *et al.*, 1986 and Fisher, 1985). It is now more usual to include a thermostated temperature control (Reifenrath, 1994) and in some cases control the environment within the donor compartment (Gummer *et al.*, 1987). Increasingly lower volumes in the receptor compartment enable low levels of permeant to be detected with increasing accuracy (Reifenrath, 1994).

1.6 *In Vitro* Absorption Barriers

Transdermal absorption experiments are designed to mimic the *in vitro* effects of drugs upon humans. This implies that the ideal *in vitro* barrier is human skin. Unfortunately, this is only available to a limited number of investigators and often then, only in relatively small quantities. Human skin does have disadvantages. Samples can be taken from various body sites and the age, sex and hairiness of donors varies. These factors are known to influence penetration (Feldman and Maibach, 1973). Samples can also come from a variety of situations, for instance surgical amputations, (reductions, mastectomies and limbs), burns patients and cadavers. The latter has especially lead to speculation that the autolytic processes within the epidermis following death may have a direct influence on the integrity of the overlying barrier (Gummer, 1989). Other possible causes of barrier-impaired skin might include, damage during the separation process and the disease or trauma of the donor, for example, many amputated limbs are due to peripheral vascular disease where the skin may already be necrotic.

Due to its availability, animal skin is used as an alternative. The majority of *in vitro* experiments are performed on the hairless mouse, although the hairy and hairless rat, guinea pig and rabbit are also used. A great deal of work has been performed correlating absorption through animal skin and human skin (Bronaugh *et al.*, 1982; Bronaugh and Maibach, 1985; Bronaugh and Stewart, 1985a). Similarities have been found, but for some chemical compounds the trend does not hold true through a homologous series. No animal skin has been found to completely mimic human skin, but weanling pig skin (Bronaugh and Maibach, 1985; Wester and Noonan, 1980) followed by monkey skin (Wester, 1975; Southwell *et al.*, 1984) are the most representative. Hairless mouse skin is known to be several-fold more permeable compared to human skin (Wester and Maibach, 1991).

Artificial membranes are used with some limited success (Nacht and Yeung, 1985) and may be useful as a convenient barrier source for comparing initial relative absorption rates from various vehicles. The advantages of artificial membranes are that they are readily available and reproducible. Silastic rubber or dimethyl polysiloxane membrane has been extensively used to study the permeation of a variety of drugs: salicylic acid (Bottari *et al.*, 1974; Walkow and McGinity, 1987a,b; Nacht and Yeung, 1985), benzoic acid (Touitou and

Abed, 1985), lidocaine (Broberg *et al.*, 1982) and steroids (Schuhmann and Touibert, 1970; Liu *et al.*, 1985 and Tanaka *et al.*, 1985). Silastic membrane is non-polar in nature and demonstrates lipid-like properties. It may be a useful model for compounds that follow the intercellular route through the stratum corneum.

A vast variety of artificial membranes have been used to mimic human skin *in vitro:* hydrophilic microporous cellulose acetate (Barry and Eleini, 1976; Barry and Brace, 1977); cellulose nitrate filters impregnated with lipids such as isopropyl myristate (Hadgraft and Ridout, 1987), dipalmitoyl phosphatidylcholine, linoleic acid and tetradecane (Hadgraft and Ridout, 1988); cellulose (Borodkin and Tucker, 1974; Samuelov *et al.*, 1979 and Donbrow and Samuelov, 1980); and multilaminate membranes (Nacht and Yeung, 1985) developed to mirror the hydrophobic-hydrophilic bilayers present within the stratum corneum.

Limitations are that the skin would appear to be more complex than simple hydrophobic/hydrophilic membranes of fixed pore size. The rate limiting characteristics of skin are still poorly understood, as evidenced by attempts to draw simple correlations between penetration kinetics and factors such as molecular weight, partition coefficients and molecular size. Artificial membranes may be useful for comparative data for individual chemicals, but it is essential to fully validate permeation with a biological membrane, preferably human skin, before embarking on relative kinetic comparisons *in vivo*.

1.7 Removal, Separation and Storage of Skin

For transdermal drug delivery *in vivo*, the whole skin, from the desquamating stratum corneum through to the viable dermis, must be considered, but it is generally accepted that the stratum corneum is the principal barrier. The dermis is vascularised *in vivo* and drugs penetrating to this layer would be carried away by the systemic circulation in a continual sink situation. When used *in vitro*, the dermis can provide a substantial barrier. This is especially true for lipophilic molecules (Scheuplein and Blank, 1973). The significance of this must be investigated before whole skin is used for *in vitro* flux measurement (Díez-Sales *et al.*, 1993). It is generally thought desirable to use epidermis or stratum corneum alone for all *in vitro* flux measurements.

There are a number of techniques for separating the epidermis, or stratum corneum from the dermis. Subcutaneous injection with staphylococcal epidermolytic toxin will separate the epidermis from the dermis as long as the tissue is quite fresh (Elias *et al.*, 1974), although there is evidence that this technique can damage the water barrier properties of stratum corneum (Smith *et al.*, 1982).

Human stratum corneum of sufficient size can be obtained from living subjects by the application of cantharidin under an occlusive dressing for 8 to 10 hours. Blisters of up to 4 cm in diameter can be obtained without scarring the subject (Kligman and Christophers, 1963). This technique is clearly best suited for studies involving small skin samples, and where there is a good supply of regular healthy "volunteers".

Chemical methods of freeing the epidermis from the corium are many and varied with a good history. Manschel in 1925 utilised maceration in acetic acid. Alkaline solutions such as lime water and ammonia were well known in the leather industry to remove hair and epidermis from animal hides and in 1947, Felsher postulated that acids and bases effected separation by causing the collagen to swell. More commonly whole skin is left immersed in various salt solutions for sometimes many hours before it is pinned out and the epidermis carefully excised with tweezers. Baumberger's method (Baumberger *et al.*, 1942) where human skin is soaked in 1N ammonium hydroxide for 20 minutes at room temperature was the technique of choice as determined by epidermal sulphydryl and disulphide concentrations

(Oguia *et al.*, 1960). Other salts that have been tried are potassium chloride (Griesmer and Gould, 1954) sodium hydroxide and, more recently, formic acid (Kligman, 1983) and sodium bromide (Scott *et al.*, 1986). In 1977, Walker *et al.*, suggested that soaking whole skin in ammonium chloride at 0°C for 30 minutes was an ideal method whereas Luis (1977) treated human skin with 2N sodium thiocyanate for 3 - 5 hours to achieve cleavage at the lamina lucida of the basal membrane zone. Although most reports carry data stating the barrier properties are unaffected, it is still questionable whether this evidence holds true over a range of animal skins and throughout a range of chemicals (Gummer, 1989).

Chemical methods can take a long time, sometimes many hours, to prepare samples before separation is achievable. However, they do appear to be the methods of choice with hairy samples. This is because the epidermis is loosened from the dermis in such a way that hair comes out with the epidermis. The use of 1.5 M sodium bromide is particularly good for separating rat epidermis from dermis, while soaking in 30% guanidine hydrochloride for several hours works quite well for hairy human skin. A variation to soaking samples in ammonium solutions is to expose them to ammonia vapour in a desiccator for 35 minutes at room temperature (Humphries and Wildnauer, 1971). The use of small aluminium alloy (Dural) frames have been implemented to facilitate the isolation and handling of stratum corneum (Ferguson, 1977). These frames are glued onto the surface of the skin before specimen removal and remain in place during the vapour exposure and subsequent removal of the dermis. Considering the size of the frames (30 x 30 mm internal measurement) and the advice to cut 1 cm from the edge of the frame, extremely large skin samples are required. Irrespective of the salt used to isolate stratum corneum all samples must be soaked in water after isolation to remove all traces of salt before they are used in transdermal transport experiments.

Enzyme digestion can be used to separate the epidermis from the dermis. Traditionally, a crude pancreatic extract was used (Medawar, 1941) but later this was improved by the use of purified trypsin in "Fan's method" (Fan, 1958). More recently, trypsin is only used to separate the stratum corneum from the viable epidermis after initial separation from the dermis (Kligman and Christophers, 1963). The epidermis is placed on filter paper pre-incubated with buffered solutions of trypsin at various strengths (between 0.0001% to 1%) depending upon the speed of separation required. Care must be taken with solution

strengths above 0.0001% as they can solubilize the horny layer. This method of preparing sheets of pure stratum corneum is often omitted after the initial separation for fear that trypsinization damages the membrane (Southwell *et al.*, 1984) by destroying lysine-rich and arginine-rich proteins, such as histones (Walker *et al.*, 1977). Mechanical methods such as producing bullae and stretching skin have been used in an attempt to minimise the use of chemicals. Bullae are produced by a heavy walled thistle tube on the epidermis. The dermis side is placed under water and the water sucked through using a vacuum pump (Blank and Miller, 1950). Van Scott (1952) recommended stretching the skin to its limit; this enables the epidermis to be removed with tweezers and a scalpel. Both these methods require sizable pieces of tissue.

Heat separation of the two layers is probably the most popular, the quickest and the most convenient method. Whole skin is first defatted and then placed in 50-60°C water or on a hot plate for a period of 60 - 120 seconds (Kligman and Christophers, 1963). This weakens the adhesion between the dermis and the epidermis so the two layers can be gently peeled apart using tweezers. In practice this method is only useful for tissue without much hair, as unlike the chemical methods the hair remains in the dermis and during separation these leave large holes in the epidermis. Another criticism of this method is that heat can severely denature some proteins (Walker *et al.*, 1977).

A very useful mechanical method of separating skin is the electric dermatome (Bronaugh *et al.*, 1981). This offers controllable thickness of specimen and although hair follicles and sweat glands that penetrate deep into the dermis are severed, this does not appear to show any difference in barrier function to that of whole skin (Gummer, 1989). Obviously this method does not ensure complete removal of the dermis which may cause assay interference in the donor phase and may act as a depot for transported drugs.

Once suitable samples have been prepared, convenient methods of storage must be employed. Freezing skin at -20°C is the method of choice. It has been demonstrated that skin samples stored frozen for 12 months did not show a significant change in water permeation (Bronaugh *et al.*, 1986; Harrison *et al.*, 1984). The tissue sample can be wrapped in aluminium foil and then sealed in occlusive film or in a sealed container and frozen. When required, the sample can be thawed and floated off the foil with water.

1.8 Aims and Objectives of Present Study

The aim of this study was to investigate the transport of ionisable compounds across human skin and silastic rubber. The pH-partition theory predicts that the percutaneous absorption of the ionic species of these compounds should be negligible. The objective of this work is to investigate four methods of enhancing this absorption; vehicle composition (Chapter 2), chemical absorption enhancers (Chapter 3 and 4), prodrug formation (Chapter 5) and protection from enzymic degradation (Chapter 6). This work should help provide an understanding of the process of absorption and the mechanisms through which absorption enhancers exert their effect.

Loftsson (1985) states that the total flux of salicylic acid through mouse skin from saturated aqueous solutions was significantly improved with increasing ionisation. Thus, under certain conditions increased ionisation can promote topical delivery. The first objective of this study was to use Franz-type *in vitro* absorption cells to investigate the effects of ionisation on transdermal delivery with excised human skin and silastic rubber as permeation barriers. The experiments were designed to test the hypothesis that the transdermal absorption of salicylic acid, a model ionogenic permeant, obeys the pH-partition theory and that the unionised molecular form is responsible for transdermal permeation and the effect from the ionised form is negligible.

It has been suggested that Azone enhances the permeation of salicylic acid across an artificial membrane by the formation of ion-pairs (Hadgraft, *et al.*, 1985). It was the second objective of this study to devise a series of experiments that questions this suggestion. These experiments test the hypothesis that, in some cases, the mechanism of absorption enhancement of Azone and other tertiary amide enhancers can be explained by partition effects alone and without recourse to ion-pair mechanisms. It was proposed to take two approaches to this objective; the first used Franz-type *in vitro* absorption cells to compare the effects of enhancers with and without a pH-gradient across the absorption barrier; the second studied the distribution of salicylic acid, as a function of pH, between an aqueous phase and isopropyl myristate containing the tertiary amide enhancers. Partition results were compared to a theoretical model for the extraction coefficients of weak acids using the relative partition coefficients of the ionised and unionised species.

Prodrugs can effectively increase the absorption potential of ionic compounds. Phosphonoacetate is an effective antiviral agent, which is ionised at physiological pH and therefore has limited permeation across cell membranes. The third objective was to assess the potential of ester prodrugs of phosphonoacetate to cross biological membranes *in vitro* and to the ability of topical absorption enhancers to further potentiate this effect.

Work in the final chapter studied the stabilising effects of cyclodextrins upon model esters in enzymic systems. The objective was to determine if cyclodextrins can protect ester prodrugs from degradation as ionic products are poorly transported. Esters (parabens) where chosen as model substrates to assess the potential of cyclodextrins to enhance the topical absorption of intact ester prodrugs for bioactivation at systemic sites of action. Examples of such prodrugs would be the esters of phosphonoacetate studied in Chapter 5.

Chapter One has considered some fundamental aspects of percutaneous studies. The objectives above require more detailed reviews on the transport of ions and the effects of ionisation, absorption enhancers, partition and extraction coefficients, phosphonates and prodrugs, and cyclodextrins. These topics will be discussed and reviewed in more detail as introductions to the relevant individual chapters.

CHAPTER TWO

PERCUTANEOUS ABSORPTION STUDIES

IONISATION AND PERCUTANEOUS ABSORPTION

2.1 Introduction

2.1.1 Ionisation and Percutaneous Drug Transport

The physical and chemical properties of the vehicle and drug have a direct influence upon the drug release rate from topical preparations. The transdermal delivery of topically applied drugs is dependent on both this release rate and the drug's permeability through the skin. The process by which compounds cross the skin layers is still in debate, but a number of mechanisms and pathways for the diffusion of drugs across the stratum corneum have been suggested (see section 1.2 for further discussion on routes of percutaneous absorption).

According to the simple pH-partition hypothesis (section 1.4), only the unionised forms of drugs are able to pass through lipoidal membranes in sufficient amounts. Earlier absorption studies on salicylates (Siddiqi and Ritschel, 1972 and Arita *et al.*, 1970), lignocaine (Menczel and Goldberg, 1978) and carboxamine (Arita *et al.*, 1970), have supported this hypothesis. However, there has been increasing evidence that the ionised species can contribute to transdermal absorption. Evidence has been provided (Wallace *et al.*, 1978) for the existence of parallel penetration pathways and shunt routes in the stratum corneum that are involved in the penetration of ionised drug species. To support this, increasing the vehicle pH increases the solubility, ionisation and steady-state penetration of methotrexate (Vaidyanathan *et al.*, 1985). Ionised compounds may also penetrate biological membranes through the hydrated keratin matrix (Flynn, 1985) or aqueous regions (Oakley and Swarbrick, 1986 and 1987), in contrast to unionised drugs which are located in the lipid regions. However, when the penetrating species exists in both ionised and unionised forms it is the unionised species that penetrates most rapidly through the skin (Touitou and Donbrow, 1982; Swarbrick *et al.*, 1984).

The total observed flux through a biological membrane (J_{obs}) is therefore dependent upon both the flux of the ionised (J_i) and unionised species (J_u) and the fraction of drug in each state, α and 1-α respectively, where the degree of ionisation (α) is given by $K_a/(K_a + [H_3O^+])$:

$$J_{obs} = \alpha J_i + (1 - \alpha) J_u \qquad \text{(Eq 2.1)}$$

which may be linearised to:

$$\frac{J_{obs}}{\alpha} = J_i + \frac{(1 - \alpha)\ J_u}{\alpha} \qquad \text{(Eq 2.2)}$$

Thus a plot of J_{obs}/α against $(1-\alpha)/\alpha$ enables the flux of the ionised and unionised species to be estimated (Irwin *et al.*, 1990a). If the plot gives a line with an intercept approximating to zero, this could suggest that in accordance with the pH-partition hypothesis, the ionised species does not penetrate the membrane to any significant extent and that when the drug is totally ionised, the permeation rate should be negligible. As from Equation 1.6, $J = D.P.C_d/\delta$, the pH-dependent partition (P_{obs}) of ionisable molecules may be modelled by:

$$\frac{P_{obs}}{\alpha} = P_i + \frac{(1 - \alpha)\ P_u}{\alpha} \qquad \text{(Eq 2.3)}$$

Where P_{obs} is the observed partition coefficients at various fractions ionised (α) and P_i and P_u are the partition coefficients of the ionised and unionised species respectively (Irwin and Li Wan Po, 1979). Further confirmation that an ionisable compound adheres to the pH-partition theory can be demonstrated by the following relationship, which is a rearrangement of Equation 2.3, assuming that $P_i = 0$ (Oakley and Swarbrick, 1987):

$$\log \frac{P_{obs}}{P_u} = \log \left(\frac{K_a}{K_a + [H_3O^+]} \right) \qquad \text{(Eq 2.4)}$$

Using this equation, it is possible to draw the curve describing the theoretical profile of variation of $\log P_{obs}/P_u$ as a function of pH. This profile expresses the partitioning of molecules adhering to the pH-partition hypothesis. Using Equation 2.4, Santi *et al.*, (1991) found that nicotine did not follow the pH-partition hypothesis when partitioned between isopropyl myristate (IPM) and McIlvaine buffers, although Verapamil did. This was in contrast to Oakley and Swarbrick (1987) who found that nicotine followed the pH-partition hypothesis with IPM, but formed ion-pairs and deviated from the hypothesis with a number of other organic compounds (excised stratum corneum, n-butanol and n-octanol). It was suggested that this discrepancy was due to the different buffers employed in the two studies.

Assuming that deviation from Equation 2.4 at pH values not far removed from a compound's

pK_a (approximately 2 to 4 pH units) will indicate its readiness to form ion-pairs. A study using proxicromil (a compound whose ionic species readily forms ion-pairs with simple counter ions) showed that it has the ability to permeate biological membranes at physiological pHs that are well removed from its pK_a (Lee *et al.*, 1985). The possibility of ion-pair formation of *m*-azidopyrimethamine with an anion present in the skin membrane was stated as the reason for the contribution of the ionised species to the observed partition coefficient into hairless mouse skin (Baker *et al.*, 1990). The partition data provided values of 16.72 for P_u and 69.90 for P_i confirming the greater involvement of the ionised component.

The theory of ion-pair facilitated transport is that the ion-pair has a greater partition coefficient between the vehicle and the skin than the parent ionic compound (Figure 2.1). The ion-pair agent, for example a counter ion or substituted amine, dissolves in the membrane and is ionised at the outer surface where there is contact with the vehicle at pH 5. This gives it the ability to combine ionically with the anionic permeant. This ion-pair can then diffuse down its

Figure 2.1 A schematic diagram of the facilitated transport of ionisable drugs using an ion-pair carrier system. $:N\text{-}R_3$, represents an ion-pair agent and P, the permeate. (From Hadgraft *et al.*, 1985)

concentration gradient to the receptor site at pH 7.4. In this region, the counter ion deprotonates, releasing the permeate into the receptor phase.

From the wide range of results and interpretations of the transport of ionised compounds across absorption barriers, the *in vitro* diffusion of compounds can be significantly influenced not only by the physicochemical properties of the vehicle and the drug, but also by experimental parameters. The membrane type, the receiver phase composition and vehicle have significant effects upon the permeation profiles of methyl salicylate (Walkow and McGinity, 1987a) and salicylic acid (Walkow and McGinty, 1987b). Lee *et al.*, (1987) found that the ionic species of sodium salicylate in aqueous media did not permeate through hydrophobic silicone rubber, which contrasted to sodium salicylate in non-aqueous media, such as ethanol and dioxane, where the formation of ion-pairs enabled significant permeation.

2.1.2 Aims and Objectives

The intent of this study was to assess the effects of ionisation upon the transport of salicylic acid across artificial and biological membranes using a buffer of similar pH in both the receiver and donor phase. This enabled comparison with work using pH-gradients and assess whether permeation is due to unionised species alone, as predicted by the pH-partition hypothesis, or if ionised species have a significant role to play in transdermal permeation. The experimental protocols are based on work by Lofftson (1985) and are designed to test his hypothesis that, under certain conditions, increased ionisation of salicylic acid can promote topical delivery. Effects upon permeation were studied using equimolar and saturated solutions of salicylic acid and a comparison was made between a silastic rubber membrane and excised human epidermis. Silastic rubber is an artificial dimethyl-polysiloxane model membrane that has been shown to yield fluxes of salicylic acid close to that of human skin (Nacth and Yeung, 1985) and is widely used in permeation studies (Houk and Guy, 1988). Also under investigation were two methods to evaluate transmembrane transport. An automated sampling method using thermostated flow-through cells and a direct UV method of analysis was compared to manual sampling with an HPLC method of analysis.

2.2 Experimental

2.2.1 Materials

Whole skin samples were obtained from the abdominal region of human cadavers at *post mortem*. The majority of subcutaneous fat was removed and the samples were stored frozen (-20°C) for up to 8 weeks prior to removal of the epidermis. Separation of the dermis was achieved by defrosting the skin, mechanically removing any remaining subdermal fat using tweezers and sharp scissors and cutting into sections (approximately 2 cm x 2 cm). Each section was then submerged in water at 60°C for 60 seconds and the epidermis was gently teased away from the dermis using blunt forceps and floated on water at room temperature (Kligman and Christophers, 1963). Separated epidermis was then wrapped in aluminium foil and sealed in polythene until ready for use or stored at 2 to 8°C for up to 48 hours. Silicone rubber membrane (Silastic^{R} Medical Grade, 500-5, Dow Corning 0.005 inch thick) was cut into circular sections of approximately 2 cm in diameter and thoroughly rinsed in distilled water prior to use to remove the surface powder. Aqueous buffer solutions were prepared over the pH range 2.0 - 8.0 using McIlvaine's citrate-phosphate system (Appendix 1). All buffer solutions were preserved using 0.002% phenylmercuric nitrate. Final pH values were adjusted as nearly as possible to 2.10, 2.37, 2.75, 3.15, 3.53, 3.96, 4.35, 4.75, 5.13, 5.48, 5.85 and 8.17, using 2M sodium hydroxide or a 10% orthophosphoric acid solution as appropriate. Reagents used were sodium salicylate (BDH) and salicylic acid (BDH). All HPLC solvents were of Hypersolv grade.

2.2.2 Assay Procedure

2.2.2.1 High-performance Liquid Chromatography

The predominant method of analysis used in this study was high-performance liquid chromatography (HPLC). This versatile technique, which enables both quantitative and qualitative determinations to be undertaken, utilises the differential absorption and partition characteristics of compounds to separate molecules. HPLC is especially useful for the analytical separation of groups of closely related compounds such as structural analogues, degradation products, metabolites and enantiomers.

The HPLC instrumentation used throughout this study was constructed from a Pye Unicam

PU4010 dual-head reciprocating pump, a Rheodyne 7125 injection valve fitted with a 20µl loop and a PU4020 UV Detector equipped with an 8µl flow cell. The detector was operated at the specified wavelength of analysis, with a filter output of 1 and sensitivity in the range 0.04-0.32 AUFS. The results were analysed by peak area measurement using a Trivector Trio chromatography computing integrator. The mobile phase was degassed immediately before use and the stationary phase was a Hicrom 10 cm x 4.9 mm internal diameter stainless steel column packed with Spherisorb S5 ODS-1 5µm reversed-phase material, which was maintained at room temperature. The concentration of salicylic acid analysed was from 2 x 10^{-3} to 1 mg ml^{-1} and was diluted where appropriate with distilled water to an analytical range of 2 x 10^{-3} to 2 x 10^{-2} mg ml^{-1}. The mobile phase composition was methanol: orthophosphoric acid: tetrahydrofuran: water (50:0.01:3:47) at a final pH of 3.2 and delivered at a rate of 1 ml min. The retention time of salicylic acid under these conditions was 3.9 minutes.

2.2.2.2 Ultra-Violet Spectroscopic Analysis

All analyses were performed on a Perkin Elmer Lambda 5 UV/VIS Spectrophotometer (2 nm slit width, 0.05 second response, peak threshold 0.02A).All solutions were assayed at a wavelength of 269 nm and calibration curves were constructed for each appropriate pH over a concentration range 1.0 x 10^{-2} to 8.0 x 10^{-2} mg ml^{-1}.

2.2.2.3 Miscellaneous

All pH values were measured using a Gallenkamp refillable general purpose glass electrode attached to a Phillips PW 9409 two decimal place digital pH meter. All accurate weights were measured using a Sartorious 2001 MP2 four decimal place balance.

2.2.3 Donor Solutions.

Salicylic acid solutions were prepared by dissolving the appropriate quantity of sodium salicylate in McIlvaine's buffer (231.8 mg in 100 ml; pH range 2 to 5.4) (Appendix 1), preserved with phenylmercuric nitrate (0.002%). Any pH adjustment required was performed using 2M sodium hydroxide or 2M hydrochloric acid. Saturated suspensions were prepared

by dissolving an excess of salicylic acid in hot McIlvaine's buffer (Appendix 1) which was then allowed to cool in a water bath at 37°C. Further pH adjustment was performed using a 30% sodium hydroxide solution or 7M hydrochloric acid. Additional salicylic acid was added as appropriate to maintain a suspension and, after the final adjustment, the solution was left at 37°C for at least 24 h to equilibrate before use.

2.2.4 Solubility Determination

Saturated suspensions were prepared as described in section 2.2.3. These were assayed by filtering an aliquot of supernatant through a pre-saturated Whatman No 1 filter into a test tube previously warmed to 37°C. The filtrate was then immediately diluted with distilled water to an appropriate concentration (Within the range 4×10^{-3} to 2×10^{-1} mg ml^{-1}) before analysis by HPLC.

2.2.5 Permeation Procedure

Jacketed Franz-type diffusion cells were used throughout the study (Franz, 1975) and the diffusion barrier (epidermis or silastic) was mounted between the two chambers and secured with a spring-clamp. The ground glass surfaces of the cell that came into contact with the membrane were smeared with high vacuum silicone grease (BDH Prod 33135) to prevent leakage. The receptor cell was maintained at 37°C by means of a thermostatically controlled water-circulator. The donor cell and the sample were sealed to minimise evaporation. The receptor chamber was filled with a solution corresponding to the donor phase vehicle to minimise any effects due to a pH-gradient. The receptor phase was de-gassed by warming to 37°C and sonication to prevent the accumulation of air bubbles at the skin-receptor interface during the course of the experiment. The receptor volume was approximately 25 ml which was determined accurately by weight and the diffusional area of approximately 2 cm^2 was accurately measured for each cell using vernier callipers. The diffusional barrier was left to equilibrate with the receptor solution overnight at room temperature. The following morning the cell was warmed to 37°C and the receptor solution allowed to equilibrate. Any air that had accumulated at the skin-receptor interface was carefully removed by tilting the cell assembly and expelling the air *via* the sample port. An aliquot of 2 ml of the formulation under study was introduced into the donor compartment.

For analysis *via* HPLC, 70 µl samples were removed from the receptor compartment at regular time intervals during a total experiment duration of 420 min. After the withdrawal of each sample the receptor fluid was replenished with an aliquot of the drug-free vehicle. The cumulative mass of drug transported was calculated according to:

$$M_t[n] = V_r \cdot C[n] + V_s \cdot \sum_{m=1}^{n-1} C[m] \qquad \text{(Eq 2.5)}$$

Where $M_t[n]$ is the current, cumulative mass transported across the membrane at time t, $C[n]$ is the current concentration in the receptor medium and $\sum\{C[m]\}$ is the summed total of the previous measured concentrations $\{(m = 1)$ to $(n - 1)\}$. V_r is the volume of the receptor medium and V_s is the volume of the sample removed for analysis (Baker *et al.*, 1990)

UV analysis was performed using a continuous sampling system, consisting of a Perkin Elmer UV/VIS Lambda 5 Spectrophotometer with a six by six thermostated cell changer. 10mm path length quartz flow through cells were used. Samples were transported from the absorption cell assembly receptor compartment to the UV spectrophotometer via polyethylene tubing with an internal diameter of 0.863 mm and PVC 0.081 inch internal diameter standard manifold tubing. A Watson Marlow 202U/l peristaltic pump was used and the total volume of the flow-through section was approximately 5 ml. The receptor solution was circulated at a rate of approximately 4.5 ml min^{-1}.

2.2.6 Determination of the Results

The amount of drug penetration through the absorption barrier per unit area was calculated by taking into consideration the volume of the receptor solution and the area of membrane available for diffusion. The cumulative amount permeated per unit area was plotted against time and the linear section of the graph taken as the steady-state flux. Lag time was estimated by extrapolation from this line. The observed permeability coefficient (k_{obs}) was calculated by dividing the flux by the solubility of the salicylic acid in the test vehicle for suspensions and by the concentration of the permeate in the test vehicles for solutions. Each profile is expressed as the mean of two determinations.

2.3 Results and Discussion

2.3.1 Solubility of Salicylic Acid with Respect to pH at 37°C

The mean saturated solubility of salicylic acid, dependent upon pH, is summarised in Table 2.1. The solubility of salicylic acid increases with pH. This is as a consequence of the greater aqueous solubility of the ionised form and that weak acids such as salicylic acid become proportionately more ionised with increasing pH.

pH	Solubility (mmolar)	Ionisation (%)
0.08	16.32 (0.18)	0.13
1.84	22.34 (0.34)	6.75
2.35	25.58 (0.39)	18.99
2.80	36.97 (0.22)	39.78
3.14	53.79 (0.62)	59.11
3.43	103.20 (0.60)	73.81
3.73	164.70 (0.80)	84.90
4.17	522.20 (7.10)	93.93
4.71	1981.0 (5.9)	98.17

Table 2.1. Effect of pH on the saturated solubility of salicylic acid in aqueous buffer at 37°C (Values in parentheses are standard errors of the mean).

The relationship between pH and solubility can be derived from the Henderson-Hasselbalch equation and for a weak acid this can be defined as:

$$pH = pK_a + \log\left(\frac{S\text{-}S_o}{S_o}\right) \qquad \text{(Eq 2.6)}$$

Where S is the overall solubility of the compound and S_o is the solubility of the unionised species or the product's solubility in distilled water. This equation can be rearranged to:

$$S = S_o\left(\frac{[H_3O^+] + K_a}{[H_3O^+]}\right) \qquad \text{(Eq 2.7)}$$

Multiplying out gives

$$S = S_o + \frac{K_a.S_o}{[H_3O^+]} \qquad \text{(Eq 2.8)}$$

Therefore, the plot of solubility (S) versus $1/[H_3O^+]$ should give a straight line with a gradient of $K_a.S_o$ and an intercept of S_o. This graph for salicylic acid is shown in Figure 2.2 and the parameters and statistics are given in Table 2.2. The value for S_o of 11.86 m compares to a solubility of salicylic acid in distilled water of 15.74 mmolar (Budavari *et al.*, 1996) and the experimental value of pK_a at 2.54 corresponds with a literature value of 2.98 (Albert and Sergeant, 1984). The errors in the experimental values with respect to the literature could be a due to the presence of buffering components from the McIlvaine buffer (Appendix 1).

2.3.2 Permeation Studies

Permeation profiles were characterised by a steady-state period that lasted for 2 to 3 hours, after which the transport rate fell and gradually reached a plateau. The non-linear section was

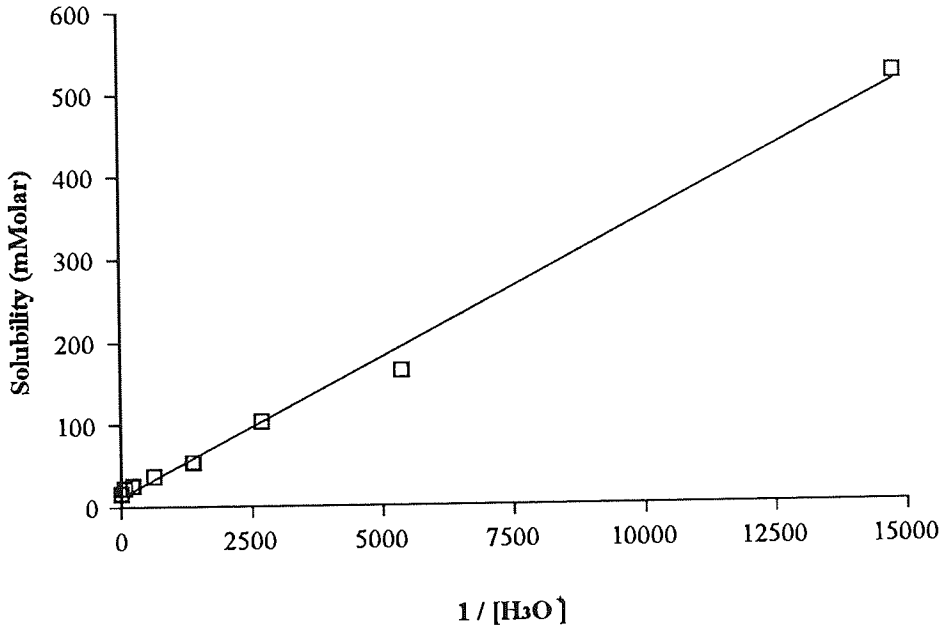

Figure 2.2 Plot of solubility versus $1/[H_3O^+]$ for salicylic acid at 37°C

Parameter	Value	± SE	± 95% CI	r
Intercept (S_0)(mM)	11.859	5.729	14.019	-
Slope (S_0K_a)	0.0337	1.010×10^{-3}	2.472×10^{-3}	0.9973
pK_a	2.54	-	-	-

Table 2.2 Calibration statistics and parameters for solubility versus $1/[H_30^+]$ for salicylic acid at 37°C in Figure 2.2 (SE, standard error; CI, confidence interval).

especially prominent with permeation from solutions (Figures 2.3 and 2.4). This effect could be explained by the gradual depletion of the donor phase and the gradual increase in salicylic acid concentration in the receptor phase. Steady-state flux is only constant when sink conditions apply. With solutions, there was a gradual lowering of the thermodynamic activity of the permeant. For example, the pH 0.44 and 2.27 donors through silastic rubber (Figure 2.3) transported 47% and 39% respectively of the donor salicylic acid in 420 minutes. With permeation profiles where this effect was especially prominent, only linear sections of the profile were used to calculate the steady-state flux (J_{obs}). Profiles using suspensions were more linear (Figures 2.9 and 2.10), but considering the concentrations of the saturated suspensions, the effect from "non -sink" conditions should have been minimal. As these profiles were not perfectly linear, reduction in thermodynamic activity could not have been the only parameter effecting the results. In later experiments, it was noted that despite the preparations to the receiver phase described in section 2.2.5, air was still accumulating at the skin-receptor interface. As a consequence, air was removed by introducing a piece of flexible polyethylene tubing down the sample port and working it up inside the cell to the skin receptor surface. The air was then gently drawn out using a syringe attached to the end of the polythene tubing. This technique, when undertaken at the beginning of the experiment and if necessary during the permeation run, produced a significant improvement in the steady-state flux profile.

For the UV method of analysis to be useful, the quantity of UV-interfering compounds that leach from the excised skin must be negligible. To study this, absorption cell assemblies were set up in triplicate with excised human epithelium as the barrier. This barrier was then left to equilibrate with McIlvaine buffer for 12 hours at 37°C. After this time a UV scan of the original buffer was compared to buffers that had been in contact with the skin. At approximately 260nm, McIlvaine's buffer began to absorb light and at wavelengths less than 240nm completely blanked out all transmitted UV light. Above 260 nm, UV-absorbable material leaching from the human epithelium was not detected above 0.03 absorption units. From these data, it was considered a suitable method of analysis for permeants through human epithelium excised by the method described in section 2.2.1 and where the wavelength of analysis is greater than 260 nm. Comparing the relative HPLC and UV assay methods, the UV flux results were consistently lower than those obtained by the HPLC method, although trends and permeation profiles were similar for both methods. The absorption of salicylic acid

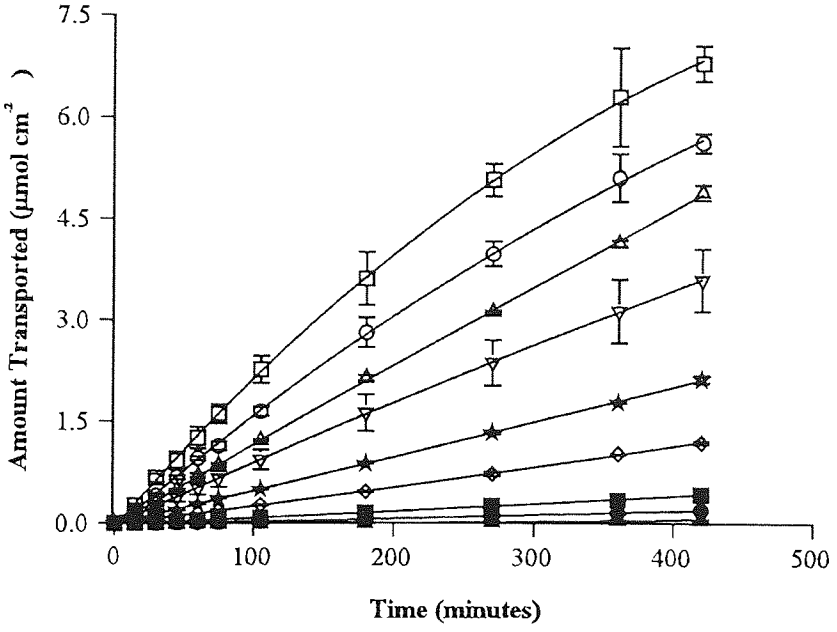

Figure 2.3 The effect of pH upon the permeation of salicylic acid from 14.48 mM aqueous solutions across silastic rubber membrane. (Each point is the mean of two determinations; error bars represent the range) [□, pH 0.44; ○, pH 2.27; △,pH 2.72; ▽, pH 3.13; ☆, pH 3.50; ◇, pH3.90; ■, pH 4.30 ; ● , pH4.71; ▲, pH 5.13]

pH	Flux ($\mu mol.cm^{-2}.hr^{-1}$)	k_{obs} ($cm.hr^{-1}$)	Lag Time (minutes)
0.44	1.3061 (6.46×10^{-2})	9.02×10^{-2} (4.46×10^{-3})	0.97 (2.86)
2.27	0.9685 (2.53×10^{-2})	6.69×10^{-2} (1.75×10^{-3})	2.50 (1.51)
2.72	0.7227 (1.30×10^{-2})	4.99×10^{-2} (8.98×10^{-4})	2.38 (1.04)
3.13	0.5470 (4.41×10^{-2})	3.78×10^{-2} (3.04×10^{-3})	1.69 (4.66)
3.50	0.3023 (4.70×10^{-3})	2.09×10^{-2} (3.24×10^{-4})	2.23 (0.91)
3.90	0.1683 (3.70×10^{-3})	1.16×10^{-2} (2.55×10^{-4})	3.92 (1.28)
4.30	0.0657 (6.58×10^{-4})	4.54×10^{-3} (4.45×10^{-5})	*11.08 (1.99)
4.71	0.0321 (6.59×10^{-4})	2.22×10^{-3} (4.55×10^{-5})	*17.25 (4.07)
5.13	0.0123 (5.51×10^{-4})	8.49×10^{-4} (3.80×10^{-5})	*35.46 (8.88)

Table 2.3 Permeation data for salicylic acid across silastic rubber from 14.48 mM solutions. * The long lag times recorded for these pH values are most likely to be artefacts caused by the particularly low levels of detection throughout these series of results. (Values in parentheses represent the standard error)

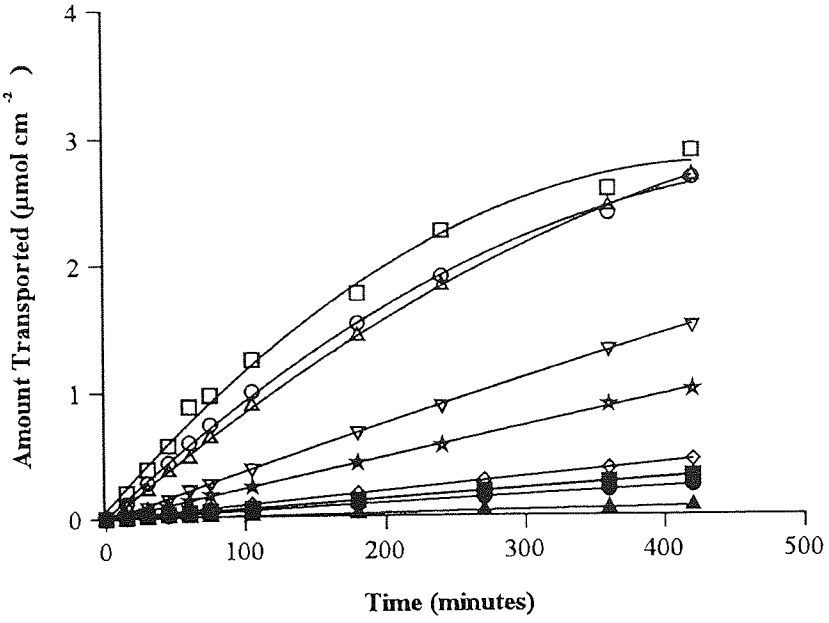

Figure 2.4 The effect of pH upon the permeation of salicylic acid from 14.48 mM aqueous solutions across human skin. (Each point is the mean of two determinations; error bars omitted for clarity; the range of all points were within 20% of the mean.) [□, pH 2.10;○, pH 2.27;△, pH2.72;▽, pH 3.13;☆, pH3.50;◇, pH 3.90;■, pH 4.30;●, pH 4.71;▲, pH5.31]

pH	Flux ($\mu mol.cm^{-2}.hr^{-1}$)	k_{obs} ($cm.hr^{-1}$)	Lag Time (minutes)
2.10	0.7216 (5.68×10^{-2})	4.98×10^{-2} (3.92×10^{-2})	2.56 (4.92)
2.27	0.5940 (1.61×10^{-2})	4.10×10^{-2} (1.11×10^{-3})	1.02 (1.70)
2.72	0.5366 (9.18×10^{-3})	3.70×10^{-2} (6.34×10^{-4})	4.39 (1.07)
3.13	0.2466 (6.18×10^{-3})	1.70×10^{-2} (4.27×10^{-4})	6.68 (1.56)
3.50	0.1556 (5.04×10^{-3})	1.07×10^{-2} (3.48×10^{-4})	5.04 (2.02)
3.90	0.0688 (1.43×10^{-3})	4.75×10^{-3} (9.87×10^{-5})	4.02 (1.29)
4.30	0.0496 (1.03×10^{-3})	3.42×10^{-3} (7.11×10^{-7})	4.04 (0.93)
4.71	0.0364 (1.66×10^{-5})	2.51×10^{-3} (1.14×10^{-6})	5.57 (3.74)
5.13	0.0118 (1.24×10^{-5})	8.17×10^{-4} (8.56×10^{-7})	9.78 (5.92)

Table 2.4 Permeation data for salicylic acid across human skin from 14.48mM solutions. (values in parentheses represent the standard error)

into the PVC tubing used in the UV method was a possible source of error. Also, receiver solution had to be pumped from the absorption cell to the detector which could cause a delay, resulting in relatively lower results at a particular time interval. Although, if this effect was significant, it would be anticipated that lag times would be longer with the UV data, which was not the case. The UV method has the advantage of being automated and can be run continuously, if necessary for periods up to a week. With alternative compounds, detection levels and low absorbance may be a problem and for analytical wavelengths below than 260 nm, an alternative buffer agent will be necessary. The automated system takes longer to set up than the HPLC system, but it is a useful method for comparative permeation work. This equipment is closely related to a standard tablet dissolution system and will be readily available in many laboratories. It could be used, especially with silastic membrane, as a routine test system to quality control the delivery from topical formulations. For the reasons expressed above, the HPLC results represented the "true" flux and as the profiles from UV and HPLC data were similar, only the HPLC data are presented in this study.

2.3.2.1 *The Effect of pH on the Transport of Salicylic Acid from Aqueous Solutions Across Silastic Rubber.*

The permeation profiles demonstrating the effect of pH on the permeation of salicylic acid from aqueous solutions across silastic membranes are recorded in Figure 2.3. Steady-state fluxes, permeability coefficients and lag times derived from the linear sections of these permeation profiles are summarised in Table 2.3. The lag times were not significant, and imply that the thickness of silastic used offers low resistance to diffusion. Permeability coefficients and flux both increase with decreasing pH. The plot of steady-state flux against pH (Figure 2.5) shows the expected sigmoidal curve which provides a linear relationship between the fraction unionised (1-α) and flux (Figure 2.6).

$$J_{obs} = 0.0124\ (0.1241)\alpha + 1.2154\ (0.0472)\ (1-\alpha) \qquad (r = 0.9947) \qquad \text{(Eq 2.9)}$$

Where (1-α) is the fraction unionised, α is the fraction ionised and the values in parentheses represent the standard errors. From Equation 2.9 (see Equation 2.1), J_i is 0.0124 µmol cm^{-2} hr^{-1}, J_U is 1.2154 µmol cm^{-2} hr^{-1}, and the predicted steady-state flux for a 14.48 mM solution where all the drug is in the undissociated form and there is no contribution from the ion form,

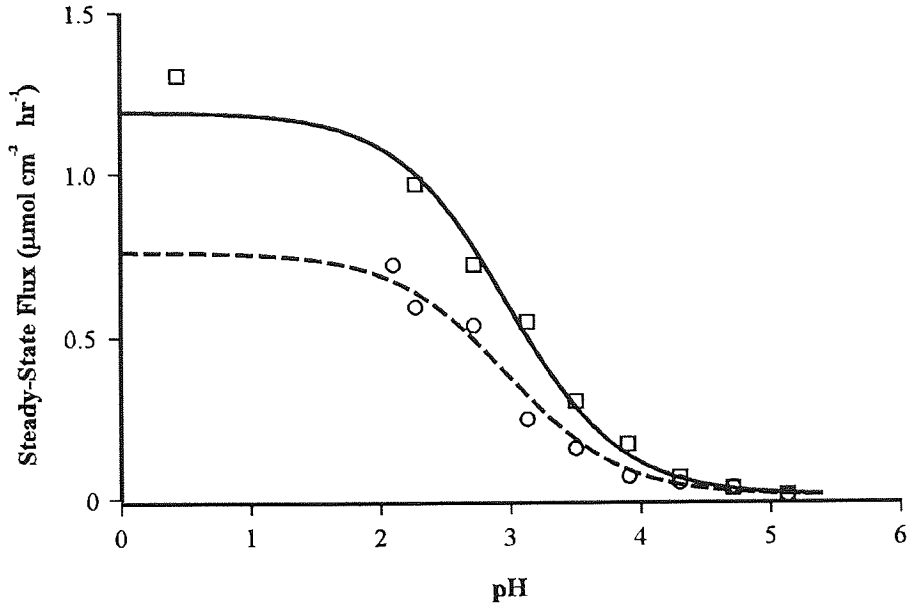

Figure 2.5 The effect of pH upon the steady-state flux of salicylic acid from 14.48 mM solutions across (□) silastic rubber membrane and (○) human skin. (Line represents $J_{obs} = \alpha J_i + (1 - \alpha) J_u$; see Equation 2.9)

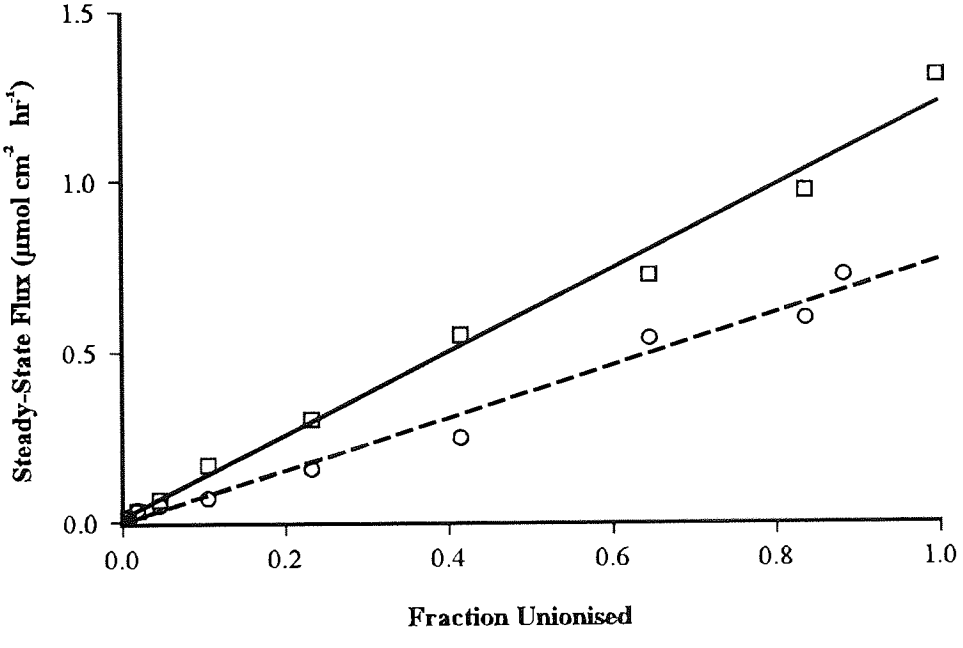

Figure 2.6 Plot of the steady-state flux of salicylic acid across (□) silastic rubber membrane and (○) human skin from solutions of differing pH, as a function of fraction salicylic acid unionised.

is 1.2278 μmol cm^{-2} hr^{-1}. From Equation 1.6, J_{obs} = (D.P.C)/δ, the apparent steady-state flux is proportional to the concentration of the permeating species. As the total apparent steady-state flux may be dependent upon the flux of both the ionised and unionised species (Equation 2.1) thus Equation 1.6 can be written as:

$$J_{obs} = \frac{(1-\alpha).P_u.D_u.C_u + \alpha.P_i.D_i.C_i}{\delta} \qquad \text{(Eq 2.10)}$$

Where subscripts u and i refer to ionised and unionised molecules respectively. If the pH-partition theory holds true under the experimental conditions quoted for this set of permeation profiles, then the ionic contribution should be negligible ($D_u.P_u \gg D_i.P_i$) then this approximates to:

$$J_{obs} = \frac{(1-\alpha)P_u.D_u.C_u}{\delta} = (1-\alpha)\ k_{obs}.C_u \qquad \text{(Eq 2.11)}$$

Thus, the linear relationship between (1-α) and J_{obs} reinforces evidence that the unionised species is solely responsible for the permeation of salicylic acid across these membranes. When applicable, the relative rates of percutaneous absorption of the unionised (J_u)and ionised (J_i) forms of a permeant may be estimated from Equation 2.2 where a plot of J_{obs}/α against (1-α)/α gives (Figure 2.7):

$$J_{obs}/\alpha = 9.44 \times 10^{-3} (6.86 \times 10^{-3}) + 1.1945\ (3.01 \times 10^{-2})\ (1-\alpha)/\alpha$$
$$(r = 0.9997) \qquad \text{(Eq 2.12)}$$

The low value for the intercept (J_i, 9.44×10^{-3} μmol cm^{-2} hr^{-1}) is further evidence that the ionised form's influence on flux is negligible. This further supports the validity of the pH-partition hypothesis in this system. The values of J_u and J_i can be transposed into Equation 2.1 to give the theoretical values of J_{obs} with respect to pH. These theoretical values for J_{obs} are plotted as the lines in Figure 2.5 and show the good correlation of the data with the theoretical plots. Equation 2.12 predicts the flux of salicylic acid from a 14.48 mM solution at a pH where all the drug is totally ionised as 1.1945 μmol cm^{-2} hr^{-1}. This value and that from Equation 2.9 are lower than that obtained experimentally at pH 0.44, but this may be a consequence of the extreme pH of the solution.

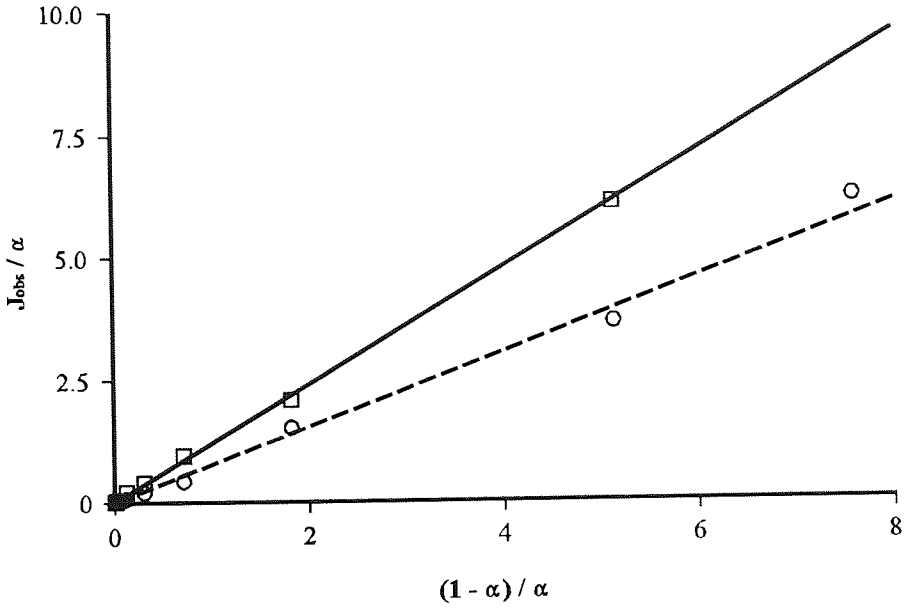

Figure 2.7 Plot of the observed flux of salicylic acid (J_{obs}) / α from aqueous solutions as a function of (1-α) / α, from which J_u (slope) and J_i (intercept) can be determined. Comparison of results derived from (○) human skin (□) silastic rubber.

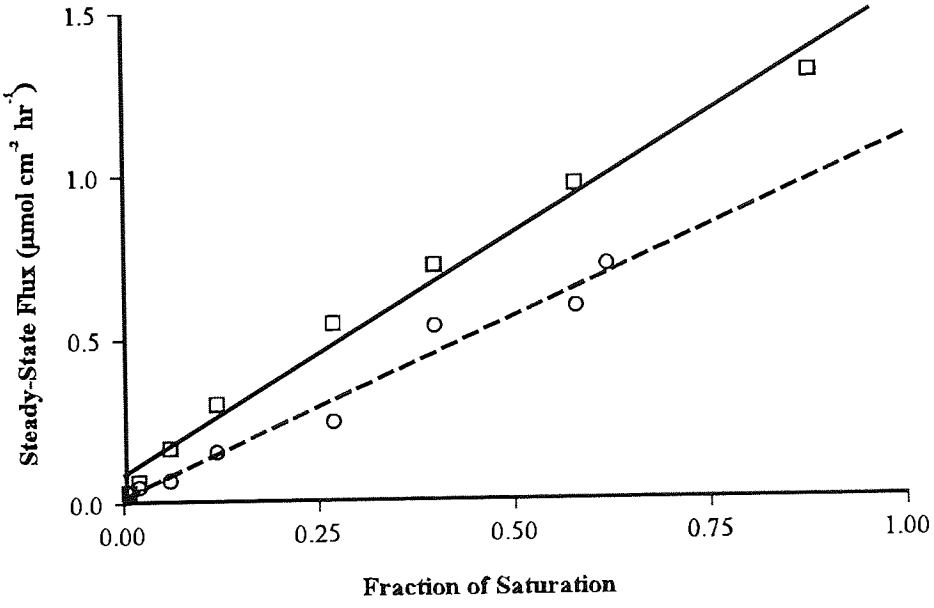

Figure 2.8 Plot of the steady-state flux of salicylic acid across (□) silastic rubber membrane and (○) human skin from solutions of differing pH, as a function of the fraction of saturation.

With increasing pH, the solubility of salicylic acid increased. As this study was performed using equimolar solutions, the thermodynamic effectiveness of the permeants penetration will be reduced with increasing pH. This effect will be relative to the degree of saturation and a plot of flux against the degree of saturation should give a linear relationship (Figure 2.8).

$$J_{obs} = 0.0866\ (0.0296) + 1.4635\ (0.0717)\ FS \qquad (r = 0.9915) \qquad (Eq\ 2.13)$$

Where FS is the fraction of saturation and is calculated by dividing the solution strength by the concentration of a saturated solution at a similar pH. Values in parentheses represent the standard error. This predicts a maximum flux (J_{max}) of 1.5743 μmol cm^{-2} hr^{-1} for a completely saturated solution. The linear relationship between J_{obs} and FS would be anticipated following a similar relationship between J_{obs} and the fraction unionised. The fraction unionised and FS are directly proportional with a plot of FS against fraction unionised giving a straight line of gradient equal to C/S_0, where S_o is the solubility of the fraction unionised and C is the concentration of the donor solution.

2.3.2.2 *The Effect of pH on the Transport of Salicylic Acid from Aqueous solutions Across Human Skin*

To compare the permeation of salicylic acid across silastic rubber to that of human skin, a similar series of permeation profiles from aqueous solutions were performed upon human skin. The permeation profiles with respect to pH are illustrated in Figure 2.4. The steady-state fluxes, permeability coefficients and lag times derived from these plots are summarised in Table 2.4. The flux and permeability coefficients increase with decreasing pH, whereas the lag times increase with increasing pH. Generally, the lag time for salicylic acid permeation through human skin was longer compared with silastic rubber, although this difference was not significant (P=0.105). This contrasts with the steady-state flux, which was greater for silastic rubber, where the comparative fluxes over the pH range 2.27 to 5.13 were on average 1.60 times greater when compared with human skin (Tables 2.3 and 2.4).

The permeation profiles from skin of different sources were normalised by using a donor solution of similar pH with each group of experiments from each skin source. The steady-state

flux at each pH was then normalised to the average flux of this common donor. Variation was most likely to result from samples being taken from male and female donors of different ages. In extreme cases, variations in flux of 10 times were observed.

The plot of steady-state flux against pH reveals a curve of similar character to that for silastic rubber (Figure 2.5). A plot of flux as a function of the fraction of drug in the unionised form (Figure 2.6) produces the following equation:

$$J_{obs} = -9.90 \times 10^{-4} (0.0205)\alpha + 0.7642 (0.0421)(1-\alpha) \quad (r = 0.9895) \quad \text{(Eq 2.14)}$$

This predicts a flux of 0.7632 μmol cm^{-2} hr^{-1} from a 14.48 mM solution at a pH where all the drug is in the undissociated form. A plot of k_{obs}/α against $(1-\alpha)/\alpha$ for the human skin data provides a linear relationship (Figure 2.7) with the equation:

$$J_{obs}/\alpha = 9.16 \times 10^{-3} (1.19 \times 10^{-2}) + 0.7599 (0.0290) (1 - \alpha)/\alpha$$
$$(r = 0.9970) \quad \text{(Eq 2.15)}$$

The low value of the intercept suggests that the ionised form does not penetrate the stratum corneum in significant quantities. A flux of 0.7599 μmol cm^{-2} hr^{-1} is predicted from a 14.48 mM solution at a pH where the drug is totally unionised. The flux obtained experimentally at pH 2.1, which represents 90.32% unionised is 0.7691 μmol cm^{-2} hr^{-1}. This correlates very closely with that predicted.

The plot of flux against the fraction of saturation gives the following relationship: (Figure 2.8)

$$J_{obs} = 0.0183 (0.0267) + 1.0896 (0.0773) FS \qquad (r = 0.9852) \quad \text{(Eq 2.16)}$$

From these data, a flux of 1.1079 μmol cm^{-2} hr^{-1} can be estimated for a completely saturated solution. Evaluating the effects of pH upon the flux of compounds across membranes from solutions encompasses a number of variables. Of these, the degree of ionisation and the degree of saturation differ as a consequence of pH. The evidence suggests that the change in flux is a direct consequence of pH, which controls the concentration of the undissociated species. To maintain the concentration of undissociated molecules and the degree of saturation as

constants, it would be appropriate to perform an analogous series of penetration profiles using saturated solutions. This should elucidate the true effect of pH upon flux and help confirm the variable responsible for the rate of transport across absorption barriers.

2.3.2.3 *The Effect of pH on the Transport of Salicylic Acid from Saturated Aqueous Suspensions Across Silastic Rubber*

Permeation data from aqueous suspensions of salicylic acid across silastic rubber are summarised in Table 2.5, the plots of the amount permeated against time (Figure 2.9) and the steady-state flux against pH demonstrate that permeation is independent of pH (Figure 2.11). The mean steady-state flux across silastic rubber from suspensions was 1.9375 ± 0.0661(SEM) μmol cm^{-2} hr^{-1}. This value is somewhat higher than that forecast from the solution data. This may possibly be due to reduced drive in the solution experiments due to the continual depletion of the donor phase, although this effect would be expected to be minimal for initial rates. Possibly, the linearity is not maintained at extremes of pH as, at very high concentrations of ionised molecules, their relatively low rates of permeation may become significant. This under-estimation could be expected considering data for azidoprofen (Naik, 1990) and ibuprofen (Irwin *et.al.*, 1990) where solution data predicted a flux of 1.1527 μmol cm^{-2} hr^{-1} for saturated suspensions across silastic rubber and 0.0161 μmol cm^{-2} hr^{-1} across hairless mouse skin respectively. This compares with experimentally obtained values of 2.1667 μmol $cm^{-2}hr^{-1}$ for azidoprofen and 0.095 μmol cm^{-2} hr^{-1} for ibuprofen.

From Equation 2.7 ($S = S_o([H_3O^+] + K_a)/[H_3O^+]$), a theoretical profile for solubility versus pH for salicylic acid is shown in Figure 2.13. S_o is constant throughout the pH range and is dependent upon the solubility of the unionised molecule. The overall increase in solubility is related to the solubility of the ionised species and the degree of ionisation is related to the pH of the vehicle. As, according to the pH-partition theory, the steady-state flux is dependent upon the concentration of the unionised molecule, J_{obs} remains constant throughout the pH range.

The overall mean lag time of 0.89 ± 0.25 (SEM) minutes serve to emphasise the low resistance to diffusion of the silastic rubber membrane. The relative permeability coefficient decreased with increasing pH. This is because k_{obs} is calculated by dividing J_{obs} by the overall solubility

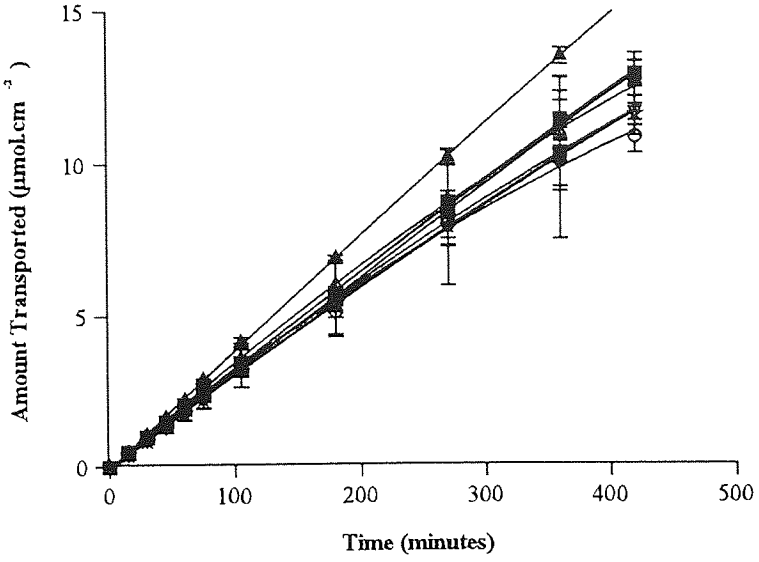

Figure 2.9 The effect of pH upon the permeation of salicylic acid from saturated aqueous suspensions across silastic rubber membranes. (Each point is the mean of two determinations; error bars represent the range) [□, pH 0.08; ○, pH 1.84; △, pH 2.35;▽,pH 2.80;☆, pH3.14;◇, pH 3.43;■, pH 3.73;●,pH 4.17;▲,pH 4.71]

pH	Flux (μmol cm^{-2} hr^{-1})	k_{obs} (cm hr^{-1})	Lag Time (minutes)
0.08	1.8012 (0.0637)	0.1104 (3.90 x 10^{-3})	0.00 (2.04)
1.84	1.9125 (0.0269)	0.0856 (1.20 x 10^{-3})	0.51 (0.81)
2.35	2.0835 (0.0442)	0.0814 (1.73 x 10^{-3})	1.16 (1.23)
2.80	1.8300 (0.0528)	0.0495 (1.43 x 10^{-4})	0.60 (1.67)
3.14	1.8246 (0.0345)	0.0339 (6.41 x 10^{-4})	1.47 (1.09)
3.45	1.8966 (0.0233)	0.0183 (2.25 x 10^{-4})	1.40 (0.71)
3.73	1.9452 (0.0482)	0.0118 (2.94 x 10^{-4})	0.00 (1.43)
4.17	1.9363 (0.0423)	0.0037 (8.03 x 10^{-5})	0.56 (1.26)
4.71	2.3798 (0.0438)	0.0012 (2.15 x 10^{-5})	2.39 (1.06)
Mean	*1.9566	-	0.90
Standard Deveation	*0.1779	-	0.78

Table 2.5 Permeation data for salicylic acid across silastic rubber from saturated suspensions. (Values in parentheses represent the standard error)
*Mean and standard deviation of flux without pH 4.71 outlier value are 1.9037 and 0.0906 respectively

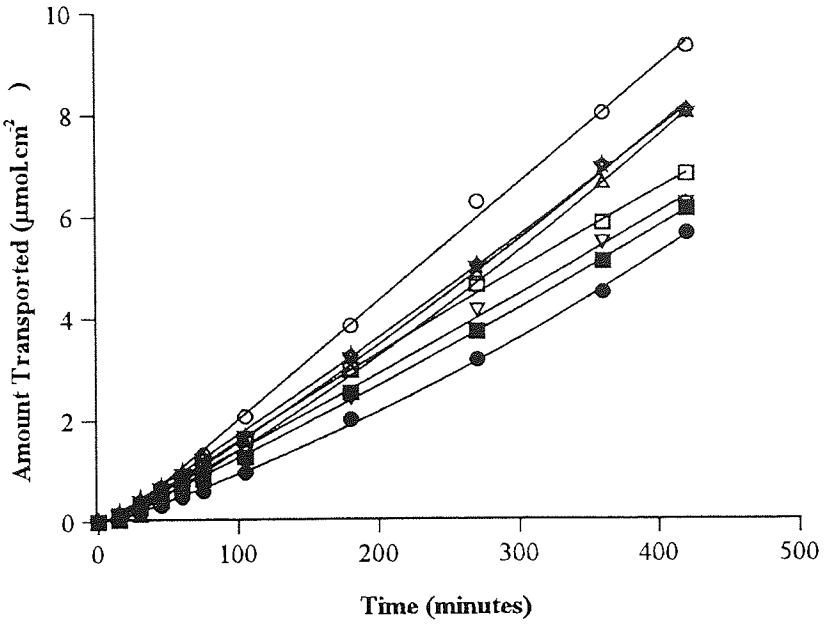

Figure 2.10 The effect of pH upon the permeation of salicylic acid from saturated aqueous suspensions across human skin. (Each point is the mean of two determinations; error bars omitted for clarity; the range of all points were within 20% of the means.) [□, pH 1.84 ; ○, pH 2.35 ; △, pH 2.80 ; ▽, pH 3.14 ; ☆, pH 3.43 ; ◇, pH 3.73 ; ■, pH 4.17 ; ●, pH 4.71]

pH	Flux ($\mu mol.cm^{-2}.hr^{-1}$)	k_{obs} ($cm.hr^{-1}$)	Lag Time (minutes)
1.84	1.0114 (0.0188)	4.53×10^{-2} (8.42×10^{-4})	7.73 (4.34)
2.35	1.4181 (0.0240)	5.54×10^{-2} (9.38×10^{-4})	17.53 (3.95)
2.80	1.2198 (0.0129)	3.29×10^{-2} (3.48×10^{-4})	30.53 (2.46)
3.14	0.9348 (0.0171)	1.74×10^{-2} (3.18×10^{-4})	10.33 (4.26)
3.45	1.1945 (0.0151)	1.16×10^{-2} (1.47×10^{-4})	13.16 (2.95)
3.73	1.2439 (0.0208)	6.10×10^{-3} (1.27×10^{-4})	26.51 (3.89)
4.17	0.9037 (0.0109)	1.70×10^{-3} (2.05×10^{-5})	16.74 (2.80)
4.71	0.8408 (0.0218)	3.89×10^{-4} (1.01×10^{-5})	31.04 (6.03)
Mean	1.0959	-	19.20
Standard Deviation	0.2021	-	9.083

Table 2.6 Permeation data for salicylic acid across human skin from saturated suspensions. (Values in parentheses represent the standard error)

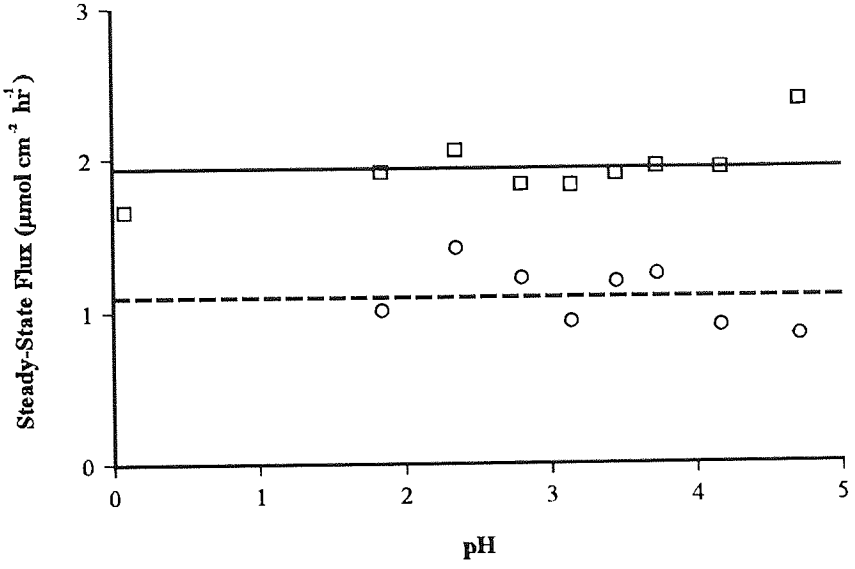

Figure 2.11 The effect of pH on the steady-state flux of salicylic acid from saturated aqueous suspensions across (□) silastic rubber membrane and (○) human skin.

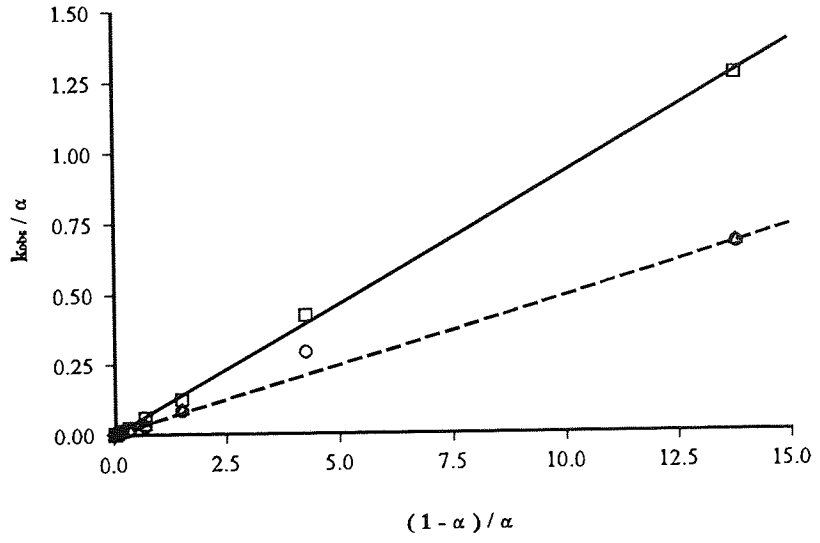

Figure 2.12 Plot of the observed permeability coefficient (k_{obs}) / α for salicylic acid from saturated aqueous suspensions as a function of (1-α)/α, from which k_u (slope) and k_i (intercept) can be determined. Comparison of results derived from (○) human skin and (□) silastic rubber.

of salicylic acid. As the solubility increases with pH due to the ionised species of salicylic acid, which does not contribute to the steady-state flux, k_{obs} decreases with increasing pH. If J_{obs}

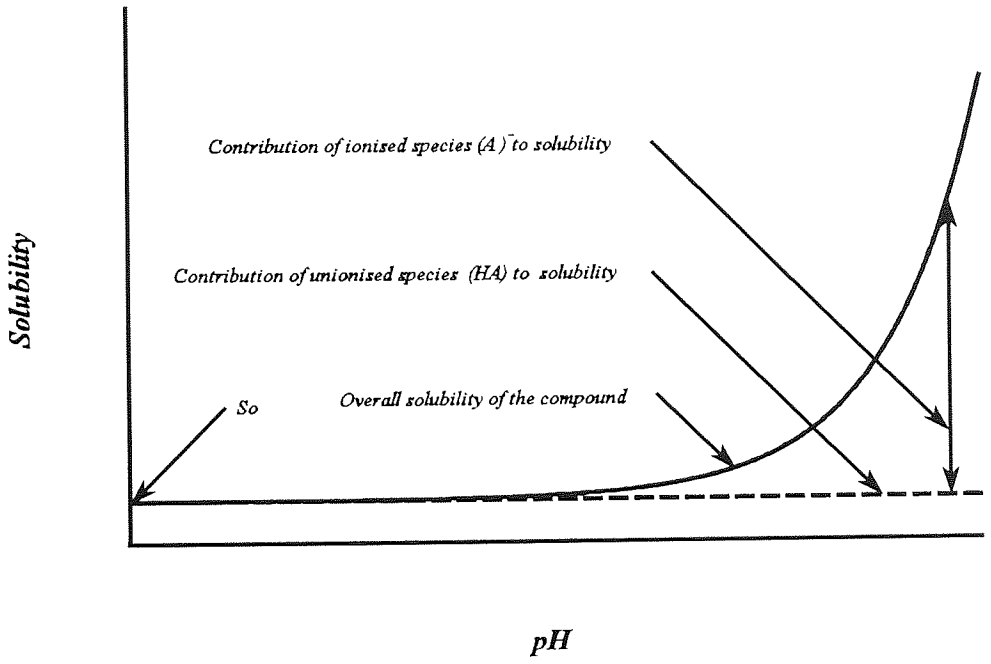

Figure 2.13 A theoretical plot showing the relationship between the solubility of an ionogenic compound and pH with the relative contributions of the ionised and unionised species.

was divided by S_o the solubility of the permeating unionised species, then the observed permeability coefficient would remain constant throughout the pH range examined. The poor skin permeability of the ionised species is reinforced by the plot of k_{obs}/α against $(1 - \alpha)/\alpha$ which provides a linear relationship with the equation.

$$k_{obs}/\alpha = 1.89 \times 10^{-3} (5.82 \times 10^{-3}) + 0.0925 (1.13 \times 10^{-3})(1 - \alpha)/\alpha \quad (r = 0.9995) \qquad \text{(Eq 2.17)}$$

The small intercept suggests the ionised form has a negligible permeability coefficient and increases evidence that the ionised molecule does not contribute to the overall flux. The values of k_u (0.0925 cm hr^{-1})and k_i (1.89×10^{-3} cm hr^{-1}) obtained from Equation 2.17 provide the information for the theoretical lines plotted in Figure 2.14, where the effect pH has upon k_{obs} is shown.

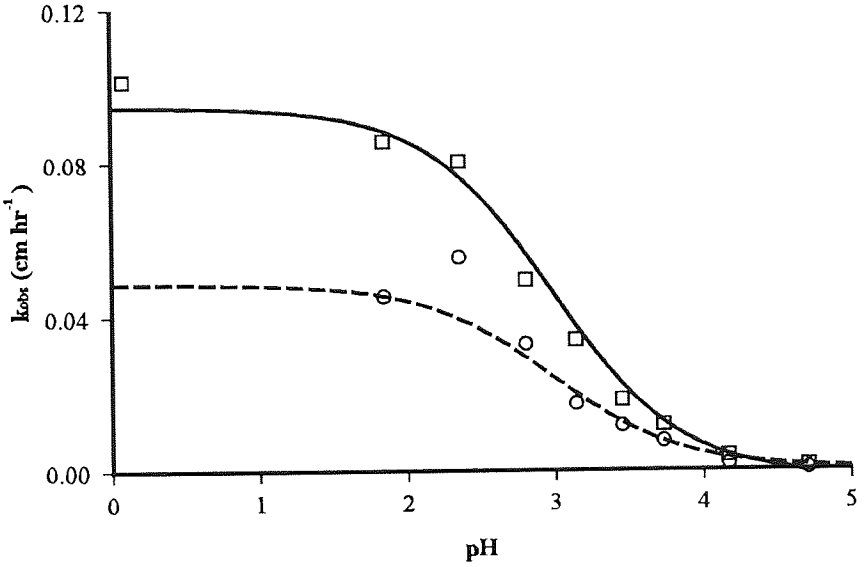

Figure 2.14 The effect of pH upon the observed permeability coefficient (k_{obs}) of salicylic acid from saturated aqueous suspensions across (□) silastic rubber and (○) human skin. (Line represented by $k_{obs} / \alpha = k_i + (1 - \alpha)k_u / \alpha$; see Equation 2.17, 2.18)

2.3.2.4 *The Effect of pH on the Transport of Salicylic Acid from Saturated Aqueous Suspensions Across Human Skin*

The permeation data for saturated suspensions of salicylic acid across human skin are summarised in Table 2.6 and Figure 2.10. These show that the penetration rates of salicylic acid from these suspensions do not vary significantly as pH increases from pH 1.84 to 4.71 and provide a mean flux of 1.0959 ± 0.0714 (SEM) μmol cm^{-2} hr^{-1}. Although this value is only 56% of those obtained from silastic rubber, the effect of pH on the fraction unionised follows similar profiles. The steady-state flux is independent of pH (Figures 2.11) and k_{obs} follows a similar sigmoidal relationship with pH (Figure 2.14). While silastic rubber did not demonstrate a significant lag time, the mean lag time with human skin was 19.20 ± 3.21 (SEM) minutes. The plot of k_{obs}/α against $(1 - \alpha)$ (Figure 2.12) shows a linear relationship where:

$$k_{obs}/\alpha = 2.92 \times 10^{-4} (1.93 \times 10^{-3}) + 0.486 (3.66 \times 10^{-4}) (1 - \alpha)/\alpha \quad (r = 0.9842) \qquad \text{(Eq 2.18)}$$

The values of k_u (0.486 cm hr^{-1})and k_i (2.92×10^{-4}) obtained from this relationship were used for the theoretical lines drawn in Figure 2.14.

2.4 Summary

This series of permeation profiles was performed to investigate the correlation between pH and its influence upon the salicylic acid flux from solutions and suspensions across excised human epithelium and silastic rubber. These experiments were deliberately set up without a pH-gradient to assess the effect this would have upon the permeation of ionisable compounds. Under these conditions, permeation followed the pH-partition theory, the transmembrane permeation was essentially due to the unionised species and the contribution of the ionised species was negligible. The results comparing flux through human skin and silastic rubber show that the trends and profiles were similar. The rates of permeation through human skin were lower than that observed through silastic rubber. For solution data, the average steady-state flux (J_{obs}) through human skin was 70% of the rate through of silastic rubber and for suspensions, the steady state flux through human skin was 56% that of silastic rubber. This compares well with previous data (Nacht and Yeung, 1985) where salicylic acid from saturated solutions was found to permeate through excised human skin at rates 58% of those recorded through silastic rubber. The majority of permeation investigations are of a comparative nature. Therefore, the results obtained in this study would indicate that silastic rubber is a useful tool to investigate and optimise vehicle pHs of topical salicylic acid formulations, though the absolute permeation values of the two barriers were not identical.

The results from this study demonstrate that the topical delivery of a model ionogenic permeant, salicylic acid, obeys the pH-partition theory and transdermal permeation is due to the unionised species. This is true over a pH range of 0.08 to 4.17 for silastic rubber and pH 1.84 to 4.71 for human skin. The contribution to flux from the ionised species is insignificant and does not have a role in transdermal delivery. These results refute those of Loftsson (1985) who proposed that under certain conditions increased ionisation can promote topical delivery of salicylic acid. This was based upon the observation of increasing flux with higher donor pH. The permeation profiles and the effect of pH on the overall flux of salicylic acid from Loftsson (1985) are shown in Figures 2.15 and 2.16.

Figure 2.15 The permeation profiles of salicylic acid through hairless mouse skin from aqueous suspensions. pH of the donor phase, ○ pH 4.73; □, 3.97; △, 3.20. (From Loftsson, 1985)

Figure 2.16 The effect of pH on the overall flux of salicylic acid through hairless mouse skin. (From Loftsson, 1985).

Considering Loftsson's results in detail there are several factors that might have contributed to the different conclusions.

- The receiver phase remained at pH 7.2 irrespective of the pH of the donor phase. This pH-gradient may have facilitated an ion-pair transport system.

- The donor phase was a saturated solution of salicylic acid, some sodium salicylate, buffer and a small amount of sodium chloride. Using this composition, the salicylic acid was unlikely to form an ion-pair with any of the donor phase components, but it may permeate as an ion-pair with a counter anion present in the skin membrane.

- Salicylic acid in its unionised form has a high partition coefficient into oily phases. The partition coefficient of the unionised form (P_u) into IPM is 28.26 (Table 4.1) and the partition coefficient of salicylic acid into IPM at pH 3.96 is 2.20. This would imply that salicylic acid should partition effectively through the stratum corneum. Results discussed in section 2.3 show that salicylic acid can be detected permeating across human skin after 15 minutes and a steady-state permeation is achieved after 45 minutes. The assessment of the permeation profile from 3 to 12 hours seems an unnecessarily long time to leave the salicylic acid in contact with the skin. Especially as hairless mouse skin has been shown to be more permeable than human skin with acetyl salicylic acid (Bronaugh *et al.*, 1982) During these long periods the absorption profiles could have been influenced by salicylic acid's keratolytic effect upon the stratum corneum.

- It is difficult to assess the effect of pH upon flux from only 3 pH points. It would have been interesting to observe whether this profile continued at even higher pH's, for example 6 and 7.

Considering these criticisms of Loftsson's work and the results demonstrated in section 2.3 the conclusion remains that the ionic species does not contribute to transdermal flux, which is almost exclusively due to the unionised species.

CHAPTER THREE

PERCUTANEOUS ABSORPTION OF SALICYLIC ACID

EFFECT OF ABSORPTION ENHANCERS ON TRANSPORT THROUGH SILASTIC RUBBER AND HUMAN SKIN

3.1 Introduction

3.1.1 Mechanisms of Action of Absorption Enhancers

The impervious nature of the stratum corneum presents major difficulties utilising the advantages of the skin as a drug administration port. The potential advantages of avoiding first-pass intestinal and hepatic metabolism, reduced side-effects from local application and easy termination of drug administration are limited by poor drug flux through the stratum corneum (Barry, 1983; Guy and Hadgraft, 1985). An increasingly popular solution to this problem is the use of absorption enhancers to increase the efficacy of topically applied local and systemic drugs. Examples of commercially available topical agents with potential absorption enhancers, detailed in parenthesis, included in their formulations are; Ibugel® (IMS, propylene glycol); Emugel® (isopropanol, propylene glycol, caprylic/capric acid fatty alcohol ester); Estraderm TTS® patch (ethanol); Feldene Gel® (ethyl alcohol, propylene glycol); Topicycline® (n-decylmethyl sulphoxide in 40% ethanol) (ABPI, 1996). Absorption enhancers ideally possess the sole property of reversibly reducing the barrier resistance of the stratum corneum, allowing the drug to reach the living tissues at a greater rate, without the enhancer damaging any cells (Barry, 1983). The mechanism of action of these absorption enhancers is not clearly understood. Increased knowledge of these mechanisms would enable the rationalisation and optimisation of their structural design (Lien and Tong, 1973; Guy and Hadgraft, 1989c; Hadgraft, 1991; Michniak *et al.*, 1995).

There are two essential approaches to potentiating the transdermal absorption of drugs. The first is to increase the driving force for drug diffusion and the second is to reduce the diffusional resistance of the skin. Chemicals that are able to increase the skin permeability by either or both of these mechanisms are referred to as "skin permeation enhancers". The precise mechanisms of action of absorption enhancers is still under investigation and in order to discuss them in further detail, it is essential to categorise these mechanisms into groups.

1. Thermodynamic effect of the permeant in its vehicle

In Chapter 1, Equation 1.13, skin permeability is expressed in terms of the permeability coefficient (k_p) which is directly proportional to the partition coefficient (P). The partition coefficient is a thermodynamic term which governs the flux of a drug molecule through the

skin and is determined by the solubility behaviour of the diffusants in the donor solution and in the skin. Therefore, regular solution theory could be applied to interpret the partition coefficient and thereby predict the drug's skin permeability under the influence of skin permeation enhancers (Liron and Cohen, 1984).

By determining the solubility of theophylline in various potential skin enhancers and comparing the calculated partition coefficients with experimentally determined skin permeabilities, it was found that the permeability coefficients from saturated solutions were inversely proportional to theophylline solubility in the skin permeation enhancers (Sloan *et al.*, 1986). A similar effect was found with Azidoprofen, which becomes more soluble with increasing propylene glycol concentration. The permeability coefficient for Azidoprofen from saturated suspensions across hairless mouse skin decreased with increasing concentrations of propylene glycol in the donor solution (Naik *et al.*, 1993).

If the absorption of drugs is proportional to the thermodynamic activity of the drug in the vehicle (Equation 1.15) and the thermodynamic activity can be expressed in terms of relative solubility (thermodynamic activity = current concentration in the vehicle/concentration of saturated vehicle), then in an ideal situation all saturated solutions of the same permeant in any mixed solvent vehicle should produce an equal flux through a membrane that is independent of solute concentrate. In actual practice, vehicle solvent/membrane interactions, especially where the vehicle is soluble in the barrier membrane, will cause significant deviations from this ideal situation (Watkinson *et al.*, 1995). To increase the percutaneous penetrations of drugs by optimising the thermodynamic activity of compounds in solutions, studies are being undertaken with supersaturated solutions (Morita and Horita, 1985; Kondo *et al.*, 1987 a,b,c, Davies, 1990). There are a number of methods of obtaining supersaturated solutions suitable for topical delivery. One of the original techniques is the use of volatile: non-volatile systems, where the solute is dissolved in a volatile solvent then mixed with a non-volatile component such as water. This solution is applied to the membrane surface and the volatile solvent evaporated off leaving a saturated solution of solute in the aqueous base (Coldman *et al.*, 1969). This technique has been used to increase the flux of hydrocortisone across ethylene vinyl acetate membranes from acetone/water systems (Theeuwes *et al.*, 1976), hydrocortisone butyrate propionate across polydimethylsiloxane from ethanol/propylene glycol/ water gels (Tanaka *et al.*, 1985) and minoxidil across excised human skin from ethanol/propylene

glycol/water solutions (Chiang *et al.*, 1989). Although this technique gives an initial increase in drug penetration, it is limited by an eventual decrease in permeation due to drug crystallisation. This crystallisation can be limited by the use of antinucleating polymers in the vehicle with consequential improvement in permeation (Kondo *et al.*, 1987 a b c). Another approach to the formation of supersaturated solutions *in situ* has been used to enhance the dermal administration of bupranolol (Kemken *et al.*, 1992). By applying bupranolol in a saturated, water-free microemulsion base, under occlusion to the dorsal skin of rabbits, supersaturated solutions were produced *in situ*. This occurred because the oily base took up water from the skin and changed the water-free microemulsion base into an emulsion. Bupranolol is insoluble in water so its solubility in the microemulsion decreases with increasing water concentration. The *in vivo* pharmacodynamic effects could be correlated with the decline of solubility versus water content of the vehicle *in vitro* (Kemken *et al.*, 1992).

An alternative method to the *in situ* production of supersaturated solution is a mixed co-solvent system technique (Davis, 1990). With this method, a solute is saturated in a co-solvent system containing a high proportion of co-solvent for example 60% propylene glycol in water. Supersaturated solutions of known concentration can then be formed by the addition of an aqueous phase to this saturated solution. Stabilisation of supersaturated solutions is achieved by the addition of antinucleant polymers to the aqueous phase. Using this technique, it is also possible to form supersaturated solutions with different degrees of saturation within a similar vehicle and solutions with different degrees of supersaturation, but containing the same concentration of solute (Megrab *et al.*, 1995). Using this procedure, supersaturated solutions have been prepared from hydrocortisone acetate (Davis and Hadgraft, 1991), piroxicam (Pellett *et al.*, 1993), and oestradiol (Megrab *et al.*, 1995) and significant levels of enhancement have been achieved. Results utilising oestradiol demonstrated a linear correlation between the degree of saturation and the uptake ratio (uptake ratio=uptake from supersaturated solution/uptake from saturated solution) and over short treatment times oestradiol uptake increased up to 18.6 and 15.8 times for human skin and silastic membranes, respectively, from an 18 times saturated donor system (Megrab *et al.*, 1995).

A unique approach to the optimisation of the thermodynamic activity of topically applied drugs is EMLA® 5% cream. It is an eutectic mixture of lignocaine base 25 mg ml^{-1} and prilocaine 25 mg ml^{-1} (Hopkins *et al.*, 1988) which has been approved by the FDA as a topical

anaesthetic for use on normal intact skin for local analgesia in adults and children older than 1 month. When lignocaine and prilocaine crystals are mixed together, the mixture forms a liquid at room temperature. Thus, the melting point is lower than if the agents were mixed separately. The significance of the lower melting point is that there is no need to dissolve the anaesthetic base in oil before adding the emulsifier, which would decrease the concentration of the anaesthetic agent. The eutectic mixture increases the concentration of the anaesthetic in the emulsion droplets from 20% lignocaine to about 80% lignocaine-prilocaine (Evers, *et al.*, 1985). EMLA® has been shown to be superior to placebo and ethyl chloride, comparable to subcutaneous lignocaine and less effective than intradermal lignocaine. Patients appear to prefer EMLA® cream treatment to the alternatives (Anon, 1993).

An alternative method of applying compounds to membrane surfaces to provide donors with high thermodynamic activity is to dissolve the compound in a volatile solvent such as ethanol or acetone. After the solution has been applied to the membrane, the solvent can be evaporated off, leaving a thin film of active compound upon the membrane (Watkinson *et al.*, 1991). This technique is especially useful in *in vitro* work where the compound of interest is either in short supply or very expensive.

2. Specific interactions with the stratum corneum

All enhancers falling within this category have the ability to alter the nature of the stratum corneum so that its diffusional resistance is reduced. This effect is being studied by a variety of techniques, including percutaneous studies across membranes, differential scanning calorimetry, infrared spectroscopy and various miscellaneous methods including vaso-assays, X-ray diffractometry and electron-spin resonance. There are various theories as to the actual mode of action of these enhancers and they can be further sub-divided (Figure 3.1).

i Site A - polar head groups

It is proposed that many absorption enhancers interact with the polar head groups of the intracellular lipids of the structured bilayer lamellae within the stratum corneum (see sections 1.1 and 1.2). These interactions modify hydrogen-bonding and ionic interactive forces between polar heads disturbing the ordered packing. Modelling of the electrostatic field

Figure 3.1 Proposed action sites for accelerants in the intercellular space of the horny layer. For enhancers, linear chains represent Azone, bent chains correspond to *cis*- unsaturated promoters and the circles stand for small polar solvents such as DMSO and its analogues, the pyrrolidones and propylene glycol (From Barry, 1991a)

around the headgroups of the ceramides which make up the lipid bilayers, show that electronegative and positive regions exist on opposite sides of the molecule. It is predicted that the interaction of these forces hold the molecules together. Disruption of these interactive electrostatic forces makes the domain more fluid and therefore promotes the diffusion of chemicals across the stratum corneum, especially those of a polar nature. This disruption may allow more aqueous liquid to enter the tissue and swell the aqueous regions between the lipid bilayers. This swelling should provide a larger fractional volume of "free" water as distinct from structured water and hence increase the cross-sectional area available for polar diffusion at site B (Barry, 1991a). However, X-ray analysis has shown that increased hydration may not expand this domain and that lipid lamellar spacings are independent of tissue water content. It is possible that lipid lamellar spacings remain independent of an increase in tissue water content due to a consequential lateral swelling of the alkyl chain length resulting in a small shortening of the mean alkyl chain length (B ouwstra, 1991). A a result of disordering the polar head group is that the packing of the lipid chains is also disrupted. Therefore, the lipid hydrophobic route, Site C, becomes disordered and the permeation of non-polar permeants is also enhanced. This explains why certain enhancers alter lipid packing, even when from simple polarity considerations, they should only affect the polar route.

ii Site B - aqueous regions of the polar route

In addition to affecting the lipid polar heads, enhancers may directly affect the composition of the aqueous region. Solvents, like enhancers, can partition into this region and alter its solubilising ability. This will alter the partition characteristics of lipophilic molecules such as steroids, which will have a more favourable partition coefficient from the donor vehicle into the skin. When the solvent diffuses out of the stratum corneum into the viable epidermis, the drug follows at a relatively high flux as it diffuses down a new, raised chemical potential gradient.

iii Site C - the lipid domain

Due to their structure absorption enhancers, such as Azone and oleic acid will insert between the hydrophobic tails of the lipid bilayer. This will disrupt the bilayer packing, increase the fluidity of the bilayer and thus permit enhanced diffusion of penetrants. Just as interaction at

Site A also affected the fluidity of Site C, the interaction at Site C will disrupt the packing of the polar heads in Site A and promote chemical penetration *via* the polar route. Some enhancers may contain both a large polar head and a lipid tail and will be capable of disruption at both Sites A and C by alignment with the ceramide lipids. An important consideration for many enhancers, especially very lipophilic molecules, is the delivery of these compounds to their site of action. If a lipophilic enhancer interacts with the polar heads in the aqueous region of the lipid bilayer, then its potential effects could be limited by poor delivery to this site. It is under these circumstances that the choice of co-solvent is important. The co-solvent may decrease the polarity of the aqueous region and so increase the solubilising ability of this region for lipophilic enhancers and potentiate the enhancing effect. This synergistic effect may increase enhancement beyond that which would have resulted from the sum of the individual effects.

iv The intracellular route

In order for an absorption enhancer to potentiate penetration *via* the intracellular route, it could potentially interact with whatever lipid remains within the corneocyte or alternatively a direct interaction with the keratin fibrils within the corneocyte.

v Permeation enhancement *via* facilitated transport systems

An ion-pair theory has been suggested for the facilitated transport mechanism of ionic drug diffusion into the stratum corneum (Barker and Hadgraft, 1981, Hadgraft *et al.*, 1985, Hadgraft *et al.*, 1986, Green and Hadgraft, 1987; Hadgraft *et al.*, 1989). By manipulation of pH and therefore drug ionisation, anions such as salicylate may be transported against their own concentration gradients. Ion-pair facilitated transport requires a pH-gradient as the driving force (Walters, 1989). Employing a pH-gradient of 5 to 7.4, it has been shown that long chain tertiary amines can facilitate the transport of anionic drug molecules across artificial membranes (Hadgraft *et al.*, 1989). The enhancer would act as an ion-pair agent to enhance the transport of an ionic compound across membranes by a similar mechanism as discussed for buffer counter-ions in section 2.1 and Figure 2.1.

The Lipid-Protein-Partitioning theory summarises a number of these potential modes of action

by suggesting that absorption enhancers usually act by one or more of three main mechanisms (Barry, 1991a; Barry, 1991b; Goodman and Barry, 1989a,b; Barry, 1988; Williams and Barry, 1992).

1. Disruption of the highly ordered structure of stratum corneum lipids.
2. Interaction with intracellular protein.
3. Improved partitioning of a drug, co-enhancer, or co-solvent into the stratum corneum.

3.1.2 Percutaneous Absorption Enhancers

For a compound to be ideal as an absorption enhancer, it should possess the following qualities (Barry, 1983; Hadgraft,1984; Woodford and Barry, 1986):

1 Pharmacologically inert
2 Non-toxic, non-irritant and non-allergenic
3 A rapid and predictable duration of action that is reversible
4 Specific mode of action
5 Chemically and physically stable
6 Cosmetically acceptable

Of the many compounds investigated for absorption enhancer properties, none fulfill all of the above criteria, but some have many of the most essential. Absorption enhancers can be broadly categorised into three chemical classes: solvents, surfactants and other miscellaneous chemicals.

Water is the simplest solvent that can affect rates of absorption. Hydration of the stratum corneum will, in the majority of cases, increase penetration. The most common way of achieving hydration is by occlusion with oil-based vehicles. Hydration is induced by sweat accumulation at the skin vehicle interface. Although there are no definite theories how hydration affects enhancement, it may be due to aqueous solvation of the polar regions of glycosphingolipids and ceramides.

Alcohols and glycols, especially ethanol and propylene glycol, have been studied as absorption

enhancers. Upon application to biological membranes, they would appear to accumulate in the stratum corneum, which results in an increased partitioning of drugs and co-enhancers into the membrane barrier (Berner *et al.*, 1989). At high concentrations, ethanol and other small alcohols can extract stratum corneum lipids (Williams and Barry, 1992).

Ethanol can increase the flux of lipophilic drugs (DeNoble *et al.*, 1987; Good *et al.*, 1985), 5-fluorouracil (Friend *et al.*, 1988a) and steroids (Pershing *et al.*, 1990; Higuchi *et al.*, 1987; Ghanem *et al.*, 1987a). The actual ratio of ethanol in an aqueous solvent, can influence the penetration rate of compounds (Kurihara - Bergstrom *et al.*, 1990). One hypothesis is that low ethanol fractions alter the lipoidal pathways, but higher concentrations significantly affect the polar pathways (Ghanem *et al.*, 1987 a;b). Nitroglycerin (Berner *et al.*, 1989) and salicylic acid (Kurihara - Bergstrom *et al.*, 1990) transdermal fluxes were optimised at ethanol volume fractions of approximately 0.7. As the ethanol volume fraction increases, altered or additional polar pathways may form from a combination of alterations in protein conformation, reorganisation within the lipid polar head regions or lipid extraction. Possible ion-pair formation may augment the enhancing effects (Lee *et al.*, 1987). Above the optimum volume fraction, the decreasing partition coefficient of the penetrant from the ethanolic vehicle becomes a dominant factor reducing the overall flux.

Although propylene glycol is a commonly used solvent for topical formulations, its use as an absorption enhancer in its own right, is a subject of debate. It has been shown to enhance oestradiol under some experimental conditions (Goodman and Barry, 1989b), but not under others (Møllgaard and Hoelgaard, 1985). These discrepancies may be due solely to differences in experimental conditions, as propylene glycol appears to be most effective when the horny layer is not fully hydrated (Møllgaard, 1993). Propylene glycol has significant enhancing properties when used as a co-solvent in conjunction with other enhancers such as oleic acid or Azone. There is a great deal of data demonstrating a synergistic effect between propylene glycol and a range of enhancers (Møllgaard, 1993).

Dimethyl sulphoxide is an earlier enhancer. It is a dipolar aprotic solvent and being miscible with both water and organic solvents, is easily incorporated into pharmaceutical preparations. Its major therapeutic use is as a solvent for idoxuridine in the treatment of herpes zoster and herpes simplex (Turnbull and MacGregor, 1969). It has also been shown to enhance the

absorption of many compounds, including non-steroidal anti-inflammatory drugs (Dallas *et al.*, 1987; Stelzer *et al.*, 1968; Muktdair *et al.*, 1986; Hwang and Danti, 1983; Chowan and Pritchard, 1978; Hsu *et al.*, 1991), and steroids (Møllgaard and Hoelgaard, 1983a; Stroughton and Cleveland, 1964; Cramer and Cates, 1974).

There are many suggestions as to the mode of action of aprotic solvents such as dimethyl sulphoxide. As with pyrrolidones and surfactants, dimethyl sulphoxide can interact with proteins contained within the corneocyte and enhance drug absorption *via* the intracellular route. Mechanisms of protein interactions include; relaxation of binding forces, alterations in the helix conformation and interactions with protein polar groups. These actions may form pore routes through the tissue. Like ethanol, dimethyl sulphoxide solvents can extract compounds from the intercellular lipid domains such as lipids, lipoproteins and nucleoproteins. This will change the composition of the intercellular regions and aid the partition of some drugs into the stratum corneum (Embery and Dugard, 1971 ; Allenby *et al.*, 1969). Polar compounds like dimethyl sulphoxide can alter partition into the aqueous or polar domains within the lipid bilayers and increase the layers solubilising ability (Figure 3.2). This enables

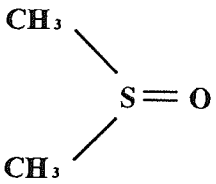

Dimethyl Sulphoxide

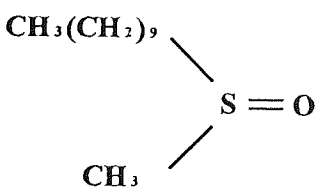

Decylmethyl Sulphoxide

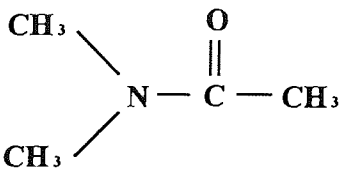

N,N-Dimethyl Acetamide

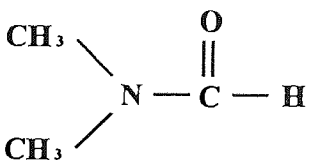

N,N-Dimethyl Formamide

Figure 3.2 Structures of aprotic solvents shown to be penetration enhancers, including alkyl methyl sulphoxides and dimethyl amides.

compounds such as steroids to dissolve in high concentrations. As the solvent diffuses out of the stratum corneum, the dissolved drug will follow down its new, raised chemical potential gradient.

Significant permeation enhancement with DMSO only occurs when it is present in concentrations in excess of 60% (Cramer and Cates, 1974; Al-Saidan *et al.*, 1987; Kurihara-Bergstrom *et al.*, 1987). At this concentration, a number of irreversible effects occur, including; elution of DMSO-soluble components, delamination of the horny layer, and the denaturing of its proteins (Kurihara - Bergstrom *et al.*, 1986; Elfbaum and Laden, 1968; Sharata and Burnette, 1988). Photomicrographs show that there is severe disruption of the stratum corneum; these effects raise toxicological problems, especially of an ocular and dermatological nature (Finkel, 1980; Kligman, 1965 and Al-Saidan, 1987).

Longer chain alkyl homologues of methyl sulphoxide have been evaluated as absorption enhancers. Decylmethyl sulphoxide has been reported as optimal (Sekura and Scala, 1972). It is effective at lower concentrations and has the advantage that its degradation products are less odorous than dimethyl sulphoxide. Decylmethyl sulphoxide can enhance polar and ionic compounds, which may suggest its mechanism of action includes the polar route (Cooper, 1982). Activity may also be due to its characteristic as a non-ionic surfactant (critical micelle concentration of 0.002M) (Cooper, 1982). Other solvents shown to affect the skin in a similar way to dimethyl sulphoxide, include dimethyl acetamide and dimethyl formamide (Aungst *et al.*, 1986; Munro and Stroughton, 1965; Munro, 1969; Akerman *et al.*, 1979; Southwell and Barry, 1984), but due to potential toxic implications, they are unlikely to be used in a clinical situation (Southwell and Barry, 1983).

In an attempt to avoid the adverse effects of the DMSO group of enhancers, natural products have been investigated. Pyrrolidone derivatives, present in natural moisturising factor, have been shown to enhance the absorption of a range of products. A constituent of natural moisturising factor, pyrrolidone carboxylic acid, has been shown to increase the water binding capacity of the stratum corneum (Barry, 1983). The primary site of this group of compounds is the polar route, and hydration would appear to be a significant factor in their mode of action. 2-pyrrolidone and N-methyl-2-pyrrolidone have shown to be two of the most effective of these

compounds, enhancing anti-inflammatory agents (Southwell and Barry, 1984; Akhter and Barry, 1985) and caffeine (Southwell and Barry, 1984). Irritation may again limit their clinical use (Bennett *et al.*, 1985).

Azone (1-Dodecylazacycloheptan-2-one; Laurocapram) has been designed and synthesised as an absorption enhancer from the pyrrolidone derivatives. It is effective with hydrophobic and hydrophilic drugs (Stoughton, 1982; Stoughton and McClure, 1983). A study of the chemical structure of Azone (Figure 3.3) shows that there is a long alkyl chain and a more polar lactam grouping. The lactam group has a significant effect upon the polarity of the molecule, which is demonstrated by the effect this has upon partitioning behaviour. There are four orders of magnitude difference between the estimated log P (using fragmental constants) of Azone, compared with the all carbon analogue (Hadgraft *et al.*, 1993). This lactam grouping, therefore, would be expected to interact with the polar regions of the lipid bilayers. The carbon side-chain would then insert into the hydrophobic tails of the lipids. Further evidence for this mechanism of interaction with lipids has been obtained using liposomes composed of dipalmitoyl phosphatidylcholine (DPPC) as a model of the stratum corneum lipid bilayers. Although there are no phospholipids present in stratum corneum, these vesicles can be used as a reproducible model to simulate potential changes that may be induced by the presence of Azone in the lipids of the stratum corneum. Any changes observed in the liposomes was determined using a simple light-scattering technique to assess phase transition temperatures. The results indicated that Azone does interact with the lipid structure, making it more fluid, reducing the diffusional resistance of penetrating species (Beastall *et al.*, 1988). Using monolayers of DPPC spread at an air-water interface, it is possible to study the Azone-lipid interaction in more detail. The interactions caused large surface expansions, measured using a Langmuir film-balance, which, in conjunction with molecular graphics, indicates that the headgroup is in a bent conformation relative to the alkyl chain and that the ring structure lies in the plane of the polar headgroups of the phospholipid (Lewis and Hadgraft, 1990). This headgroup arrangement of Azone has an electronegative site at the carbonyl moiety, but no complementary positive site. This is in contrast to the natural polar head of the ceramide lipids which have complementary electropositive and negative groups on opposite sides of the molecule. When Azone inserts into the lipid structure, it will leave an unbalanced electronegative site on the ceramide, which could give rise to a permeability defect.

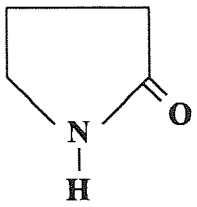

2-Pyrrolidone

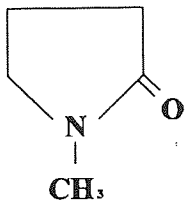

N-Methyl-2-Pyrrolidone

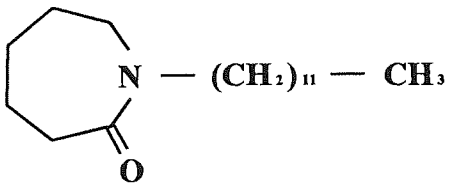

1-Dodecylazacycloheptan-2-one (Azone)

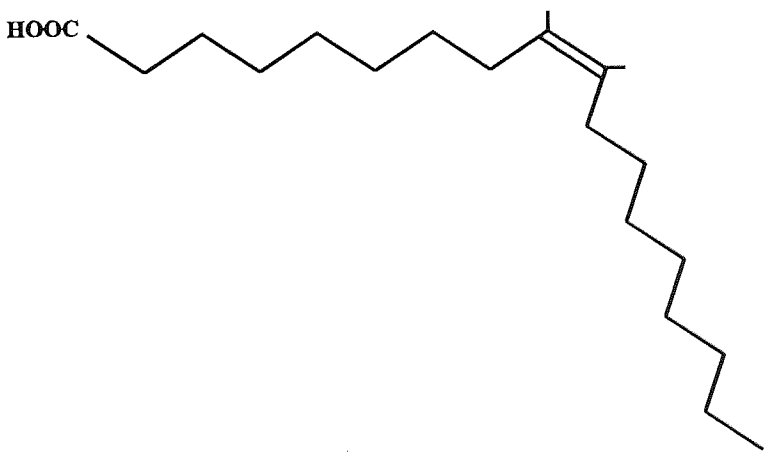

cis-9-Octadecenoic Acid (Oleic Acid)

Figure 3.3 Structures of some penetration enhancers

The generally accepted mechanism of action for Azone is that it disrupts the ordered lipid packing within the bilayers and increases the fluidity of this layer (Golden *et al.*, 1987; Goodman and Barry, 1985; Hadgraft, 1991). This increased fluidity will allow easier diffusion of hydrophobic penetrants. The structure of the Azone hydrocarbon chain is linear, unlike the kinked nature of oleic acid with its *cis* - double bond. This would imply that the hydrophobic tail is not responsible for the lipid structure disruption. Computer graphic representations and monolayer experiments suggest that the positioning of the seven-membered ring among the lipid polar head groups at site B (Figure 3.1) forces the polar heads apart. This prevents the alkyl chains packing efficiently, imparts disorder and facilitates diffusion (Beastall *et al.*, 1987; 1988). The disruption created by the lactam ring at the polar head region will promote permeation of hydrophilic compounds *via* the polar route (Barry, 1991a; Hadgraft *et al.*, 1993). There is also evidence to suggest that Azone disrupts the horny lipids structure (Goodman and Barry, 1985 and Goodman and Barry, 1986).

Concentrations of 1 to 10% Azone appear to be most appropriate, but care must be taken with the final formulation. Actual concentration depends upon the physicochemical properties of the active drug and recipients. Co-solvents such as polyethylene glycol 400 and white soft paraffins can inhibit any enhancing action. This may be due to the preferential partitioning of Azone into the fatty base, rather than the stratum corneum. Polar co-solvents such as propylene glycol have marked synergistic effects upon absorption (Wotton *et al.*, 1985). This synergy between polar co-solvents such as ethanol and propylene glycol has been observed with many lipophilic enhancer compounds besides Azone, for example; terpenes and long-chain unsaturated compounds such as oleic acid and oleyl alcohol.

A single dose of Azone can enhance the penetration of subsequent drug doses for at least five days (Wotton *et al.*, 1985), indicating preferential partitioning into the stratum corneum rather than the viable epidermis. This has significant potential advantages for a topical drug absorption enhancer. Azone has the potential to enhance the transdermal absorption of a range of compounds. This effect can be optimised by tailoring the concentration of the enhancer to the lipophilicity of the penetrant. At concentrations of 1% w/w Azone acts upon compounds with a lipophilicity value of log $PC_{oct} \leq 1$ (5-fluorouracil and aniline). With a 5% w/w concentration, the lipophilicity limit for enhancement is increased to log $PC_{oct} = 2.69$. This trend continues with membrane treatments with 10% w/w Azone solutions. Compounds of high lipophilicity

(log $PC_{oct} \geq 3$) may not demonstrate enhanced permeation rates irrespective of the concentration of applied Azone solutions (Diez-Sales *et al.*, 1996).

Surfactants are characterised by the presence of both polar and non-polar groups on the same molecule. They are broadly categorized into three groups, anionic, cationic and nonionic surfactants. Their traditional use in pharmaceutical formulations is as emulsion and suspension stabilisers, wetting agents, solubilisers and detergents. This function is attributed to their ability to congregate at the interface of two immiscible substances and lower interfacial tension. Two phases can be emulsified by the incorporation of one phase within micelles of surfactant. It has also been shown that at low concentrations, surfactants have penetration enhancer capabilities. This is attributed to the molecule's ability to penetrate and eventually disrupt the cell membrane structure. If there is a possible interaction between surfactant and penetrant, then once the critical micelle concentration of surfactant is reached, the penetrant can be solubilised within the micelle. This lowers the thermodynamic activity of the penetrant, therefore inhibiting further absorption enhancement (Florence and Gillian, 1975).

Anionic surfactants can penetrate and interact strongly with skin (Bettley, 1965; Gibson and Teall, 1983). The amount of penetration is influenced by the surfactant structure, principally on the alkyl chain length. Anionic surfactants, once absorbed, induce large alterations upon the barrier function of the skin. They induce swelling of the stratum corneum and the viable epidermis (Scheuplein and Ross, 1970; Blake-Hoskins *et al.*, 1986) and destroy its integrity within hours of application (Rhein *et al.*, 1986). A possible mechanism of action is that the hydrophobic interaction of the alkyl chains with the substrate leaves the negative end group of the surfactant exposed, creating additional anionic sites on the membrane. This results in the development of repulsive forces that separate the protein matrix, uncoil the filaments, and expose more water-binding sites, possibly increasing the hydration level of the tissue. Separation of the protein matrix could also result in a disruption of the long range order within the keratinocyte, leading to increased intracellular diffusivity and enhanced percutaneous absorption. Although anionic surfactants can significantly increase drug penetration, their therapeutic use is limited by the skin irritation they can cause (Novac and Francom, 1984).

Cationic surfactants such as cetyltrimethyl ammonium bromide, have not been extensively investigated as enhancers, because they are allegedly the most topically irritant of the

surfactants. Alkyl amines are generally less irritant surfactants than the alkyl ammonium bromides. Their mode of action may be different to that of anionic surfactants in that cationic surfactants do not cause swelling of the epidermis (Choman, 1963). It is suggested that these may facilitate the transport of ionised drugs across the skin *via* an ion-pair carrier system (Barker and Hadgraft, 1981 and Hadgraft *et al.*, 1986). Ion-pair facilitation cannot be the sole means of transport, as Ethomeen S12 (N, N-bis[2-hydroxyethyl] oleylamine) is reported to enhance permeation of caffeine, a weakly basic drug, across skin, but it has no effect upon the permeation of caffeine across artificial membranes. This would imply that Ethomeen S12 exerts an effect upon stratum corneum unrelated to its ion-pair carrier properties (Hadgraft *et al.*, 1986).

The non-ionic surfactants are potentially the most therapeutically useful of the surface active agents, as they have the least potential for irritancy. Of the many different types of non-ionic surfactants, studies of skin enhancers are limited to four main groups. These are the polysorbates, which are mixtures of partial esters of sorbitol and its mono and dianhydrides condensed with approximately 20 mol of ethylene oxide; polyethoxylated alkyl ethers and esters, in which the alkyl chain can be saturated, unsaturated, branched or linear, polyethoxylated alkyl phenols, in which the hydrophobic group is normally octyl or nonyl-phenyl; and poloxamers, polyoxyethylene - polyoxypropylene block copolymers, in which the polyoxypropylene chain acts as the hydrophobic moiety. The polysorbates have been shown to have a variety of actions upon skin absorption, from retarding to enhancing (Mezei and Ryan, 1972; Ryan and Mezei, 1975; Behl *et al.*, 1980; Chowan and Pritchard, 1978; Aungst *et al.*, 1986; Aguiar and Weiner, 1978; Sarpotdar and Katz, 1986a; 1986b). This is because, at low concentrations, these compounds can alter the barrier properties of the skin, but at higher relative concentrations, they have a significant capacity to solubilise penetrants into micelles. Polyoxyethylene aryl ethers tend to enhance ionised species more significantly than unionised (Hwang and Danti, 1983). Polyoxyethylene aryl ethers and the polyoxamers have limited action as enhancers and have maximum effect only when used in combination with other groups of absorption enhancers.

The suggested mechanism of action of non-ionic surfactants, is that they partition into the intracellular lipid phases of the stratum corneum. This results in increased fluidity in this region, which reduces diffusional resistance. The incorporation of polyethylene alkyl ethers increases the lipid monolayer fluidity (Walters *et al.*, 1982). This interaction is dependent on alkyl chain

length, such that dodecyl chains cause a greater increase in fluidity at lower concentrations than octadecyl. Surfactants whose hydrophobic portions are composed of branched chains or aromatic groups lack enhancing activity. This theory suggests they are not readily amalgamated into the stratum corneum lipid structure. At high surfactant concentration, lipid extraction may occur, further reducing diffusional resistance. A mechanism that may augment the effect above, especially for dodecyl-based surfactants, is the penetration into the intracellular matrix, followed by interaction and binding with the keratin filaments.

Long-chain fatty acids and alcohols have been shown to be effective absorption enhancers (Aungst *et al.*, 1986; Cooper *et al.*, 1985; Bennett and Barry, 1985; Davidson *et al.*, 1986). The ability to function as absorption enhancers varies, dependent upon chain length, saturation, position and type of double bonds. The C12 analogue is the most effective straight chain fatty acid (Aungst *et al.*, 1986) and in all cases, the *cis* configuration is more effective than the trans linkage (Table 5.1)(Cooper, 1984a; Golden *et al.*, 1987). It is almost universally believed that the "kinked" *cis* molecule positions itself within the lipid bilayers (Site C Figure 3.1) and disorders the packing and imparts fluidity (Hadgraft, 1991; Green *et al.*, 1988).

Table 3.1 Effect of double bond position on the enhancement of salicylic acid flux. (From Golden *et al.*, 1987 and Walters, 1989).

A proposed mechanism of action for oleic acid is that the kinked structure inserts within the normal intercellular lipid arrangement of the stratum corneum. This fluidises the lipid bilayers and increases the permeability of this region (Green *et al.*, 1988). There is evidence from FTIR that oleic acid exist as "pools" within the stratum corneum (Ongpipattanakul *et al.*, 1991) rather than homogeneously distributed. The existence of these separated domains within the intercellular spaces disrupts the barrier function by creating highly permeable border regions or interfacial defects between the ceramide and oleic acid molecules. These "fluid-like oleic acid channels" are introduced within the stratum corneum at physiological temperatures (Walker and Hadgraft, 1991).

More recently, evidence from thermal analysis and freeze-fracture electron microscopy of stratum corneum pretreated with oleic acid (0.16 M in propylene glycol), indicates that oleic acid builds up a new type of structure within the skin lipids, which differs from the normal lipid structure and from the structure of oleic acid in propylene glycol itself. It is suggested that this new structure is created by eutectic mixing of oleic acid with the skin lipids and this has a reduced barrier capacity in comparison to untreated skin (Tanojo *et al.*, 1995).

From a group of oleyl surfactants, including oxyethylene oleyl ethers and esters and oleic acid, oleic acid was the most effective for promoting transdermal absorption of nitroglycerin (Kadir *et al.*, 1993). This was in spite of evidence that oleic acid was the least toxic, demonstrating that a powerful skin penetration enhancer does not have to be strongly toxic for skin cells. Enzymatic hydrolysis of the surfactants leads to the suggestion of biodegradable penetration enhancers. These would remain intact and effective while in the stratum corneum, but biodegrade on arrival in a more enzymatically active skin strata, such as the viable epidermis.

A "push-pull" mechanism of action has been proposed for alkanecarboxylic acids (Kadir *et al.*, 1987;1988). Incorporation of these surfactants into topical preparations changes the thermodynamic activity of the penetrating species, leading to a "push" affect. The "push" originating from a change in the substrates solubility characteristics in the vehicle. "Pull" effects are due to surfactants, especially those containing an oleyl chain, penetrating into the highly ordered intercellular lipid structure of the stratum corneum and reduce its resistance by increasing lipid acyl chain mobility (Ashton *et al.*, 1986; Mak *et al.*, 1990).

It is now generally accepted that the choice of solvent is influential in obtaining the full enhancing potential of some lipophilic enhancers (Wotton *et al.*, 1985). Polar co-solvents such as propylene glycol are synergistic with Azone and fatty acids, for example oleic acid and some surfactants (Cooper, 1984a; Bennett *et al.*, 1985; Barry and Bennett, 1987). It is hypothesised that the functional site of these lipophilic enhancers, especially Azone, is the polar surface of the lipid bilayer (site A Figure 3.1). To enable the lipophilic enhancer to reach this site in sufficient quantities, propylene glycol decreases the polarity of the aqueous regions and so increases its potential to solubilise Azone. The disruption of the lipid layer caused by Azone promotes the flux of propylene glycol. This mutual effect could result in a more rapid diffusion of drug molecules across the skin (Møllgaard, 1993).

Natural products are currently receiving considerable interest, for example compounds which are or which were derived from essential oils, terpenes and terpenoids. These may provide a series of relatively safe, clinically acceptable absorption enhancers for lipophilic and hydrophilic drugs (Williams and Barry, 1992), although they may be prone to oxidation. The essential oils of eucalyptus, chenopodium, and ylang ylang have been used as penetration enhancers in excised human skin (Williams and Barry, 1989). Eucalyptus was the most active oil and increased the membrane-permeability coefficient of 5-fluorouracil by 34 times. Acetone extracts of cardamom seed enhanced the transdermal permeation of prednisolone (Yamahara *et al.*, 1989). The active constituents of the extract, the monoterpene terpineol and acetyl terpineol, were more effective than Azone in promoting drug diffusion through excised, shaved mouse skin. Using 5-fluorouracil as a model hydrophilic compound, the terpenes d-limonene, 1,8-cineole, menthone and nerolidol all increased transdermal permeation by a proposed mechanism of disruption of the intracellular lipid lamellar structure (Yamane *et al.*, 1995a). The activity of these terpenes as enhancers is dependent upon the propylene glycol content of their co-solvent vehicles with maximum fluxes obtained with formulations containing 80% propylene glycol systems (Yamane *et al.*, 1995b). The mechanism for this synergy remains unclear, but with 1,8-cineole the effect may occur through synergistically enhanced lipid disruption. There is no evidence for propylene glycol improving enhancer delivery into the stratum corneum or lipid extraction (Cornwell *et al.*, 1996). Evidence has been presented that terpene enhancers pool within the stratum corneum due to high enhancer uptake values. Further evidence is required to determine exactly where this pooling occurs, but it is suggested that it may be found outside the lipid bilayers as DSC traces following terpene treatment continue to display lipid

bilayer transitions (Cornwell *et al.*, 1996).

By hydrating the stratum corneum, urea enhances the penetration of several compounds, the most significant of which is hydrocortisone (Feldman and Maibach, 1974). The keratolytic effect of urea limits its long term usage (Idson, 1975; Hadgraft, 1984). Other miscellaneous chemicals known to act as penetration enhancers are N,N-dimethyl-m-toluamide (Windheuser *et al.*, 1982), calcium thioglycolate (Kushida, *et al.*, 1984), and some anticholinergic agents (Bodor, 1986). The epidermis itself is a living entity and has the potential to respond biologically to chemicals such as drugs and penetration enhancers. The pathological response of the skin, for example, inflammatory and immune reactions, can induce changes in the chemical structure and composition of lipids and proteins in the skin. This response may cause disruption and potentiate transdermal absorption. This possible effect should be considered when extrapolating *in vitro* data to *in vivo* situations (Xu and Chien, 1991).

3.1.3 Aims and Objectives

Excised human skin and silastic rubber were used to investigate the effects of various putative enhancers in co-solvents upon the permeation of salicylic acid. The primary objective was to to study the effects and relative enhancement ratios these putative enhancers had upon the model permeant, salicylic acid, with and without a pH-gradient across the membrane. The purpose was to determine whether, in some cases, the mechanism of enhancement of absorption enhancers can be explained by partition effects alone without recourse to ion-pair mechanisms. In section 2.1, the mechanism of ion-pair facilitated transport was discussed where a pH-gradient enables the formation of an ion-pair on the donor side of the membrane which then travels down its concentration gradient be dissociated on the other side of the membrane, releasing the permeant into the receiver solution. The pH-gradient is an important parameter in this process, because without it the ion-pair can neither form on the donor side nor can it dissociate into the receiver solution. Hence, without a pH-gradient ion-pair facilitated transport should not occur. If percutaneous absorption enhancement occurs with pretreatment of membranes without a pH-gradient it can be assumed this is due to increased partitioning into the membrane. If this enhancement is augmented by a pH-gradient then this potentiation should be due to ion-pair facilitated transport. It is proposed to pretreat membranes with enhancer

solutions using Franz-type *in vitro* absorption cells with and without a trans-membrane pH-gradient while maintaining all other variables constant.

The action plan to achieve this primary objective is :

- Study the effect of a pH-gradient upon the transport of salicylic acid.

  The results in chapter 2 showed that it was the unionised species that was responsible for percutaneous transport. This conclusion was achieved using donors and receivers of similar pH to prevent the possibility of a pH-gradient influencing the results. The first objective of work in Chapter 3 was to see if a pH-gradient would modify these results. This was studied by varying the donor pH while maintaining the receiver pH at 7.2 and then by maintaining the donor at pH 4 while varying the receiver pH.

- Study the effect of a pH-gradient upon the chemical enhancement of salicylic acid across silastic rubber.

  This objective was two-fold, the first to see if this membrane was an appropriate model to study enhancer pretreatment and the second to study the effect of the pH-gradient on enhanced transport of salicylic acid. The enhancement with and without the pH-gradient would be compared statistically to test the difference for significance.

- Study the effect of a pH-gradient upon the chemical enhancement of salicylic acid across excised human skin.

  Using human skin the effects of a pH-gradient were studied upon the chemical enhancement of salicylic acid. The results with and without a pH-gradient were compared statistically in order to determine modes of action of various chemical enhancers of percutaneous absorption.

3.2 Experimental

3.2.1 Materials

Chemicals and permeation membranes were obtained and prepared as detailed in section 2.2.1. Enhancers used, were lauric acid N,N-dimethylamide (LDA) (Sigma), caproic acid N,N-dimethylamide (CDA) (Sigma), dodecylamine (DCA) (BDH), Azone® (Nelson Research, a gift), oleic acid (OA) (Merck) and Transcutol®(TC) (Gattefossé, a gift). All the enhancers were presented as 0.5M solutions in propylene glycol (PG) (BDH) or isopropyl myristate (IPM) (Croda). The ibuprofen was a gift from Boots.

3.2.2 Assay Procedures.

All salicylic acid assays were carried out as discussed in section 2.2.2. Ibuprofen was assayed using similar HPLC instrumentation to salicylic acid (section 2.2.2.1). The ibuprofen mobile phase comprised aqueous acetonitrile (55%), adjusted to pH 2.0 with phosphoric acid (0.45%) and an analytical wavelength of 225 nm was used (Irwin *et al.*, 1990a).

3.2.3 Donor Solutions.

All vehicles were prepared as section 2.2.3, except all permeation profiles were carried out at 32°C.

3.2.4 Solubility Determination.

The solubility of salicylic acid was determined at 32°C by the method described in section 2.2.4.

3.2.5 Permeation Procedure.

Jacketed Franz-type diffusion cells were set up as described in section 2.2.5, except that the receptor cell was maintained at 32°C by means of a thermostatically controlled water circulator. The donor cell and the sample were sealed to minimise evaporation. The receptor chamber was filled with a McIlvaine buffer of the appropriate pH. The receiver phase was de-gassed by warming to 32°C and sonication to minimise the accumulation of air bubbles at the skin-receptor interface during the experiment. Any further pockets of air that developed were removed by a syringe connected to a piece of flexible polyethylene tubing passed down the sample port and into the air bubble. The receptor volume was approximately 30 ml. This was

determined accurately by weight. The diffusional barrier was left to equilibrate with the receptor solution overnight at room temperature. The following morning, the cell was warmed to 32°C and the receptor solution allowed to equilibrate. Any air that had accumulated at the skin-receptor interface was carefully removed. An aliquot of 2 ml of the formulation under study was introduced into the donor compartment. Samples of the receptor phase (1 ml) were removed at appropriate time intervals over 15 to 420 minutes and were assayed by HPLC following suitable dilution (section 2.2.2.1). Receiver solutions of pH 3.40 buffer were diluted with distilled water and pH 7.22 receiver solutions were diluted with 0.1M HCl. Diluting the pH 7.22 buffer with 0.1M HCl quenched the chromatographic interference induced by the relatively high pH of this buffer.

After the permeation cells had been assembled with buffer solutions in the receiver compartment, pretreatment with enhancers was effected by applying 1 ml of the enhancing solution (section 3.2.1) to the membrane surface for 12 hours at room temperature. After this period the cells were warmed to 32°C and the pretreatment solution carefully removed. This surface was then rinsed a number of times with distilled water. Excess water was then removed and the membrane surface dabbed dry with soft tissue. Following this procedure 2ml of the saturated suspension of salicylic acid (SA) was then applied to the membrane surface. Six Franz-type cells were used for each experimental run, each held membrane from a similar source. Three of these cells were pretreated with enhancer and the remaining cells remained untreated as controls.

Unless otherwise stated, permeation profiles with a pH-gradient utilised a saturated salicylic acid suspension at pH 4.04 as a donor and a McIlvaine buffer at pH 7.2 (Appendix 1) as a receiver. Profiles without a pH-gradient used a similar salicylic acid suspension at pH 4.04 as a donor and a McIlvaine buffer at pH 3.4 (Appendix 1) as a receiver.

3.3 Results and Discussion

3.3.1 The Effect of the Receiver Phase Buffering Capacity Upon Chromatography

Results from Chapter 2 demonstrated that the rate of flux of salicylic acid across human skin and silastic rubber was proportional to the concentration of unionised molecules in the donor phase. The experimental protocol used eliminated the potential effects of a pH-gradient by the utilisation of donors and receivers of similar pH. To study the ion-pair effects of putative enhancers, a pH-gradient is essential. It was assumed that an ideal pH-gradient to test the ion-pair hypothesis (Hadgraft *et al.*, 1985) was a donor at approximately pH 4 and a receiver at approximately pH 7. These particular solutions were chosen because the pH of the lower skin layers of the viable epidermis is about 7.4 (Katz and Poulsen, 1971). The receiver pH of about 3.5 would ensure the ion-pair would not deprotonate releasing the donor anion into the receiver phase.

Initial work was to determine whether the flux from an aqueous suspension of salicylic acid at pH 4.04 would be the same into both the pH 7.22 and the 3.42 receiver. The experimental protocol in Chapter 2.2.5 took samples directly from the receiver and injected them directly onto the HPLC. Samples with pH as high as 7 had not been previously studied, but problems were not anticipated. The developmental work was undertaken using silastic rubber as the model membrane. The initial results are graphically represented in Figure 3.4. They clearly demonstrate that the flux was significantly greater into the pH 3.42 receiver than the 7.22. This effect was not only unexpected, but it was the reverse of any predicted influence due to pH-partition. This experiment was repeated pretreating the membrane with enhancers, but the increased rate of flux into the pH 3.42 receiver continued to be observed.

To establish the pH at which the reduction in flux occurs, a series of experiments were prepared using a pH 4.04 saturated suspension of salicylic acid as a donor and a series of McIlvaine buffers in the pH range 3.14 to 8.13 as the receiver phases. The results of this work show a marked reduction in rate between pH 5.5 and 6.5 (Figure 3.5). This does not correspond with the pK_a of salicylic acid, so the effect is not due to the ionisation of salicylic acid , but it is dependent upon pH. Ruling out any physicochemical influence of salicylic acid, investigations were focused upon the experimental design. Three areas were investigated: whether the donor solution was influencing the pH of the receiver; the receiver was influencing

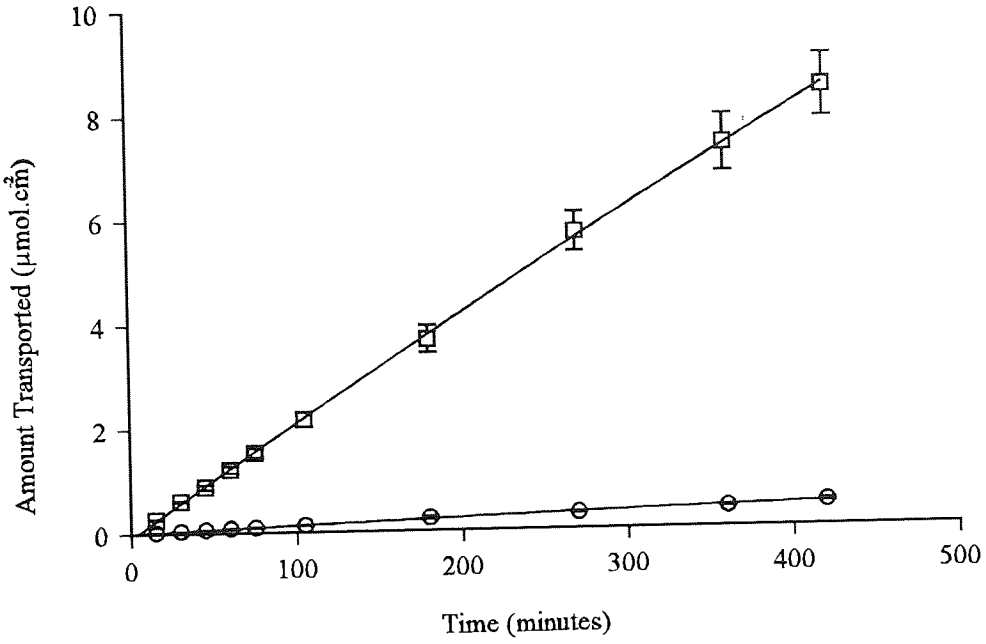

Figure 3.4 The effect of the receiver pH upon the permeation of salicylic acid from saturated aqueous suspensions at pH 4.04 across silastic rubber membrane (□, pH 3.42 receiver; ○, pH 7.22 receiver).

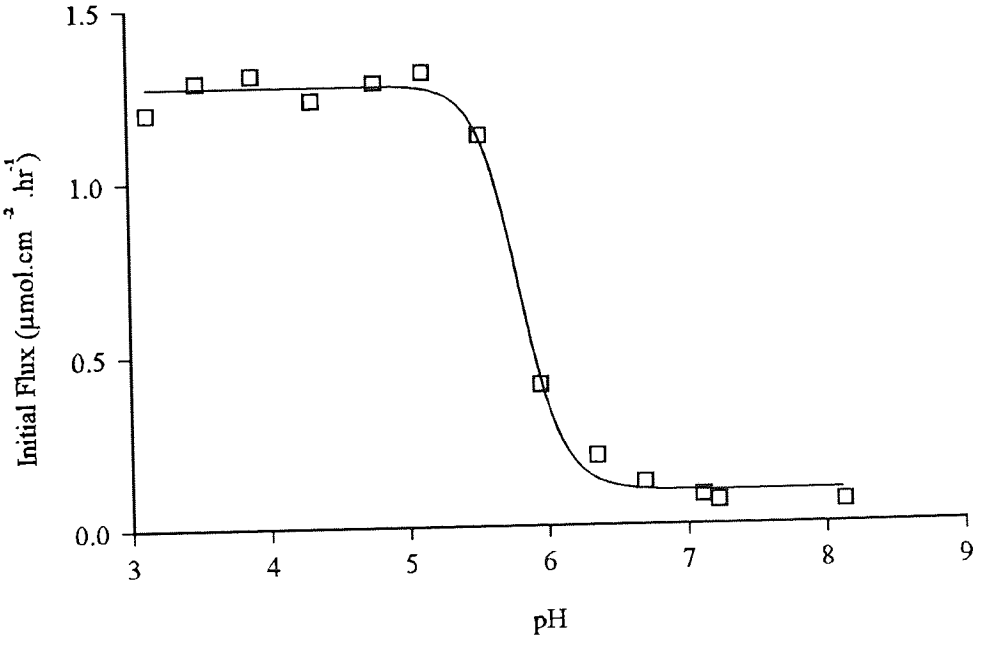

Figure 3.5 The effect of the receiver solution pH upon the initial flux of salicylic acid from saturated aqueous suspensions at pH 4.04 across silastic rubber.

the pH of the donor; or alternatively the setting up of the cells over night allowed the pH 7.22 buffer to partition into the silastic rubber enabling the rubber to act as a significant depot for the salicylic acid. By adjusting experimental parameters, including the use of horizontal diffusion cells, each of these hypotheses were eliminated. Further experiments were undertaken to see if this phenomenon could be observed with other weak acids. Ibuprofen was selected and the permeation profiles were repeated. The receiver solutions were modified to contain 50% propylene glycol due to the low aqueous solubility of ibuprofen.

The ibuprofen experiments revealed the answer to the unusual rates observed with salicylic acid. By injecting samples of ibuprofen in the pH 7.22 double strength McIlvaine buffer in 50% propylene glycol onto the HPLC split peaks were observed (Figure 3.6A). These chromatograms could be modified to a peak with a shoulder by using single strength buffer in propylene glycol (Figure 3.6B) and the effect was eliminated by diluting the single strength buffer in propylene glycol 1 to 10 with 0.1M hydrochloric acid (Figure 3.6C).

Looking again at the salicylate chromatograms with this new information, the unusual results could be explained. The buffering capacity of the pH 7.22 receiver phase was sufficient to influence the mobile phase pH and create an artifact in the chromatography. The lack of ionisation control resulted in peak splitting with the component equivalent to the pure acid, the peak at 3.2 minutes being taken as the total salicylic acid concentration. Unlike the ibuprofen experiments, the salicylic acid did not split into 2 visible peaks, but one visible peak and one that originated in the solvent front. It was for this reason that the problem was not identified earlier. The apparent differences in flux resulted entirely from this artifact which can be clearly seen in Figure 3.7 when the chromatograms of equimolar solutions of salicylic acid in various solvents give apparently significantly different peak areas.

The problem was overcome in the *in vitro* permeation profiles by taking 1 ml samples of receiver and diluting the pH 7.22 receiver in 0.1M hydrochloric acid and the pH 3.42 buffer receiver in distilled water. The sample volume was replaced with fresh buffer and the cumulative mass of salicylic acid transported was calculated mathematically. In all future experiments, the assays were validated using an appropriate solvent equivalent to the final dilution and solvents for calibration curves were more carefully selected.

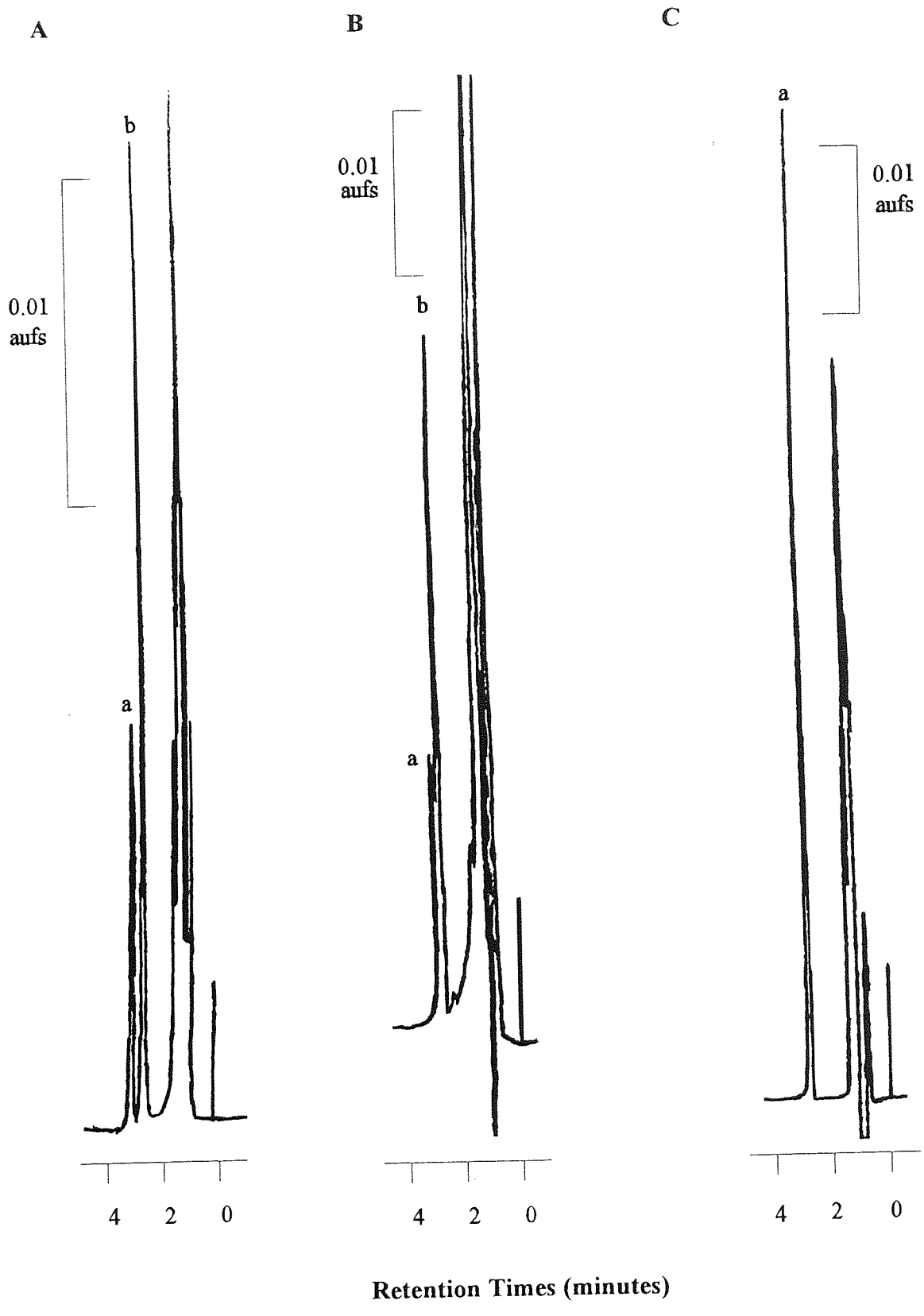

Figure 3.6 Example HPLC chromatograms of ibuprofen (peak a) in various buffer solutions showing peak splitting (peak b) (Ibuprofen retention time 2.9 mins).

A Double strength McIlvaine's buffer pH 7.2 in 50% propylene glycol
B McIlvaine's buffer pH 7.2 in 50% propylene glycol
C McIlvaine's buffer pH 7.2 in 50% propylene glycol diluted 1 in 10 with 0.5M HCl

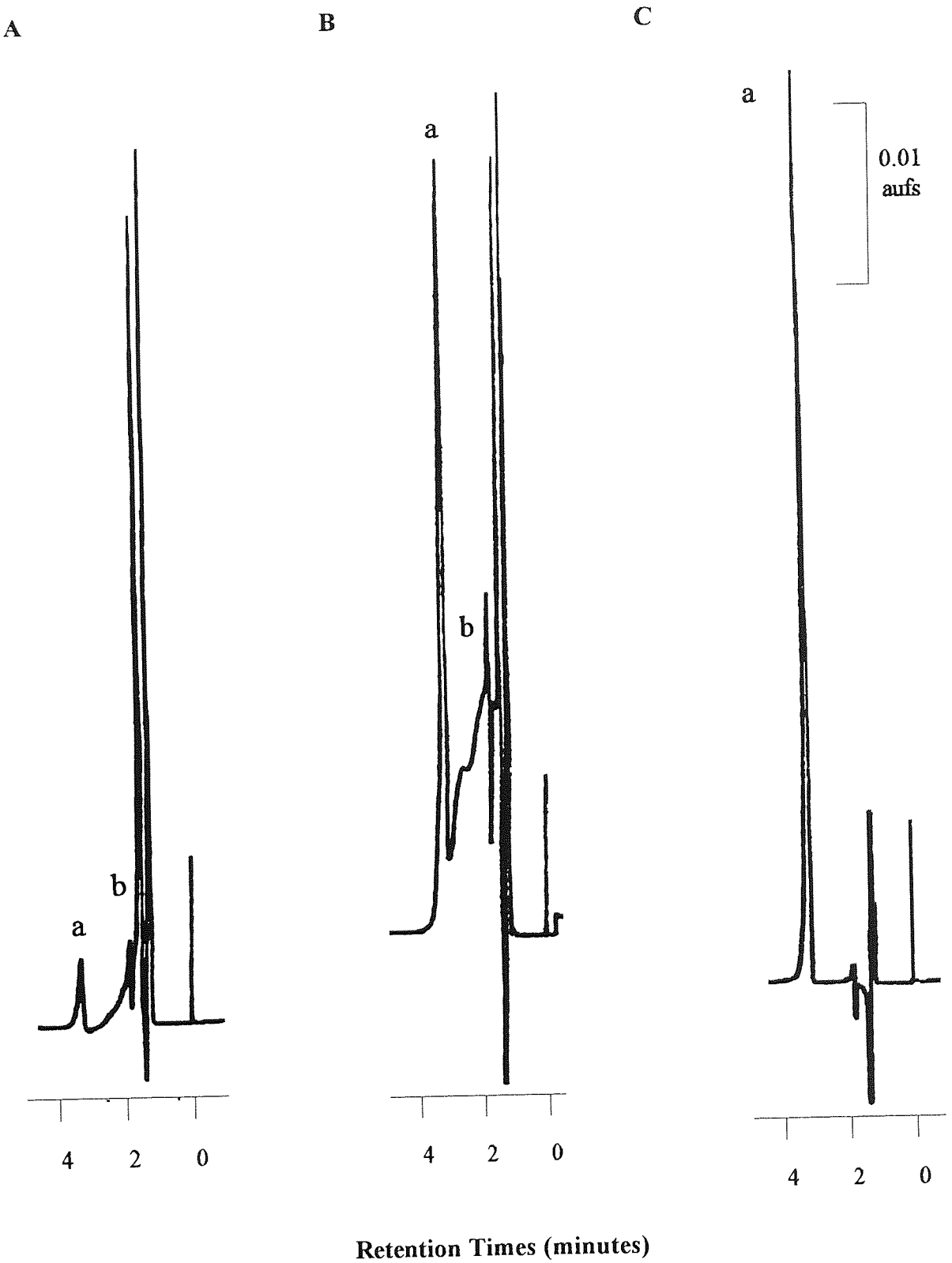

Figure 3.7 Example HPLC chromatograms of equimolar solutions of salicylic acid (peak a) in various pH buffer solutions showing peak splitting (peak b) (Retention time of salicylic acid is 3.2 minutes).

A McIlvaines buffer pH 7.2
B McIlvaines buffer pH 5.8
C Distilled water

3.3.2 Solubility of Salicylic Acid with Respect to pH at 32°C

The effect of pH on the saturated solubility of salicylic acid in aqueous buffer at 32°C was determined and is recorded in Table 3.2. The solubility increases with respect to pH as discussed in section 2.3.1 and is determined by the extent of ionisation. As salicylic acid is a weak acid with a pK_a of 2.98 the more hydrophilic ionised species is favoured at the higher pH values. Comparing the results at 32°C with those at 37°C (Table 2.1), the solubilities are similar at lower pHs with a solubility of 24.841 mmolar at pH 2.57 at 32°C and 25.58 at pH 2.35 at 37°C. The differences become more significant at higher pHs with a solubility of 343.957 mmolar at pH 4.29 at 32°C and 522.20 at pH 4.17 at 37°C. As would be expected, the solubilities are greater at the higher temperature.

The plot of solubility versus $1/[H_3O^+]$ for salicylic acid at 32°C is shown in Figure 3.8 and the statistics for this graph are given in Table 3.3. The values of S_0 and pK_a of 30.08 and 3.30 respectively compare to the literature values for solubility in distilled water of 15.74 mmolar (Budavari, *et al.*, 1996) and pK_a of 2.98 (Albert and Sergeant, 1984). The types of errors in this determination with respect to the literature values are discussed further in section 2.3.1

pH	Salicylic Acid Solubility (mmolar)	Percentage Ionisation
2.16	18.566	13.15
2.57	24.841	28.01
3.04	43.038	53.45
3.64	130.594	82.05
3.96	172.309	90.52
4.27	277.660	95.12
4.29	343.957	96.72
4.60	629.890	98.13

Table 3.2 Effect of pH on the saturated solubility of salicylic acid in aqueous buffer at 32°C

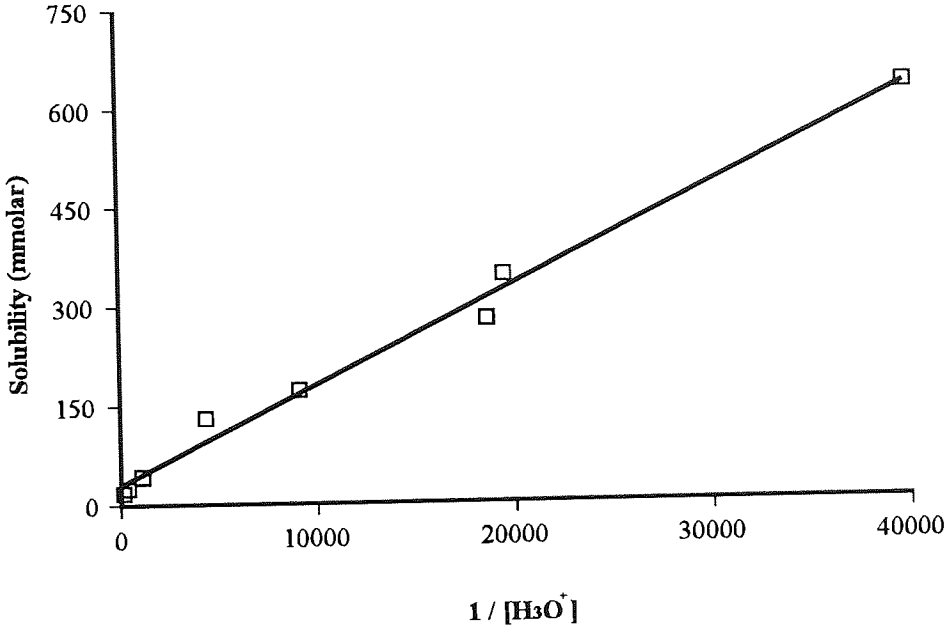

Figure 3.8 Plot of solubility versus $1/[H_3O^+]$ for salicylic acid at 32°C

Parameter	Value	± SE	± 95% CI	r
Intercept (S_0)(mM)	30.081	10.708	26.202	-
Slope (S_0K_a)	0.01505	6.162×10^{-4}	0.00151	0.9950
pK_a	3.30	-	-	-

Table 3.3 Calibration statistics and parameters for solubility versus $1 / [H_3O^+]$ for salicylic acid at 32°C in Figure 3.8 (SE, standard error; CI, confidence interval).

3.3.3 The Effect of a pH-Gradient Upon the Flux of Salicylic Acid Across Human Skin and Silastic Rubber.

Work described in Chapter 2 has shown that the rate of penetration from saturated suspensions of salicylic acid is independent of the donor pH. This was determined using a receiver solution of a similar pH to that of the donor. Results obtained without a pH-gradient could not demonstrate any effect from ion-pairing. The results presented here maintain the receiver pH at 7.22. Those recorded in Table 3.4 represent the silastic rubber results and Table 3.5 represent the permeation through human skin. Both absorption barriers show similar trends for flux with relation to pH. Figure 3.9 is graphical representation of the flux through each membrane versus the donor pH. The mean flux for silastic rubber was 1.505 μmol cm^{-2} hr^{-1} (SEM = 0.025) and for human skin was 0.925 μmol cm^{-2} hr^{-1} (SEM = 0.034). The rate of permeation remains independent of the donor pH and is related to the concentration of unionised molecules.

A sigmoidal relationship for k_{obs} and pH is described for both membranes and is illustrated in Figure 3.10. k_{obs} is dependent upon both the permeability of the ionised (k_i) and unionised species (k_u), where the fraction of drug in each state, α and 1-α respectively. The relationship is described by $k_{obs} = \alpha k_i + (1-\alpha)k_u$, where the degree of ionisation is given by $K_a/(K_a+[H_3O^+])$. By linearisation of this relationship (see Equation 2.1) and plotting k_{obs}/α against $(1-\alpha)/\alpha$ the values of k_i and k_u can be obtained from the intercept and gradient respectively. The lines in Figure 3.10 are plotted based on this theoretical relationship (Silastic rubber $k_i = 5.90 \times 10^{-5}$, $k_u = 0.0916$; Human skin $k_i = 9.23 \times 10^{-4}$, $k_u = 0.0543$). This relationship is discussed in more detailed in section 2.3.2.

Table 3.6 details salicylic acid permeation data from a pH 4.04 suspension across silastic membrane into receivers formulated over the pH range 0.44 to 8.13. The evidence here shows that a change in the pH-gradient alone is not sufficient to affect the flux. As the pH of the receiver does not affect the partition of salicylic acid from the donor, the membrane itself is most probably the rate-limiting step.

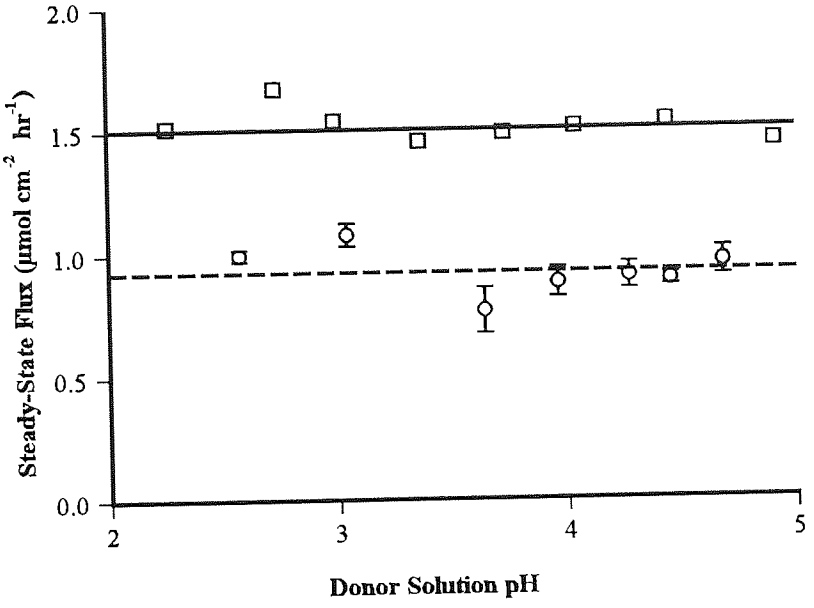

Figure 3.9 The effect of donor pH upon the steady-state flux of salicylic acid from saturated aqueous suspensions across (□) silastic rubber and (○) human skin into McIlvaine's buffer receiver of pH 7.22. (Error bars represent the standard errors of the mean)

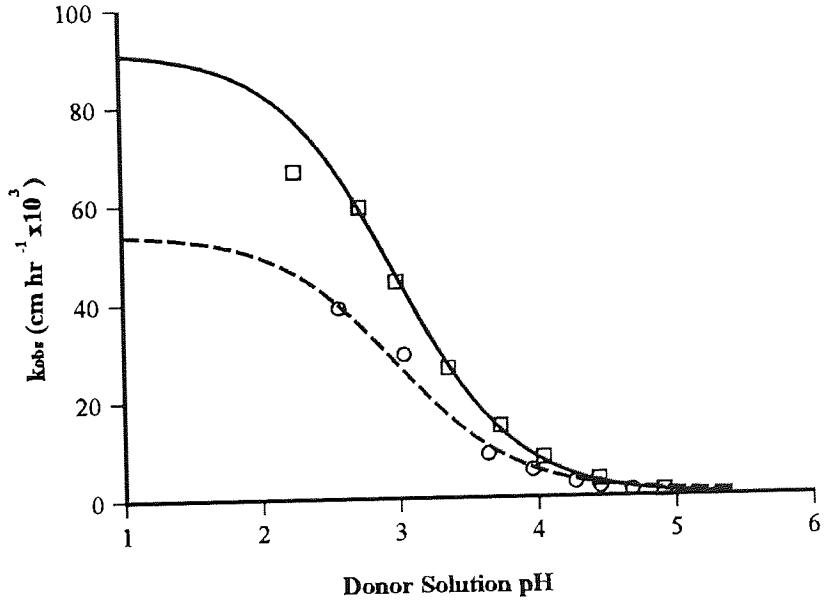

Figure 3.10 Plot of the observed permeability coefficient (k_{obs}) for salicylic acid from saturated aqueous suspensions across (□) silastic rubber and (○) human skin into a McIlvaine buffer receiver pH 7.22 versus the pH of the donor solution. (The line is described by $k_{obs} = \alpha k_i + (1 - \alpha)k_u$, see text for details) (Error bars represent the standard error of the mean).

Donor pH	Flux (μmol cm^{-2} hr^{-1})	k_{obs} (cm $hr^{-1}x10^{3}$)	Lag Time (minutes)
0.29	1.379	68.95	0.83
2.26	1.516	66.60	7.52
2.73	1.670	59.22	0.49
2.99	1.540	44.07	3.17
3.36	1.456	26.44	0.75
3.73	1.488	14.56	2.21
4.04	1.512	8.05	6.96
4.44	1.533	3.47	6.66
4.91	1.450	1.15	11.69

Table 3.4 The effect of donor pH upon the steady-state flux of salicylic acid from saturated aqueous suspensions across silastic rubber into a receiver of McIlvaine's buffer at pH 7.22. (Each result represents the mean of 2 determinations){ANOVA: single factor analysis for significance of difference between flux means P = 0.241, *i.e.* no significant difference}

Donor pH	Flux (μmol cm^{-2} hr^{-1})	k_{obs} (cm hr^{-1} x 10^{3})	Lag Time (minutes)
2.57	0.996 (0.024)	38.81	35.04 (3.645)
3.04	1.078 (0.047)	29.32	26.23 (5.010)
3.64	0.767 (0.092)	8.83	35.42 (0.686)
3.96	0.880 (0.060)	5.51	26.59 (3.892)
4.27	0.904 (0.054)	2.96	23.49 (4.335)
4.45	0.931 (0.023)	2.00	19.14 (1.810)
4.68	0.962 (0.057)	1.28	41.01 (1.794)

Table 3.5 The effect of donor pH upon the steady-state flux of salicylic acid from saturated aqueous suspensions across human skin into a receiver of McIlvaine's buffer at pH 7.22. (Each result represents the mean of at least three determinations, values in parentheses are the standard errors of the mean){ANOVA: single factor analysis for significance of difference between flux means P = 0.065, *i.e.* no significant difference}.

Receiver pH	Flux (μmol cm^{-2} hr^{-1})	k_{obs} (cm hr^{-1})	Lag Time (minutes)
0.44	1.6052	7.15×10^{-3}	0.0
2.01	1.6863	7.51×10^{-3}	0.0
2.72	1.8143	8.08×10^{-3}	0.0
3.14	1.2131	5.40×10^{-3}	0.0
3.50	1.2891	5.74×10^{-3}	0.0
3.90	1.3080	5.82×10^{-3}	3.9
4.33	1.2348	5.50×10^{-3}	2.1
4.73	1.2839	5.72×10^{-3}	0.4
5.13	1.3124	5.84×10^{-3}	0.0
5.53	1.4223	6.33×10^{-3}	0.0
5.95	1.6754	7.46×10^{-3}	0.0
6.35	1.4965	6.66×10^{-3}	4.7
6.69	1.3282	5.91×10^{-3}	1.1
7.11	1.4983	6.67×10^{-3}	6.8
8.13	1.5050	6.70×10^{-3}	2.6
Mean	1.4448	6.43×10^{-3}	1.44
Standard Deviation	0.1854	8.26×10^{-4}	2.15

Table 3.6 The effect of the receiver solution pH upon the initial flux of salicylic acid from saturated aqueous suspensions at pH 4.04 across silastic rubber (Each result is the mean of 2 determinations).

In comparison to the silastic rubber results (Table 3.6) the flux from similar pH 4.04 salicylic acid suspensions across human skin into a pH 7.22 receiver was 0.649 μmol cm^{-2} hr^{-1} (SEM = 0.141) and into a pH 3.40 receiver was 0.639 μmol cm^{-2} hr^{-1} (SEM = 0.069). As with the silastic rubber the pH-gradient alone does not have an effect upon the salicylic acid flux and it is the membrane that is the major barrier to diffusion.

3.3.4 The Effect of a pH-Gradient Upon the Chemical Enhancement of Salicylic Acid Across Silastic Rubber.

To differentiate between the LPP and ion-pairing modes of action of an absorption enhancer, it was essential to determine if a pH-gradient had any effect upon the salicylic acid flux across untreated membranes. If pretreatment with an enhancer has a greater effect upon flux under the influence of a pH-gradient, the mode of action may be due, to some extent, to ion-pairing. If the flux is similar with and without a gradient, the mode of action is more likely to be due to LPP, with little or no influence from ion-pairing.

The model of ion-pair facilitated transport assumes that at the lower pH of the donor compartment-membrane interface the carrier protonates and can combine with the anions present to form ion-pairs, in the interfacial region. The ion-pairs can then partition into the bulk lipid phase and diffuse down their concentration gradient to the opposite interface. In the interfacial region at the higher pH the carrier deprotonates to release the anions (Hadgraft *et al.*, 1985). A pH-gradient is essential for this facilitated transport mechanism. A comparison of absorption enhancer activity with and without a pH-gradient would help ascertain the likely existence of this model (for further discussion see section 2.1).

The enhancers and co-solvents used in this study were chosen with reference to previous work investigating the effects of percutaneous absorption enhancers. Propylene glycol was employed as a co-solvent because it is widely used for topical pharmaceutical products (Cooper, 1984a) and can effectively increase the skin penetration of various topical drugs (Lorenzetti, 1979). It has also shown a synergistic enhancing effect with both oleic acid and Azone (Wotton *et al.*, 1985). As propylene glycol and its solutions are miscible in water they are readily washed from the membrane surface following pretreatment. Isopropyl myristate was used to enable a comparison with the partition and extraction coefficients determined for salicylic acid between buffered aqueous phases and IPM containing various tertiary amide enhancers (Irwin and Smith, 1991). IPM has been shown to be an absorption enhancer in its own right by promoting the percutaneous absorption of nicorandil (Sato *et al.*, 1988) and also claims to be a liquid representative of skin lipids (Poulsen *et.al.*, 1968).

LDA and CDA, alkanoic N,N-dimethylamides ($[(CH_3)_2N\text{-}CO\text{-}(CH_2)_n\text{-}CH_3]$, caproic, n = 4;

lauric, n = 10) were chosen as potential absorption enhancers as compounds of this type have been shown to enhance an organophosphorous anticholinesterase the authors named VX (Wiles and Narcisse, 1971). The medium chain amides were selected as they appear active at lower concentrations than the short chain amides such as N,N-dimethylformamide and N,N-dimethylacetamide. This trend is endorsed by the well-documented effects of Azone, although Azone may have special steric properties. CDA and LDA in low concentrations have been found to enhance the percutaneous absorption of Naproxen by a flux ratio of 1.5 and 3.2 respectively (Irwin *et al.*, 1990b).

The lipophilic amine, dodecylamine was selected as a potential ion-pairing agent and absorption enhancer for salicylic acid. N-substituted bis (2-hydroxypropyl) amines have been reported to facilitate the transport of anionic drugs by ion-pairing (Barker and Hadgraft, 1981). However, this role for DCA has been questioned by Naik *et al.*, (1993), who suggested the potentiation of caffeine's transdermal flux was due to a reduction in barrier resistance, *via* a change in the skin's integrity.

The effects of Azone and oleic acid have been extensively studied as penetration enhancers upon a variety of chemicals. OA is deemed to exert its enhancing effect by lipid perturbation (Ruland and Kreuter, 1992) possibly by pooling and interfacial defects or increased lipid fluidity (Barry, 1987b). Mechanisms of lipid disruption have been proposed for Azone, although there is evidence that some of its action may be attributed to ion-pairing (Hadgraft *et al.*, 1985). Transcutol increases the solubilising potential of the stratum corneum and is an effective enhancer for the transdermal delivery of prostaglandins, especially in association with Azone (Watkinson *et al.*, 1991).

The permeation profiles showing the effect of putative enhancers on salicylic acid permeation from aqueous suspensions across silastic rubber are illustrated in Figures 3.11 to 3.14. The data corresponding to these profiles are summarised in Tables 3.7 and 3.9 and the statistics showing the probability of the enhancers having significantly different effects upon the permeability of salicylic acid are shown in Tables 3.8, 3.10 and 3.11. The means of the flux after enhancer pretreatment are assessed for a significance in difference with and without a pH-gradient using the students t-test. It is assumed that the two samples, with and without a pH-gradient, have unequal variances. This type of t-test is described as a heteroscedastic t-test and

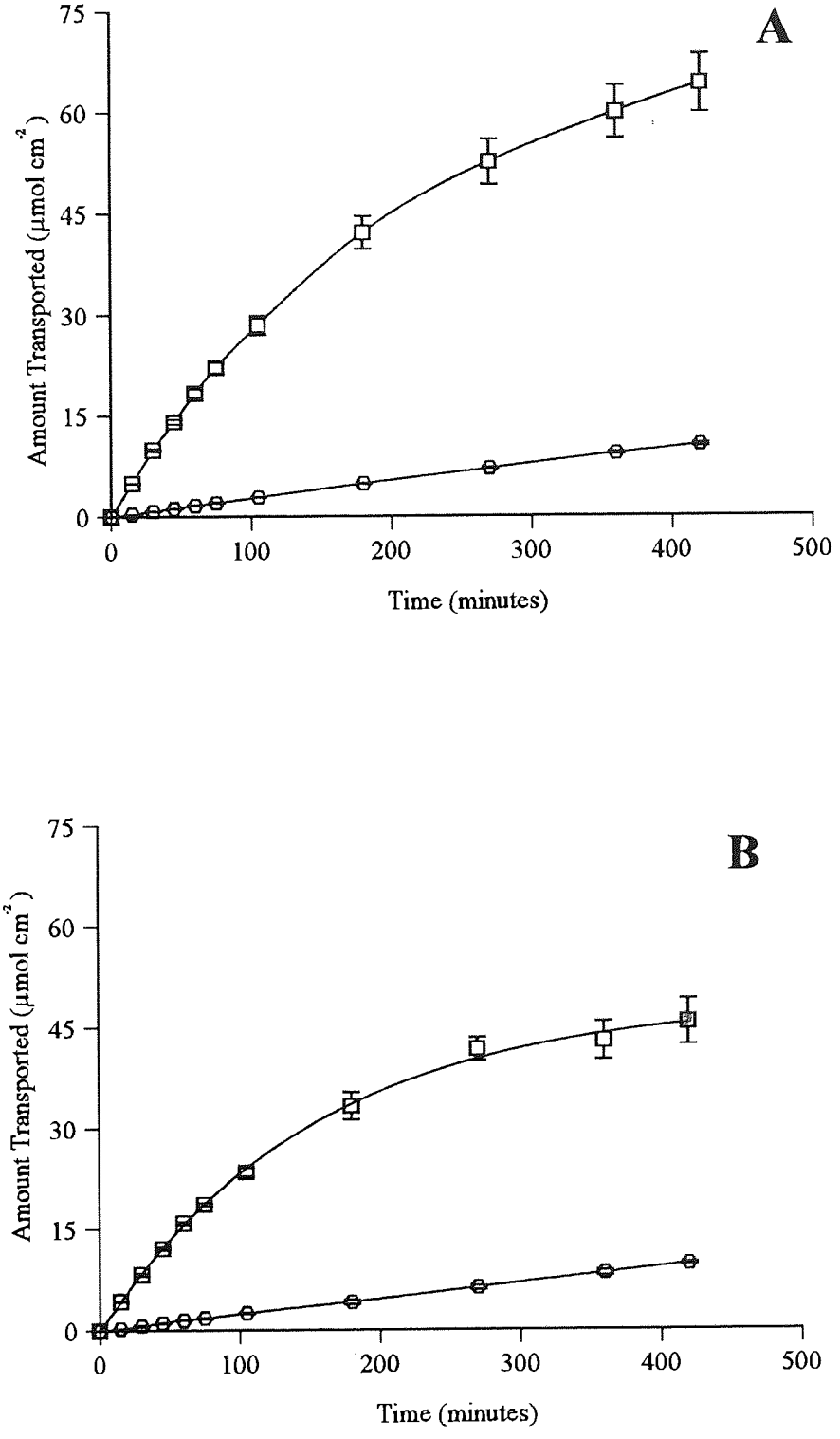

Figure 3.11 The effect of pretreatment with propylene glycol (○) and isopropyl myristate (□) upon the permeation of salicylic acid from saturated aqueous suspensions across silastic rubber membrane. (Error bars represent SEM)

A McIlvaine buffer pH 7.22 receiver phase; pH 4.04 donor phase
B McIlvaine buffer pH 3.42 receiver phase; pH 4.04 donor phase

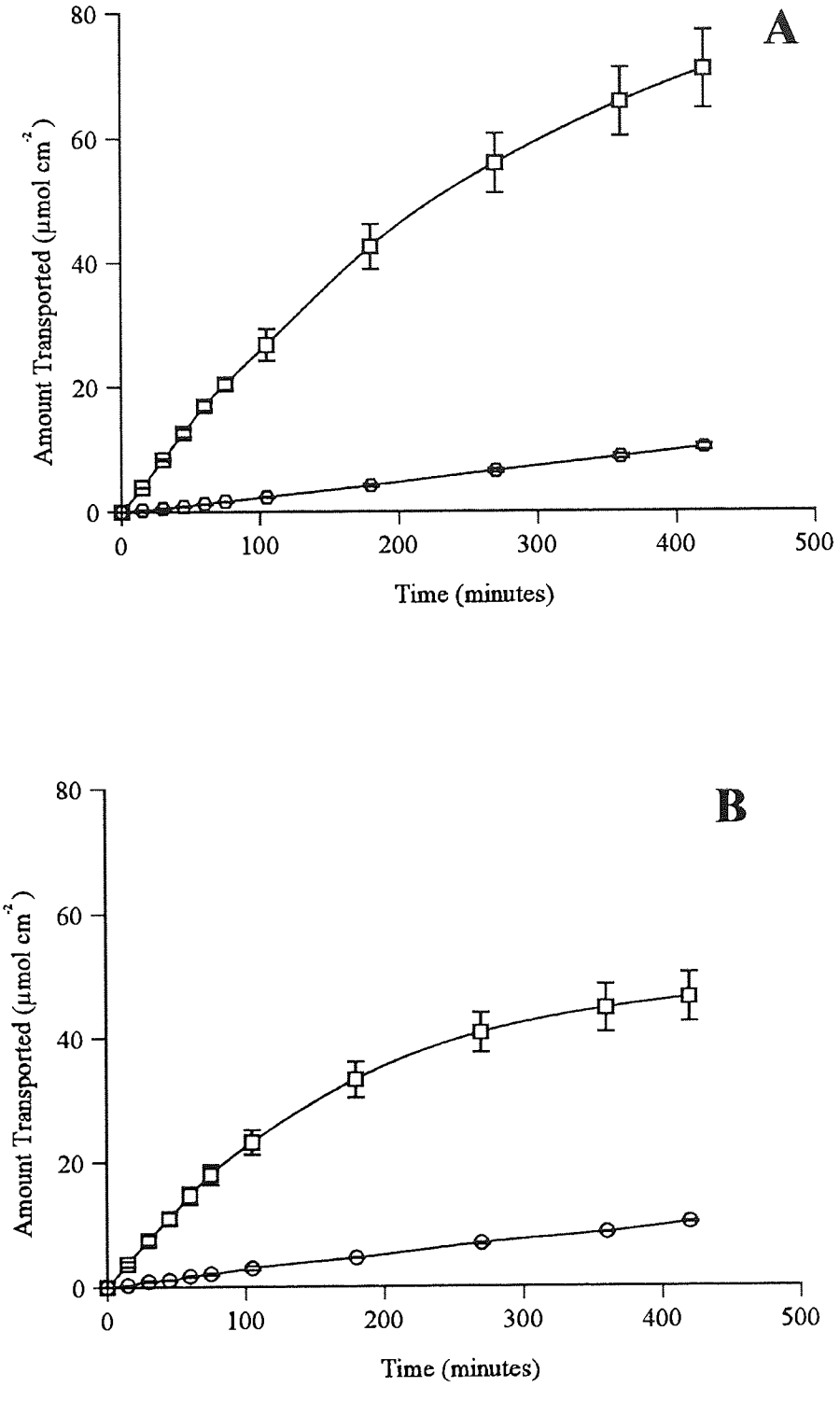

Figure 3.12 The effect of pretreatment with 0.5M caproic acid dimethylamide in propylene glycol (○) and isopropyl myristate (□) upon the permeation of salicylic acid from saturated aqueous suspensions across silastic rubber membrane.(Error bars represent SEM)

A McIlvaine buffer pH 7.22 receiver phase; pH 4.04 donor phase
B McIlvaine buffer pH 3.42 receiver phase; pH 4.04 donor phase

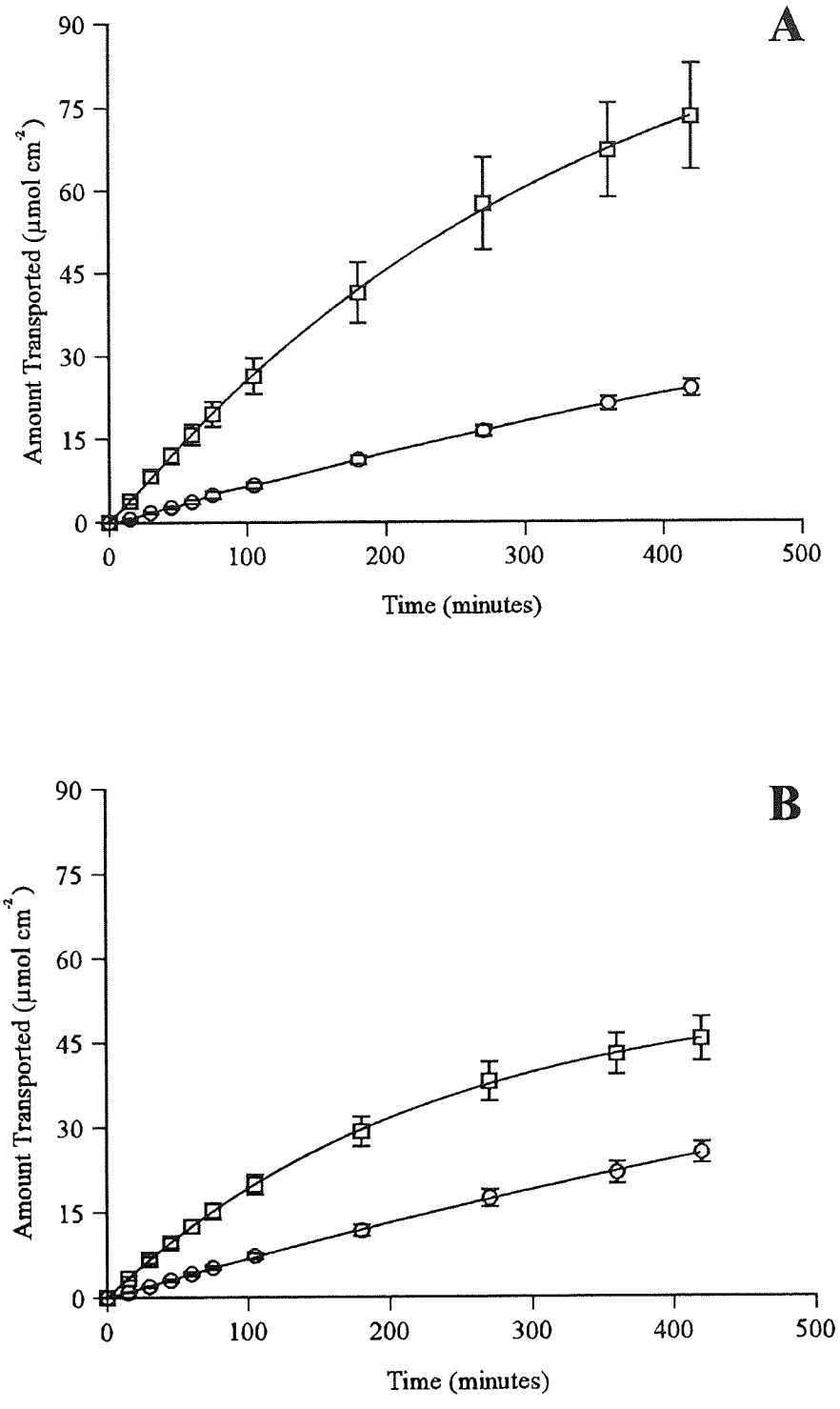

Figure 3.13 The effect of pretreatment with 0.5M lauric acid dimethylamide in propylene glycol (○) and isopropyl myristate (□) upon the permeation of salicylic acid from saturated aqueous suspensions across silastic rubber membrane. (Error bars represent SEM)

A McIlvaine buffer pH 7.22 receiver phase; pH 4.04 donor phase
B McIlvaine buffer pH 3.42 receiver phase; pH 4.04 donor phase

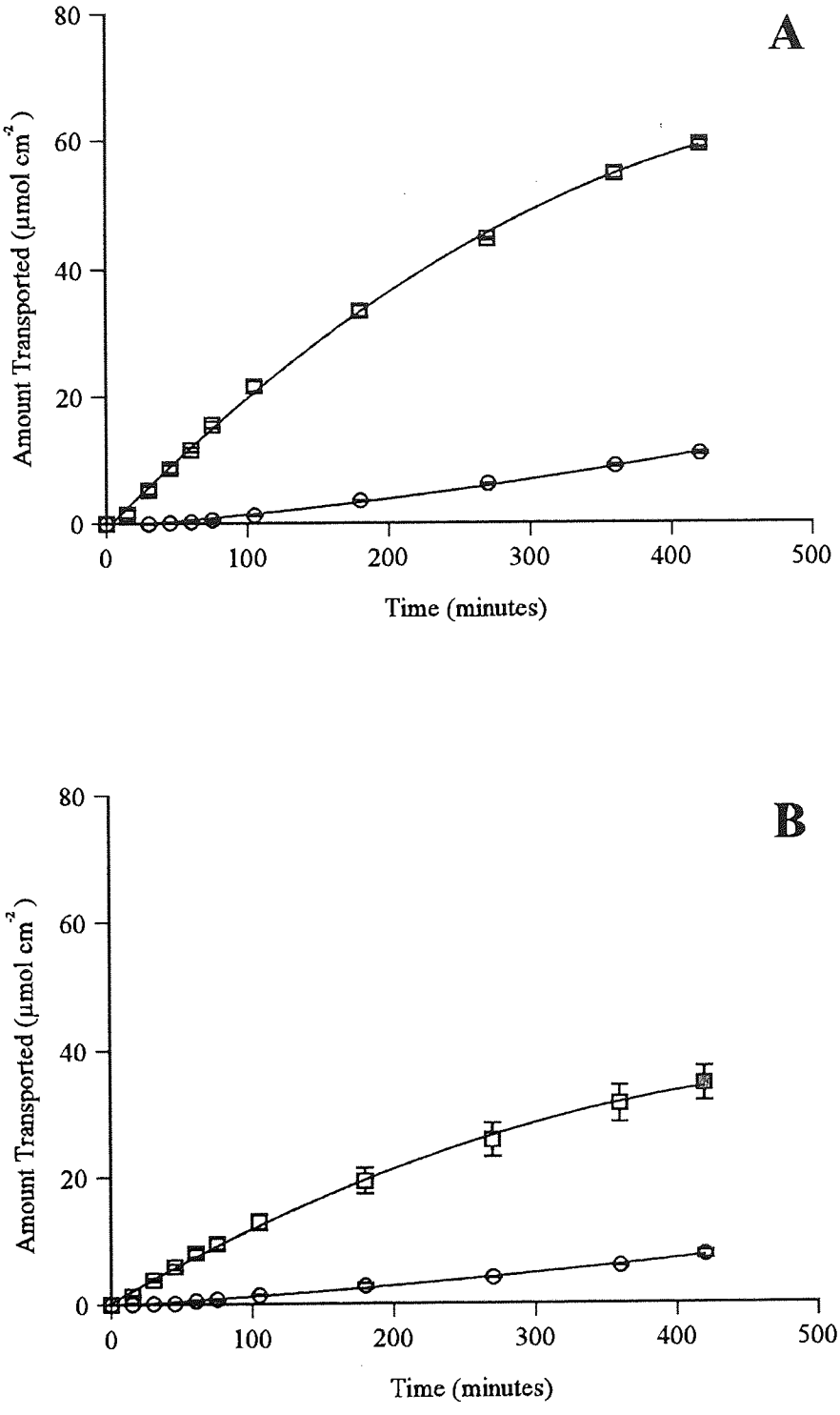

Figure 3.14 The effect of pretreatment with 0.5M dodecylamine in propylene glycol (○) and isopropyl myristate (□) upon the permeation of salicylic acid from saturated aqueous suspensions across silastic rubber membrane. (Error bars represent SEM)

A McIlvaine buffer pH 7.22 receiver phase; pH 4.04 donor phase
B McIlvaine buffer pH 3.42 receiver phase; pH 4.04 donor phase

Pretreatment[a]	Flux (μmol cm^{-2} hr^{-1})	k_{obs} (cm hr^{-1}x10^{3})	Flux Ratio[b]
None	1.488 (0.043)	6.62 (0.190)	1.0
PG	1.524 (0.028)	6.78 (0.126)	1.031
IPM	17.273 (0.682)	76.90 (3.038)	11.681
CDA in PG	1.501 (0.054)	6.68 (0.242)	1.015
CDA in IPM	16.653 (0.718)	74.14 (3.20)	11.261
LDA in PG	3.501 (0.155)	15.59 (0.689)	2.368
LDA in IPM	15.537 (1.400)	69.17 (6.231)	10.507
DCA in PG	1.694 (0.032)	7.54 (0.142)	1.145
DCA in IPM	13.753 (0.262)	61.23 (1.167)	9.300

[a] Enhancer concentrations are 0.5M in their respective vehicles
[b] Flux ratio is the flux following pretreatment with enhancer / no pretreatment

Table 3.7 Permeation data following enhancer pretreatment of salicylic acid from saturated suspensions at pH 4.04 across silastic membrane into a buffer receiver at pH 7.22. (Values in parentheses are the standard errors of the mean; CDA, caproic acid N,N-dimethylamide; LDA, lauric acid N,N-dimethylamide; DCA, dodecylamine).

	PG	CDA in PG	LDA in PG	DCA in PG
None	0.6432	0.8936	**0.0049**	0.0592
PG	-	0.7756	**0.0075**	0.0320
CDA in PG	-	-	**0.0046**	0.0816
LDA in PG	-	-	-	**0.0086**

Table 3.8 The probability (P) of a difference between rates of permeation of salicylic acid through silastic rubber into a pH 7.22 receiver relative to the enhancer used. (Two-tailed heteroscedastic t-test; values in bold are significant at $P \leq 0.01$; CDA, caproic acid N,N-dimethylamide; LDA, lauric acid N,N-dimethylamide; DCA, dodecylamine).

Pretreatment[a]	Flux (μmol cm^{-2} hr^{-1})	k_{obs} (cm hr^{-1}x10^{3})	Flux Ratio[b]
None	1.226 (0.075)	5.46 (0.236)	1.0
PG	1.389 (0.036)	6.19 (0.162)	1.133
IPM	14.453 (0.166)	64.35 (0.741)	11.787
CDA in PG	1.457 (0.009)	6.49 (0.038)	1.188
CDA in IPM	14.280 (0.957)	63.58 (4.260)	11.646
LDA in PG	3.619 (0.242)	16.11 (1.076)	2.952
LDA in IPM	11.719 (0.850)	52.18 (3.786)	9.558
DCA in PG	1.109 (0.031)	4.94 (0.136)	0.905
DCA in IPM	8.882 (0.529)	39.54 (2.355)	7.244

[a] Enhancer concentrations are 0.5M in their respective vehicles
[b] Flux ratio is the flux following pretreatment with enhancer / no pretreatment

Table 3.9 Permeation data following enhancer pretreatment of salicylic acid from saturated suspensions at pH 4.04 across silastic membrane into a buffer receiver at pH 3.40. (Values in parentheses are the standard errors of the mean; CDA, caproic acid N,N-dimethylamide; LDA, lauric acid N,N-dimethylamide; DCA, dodecylamine).

	PG	CDA in PG	LDA in PG	DCA in PG
None	0.2112	0.1264	**0.0097**	0.3324
PG	-	0.2670	0.0155	**0.0093**
CDA in PG	-	-	0.0181	**0.0076**
LDA in PG	-	-	-	**0.0126**

Table 3.10 The probability (P) of a difference between rates of permeation of salicylic acid through silastic rubber into a pH 3.40 receiver relative to the enhancer used. (Two-tailed heteroscedastic t-test; values in bold are significant at $P \leq 0.01$; CDA, caproic acid N,N-dimethylamide; LDA, lauric acid N,N-dimethylamide; DCA, dodecylamine).

Absorption Enhancer	None	PG	CDA in PG	LDA in PG	DCA in PG
Probability P (T≤t) two-tail	0.0865	0.0796	0.5800	0.7560	**0.0004**

Table 3.11 The probability of a difference between the level of enhancement of salicylic acid permeation across silastic rubber by absorption enhancers with and without a pH-gradient. (Two-tailed heteroscedastic t-test; values in bold are significant at $P \leq 0.01$; CDA, caproic acid N,N-dimethylamide; LDA, lauric acid N,N-dimethylamide; DCA, dodecylamine).

the probability (P) is quoted is the chance of the means of the two groups being equal. The probability is expressed as a fraction of one, for example a value of P=0.01 shows there is a 1% chance of the means from each group being equal. The t-test is performed "two-tailed" to ensure the probability of any difference, either higher or lower, is assessed. The formula to determine the t-test statistical value for t is:

$$t = \frac{\bar{x} - \bar{y}}{\sqrt{\frac{s_1^2}{m} + \frac{s_2^2}{n}}} \qquad \text{(Eq 3.1)}$$

Where s_1 and s_2 are the variances and m and n are the number in the population of the x and y populations respectively. The probability is obtained for the particular calculated value of t from a t-table with respect to the number of degrees of freedom (df) which is calculated from:

$$df = \frac{\left(\frac{s_1^2}{m} + \frac{s_2^2}{n}\right)^2}{\frac{(s_1^2/m)^2}{m-1} + \frac{(s_2^2/n)^2}{n-1}} \qquad \text{(Eq 3.2)}$$

The actual number of degrees of freedom is taken as the nearest integer, as this calculation does not usually give a whole number.

The effectiveness of penetration enhancers was determined by comparing salicylic acid flux after pretreatment with enhancers to flux with no pretreatment upon similar samples of silastic rubber or human skin. This as defined as the flux ratio (otherwise termed the enhancement factor, (Bonina and Montenegro 1992; Ruland and Kreuter 1992)).

$$\text{Flux ratio} = \frac{\text{Initial Steady State Flux Following Enhancer Pretreatment}}{\text{Initial Steady State Flux With No Pretreatment}} \qquad \text{(Eq 3.3)}$$

The results with silastic rubber show that rates from enhancers in IPM vehicles are significantly greater than those in PG vehicles. After pretreatment with IPM, the silastic rubber becomes appreciably distorted, implying that the additional potentiation attributed to IPM over PG is due to membrane damage. The flux ratio of enhancers in IPM is approximately 10 times greater than that of similar enhancers in PG. The addition of enhancers to the IPM vehicle had very little discernible effect and if anything they suppressed penetration. This was probably due to their low potential to damage the rubber membrane in comparison to IPM and their inclusion in the pretreatment solution helped to protect the silastic rubber from damage. This effect of IPM on silastic rubber is considerable and demonstrates that silastic rubber is an inappropriate model for determining the effect of enhancers in this vehicle.

Pretreatment with PG alone did not have a significant enhancing effect upon silastic rubber. PG has been reported to promote skin penetration of metronidazole and oestradiol (Møllgaard and Hoelgaard, 1983b,c) and can promote drug partitioning into the skin (Woodford and Barry, 1986). However, an increasing number of investigators report similar negative effects for PG when used alone. The flux of mannitol, hydrocortisone and progesterone was not increased through human skin (Barry and Bennett 1987). Pretreatment periods of either 1 or 12 hours had little effect upon azidoprofen through hairless mouse skin (Naik *et al.*, 1993). The penetration of various amino acids was not promoted through hairless mouse skin (Ruland and Kreuter, 1992). This lack of effect made the interpretation of the effect of putative enhancers more straightforward. From the flux ratios,0.5M CDA in PG had very little effect upon the penetration of salicylic acid into receivers of either pH. In contrast, 0.5M LDA in PG increased the flux 2.6 and 2.3 times over the vehicle into the pH 7.22 and pH 3.40 receiver

respectively. These results follow a similar trend to salicylic acid partition data into IPM(Irwin and Smith, 1991). Where 0.5M CDA in IPM had only a 2-fold effect on the salicylic acid partition coefficient from aqueous solutions, whereas the LDA had a 10-fold effect.

Using excised hairless mouse skin and a similar pH receiver and donor phase, Naik *et al.* (1993) found that the inclusion of DCA in the donor formulation suppressed penetration of azidoprofen across hairless mouse skin. It was postulated that a large counter-ion may be associated with lower diffusivity, or that a pH-gradient may be essential to facilitate this mode of enhanced drug transport. Membrane pretreatment with DCA in PG increased the flux of caffeine, an essentially unionised molecule, at the experimental pH used. It was surmised that this enhancement was due to a reduction in barrier resistance. Silastic rubber is possibly resistant to this membrane effect resulting in a suppressed permeation of salicylic acid without a pH-gradient. The flux ratio for DCA in PG increases to 1.14 in the pH 7.22 experiments where a pH-gradient is employed. Although this is only 11% increase in flux over the vehicle it is worthwhile noting that the increase in flux over the pH 3.40 experiments is significant at $P < 0.001$ (Table 3.11). The increase in flux observed by both CDA and LDA into the two pH receivers was not significantly different ($P > 0.5$, Table 3.11). Across silastic rubber, the enhancement due to DCA is facilitated by a pH-gradient, whereas that by LDA and CDA is not. This would imply that the effect of DCA is due, at least to some extent to ion-pairing (see sections 2.1 and 3.1.2), whereas the enhancement due to CDA and LDA is due to partitioning phenomena alone. The medium chain LDA (C=12) in PG enhanced permeation of salicylic acid by a flux ratio of 2.37 into the pH 7.22 receiver and 2.95 into the pH 3.40 receiver. In comparison, the shorter chain CDA (C=6) in PG which enhanced salicylic acid by a flux ratio of 1.015 into the pH 7.22 receiver and 1.188 into the pH 3.40 receiver (Tables 3.7 and 3.9). This difference in the enhancing effect between LDA and CDA, which is significant (P=0.0046, pH 7.2 receiver, Table 3.10; P=0.0181, pH 3.4 receiver, Table 3.8) agrees with the data for the enhancement of naproxen across rat skin by a series of N,N-dimethylamides where the C_8 - C_{14} range were found to give the maximum enhancement (Irwin *et al.*, 1990b).

3.3.5 The Effect of a pH-Gradient Upon the Chemical Enhancement of Salicylic Acid Across Excised Human Skin.

To investigate the suitability of silastic rubber as an artificial substitute for human skin, a similar series of experiments was repeated using human skin. Penetration profiles are shown in Figures 3.15 to 3.22, the flux values are numerically detailed in Tables 3.12 and 3.14 and the probability statistics are shown in Tables 3.13, 3.15 and 3.16. Bar chart comparisons of the enhancer flux ratios into the two buffers are shown in Figure 3.23.

PG has a limited effect upon salicylic acid permeation across human skin. This is similar to that observed with silastic rubber. However, in direct contrast to the silastic rubber results, the IPM effect upon human skin is also negligible. Isopropyl myristate does not affect the integrity of human skin as it affects silastic rubber. This is confirmed from the macroscopic detail of the skin, where no obvious destruction was observed. This is anticipated, as isopropyl myristate is frequently used in cosmetic and pharmaceutical topical formulations as a vehicle and moisturising agent (Croda, 1985; 1996)

The LDA in PG had a flux ratio of 3.53 utilising a pH-gradient and 2.93 into the pH 3.40 receiver. These results did not represent a significant difference ($P = 0.3568$, Table 3.16). It can be concluded that the enhancement observed is not due to an ion-pair facilitated mechanism. These results are in agreement with the physicochemical data for N,N-dimethylamides, which are very weak bases with pK_a values of less than 1 (Higuchi *et al.*, 1962; Adelman, 1964). Under these experimental conditions they would not be expected to be sufficiently ionised to promote ion-pairing. This type of potentiation would correspond with the LPP theory of absorption enhancer mechanisms and a significant proportion of enhancement due to these N,N-dimethylamides is probably due to a modification of drug partition into the stratum corneum.

DCA has a massive absorption enhancing effect on salicylic acid through human skin, with flux ratios of 58 into the pH 7.2 receiver and 29 into the pH 3.4 receiver. This degree of potentiation would be consistent with DCA causing a significant reduction in barrier resistance or destruction of the membrane. Naik *et al.*, (1993) studying the enhancement of azidoprofen

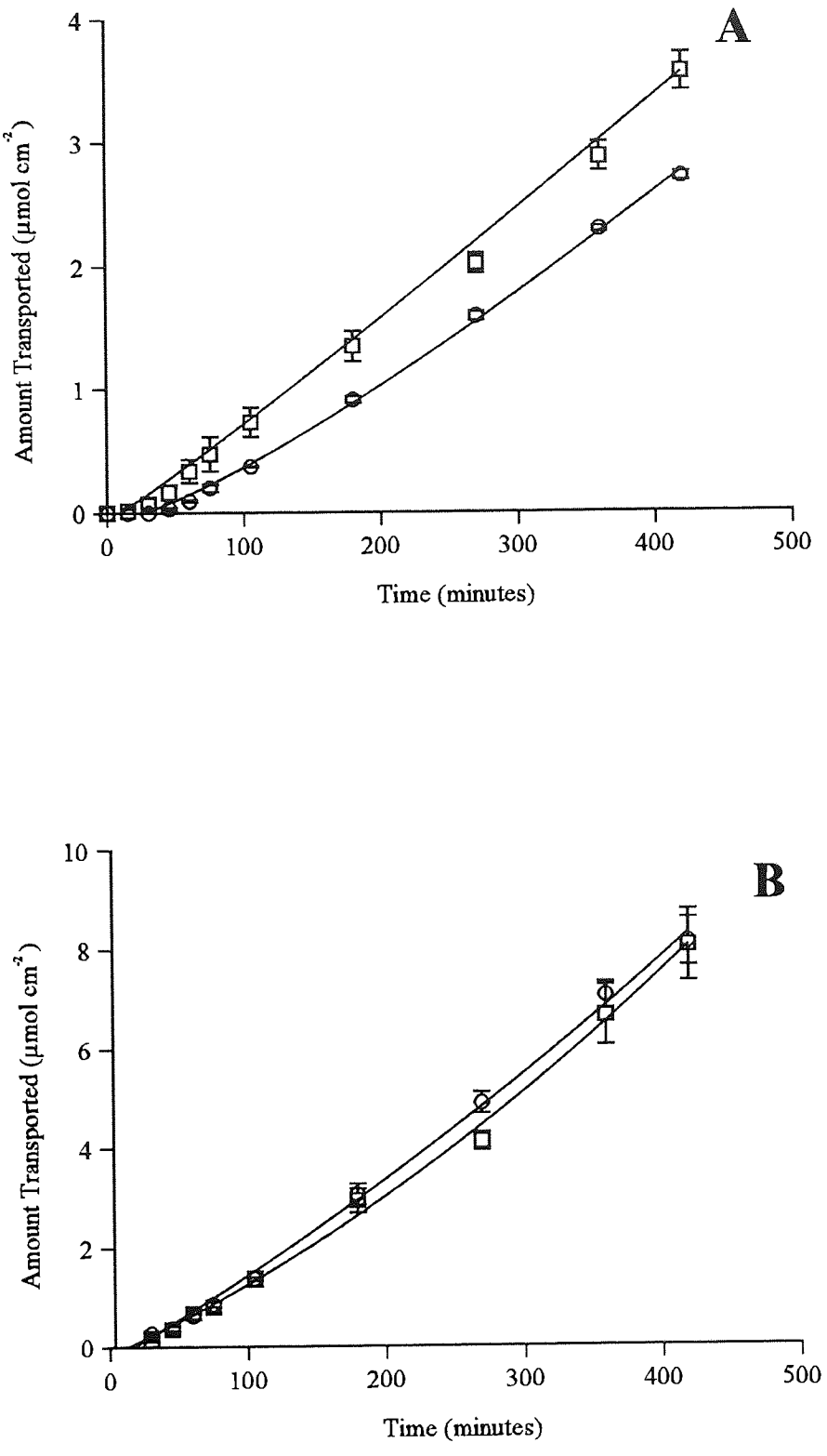

Figure 3.15 The effect of pretreatment with propylene glycol upon the permeation of salicylic acid from saturated aqueous suspensions at pH 4.04 across human skin (○ Control; □ Pretreated skin; Error bars represent SEM) .

A McIlvaine buffer pH 7.22 receiver phase; pH 4.04 donor phase
B McIlvaine buffer pH 3.42 receiver phase; pH 4.04 donor phase

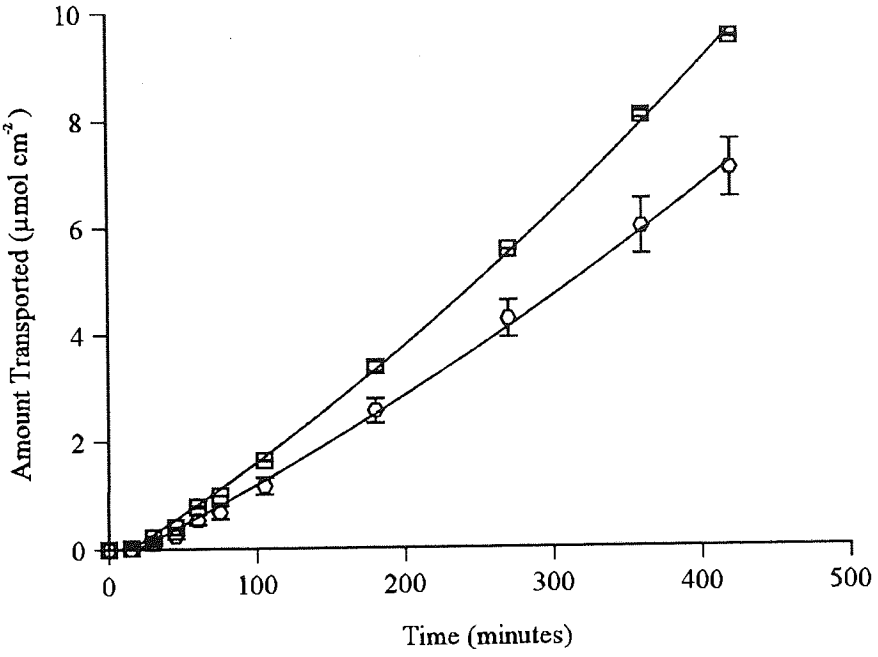

Figure 3.16 The effect of pretreatment with isopropyl myristate upon the permeation of salicylic acid from saturated aqueous suspensions at pH 4.04 across human skin into a pH 7.22 McIlvaine buffer receiver (○, Control; □, Pretreated skin; Error bars represent SEM).

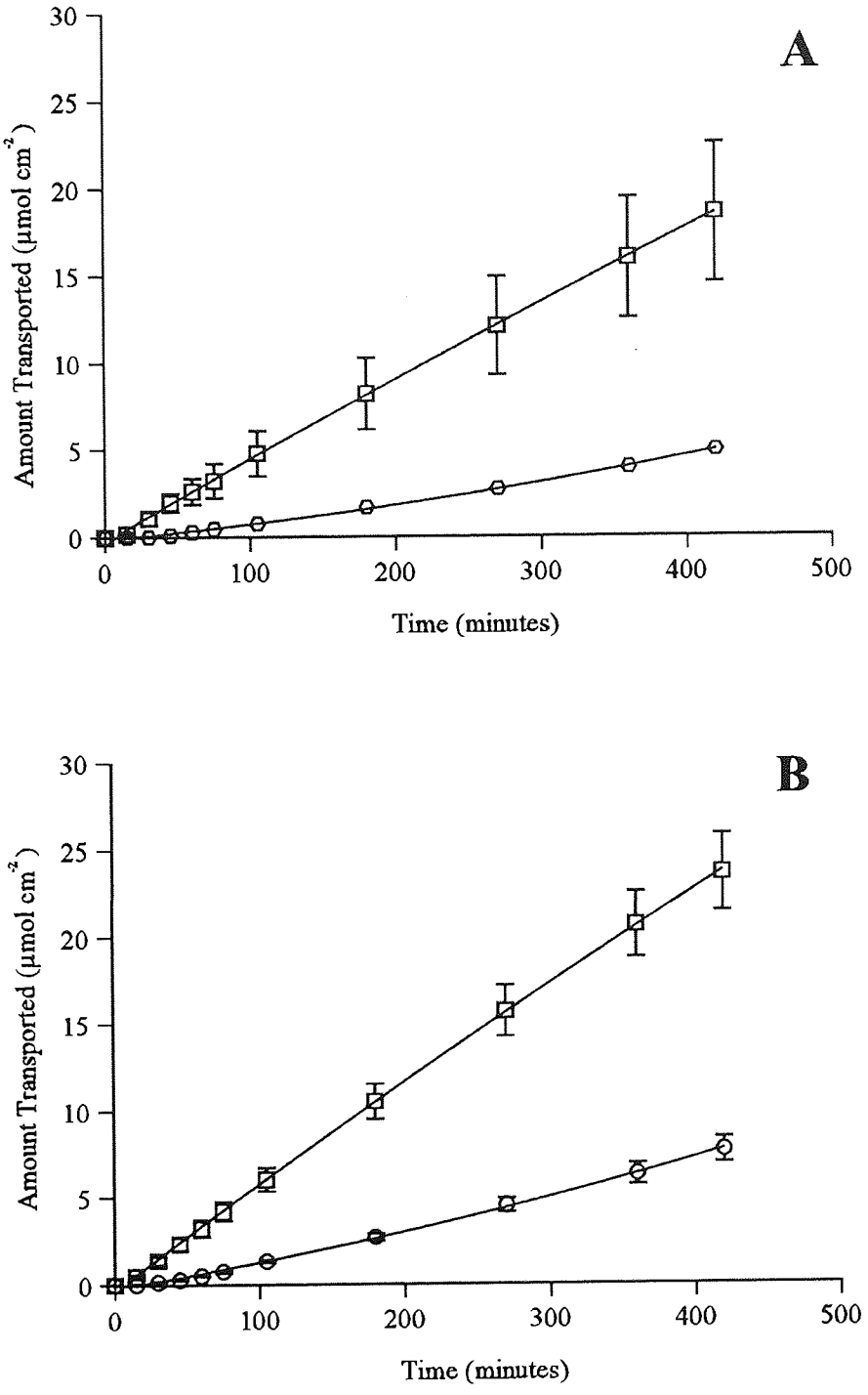

Figure 3.17 The effect of pretreatment with 0.5M lauric acid dimethylamide in propylene glycol upon the permeation of salicylic acid from saturated aqueous suspensions at pH 4.04 across human skin (○, Control; □, Pretreated skin; Error bars represent SEM).

A McIlvaine buffer receiver pH 7.22; pH 4.04 donor phase
B McIlvaine buffer receiver pH 3.42; pH 4.04 donor phase

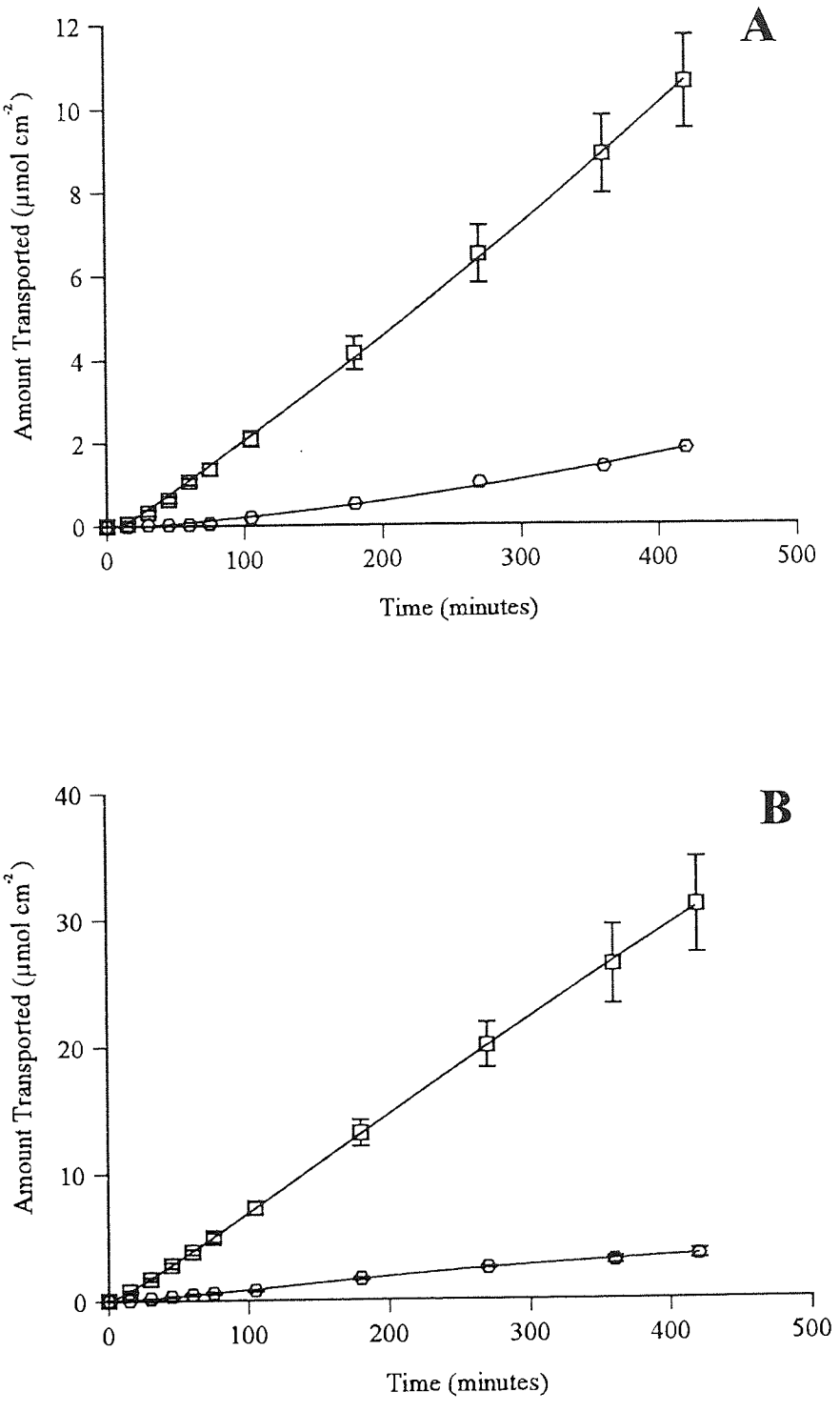

Figure 3.18 The effect of pretreatment with 0.5M lauric acid dimethylamide in isopropyl myristate upon the permeation of salicylic acid from saturated aqueous suspensions at pH 4.04 across human skin (○, Control; □, Pretreated skin; Error bars represent SEM).

A McIlvaine buffer receiver pH 7.22; pH 4.04 donor phase
B McIlvaine buffer receiver pH 3.42; pH 4.04 donor phase

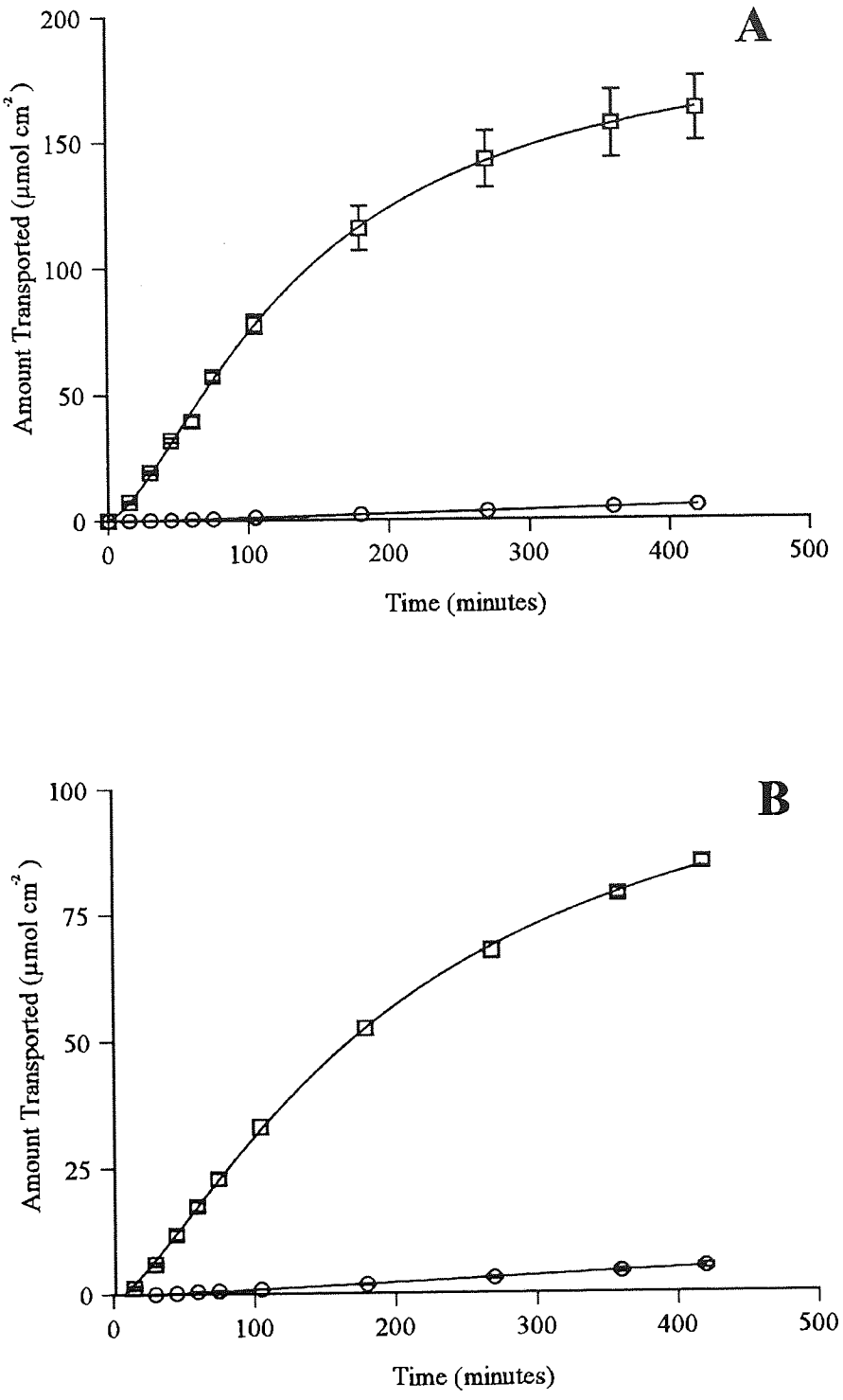

Figure 3.19 The effect of pretreatment with 0.5M dodecylamine in isopropyl myristate upon the permeation of salicylic acid from saturated aqueous suspensions at pH 4.04 across human skin (○, Control; □, Pretreated skin; Error bars represent SEM).

A McIlvaine buffer receiver pH 7.22; pH 4.04 donor phase
B McIlvaine buffer receiver pH 3.42; pH 4.04 donor phase

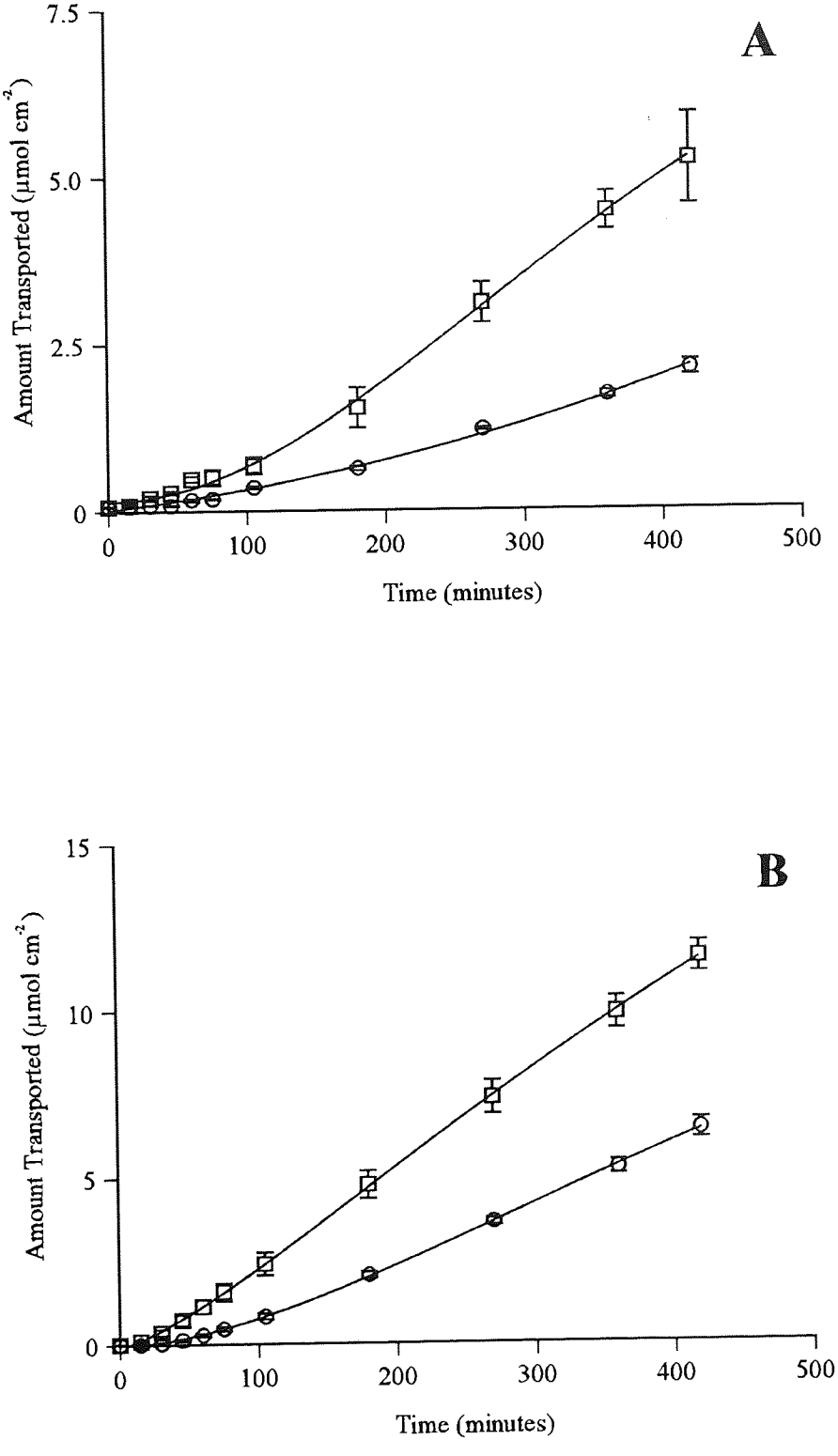

Figure 3.20 The effect of pretreatment with 0.5M Azone in propylene glycol upon the permeation of salicylic acid from saturated aqueous suspensions at pH 4.04 across human skin (○, Control; □, Pretreated skin; Error bars represent SEM).

A McIlvaine buffer receiver pH 7.22; pH 4.04 donor phase
B McIlvaine buffer receiver pH 3.42; pH 4.04 donor phase

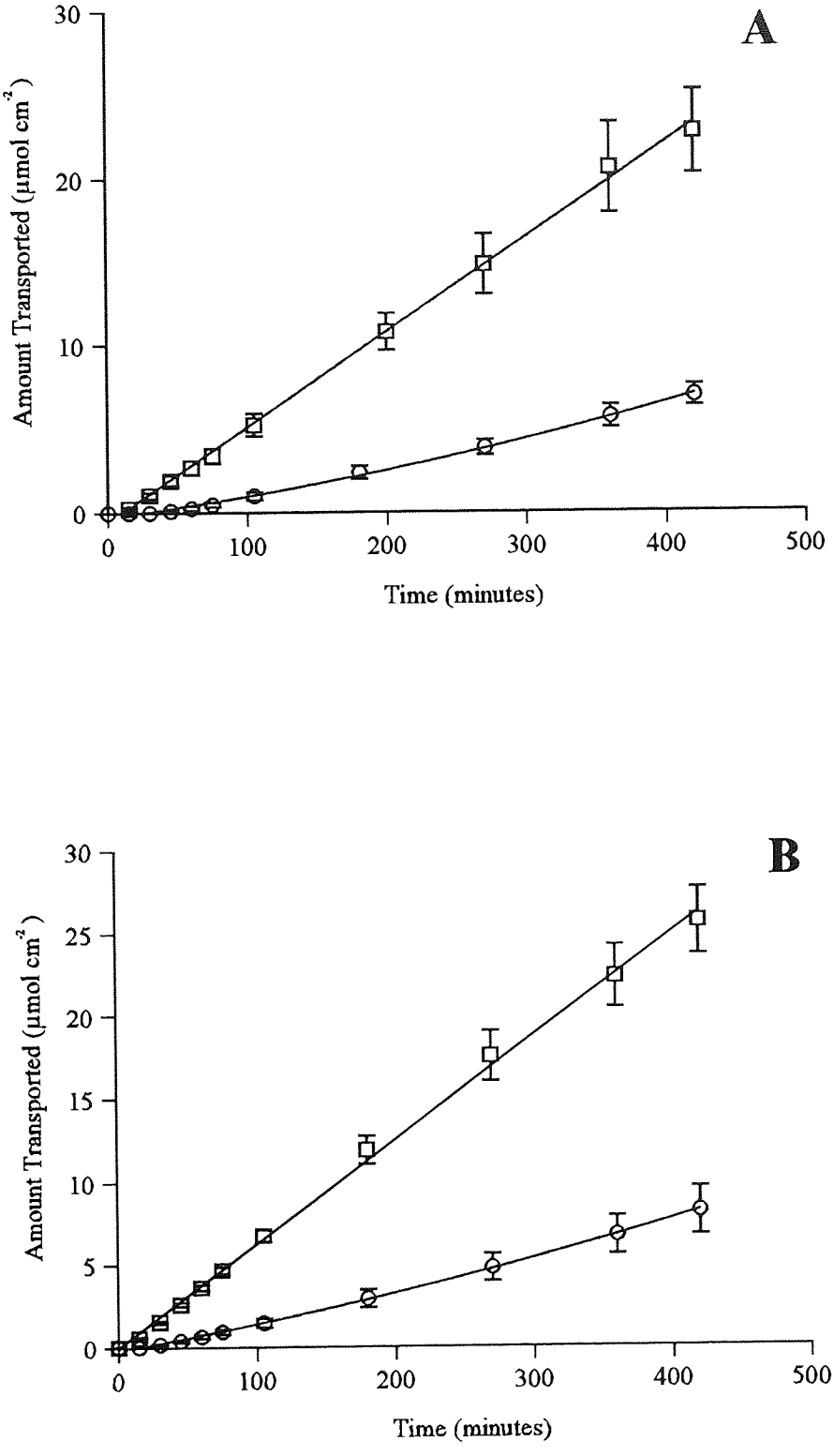

Figure 3.21 The effect of pretreatment with 0.5M oleic acid in propylene glycol upon the permeation of salicylic acid from saturated aqueous suspensions at pH 4.04 across human skin (○, Control; □, Pretreated skin; Error bars represent SEM).

A McIlvaine buffer receiver pH 7.22; pH 4.04 donor phase
B McIlvaine buffer receiver pH 3.42; pH 4.04 donor phase

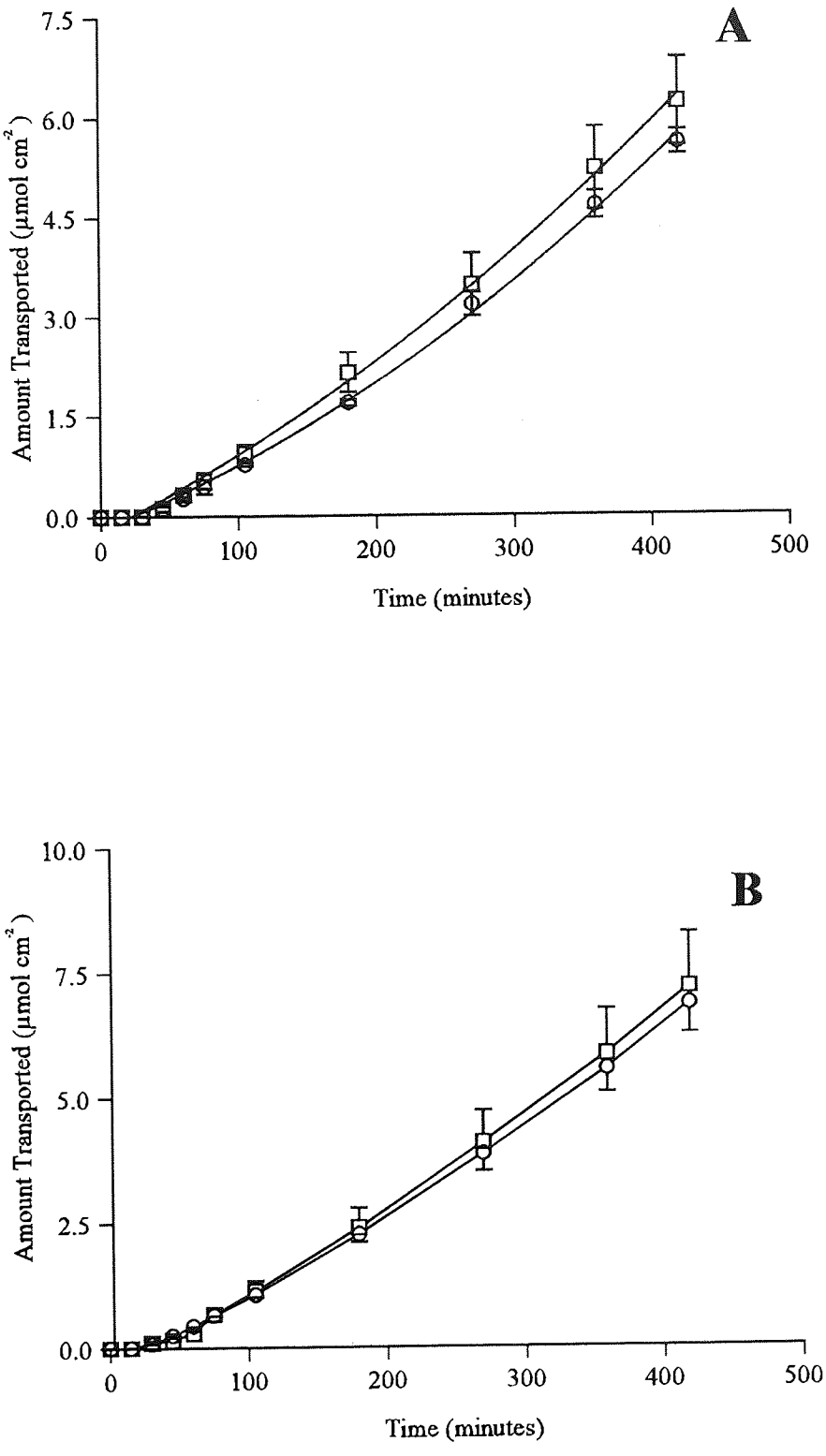

Figure 3.22 The effect of pretreatment with 0.5M transcutol in propylene glycol upon the permeation of salicylic acid from saturated aqueous suspensions at pH 4.04 across human skin (○, Control; □, Pretreated skin; Error bars represent SEM).

A McIlvaine buffer receiver pH 7.22; pH 4.04 donor phase
B McIlvaine buffer receiver pH 3.42; pH 4.04 donor phase

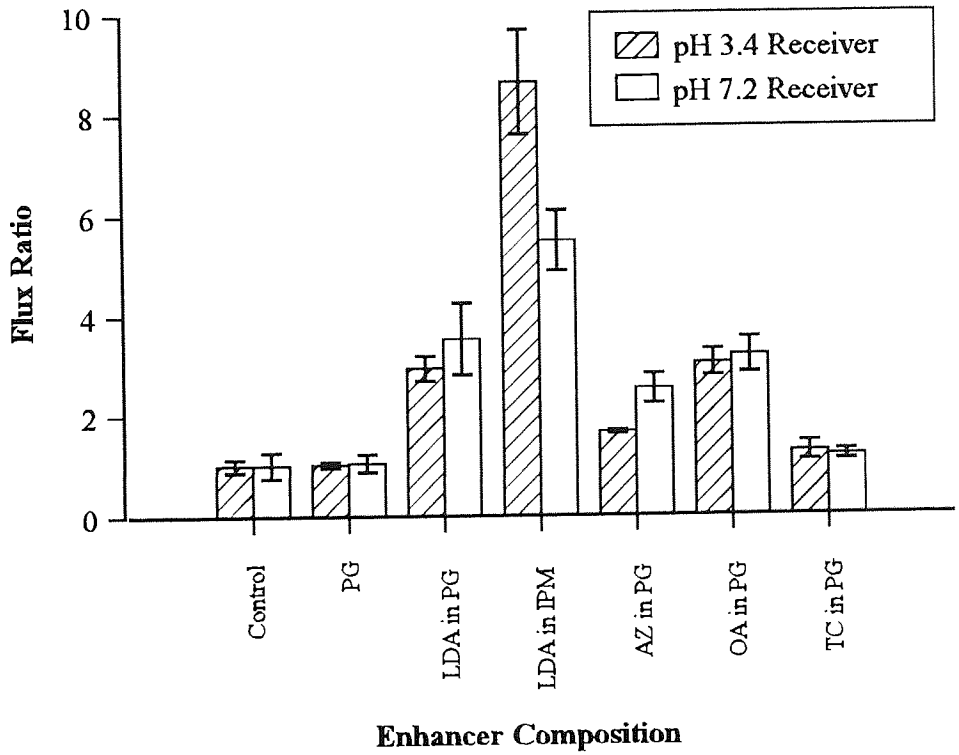

Figure 3.23 The effect of enhancer pretreatment on the flux ratio of salicylic acid from saturated suspensions at pH 4.04 across human skin with and without a pH gradient (Error bars represent the standard error of the mean).

Pretreatment[a]	Flux (μmol cm^{-2} hr^{-1})	k_{obs} (cm hr^{-1}x10^{3})	Flux Ratio[b]
None	0.649 (0.141)	2.89 (0.628)	-
PG	0.788 (0.008)	3.55 (0.034)	1.215
IPM	0.868 (0.002)	3.86 (0.008)	1.335
LDA in PG	2.625 (0.323)	11.69 (1.437)	3.529
LDA in IPM	3.235 (0.201)	14.40 (0.897)	5.496
DCA in IPM	38.101 (1.385)	169.6 (6.168)	57.839
Azone in PG	1.306 (0.095)	6.55 (0.423)	2.522
OA in PG	2.264 (0.128)	10.08 (0.570)	3.192
TC in PG	0.758 (0.063)	3.37 (0.0280)	1.174

[a] Enhancer concentrations are 0.5M in their respective vehicles
[b] Flux ratio is the flux following pretreatment with enhancer / no pretreatment

Table 3.12 Permeation data following enhancer pretreatment of salicylic acid from saturated suspensions at pH 4.04 across human skin into a buffer receiver at pH 7.22. (Values in parentheses are the standard errors of the mean; Rates are normalised to none pretreated controls).

and caffeine across excised hairless mouse skin came to similar conclusions. Although the amount transported versus time profile showed a marked reduction in flux after 3 hours (Figure 3.19), which could be interpreted as a reversible effect due to an exhausting enhancer effect. A more likely explanation is a thermodynamic effect due to the reduction of the concentration gradient of the salicylic acid. The quantity of salicylic acid transported into the pH 7.2 receiver gave a concentration of representing 6.2% of the donor concentration which would have reduced the true "sink" conditions of the experiment. It may be relevant to test this hypothesis by a more exacting "reversibility experiment".

Without a pH-gradient, Azone demonstrated a flux ratio of 1.65, implying that this aspect of Azone enhancement is achieved *via* a direct membrane effect. Azone is a non-polar molecule that partitions directly into the lipid regions of the stratum corneum and prevents the lipid chains from associating and crystallising. The increased fluidity reduces the diffusional resistance to drugs (Barry, 1991b, Beastall *et al.*, 1988). Azone has also been associated with the ion-pairing theory of facilitated drug transport (Hadgraft *et al.*, 1985). The results utilising

	PG	IPM	LDA in PG	LDA in IPM	DCA in PG	Azone in PG	OA in PG	TC in PG
None	0.4558	0.1123	0.0326	**0.0139**	**0.0001**	**0.0139**	**0.0082**	0.5538
PG	-	0.0869	0.0485	**0.0055**	**0.0001**	0.0463	0.0308	0.7206
IPM	-	-	0.0269	**0.0018**	**0.0001**	0.0285	0.0188	0.1905
LDA in PG	-	-	-	0.0813	**0.0001**	0.1810	0.6358	0.0229
LDA in IPM	-	-	-	-	**0.0001**	**0.0019**	**0.0079**	**0.0011**
DCA in PG	-	-	-	-	-	**0.0001**	**0.0001**	**0.0001**
Azone in PG	-	-	-	-	-	-	0.2232	0.0338
OA in PG	-	-	-	-	-	-	-	0.0235

Table 3.13 The probability (P) of a difference between rates of permeation of salicylic acid from saturated suspensions at pH 4.04 through human skin into a pH 7.22 receiver relative to the enhancer used. (Two-tailed heteroscedastic t-test; values in bold are significant at $P \leq 0.01$; CDA, caproic acid N,N-dimethylamide; LDA, lauric acid N,N-dimethylamide; DCA, dodecylamine; OA, oleic acid; TC, transcutol).

a pH-gradient show a further enhancement of transdermal flux, with a flux ratio of 2.52. With Azone as an enhancer the flux with and without a pH-gradient is not significantly different (P=0.0915, Table 3.16). This suggests that Azone does not enhance transdermal flux of salicylic acid *via* an ion-pairing mechanism. These results support the hypothesis developed in Chapter 4 that, in some cases, the action of Azone can be explained by partition effects alone. In these experiments it is assumed that the buffer solutions on either side of the skin will affect the ionic state of the absorption enhancers and permeant during their passage across the skin. The skin has a good buffering capacity and the receiver and donor phase buffers may not necessarily affect the pH of the skin itself.

In the PG vehicle, OA is the most efficient penetration enhancer. The flux ratio was similar with and without a pH-gradient. This effect would confirm the hypothesis that OA exerts its action by the disruption of the lipid layer. Once OA has penetrated into the stratum corneum lipids its "kinked" structure due to the *cis*- double bond, disrupts and increases the fluidity of the lipid packing. Co-solvents such as PG have a synergistic action with OA. This may be due

Pretreatment[a]	Flux (μmol cm^{-2} hr^{-1})	k_{obs} (cm hr^{-1}x10^{3})	Flux Ratio[b]
None	0.639 (0.069)	2.85 (0.309)	-
PG	0.650 (0.027)	2.89 (0.121)	1.017
LDA in PG	1.875 (0.134)	8.35 (0.592)	2.932
LDA in IPM	5.529 (0.577)	24.62 (2.571)	8.648
DCA in IPM	18.446 (0.624)	82.12 (2.781)	28.849
Azone in PG	1.057 (0.017)	4.70 (0.074)	1.653
OA in PG	1.942 (0.138)	8.64 (0.616)	3.037
TC in PG	0.803 (0.097)	3.575 (0.433)	1.256

[a] Enhancer concentrations are 0.5M in their respective vehicles
[b] Flux ratio is the flux following pretreatment with enhancer / no pretreatment

Table 3.14 Permeation data following enhancer pretreatment of salicylic acid from saturated suspensions at pH 4.04 across human skin into a buffer receiver at pH 3.40. Values in parentheses are the standard errors of the mean. (Rates are normalised to none pretreated controls)

	PG	LDA in PG	LDA in IPM	DCA in IPM	Azone in PG	OA in PG	TC in PG
None	0.8753	0.0104	0.0048	0.0017	0.0026	0.0104	0.3047
PG	-	0.0143	0.0052	0.0018	0.0012	0.0141	0.3269
LDA in PG	-	-	0.0097	0.0014	0.0356	0.7908	0.0077
LDA in IPM	-	-	-	0.0001	0.0067	0.0101	0.0049
DCA in IPM	-	-	-	-	0.0019	0.0014	0.0015
Azone in PG	-	-	-	-	-	0.0331	0.1632
OA in PG	-	-	-	-	-	-	0.0073

Table 3.15 The probability (P) of a difference between rates of permeation of salicylic acid through human skin into a pH 3.40 receiver relative to the enhancer used. (Two tailed heteroscedastic t-test; CDA, caproic acid N,N-dimethylamide; LDA, lauric acid N,N-dimethylamide; DCA, dodecylamine; P ($T \leq t$) two-tail).

Absorption Enhancer	None	PG	LDA in PG	LDA in IPM	DCA in IPM	Azone in PG	OA in PG
Probability P (T≤t) two-tail	0.9612	0.0395	0.3568	0.0532	0.0001	0.0915	0.6778

Table 3.16 The probability of a difference between the level of enhancement of salicylic acid permeation across human skin by absorption enhancers with and without a pH-gradient. (Two tailed heteroscedastic t-test; CDA, caproic acid N,N-dimethylamide; LDA, lauric acid N,N-dimethylamide; DCA, dodecylamine; OA, oleic acid; TC, transcutol).

to the co-solvent's ability to reduce the polarity of the aqueous regions of the stratum corneum, so increasing the ability of the stratum corneum to solubilise OA.

Transcutol in PG had a very limited apparent effect upon the flux of salicylic acid across human skin. However, it has been shown that Transcutol increases the flux of model drugs into the human stratum corneum possibly by increasing the solubility of the penetrant in the stratum corneum (Harrison *et al.*, 1996), but the drugs remain in this layer as a depot (Panchagnula and Ritschel, 1991). Transcutol is believed to cause intercellular lipid swelling without altering the multiple bilayer structure. This effect results in the drug depot developing within the stratum corneum, hence the increased penetration of drugs into the skin and the decreased permeation across the skin. The experimental method used in this study only measured the drug penetrating through the skin so this depot effect of Transcutol would not have been observed. This mode of action may be usefully exploited as a co-solvent of other enhancers such as Azone or oleic acid.

3.4 Summary

The penetration of salicylic acid from saturated suspensions through excised human epidermis and silastic membrane was investigated. The influence of a pH-gradient, donor pH and receiver pH upon skin penetration was studied to correlate these parameters to the drug-vehicle-membrane inter-relationships governing penetration. Results showed that salicylic acid

flux was not influenced by a pH-gradient with respect to either the donor or receiver pH. These results provided further evidence that transport of salicylic acid obeyed the pH-partition hypothesis. Permeation studies using skin and silastic membrane as model membranes to study the influence of ionisation gave similar profiles, again demonstrating the suitability of the silastic rubber model for this type of study.

Silastic rubber was not ideal for studies with absorption enhancers. It showed a number of characteristics at variance with the excised skin model. This was especially apparent using isopropyl myristate as the enhancer vehicle. The isopropyl myristate disrupted the silastic rubber both visually, leaving the membrane puckered and distorted, and physically by disrupting the membranes properties towards salicylic acid. Dodecylamine, which had a significant effect upon human skin, probably reducing the barrier resistance *via* a change in the skins integrity, had very little effect on the transport of salicylic acid through silastic rubber. For these reasons, studies were not extended to the use of Azone, oleic acid and Transcutol on this membrane.

Investigations using human skin confirmed that oleic acid and Azone are valuable compounds for enhancing transdermal penetration. Both demonstrate actions of lipid perturbation, but comparing enhancement potential with and without a pH-gradient, neither compound demonstrated potential for enhanced permeation due to ion-pairing. LDA also showed potential for enhancing transdermal penetration. An increased partition into the absorption barrier is a likely mode of action. The system did not show evidence of an ion-pair facilitated transport which is as expected with this compound as it would be unionised at the experimental pHs. The increase in transdermal flux of salicylic acid with LDA as an enhancer was further potentiated using IPM as a vehicle as opposed to PG. Transcutol in PG and the two vehicles alone, IPM and PG had minimal effects upon the rate of flux, but these observations may be due to some extent to methodology.

The evidence from this series of experiments with and without pH-gradients demonstrate that, under certain conditions, the transdermal penetration enhancement of a number of topical enhancing compounds, including Azone and oleic acid, can be explained without recourse to ion-pair phenomenon.

CHAPTER FOUR

EXTRACTION COEFFICIENTS AND FACILITATED TRANSPORT.

THE EFFECT OF ABSORPTION ENHANCERS

4.1 Introduction

4.1.1 Extraction Coefficients and Absorption Enhancers

The factors that control the rates of percutaneous absorption and moderate topical delivery of medicinal agents are under intensive study (Bronaugh and Maibach, 1989; Hadgraft and Guy, 1989; Walters and Hadgraft, 1993; Yamane *et al.*, 1995). The rate-limiting nature of the stratum corneum in healthy skin is well recognised and strategies are being developed to enhance the frequently low delivery rates of topical drugs. These approaches include the use of absorption enhancers such as Azone (Stoughton, 1983; Stoughton and McClure, 1983) or alkyl methyl sulphoxides (Sekura and Scala, 1972), the design of facilitated absorption systems that involve ion-pair enhancement of delivery profiles (Barker and Hadgraft, 1981; Barker *et al.*, 1984) and the use of iontophoresis to drive a flux of ionic or neutral compounds across the skin under the influence of an electric potential (Tyle and Kari, 1988).

It has been observed that the transport of salicylate across an isopropyl myristate membrane using a rotating diffusion cell (Albery *et al.*, 1976; Guy and Fleming, 1979) is enhanced in the presence of Azone (Hadgraft *et al.*, 1985). Utilising a pH-gradient of 5 to 7.4 across the membrane to represent the natural pH-gradient that exists across skin, it was suggested that a facilitated transport system as described in Chapter 2.1 and Figure 2.1 was established in the rotating diffusion cell. This transport system is dependent upon the formation of ion-pairs in the pH 5 donor vehicle which can then partition into the bulk lipid phase and diffuse down their concentration gradient to the opposite interface. In the interfacial region at the higher pH, the carrier deprotonates to release the anions. The extraction of the salicylate anion from aqueous solutions into the IPM organic phase was studied in order to determine whether this enhancement is due to ion-pair formation by Azone or a co-solvent effect. The extraction into the organic phase was investigated with and without Azone and as a function of the pH of the aqueous phase.

A sigmoidal relationship was seen for the extraction coefficients of salicylate between the aqueous buffer solutions and isopropyl myristate phases (Figure 4.1). This relationship is due to the favourable extraction into the organic phase by the unionised form of salicylate present at low pHs. With increasing pH the ionised form of salicylate becomes predominant. This has a less favourable extraction into the organic phase. The addition of Azone to the isopropyl

Figure 4.1 pH extraction profiles for salicylate between aqueous solution and IPM (○), and 0.1M Azone in IPM (●). The relation between the extraction coefficient into 0.1M Azone in IPM, divided by the extraction coefficient into IPM is also shown (■). (From Hadgraft *et al.*, 1985).

myristate phase shifts the sigmoidal curve to the right (Figure 4.1). This has been explained by the ionisation state of Azone, which was stated to be fully ionised at low pH and only partially ionised at high pH. Therefore, as the pH approaches 5.5 the amount of salicylate which can form ion-pairs with Azone increases. With further increase in pH the proportion of ionised Azone available for ion-pairing decreases and the extraction of salicylate ions becomes less efficient. This relationship is illustrated by a plot of the ratios of extraction coefficients determined with and without Azone, as a function of pH, which produces a bell-shaped curve (Hadgraft *et al.*, 1985). The peak of this curve represents the optimum pH conditions for ion-pair formation (Figure 4.1). The conclusions that Azone could be used to enhance the percutaneous absorption of anionic entities by an ion-pair facilitated transport mechanism have reached the review literature (Neubert, 1989).

While these ion-pair interactions may not be totally excluded, particularly in the low polarity solvents used, this study is presented to show that an enhancement of salicylate partitioning is caused by amide additives to the organic phase and the extraction coefficient versus pH profiles and ratio plots follow similar profiles to Azone. The amides used are very weak bases

with pKa values of less than 1 (Higuchi *et al.*, 1962; Adelman, 1964) and under the experimental conditions studied would not be expected to be sufficiently ionised to promote ion-pairing. Therefore, it is proposed that these effects may be explained solely on the basis of partition and ionisation equilibria without recourse to ion-pair formation.

4.1.2 Aims and Objectives

The aim of this study was to develop a mathematical model to predict the extraction coefficients of weak acids using parameters based only upon partition coefficients of ionised and unionised species between aqueous and organic phases. This model would not include any mathematical parameters based upon ion-pairing. Experimental data resulting from the distribution of salicylic acid between an aqueous phase and IPM containing tertiary amide enhancers of percutaneous absorption was assessed for goodness of fit with this theoretical model.

4.2 Experimental

4.2.1 Materials

Aqueous buffer solutions were prepared over the pH range 2.0 - 8.0 using McIlvaine's citrate-phosphate system (Appendix 1). All buffer solutions were preserved using 0.002% phenyl-mercuric nitrate. Final pH values were measured using a Gallenkamp refillable general-purpose combination glass electrode attached to a Phillips PW 9409 digital pH meter. Values were adjusted as nearly as possible to pH 2.10, 2.37, 2.75, 3.15, 3.53, 3.96, 4.35, 4.75, 5.13, 5,48, 5.85 and 8.17. Reagents used were isopropyl myristate (Croda), sodium salicylate (BDH), lauric acid *N,N*-dimethylamide (Sigma), caproic acid *N,N*-dimethylamide (Sigma) and Azone^{R} (Nelson Research). All HPLC solvents were of Hypersolv grade. Analyses were undertaken using an HPLC system constructed from a Pye Unicam PU 4010 dual-head reciprocating pump, a Rheodyne 7125 injection valve fitted with a 20µl loop, a stainless-steel column (10 cm x 4.6 mm i.d.) containing Spherisorb S5 ODS-1 (5µm) stationary phase and a Pye Unicam PU 4020 UV detector equipped with an 8µl flow cell. The detector was operated at a wavelength of 0.08 AUFS and results were analysed using a Trivector Trio Chromatography computing integrator. The mobile phase, comprising methanol / water / tetrahydrofuran / orthophosphoric acid (50 : 47 : 3 : 0.01), was degassed in an ultrasonic bath

immediately prior to use and was delivered at a flow rate of 1 ml min^{-1}. The retention time of salicylic acid under these conditions was 3.87 minutes.

4.2.2 Methods

Partition coefficients of salicylic acid and isopropyl myristate were obtained with and without the presence of added enhancer over the pH range 2.1-8.2. Organic phases comprising isopropyl myristate (IPM), 0.1 and 0.5 M lauric acid *N,N*-dimethylamide (LDA) in IPM, 0.1 and 0.5 M caproic acid *N,N*-dimethylamide (CDA) in IPM and 0.1 M Azone^{R} in IPM were prepared and presaturated with the range of buffer solutions. Aqueous buffer phases were also presaturated with the appropriate organic phase and were prepared to contain sodium salicylate (approximately 2 mg ml^{-1}). Aliquots of the aqueous phases (15 ml) were pipetted into 25 ml volumetric flasks which were then made up to volume with the organic phase. Flasks were maintained at 25°C and were stored, with stirring, for 2 days. Aqueous phases were removed using a glass syringe, centrifuged twice to remove any residual organic phase and were then diluted appropriately and assayed by HPLC. A calibration curve over the range 4×10^{-3} to 2×10^{-2} mg ml^{-1} was prepared and residual concentrations were obtained by interpolation after appropriate dilution dependent upon pH. Extraction ratios were calculated according to Equation 4.2 and were modelled theoretically using an IBM PC computer simulation based upon Equations 4.11 and 4.12.

4.3 Theoretical

The extraction ratio is a measure of the partitioning behaviour of species between two immiscible solvents. It may be defined as the ratio of material extracted by an immiscible solvent to the original amount of material present. If the initial aqueous solution has a concentration of solute C_1 in a volume V_w and, after extraction with an immiscible solvent of volume V_o, the aqueous concentration of solute is C_2, the extraction ratio (ER') is given by:

$$ER' = \frac{C_1 - C_2}{C_1} \qquad \text{(Eq 4.1)}$$

As such, these values are dependent upon the phase volume ratio. An alternative expression which defines the extraction ratio (ER) as a volume-dependent parameter is:

$$ER = \frac{C_1V - C_2V}{C_1V - C_2V + C_2} \qquad \text{(Eq 4.2)}$$

Where the phase volume ratio $V = V_w / V_o$. When equal volumes of aqueous and organic phases are used ($V = 1$) this expression reduces to Equation 4.1. For an ionisable molecule, the value of the extraction coefficient depends upon the partition coefficients of the molecule and ion, and upon the dissociation constant of the acid. This may be shown as follows for a weak acid (HA) partitioning between aqueous and oil phases and undergoing ionisation.

$$HA_o \underset{oil}{\overset{K_2}{\rightleftharpoons}} HA_w \underset{water}{\overset{K_1}{\rightleftharpoons}} H^+ + A_w^- \underset{oil}{\overset{K_3}{\rightleftharpoons}} A_o^-$$

Where subscripts o and w refer to oil and water phases, K_1 is the acid dissociation constant and K_2 and K_3 are the partition coefficients of the neutral molecule and anion respectively. The equilibria may be defined as :

$$K_1 = \frac{[H^+][A_w^-]}{[HA_w]} \qquad \text{(Eq 4.3)}$$

$$K_2 = \frac{[HA_o]}{[HA_w]} \qquad \text{(Eq 4.4)}$$

$$K_3 = \frac{[A_o^-]}{[A_w^-]} \qquad \text{(Eq 4.5)}$$

The total acid in the system (HA_T) is given by :

$$HA_T = [HA_w]V_w + [A_w^-]V_w + [HA_o]V_o + [A_o^-]V_o$$

expressing this in terms of the initial aqueous concentration ($[HA]_T = HA_T / V_w$) leads to :

$$[HA]_T = [HA_w] + [A_w^-] + [HA_o]/V + [A_o^-]/V$$

Substitution for $[A_w^-]$, $[HA_o]$ and $[A_o^-]$ using transformations of equations 4.3 to 4.5 detailed below, leads to a solution for $[HA]_T$ as a function of $[HA_w]$:

Equation 4.3 becomes :

$$[A_w^-] = \frac{[HA_w]\ K_1}{[H^+]} \qquad \text{(Eq 4.3a)}$$

Equation 4.4 becomes :

$$[HA_o] = [HA_w]K_2 \qquad \text{(Eq 4.4a)}$$

Equation 4.5 becomes :

$$[A_o^-] = [A_w^-]K_3 \qquad \text{(Eq 4.5a)}$$

substitution of Equation 4.3a with Equation 4.5a gives :

$$[A_o^-] = \frac{[HA_w]K_1K_3}{[H^+]} \qquad \text{(Eq 4.5b)}$$

Therefore $[HA_T]$ as a function of $[HA_w]$ becomes :

$$[HA]_T = [HA_w] + \frac{[HA_w]K_1}{[H^+]} + \frac{[HA_w]K_2}{V} + \frac{[HA_w]K_1K_3}{V[H^+]}$$

Multiplying out $[HA_w]$:

$$[HA]_T = [HA_w]\left(1 + \frac{K_1}{[H^+]} + \frac{K_2}{V} + \frac{K_1K_3}{V[H^+]}\right)$$

Divided through by $V[H^+]$ gives :

$$[HA]_T = [HA_w]\left(\frac{[H^+]V + K_1V + K_2[H^+] + K_1K_3}{[H^+]V}\right) \qquad \text{(Eq 4.6)}$$

Equations 4.3 to 4.5 and 4.6 lead to the following species concentrations as a function of the initial aqueous concentration of acid in the system $[HA]_T$:

Arranging Equation 4.6 with respect to $[HA_w]$:

$$[HA_w] = [HA]_T\left(\frac{[H^+]V}{[H^+]V + K_1V + K_2[H^+] + K_1K_3}\right)$$

Multiplying out :

$$[HA_w] = \frac{[HA]_T[H^+]V}{[H^+]V + K_1V + K_2[H^+] + K_1K_3} \qquad \text{(Eq 4.7)}$$

Substituting $[HA_w]$ in Equation 4.7 with $[A_w^-]$ from Equation 4.3a :

$$[A_w^-] = \frac{[HA]_TK_1V}{[H+]V + K_1V + K_2[H^+] + K_1K_3} \qquad \text{(Eq 4.8)}$$

Substituting [HA $_w$] in Equation 4.7 with [HA $_o$] from Equation 4.4a :

$$[HA_o] = \frac{[HA]_T K_2 [H^+] V}{[H^+]V + K_1 V + K_2[H^+] + K_1 K_3} \qquad \text{(Eq 4.9)}$$

Substituting [HA $_w$] in Equation 4.7 with [A $_o^-$] from Equation 4.5b :

$$[A_o^-] = \frac{[HA]_T K_1 K_3 V}{[H^+]V + K_1 V + K_2[H^+] + K_1 K_3} \qquad \text{(Eq 4.10)}$$

When no significant ion partition occurs ($K_3 = 0$) or in the absence of partitioning ($K_2 = 0$, $K_3 = 0$) these expressions reduce to :

Species	No ion partition $K_3 = 0$	No partition $K_2 = 0$ $K_3 = 0$
[HA $_w$]	$\frac{[HA]_T [H^+] V}{[H^+]V + K_1 V + K_2[H^+]}$	$\frac{[HA]_T [H^+]}{[H^+] + K_1}$
[A $_w^-$]	$\frac{[HA]_T K_1 V}{[H^+]V + K_1 V + K_2[H^+]}$	$\frac{[HA]_T K_1}{[H^+] + K_1}$
[HA $_o$]	$\frac{[HA]_T K_2 [H^+] V}{[H^+]V + K_1 V + K_2[H^+]}$	0
[A $_o^-$]	0	

Substitution of these values into Equations 4.1 and 4.2, where $C_1 = [HA]_T$ and $C_2 = [HA_w] + [A_w^-]$, provides an estimate for the extraction coefficient of the system such that :

$$ER' = \frac{K_2[H^+] + K_1K_3}{[H^+] + K_1 + K_2[H^+] + K_1K_3} \qquad \text{(Eq 4.11)}$$

and

$$ER = \frac{K_2[H^+] + K_1K_3}{[H^+]V + K_1V + K_2[H^+] + K_1K_3} \qquad \text{(Eq 4.12)}$$

In systems where no significant ion partition is observed ($K_3 = 0$) this reduces to :

$$ER' = \frac{K_2[H^+]}{[H^+] + K_1 + K_2[H^+]} \qquad \text{(Eq 4.13)}$$

and

$$ER = \frac{K_2[H^+]}{[H^+]V + K_1V + K_2[H^+]} \qquad \text{(Eq 4.14)}$$

When no ionisation occurs ($K_1 = 0$, $K_3 = 0$) the extraction ratio is related to the partition coefficient (K_2, P) by :

$$ER' = \frac{K_2}{K_2 + 1} \qquad \text{(Eq 4.15)}$$

and

$$ER = \frac{K_2}{K_2 + V} \qquad \text{(Eq 4.16)}$$

4.4 Results and Discussion

The consequences of Equations 4.11 and 4.12 are illustrated in Figures 4. 2 to 4 where the effects of a change in the system variables are examined as a function of pH. The ratios of the extraction ratios are also illustrated. Each curve is referenced to the $pK_a = 2.98$, $K_2 = 50$, $K_3 = 0.1$ data as this type of plot was used previously to indicate the pH of the maximum enhancement effect (Hadgraft *et al.*, 1985). Figure 4.2A deals with the effects of a change in the pK_a of the acid over the range 2.5 to 3.5 pH units. This parameter could change during partition experiments involving added enhancer if the later component is extracted to a significant level into the aqueous phase. In general, the strength of acids in mixed aqueous-organic solvents is less than in pure water (Albert and Sergeant, 1984). This occurs in a distribution because the pH changes as the equilibrium is altered by removal of the unionised component into the organic solvent. It is noted that such an increase in pK_a causes curves to shift significantly to the right (higher pH) as more material is extracted at a particular pH due to reduced ionisation. The ratio plot (Figure 4.2B) shows this variation normalised to the $pK_a = 2.98$, $K_2 = 50$, $K_3 = 0.1$ data. No deviation from the reference curve is observed at either extreme of the ionisation profile but at intermediate values a maximum deviation develops. The direction of deviation depends upon the relative magnitudes of the two pK_a values involved in the normalisation. Although changes in pK_a value produce profiles analogous to those sought, it is unlikely that this is responsible for the effect of Azone in the experimental system. Significant changes in pK_a require substantial concentrations of co-solvent. The highly lipophilic nature of Azone renders it only very sparingly water-soluble and it is unlikely that sufficient is in solution to modify ionisation to any measurable extent.

Addition of an amide percutaneous absorption enhancer to the largely lipoidal isopropyl myristate may increase the partition coefficient (K_2) of the undissociated salicylic acid. The effect of this variation over a range of $P_u = 10 - 100$ is illustrated in Figure 4.3A where shifts in extraction ratios analogous to those recorded for pK_a variation are observed. In this example, the limiting extraction ratios at low pH values do not converge but the ratio plot (Figure 4.3B) continues to show the same behaviour with a clear maximum deviation.

In contrast, variation in the partition coefficient of the ion (K_3) over the range $P_i = 0.01 - 0.5$, as shown in Figure 4.4A, changes the relationship between the curves significantly. The

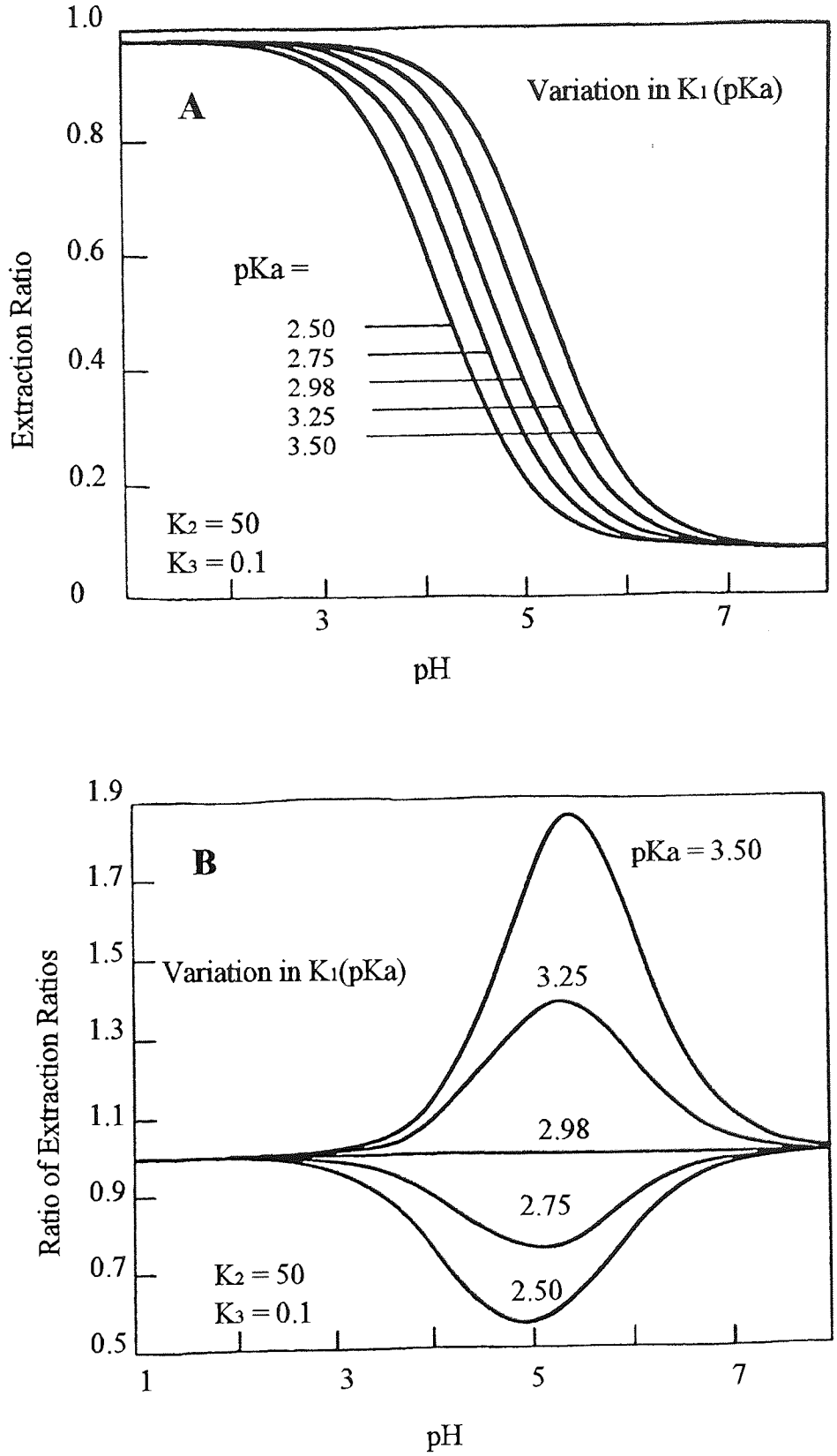

Figure 4.2 Theoretical plots of the effect of pK_a (K_1) variation upon extraction ratios of a weak acid ($K_2 = 50$, $K_3 = 0.1$). Curve A illustrates the effect on the extraction ratio and curve B presents the ratios of extraction ratios. The centre, standard curve, with values of $pK_a = 2.98$, $K_2 = 50$ and $K_3 = 0.1$ was used as reference.

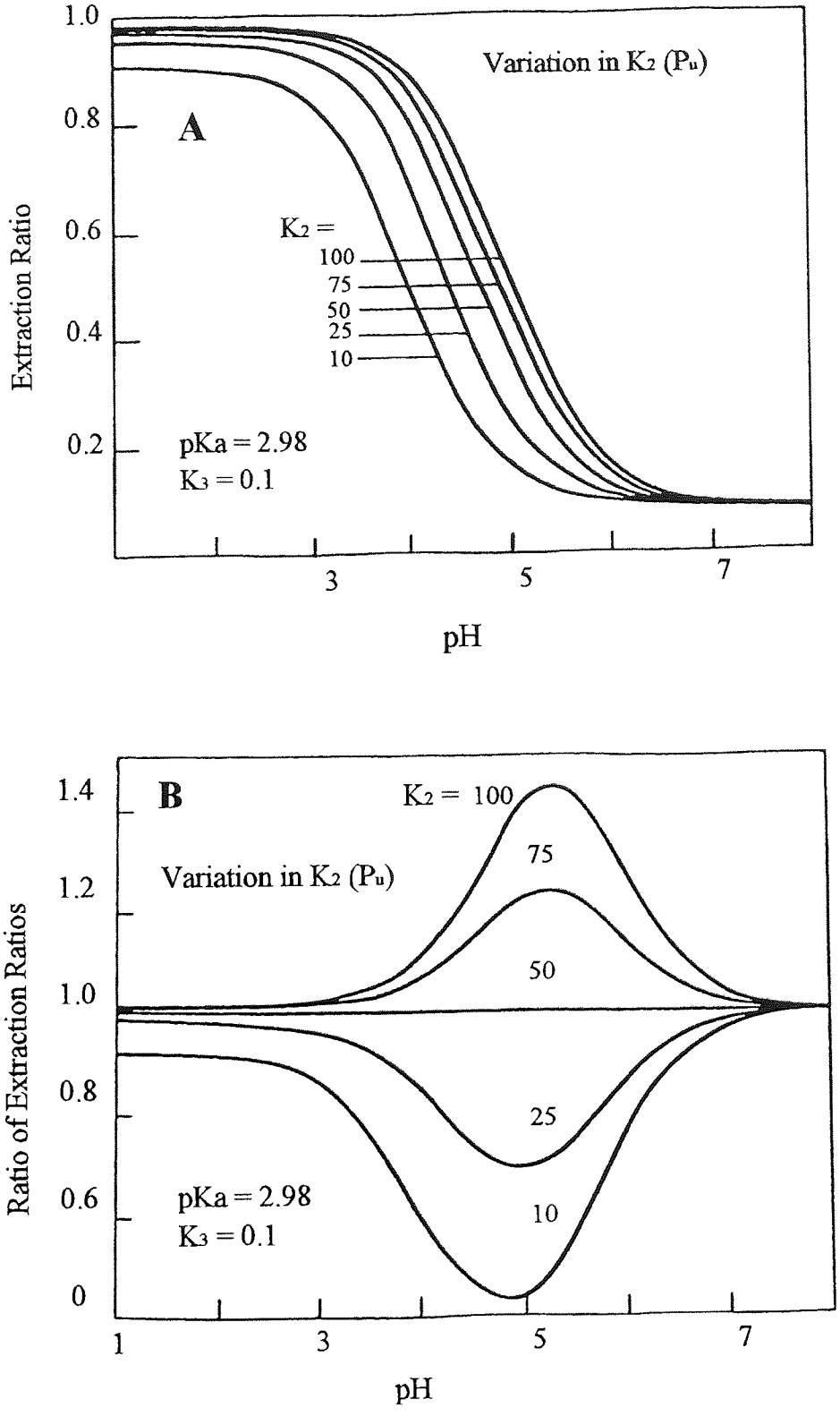

Figure 4.3 Theoretical plots of the effect of partition coefficient (K_2) variation upon extraction ratios of a weak acid ($pK_a = 2.98$, $K_3 = 0.1$). Curve A illustrates the effect on the extraction ratio and curve B presents the reatio of the extraction ratios. The centre, standard curve, with values of $pK_a = 2.98$, $K_2 = 50$ and $K_3 = 0.1$ was used as reference.

extraction ratios at high pH are solely due to this variable and the ratio plots (Figure 4.4B) are divergent. This trend is continued when simultaneous changes in K_1 and K_2 are modelled. Only when the ion partition coefficients of both curves are close to equality are the ratio plots symmetrical and non divergent.

To examine these conclusions experimentally, the partition coefficients of salicylic acid between an aqueous phase of variable pH and an isopropyl myristate phase containing an amide enhancer of percutaneous absorption were determined. Enhancers used were lauric acid *N,N*-dimethylamide (LDA), caproic acid *N,N*-dimethylamide (CDA) (Irwin *et al.*, 1990a,b) and Azone and data are recorded in Table 4.1. The partition coefficients measured at pH = 8.17 were taken as those of the salicylate ion (P_i, K_3) as this pH exceeds the pK_a value (2.98) by over 5 units and thus ensures virtually total ionisation. The phenolic ionisation of salicylic acid has a pK_a of 13.8, which is too far removed to play any part in the equilibria described here. The partition coefficients of the unionised molecule were calculated from the slope of the appropriate plots using the relationship (Tsuji *et al.*, 1977; Irwin and Li Wan Po, 1979; Oakley and Swarbrick, 1987):

$$\frac{P_{obs}}{\alpha} = P_i + \frac{(1 - \alpha)\ P_u}{\alpha} \qquad \text{(Eq. 4.17)}$$

and from nonlinear fitting (Metzler and Weiner, 1986; Irwin, 1990) to the alternative presentation:

$$P_{obs} = \alpha P_i + (1 - \alpha) P_u \qquad \text{(Eq. 4.18)}$$

where P_{obs} is the apparent partition coefficient recorded in Table 4.1, P_i and P_u are the true partition coefficients of the ion and unionised molecule (K_3, K_2), respectively, and α is the fraction ionised. these values are also listed in Table 4.1.

To relate this approach to that adopted earlier (Hadgraft *et al.* 1985), the data were also expressed as extraction ratios using Equation 4.2. The experimental values thus obtained were compared to those derived from the theoretical model in Equation 4.12 using the appropriate

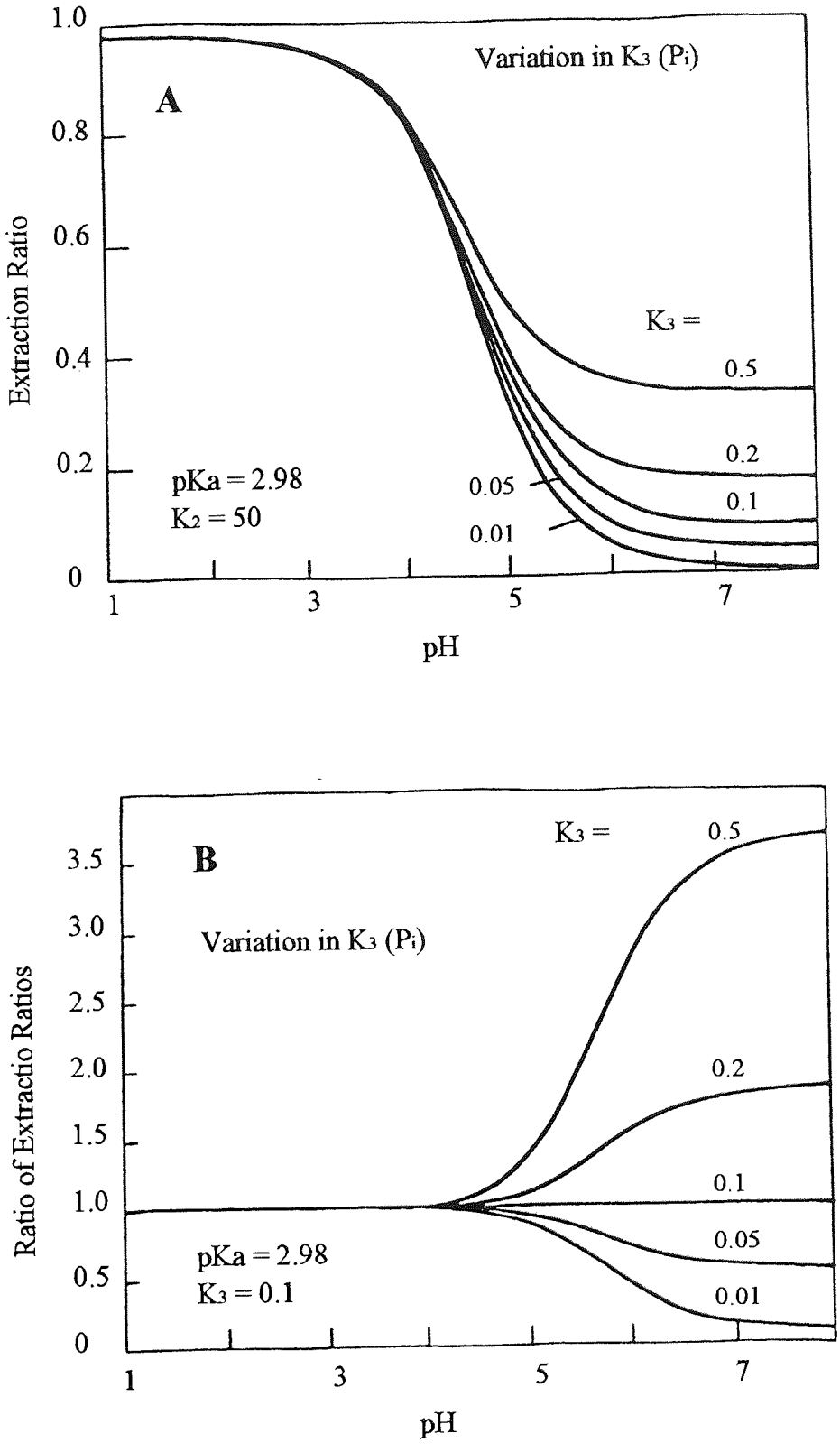

Figure 4.4 Theoretical plots of the effect of ion partition coefficient (K_3) variation upon extraction ratios of a weak acid ($pK_a = 2.98$, $K_2 = 50$). Curve A illustrates the effect on the extraction ratio and curve B presents the ratios of extraction ratios. The centre, standard curve, with values of $pK_a = 2.98$, $K_2 = 50$ and $K_3 = 0.1$ was used as reference.

pH	Partition Coefficient of Salicylic Acid into					
	IPM	CDA (0.1M)	CDA (0.5M)	LDA (0.1M)	LDA (0.5M)	Azone (0.1M)
2.10	25.32			106.64	203.15	97.99
2.37	24.13	32.85		74.36	196.40	63.21
2.75	17.48	22.71	38.53	32.55	142.67	53.95
3.15	10.45	12.59	20.96	19.83	75.41	31.87
3.53	4.72	5.95	11.88	9.26	31.79	11.63
3.96	2.20	2.70	4.89	4.71	13.60	6.04
4.35	1.05	1.38	2.30	1.93	6.29	2.67
4.75	0.49	0.52	1.09	0.80	2.27	1.06
5.13	0.053		0.56	0.058		0.57
5.48			0.26		0.47	
5.85			0.11		0.20	
P_u	28.26	36.9	56.8	85.15	222.83	83.14
P_i	0.03403	0.0041	0.0178	0.00197	0.0052	0

IPM, isopropyl myristate; LDA, lauric acid dimethylamide; CDA, caproic acid dimethylamide.

Table 4.1 Partition of salicylic acid between an aqueous phase of variable pH and an isopropyl myristate phase containing various tertiary amide additives.

estimates of K_1, K_2 and K_3 (K_a, P_u and P_i). Plots comparing the extraction ratio profiles for each system are shown in Figures 4.5 to 7 which also illustrate the degree of correspondence between the experimental and theoretical estimations.

Figure 4.5 compares the data from IPM alone and systems including caproic acid *N,N*-dimethylamide. The partition follows the expected pH dependence with the salicylate showing little affinity for the organic phase as concentrations of the ionised form predominate. Figure 4.5A also reveals that significant modification of the partition profile results from the inclusion of the tertiary amide enhancers of percutaneous absorption. The inclusion of 0.1 M CDA in the lipid phase causes an increase in P_u (K_2) of some 30% while a doubling is seen when the

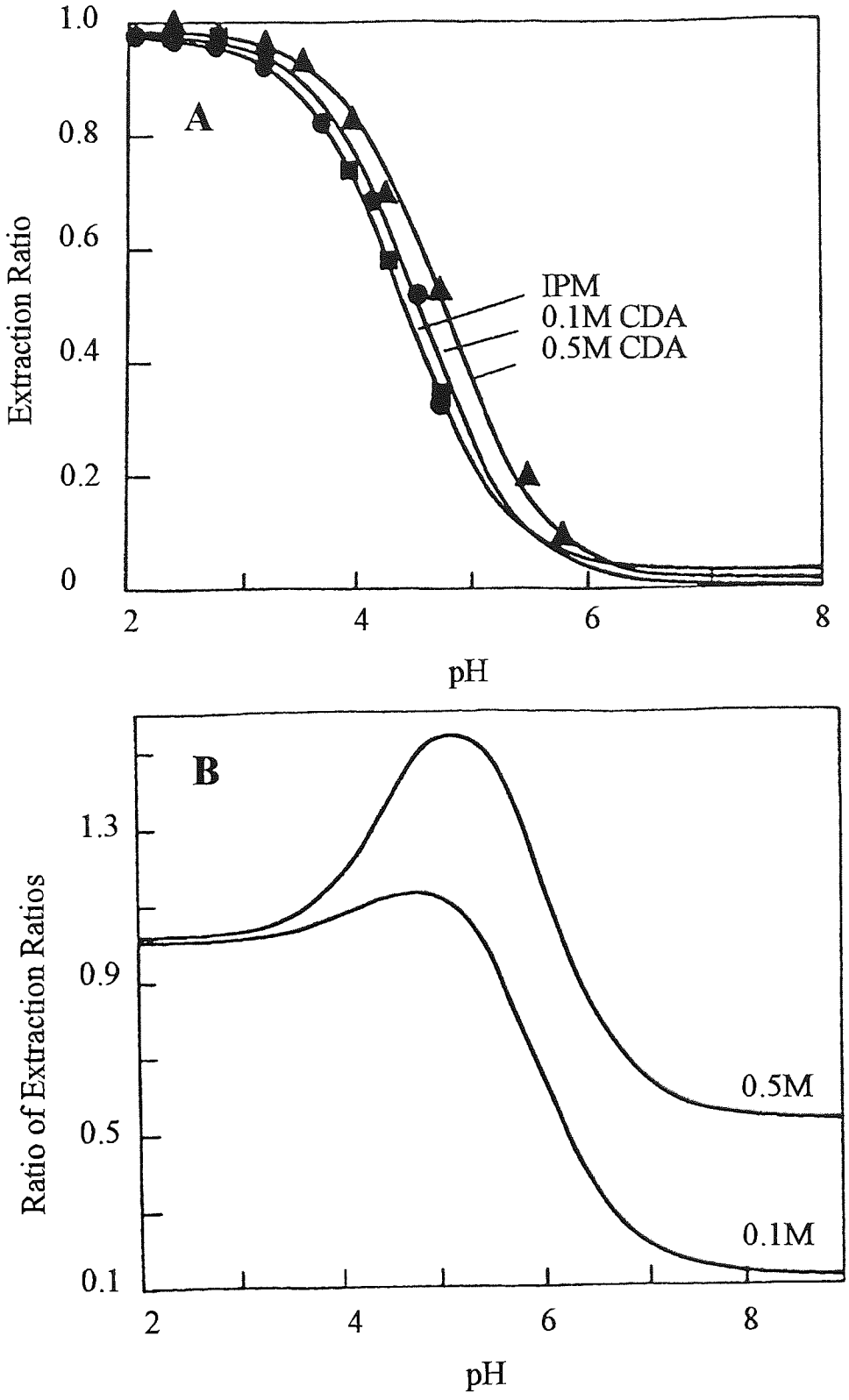

Figure 4.5 Extraction ratios for the partition of salicylic acid between an aqueous phase of variable pH and an isopropyl myristate phase containing caproic acid *N,N*-dimethylamide (0.1M, 0.5M). [A, Extraction ratios; B, ratio of extraction ratios using pure IPM as the reference; ●, IPM; ■, 0.1M; ▲, 0.5M.]

additive concentration is increased to 0.5 M. The coincidence of the theoretical lines and the values determined by experiment confirm the validity of the model. Figure 4.5B displays the curves resulting from calculating the ratios of the extraction coefficients at corresponding pH values. The appearance is similar to that shown in Figure 4.3B and shows clear maxima, increasing with co-solvent concentration confirming that this position is dependent upon the partition coefficient of the unionised species (P_u). No ion-pairing assumptions have been made in establishing this model and it seems unnecessary, therefore, to invoke their existence. The curves are somewhat distorted compared to the theoretical plots shown in Figure 4.3. This is due to simultaneous variation in P_i (K_3) where it appears that the presence of the enhancers reduces the affinity for the anion resulting in a lowering of this parameter. This observation is at variance with an ion-pairing phenomenon. Moreover, amides are not generally regarded as bases in aqueous systems and pK_a values of -0.7 for dimethylformamide and 0.1 for dimethylacetamide have been quoted (Adelman, 1964). Such values show little indication of significant ion-pairing potential.

Similar results are afforded with the longer chain enhancer lauric acid *N,N*-dimethylamide and representative plots are shown in Figure 4.6. Analogous, but larger, increases in P_u (K_2) are seen with 0.1 M (3-fold increase) and 0.5 M (~ 8-fold increase) incorporation of the co-solvent. The ratio plots show effects comparable to those seen with CDA. The presence of 0.1 M Azone exerts an effect almost identical to that observed with 0.1 M LDA, as shown in Figure 4.6, with P_u (K_2) increasing almost 3-fold in the presence of the enhancer. Values for P_i (K_3) are also suppressed and no ion-partition could be detected here. Ratio plots in Figure 4.7B again follow the previous trend and indicate no evidence for processes other than simple partition and ionisation. The maximum of this plot occurs at pH 5.3, which is comparable to the value of 5.5 quoted earlier (Hadgraft *et al.*, 1985). It is also noteworthy to observe the exquisite dependence of the shape of the ratio curves upon P_i (K_3) as a result of the low values observed. This effect is illustrated in Figure 4.8 that shows the consequence of varying P_i from zero, the measured value, to 0.2, which represents a value of less than 0.25% of P_u. Over this range, the maximum entirely disappears and is replaced by a sigmoidal curve as P_i in the co-solvent system progressively exceeds that in the pure solvent reference. The low values of P_i make their determination to any degree of precision difficult. The high dependence of the ratio profile on this parameter suggests that this mode of data analysis is unreliable as a guide to mechanistic events.

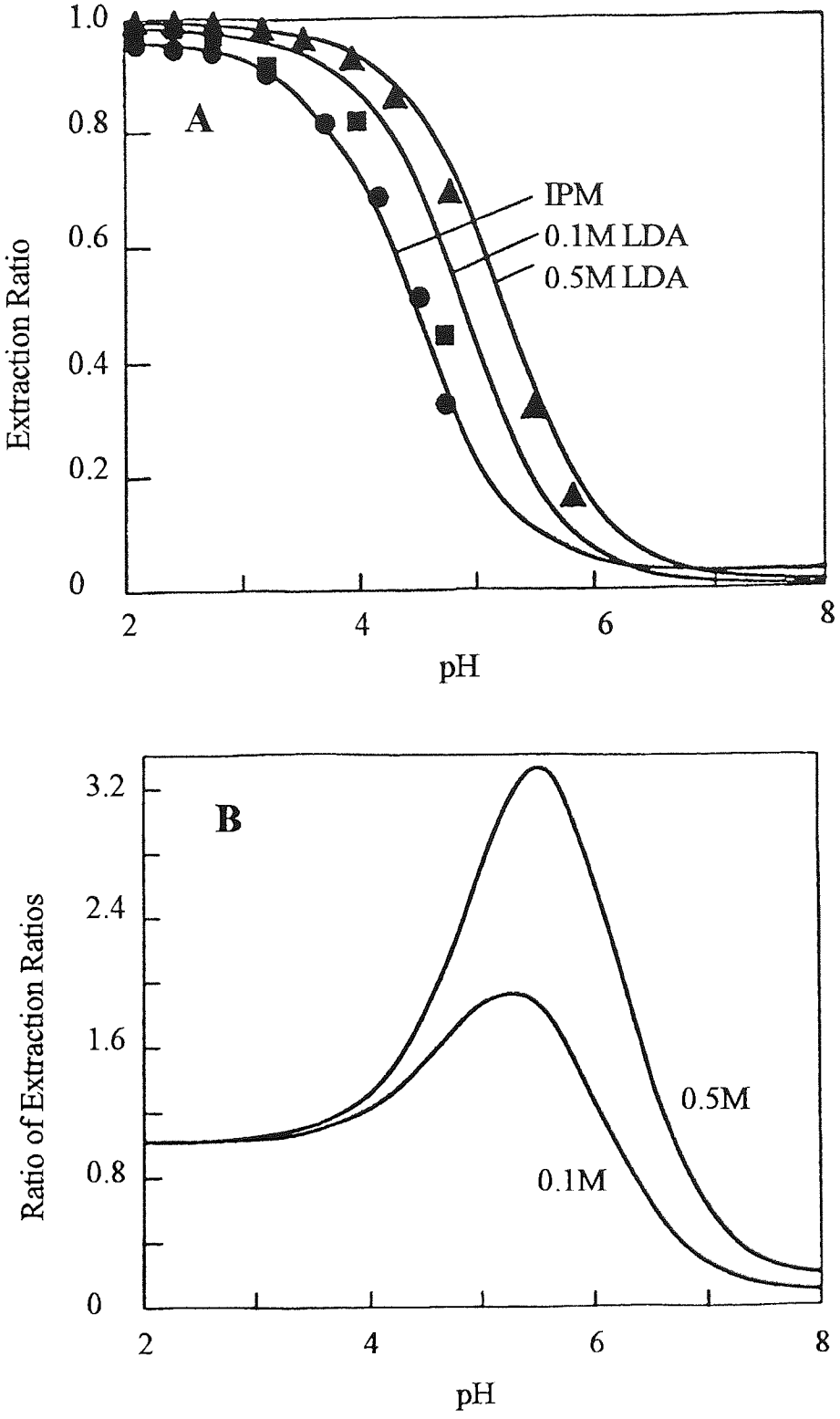

Figure 4.6 Extraction ratios for the partition of salicylic acid between an aqueous phase of variable pH and an isopropyl myristate phase containing lauric acid *N,N*-dimethylamide (0.1M, 0.5M). [A, Extraction ratios; B, ratio of extraction ratios using pure IPM as the reference; ●, IPM; ■, 0.1M; ▲, 0.5M.]

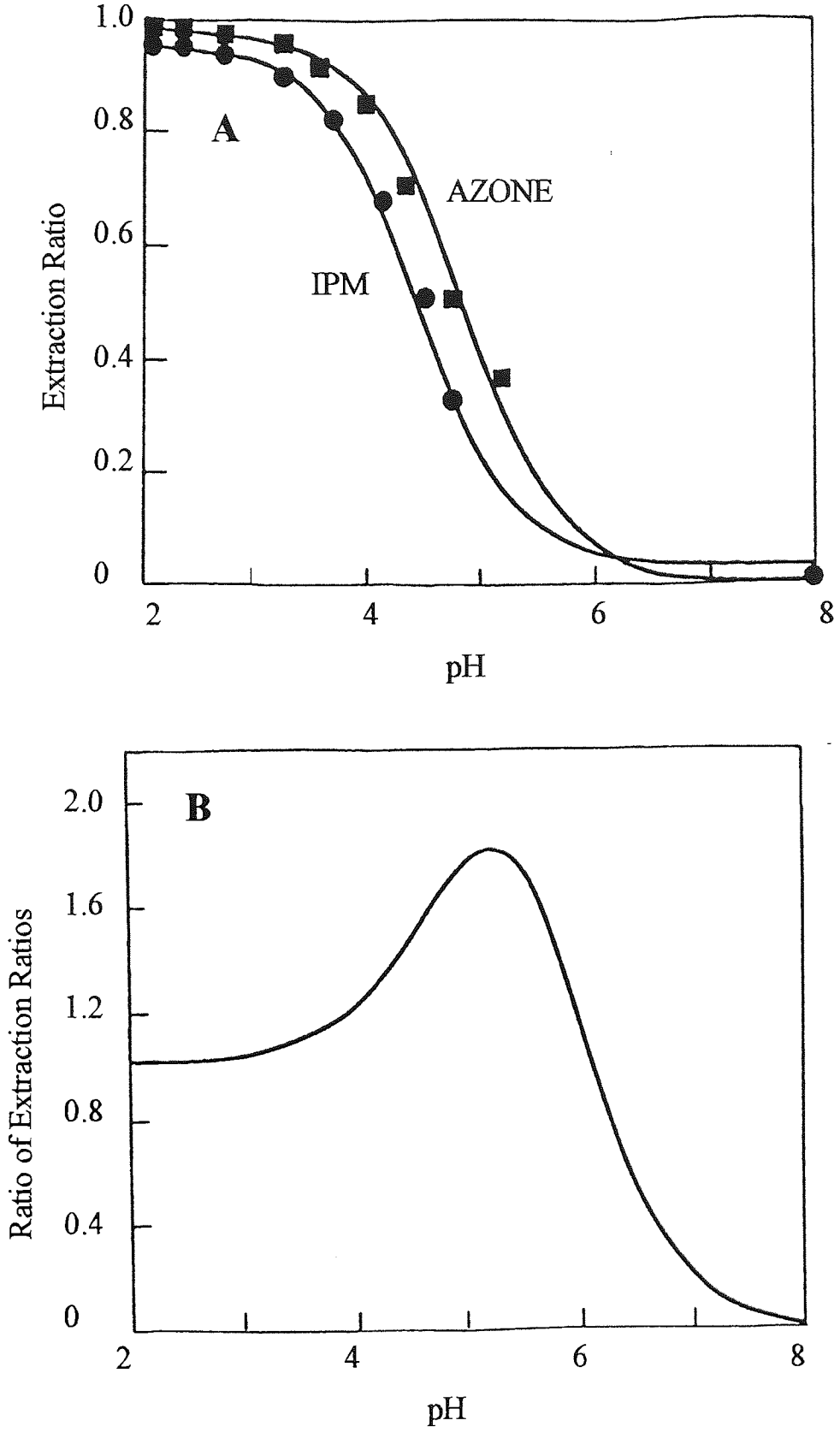

Figure 4.7 Extraction ratios for the partition of salicylic acid between an aqueous phase of variable pH and an isopropyl myristate phase containing Azone (0.1M). [A, Extraction ratios; B, ratio of extraction ratios using pure IPM as the reference; ●, IPM; ■, 0.1M Azone.

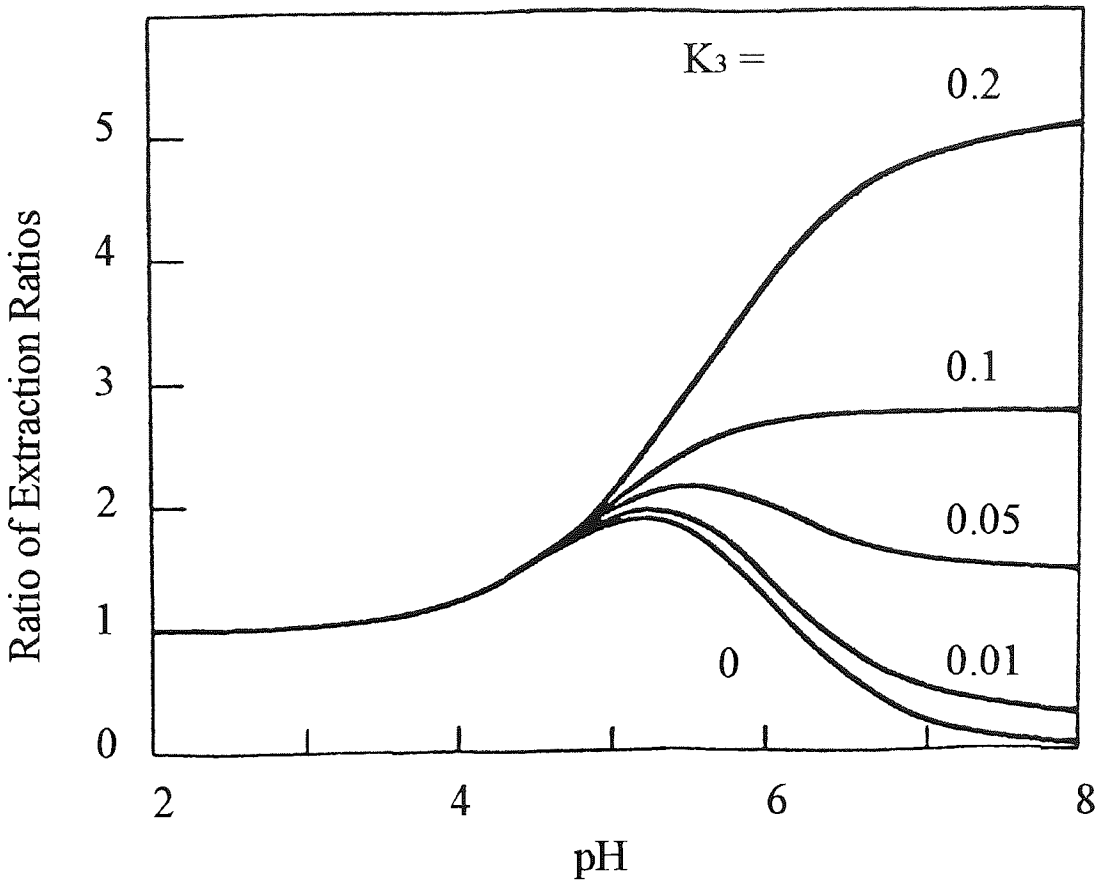

Figure 4.8 Theoretical ratios of extraction ratios for the partition of salicylic acid between an aqueous phase of variable pH and an isopropyl myristate phase containing Azone (0.1M) showing the effect of Pi on curve shape.

Partition studies as a function of concentration and pH have shown that carboxylic acids, including salicylic acid, show some association in the organic phase (Smith and White 1929). This association is usually neglected in partitions determined to model topical delivery. Although expressions analogous to Equations 4.11 and 4.12 may be derived which model association in the organic phase, the system described here fits the derived model well. This indicates that this modification is not required in this instance.

4.5 Summary

The partition of salicylic acid from aqueous buffers into isopropyl myristate organic phases was studied. The enhancement of this partition by amide additives was investigated and compared with a theoretical model. The theoretical model was based upon the extraction ratio (ER) of weak acids :

$$ER = \frac{C_1 - C_2}{C_1}$$

Where C_1 is the initial aqueous concentration of the solute and C_2 is the concentration after extraction. Using the partition coefficients of the ionised and unionised species (P_i, P_u) obtained from $P_{obs}/\alpha = P_i + (1 - \alpha) P_u/\alpha$, a theoretical model was developed to account for the variation in partition dependent upon pK_a.

The ratio of extraction coefficients was plotted to compare the effects of Azone with LDA and CDA. All the plots produced bell-shaped curves with maximums between pH 5 and 6. It has been proposed that a bell-shaped curve demonstrates the optimum pH for ion-paired facilitated transport to take place. However, the shape of the plot is a natural outcome of the ion-pair-independent model. Due to the low pK_as of LDA and DCA, these compounds would not be expected to be ionised at the pH value used and are therefore unavailable for ion-pairing. These data provide evidence to suggest that enhancement of salicylic acid partition by amide enhancers can be explained by partition and ionisation equilibria alone, without the involvement of ion-pairs.

CHAPTER FIVE

PRODRUGS OF PHOSPHONOACETATE

METHODS OF ANALYSIS, STABILITY AND PERCUTANEOUS ABSORPTION

5.1 Introduction

5.1.1 Antiviral Properties of Phosphonates

In 1973, Shipkowitz *et al.* demonstrated that phosphonoacetic acid **5.1** had antiviral properties. It was a compound that inhibited viral growth whilst having little or no toxic effect on the host cell. These early studies documented the effectiveness of phosphonoacetate against herpes simplex virus in experimental mouse dermatitis and rabbit keratitis. Further studies on ocular herpetic keratitis in rabbits (Meyer *et al.*, 1976; Gersetin *et al.*, 1975), herpes virus skin infections in mice (Klein and Friedman - Kien, 1975), mouse and human cytomegalovirus, herpes simplex type 1 (Tateishi *et al.*, 1994) and type 2 (Overby *et al.*, 1977 and Hay *et al.*, 1977), herpes virus saimiri, Epstein-Barr Virus (Huang, 1975), pseudorabies virus, equine abortion virus and Marek's disease virus (Leinbach *et al.*, 1979) have shown the success of phosphonoacetates in controlling viral infection.

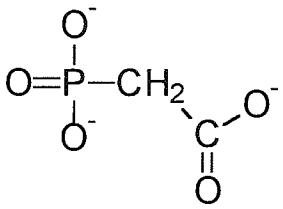

Phosphonoacetate (5.1)

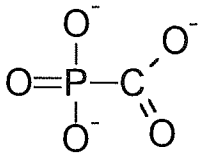

Phosphonoformate (5.2)

In developing viral chemotherapeutic agents, a rational approach would involve designing compounds that interact specifically with viral enzymes leaving cellular enzymes unaffected (Cohen, 1977). As part of a screening programme to select specific viral DNA polymerase inhibitors, a series of compounds including pyrophosphate analogues were found, which may interact with the binding of nucleoside triphosphates to polymerases. (Leinbach *et al.*, 1979).

The pyrophosphate analogues, phosphonoacetate **5.1** and phosphonoformate **5.2**, inhibit the functions of herpes virus DNA polymerase (Mao *et al.*, 1975; Mao and Robishaw, 1975). This was initially demonstrated for herpes simplex virus (Helgstrand *et al.*, 1978; Eriksson and Oberg, 1979) and then subsequently for cytomegalovirus (Eriksson *et al.*, 1982), varicella zoster virus (Öberg, 1986) and Epstein-Barr Virus (Datta and Hood, 1981).

A significantly higher concentration of phosphonoacetate is required to inhibit human DNA polymerases than viral DNA polymerases. The concentration required to give a 50 per cent inhibition of HSV-1 plaque formation (IC_{50}), is 20 μM, but a concentration of 1000 μM is required to inhibit cellular DNA synthesis by a similar amount (Helgstrand *et al.*, 1978). Comparisons can be made to Idoxuridine, Vidarabine and Ribavirin, where viral to cellular DNA inhibition concentrations (IC_{50}) are 5 μM to 30 μM, 15 μM to 70 μM and 2 μM to 25 μM respectively.

In the presence of phosphonates the production of viral late antigens, such as structural proteins, are decreased. Early antigens which are synthesised prior to viral DNA replication continue to be produced (Wahren and Öberg, 1979; 1980). This is because the phosphonates are analogues of pyrophosphate and inhibit DNA chain elongation catalysed by the viral DNA polymerase by preventing pyrophosphate exchange. The kinetics of this inhibition is non-competitive with respect to deoxynucleoside triphosphate and uncompetitive with respect to the activated DNA template primer (Eriksson *et al.*, 1982; Derse *et al.*, 1982; Eriksson, 1980 and Ostrander and Cheng, 1980). Phosphonates are competitive with pyrophosphate indicating that the compounds block the pyrophosphate binding site on the viral DNA polymerase enzyme, interfering with exchange of pyrophosphate (Derse *et al.*, 1982; Leinbach *et al.*, 1979). Kinetic data suggest that the interaction between these compounds may not be completely straightforward as inhibitory constant results indicate that the phosphonates and pyrophosphate may bind to distinct sites on the viral enzyme, which are closely linked (Derse *et al.*, 1982).

One of the more successful approaches to human acquired immunodeficiency syndrome (AIDS) chemotherapy, is the development of reverse transcriptase inhibitors (De Clercq, 1986; Mitsuya and Broder, 1987). Phosphonoformate is a potent and reasonably selective inhibitor of HIV reverse transcriptase enzyme (Sandström *et al.*, 1985; Sarin *et al.*,1985) in a dose dependent manner and has received attention as a potential AIDS drug (De Clercq, 1986; Mitsuya and Broder, 1987; Oberg, 1989; Wordrak *et al.*, 1988). This inhibitory activity against HIV reverse transcriptase, is non-competitive and reversible (Crumpacker, 1992). Phosphonoformate appears to bind to the reverse transcriptase at a site that is distinct from the nucleoside triphosphate binding site (Nunberg, 1991).

Pyrophosphate analogues have a place in clinical therapy in the treatment of cytomegalovirus retinitis and acyclovir-resistant herpes simplex virus infection (Chrisp and Clissold, 1991; Safrin *et al.*, 1991). The well documented properties of these compounds, that act directly on viral polymerases without requiring activation by viral or cellular proteins, have established the basis for their development as useful antiviral drugs. To continue the development of these compounds, it is essential to understand their basic mechanisms and the process of viral resistance. In this regard, phosphonates serve as an important model for further progress in the development of antiviral drugs (Crumpacker, 1992).

5.1.2 Prodrugs of Phosphonate Antiviral Agents

The Phosphonate antiviral agents are clinically limited by their highly ionic nature. At a physiological pH, phosphonoacetic acid **5.1** is partially triionic with pKa values of 2.30 (P-OH), 5.40 (COOH) and 8.60 (P-OH) (Boezi, 1979) and phosphonoformate **5.2** is triionic with pKa values of 0.49, 3.41 and 7.27 (Warren and Williams, 1971). This is presumably why these compounds do not readily cross mucosal or cellular membranes (Oberg, 1989 and Wandrak *et al.*, 1988). When 20 mg kg^{-1} was administered to rabbits and monkeys, only 2 and 8 percent respectively of the dose was absorbed (Bopp *et al.*, 1977) and high-dose infusions of phosphonoformate **5.2** (foscarnet) are required to achieve clinically therapeutic effects (Jacobson *et al.*, 1988). Phosphonoformate **5.2** is absorbed to a limited and variable extent, less than 22 percent when administered to humans *via* the oral route (Sjovall, 1988) and is unstable at pH 2, with a half-life of hydrolysis of approximately 1 hour (Warren and Williams, 1971). Despite being unstable at gastric pH, neutralisation of gastric acidity only increases the absorption of phosphonoformate **5.2** by approximately 50 percent, from an average of 6.2 to 9.9 percent (Barditch-Crovo *et al.*, 1991). Hence, chemical instability probably only accounts for a small part of the drugs limited absorption (Lietman, 1992). Compounds that do not readily cross cellular membranes are also unlikely to penetrate into the brain (Bundgaard, 1985). These include the ionic phosphonates (Oberg, 1989) which are therefore ineffective against viral infection at this site (Elder and Sever, 1988). Drug penetration here is poor because the brain microvessel endothelial cells, commonly known as the blood-brain barrier, limit extravasation (Rapoport, 1976). This barrier is intended to protect this vital organ from harmful chemicals but, in doing so, makes the administration of potentially beneficial drugs to

the affected brain very difficult. Endothelial cells in the brain's capillaries differ from those in most other tissues by the absence of intercellular pores and pinocytotic vesicles (Benet *et al.*, 1995). The "tight junctions" between cells create a virtually impenetrable barrier, unless an active transport system exists, for example with sugars, or compounds are sufficiently lipophilic such as diamorphine. Endothelial cells in the rest of the body are joined by permeable junctions that allow diffusion of small and large molecules between the blood-stream and peripheral organs. Brain capillary endothelial cells also have the ability to regulate the traffic of specific molecules into and out of the brain, which is accomplished by receptors located in the endothelial cell surface (Hsieh, 1994). It is likely that a unique arrangement of pericapillary glial cells contributes to the slow diffusion of organic acids and bases into the CNS. Drug molecules probably have to traverse not only endothelial, but perivascular cell membranes before reaching neurones or other target cells in the CNS. Highly lipid soluble compounds can permeate the blood brain barrier and their rate of transport is probably only limited by cerebral blood flow. With increasing drug polarity, the rate of diffusion into the CNS is proportional to the lipid solubility of the unionised species (Benet *et al.*, 1990). One approach to increase the effective permeation of ionic compounds is to design a prodrug form (Silverman, 1992; Bundgaard, 1985).

The term prodrug was first introduced by Albert (1951; 1958) to describe pharmacologically inactive compounds which undergo metabolic biotransformations into an active drug, for example by esterases. More recently the term has been broadened to include compounds which undergo chemical as well as biological transformations (Kupchan *et.al.*, 1965). The physicochemical and biological properties of the parent drug can be temporarily overcome to mask some intrinsic problem associated with its therapeutic use. Once the desired goal for the prodrug has been achieved it should be converted back to its active parent form. This could occur during or after absorption, or alternatively at a specified site in the body.

A carrier-linked prodrug is a compound that contains an active drug linked to a carrier group that can be removed enzymatically. An ester which is hydrolysed to an active caboxylic acid-containing drug would be an example of this type. The bond to the carrier group must be sufficiently labile to allow the drug to be released efficiently *in vivo*. The carrier group must be non-toxic and biologically inactive when detached from the drug. Bipartate, tripartate and mutual prodrugs are further classifications of carrier-linked prodrugs. These classifications

describe the carrier arrangement of the prodrug. Bipartate prodrugs are comprised of one carrier attached to the parent drug. Tripartate prodrugs connect the carrier to the drug *via* a linker arm. Mutual prodrugs consist of two drugs, usually synergistic, attached to each other. One drug is the carrier for the other and *vice versa*. 4-azidobenzyl carbonates **5.3** (Figure 5.1) are model examples of tripartite prodrugs, where the azide (N_3) substituent serves as the carrier group, the benzyloxycarbonyl group as the linker arm and the aniline substituent represents the amine drug.

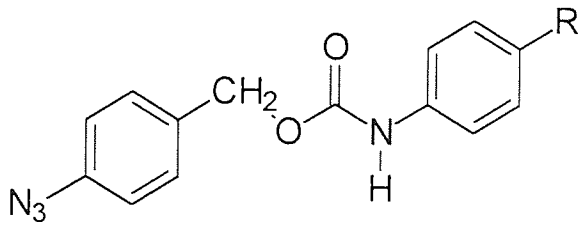

Figure 5.1 4-Azidobenzyl carbamates **(5.3)** ; models for potential amine prodrugs.

Aromatic azides are rapidly reduced to the corresponding amines by thiols under mild conditions (Staros *et al.*, 1978). The analogous reaction of a 4-azidobenzyl carbamate prodrug (Griffin *et al.*, 1996) with a biological thiol such as glutathione will generate the corresponding 4-aminobenzyl carbamates. This is unstable and decomposes spontaneously to release the appropriate aniline (Robinson *et al.*, 1988). Modification of the physicochemical properties of a drug *via* the prodrug approach represents a promising method for optimisation of drug delivery. This not only includes the traditional parenteral and oral routes of delivery, but it has great potential for transdermal delivery (Sloan, 1992). Only a small number of the possible prodrug approaches to enhancing topical delivery has been evaluated: some of these have achieved significant improvements. Individual promoieties of S^6-acyloxymethyl and 9-dialkylaminomethyl gave an increase in the transdermal delivery of 6-mercaptopurine of up to 66 and 180 times respectively. The combination of both promoieties increased the transdermal delivery by up to 240 times. Simple N-acyl derivatives increased the transdermal delivery of 5-fluorouracil by up to 40 times (Sloan, 1992) and dihydroxyalkoxycarbonyl derivatives of levonorgestrel increased the transdermal delivery of the parent compound by 30 times (Friend *et al.*, 1988b). Esters of steroids are commonly used as prodrugs in commercially available

topical products, for example betamethasone-17-valerate and hydrocortisone-21-acetate. Thus, by transiently increasing the biphasic solubility, the prodrug approach can promote both 5-fluorouracil, a polar drug that can permeate skin reasonably well, and levonorgestrel, a lipophilic compound with low transdermal permeation. This potential ability of the prodrug approach to increase the effective solubility of the parent drug in the skin gives it a significant advantage over any formulation approach to increase the dermal or transdermal delivery of the parent drug. This is because primarily, a formulation approach affects the solubility of the parent drug in the vehicle and only secondarily affects its solubility in the skin. An ideal approach would be the utilisation of both formulation and prodrug variations (Sloan, 1992).

For prodrug synthesis to be a practical approach, the rate of metabolism or biotransformation must be optimal. It is impractical to design a prodrug with an ideal transdermal absorption rate if the compound is not converted to the active parent drug in sufficient concentrations before it is carried away from the site of action by the systemic circulation. The ideal transdermal prodrug must also have physicochemical properties that enable its formulation in practical vehicles (Guy and Hadgraft, 1992).

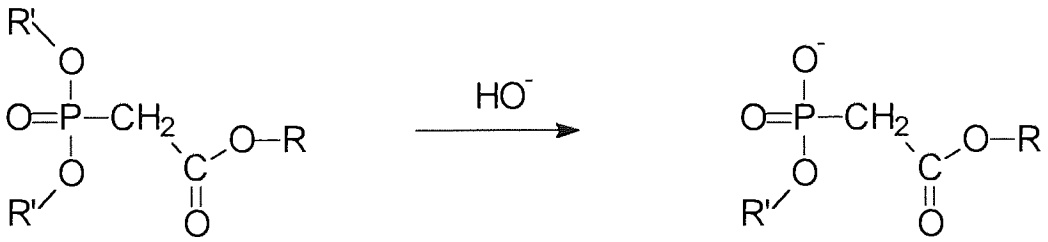

Figure 5.2 Hydrolysis of lipophilic phosphoester **(5.4)** to unreactive anionic intermediate **(5.5)**.

Drugs that comprise a phospho group [-$PO(OH)_2$] within their structure, such as phosphonoacetate and phosphonoformate, present a challenge to prodrug design. The objective is to design a prodrug form that will convert the parent hydrophilic phosphonate into a lipophilic phosphoester prodrug that can cross biological barriers. A neutral lipophilic phosphoester, for example dimethyl benzyloxycarbonylmethyl phosphonate **5.4,** is then chemically or enzymatically transformed within the target organ to regenerate the active compound. However, if R' is represented by simple alkyl analogues, hydrolysis under physiological conditioning will remove the first R' group, but the second group is significantly,

at least a million-fold, more resistant to cleavage. This is because the phosphorus of the anionic intermediate **(5.5)** is unreactive to nucleophilic attack (Figure 5.2)(Bel'skii, 1971). To enable the release of the phospho group, a tripartite prodrug design is required which does not require nucleophilic attack at the phosphorous and subsequent P-O bond cleavage for the removal of the promoiety. Prodrugs of phosphonoformate **5.2** have been studied in an effort to improve the bioavailibility of the drug. A range of P,P-di(alkyl) triesters (Norén *et al.*, 1983) and P,P-di (acyloxymethyl) esters (Iyer *et al.*, 1989) have been synthesised, but none of these compounds showed antiviral activity greater than that of the parent compound. Another approach was the preparation of the triester of phosphonoformate, dibenzyl methoxycarbonylphosphonate **5.6** (Mitchell *et al.*, 1991). This was a lipophilic prodrug designed to pass the blood brain barrier.

Figure 5.3 Scheme of degradation of dibenzyl methoxycarbonyl phosphonate (from Mitchell *et al.*, 1991).

The hydrolysis scheme of dibenzyl methoxycarbonyl phosphonate **5.6** is shown in Figure 5.3. Although it was anticipated that benzyl methoxycarbonyl phosphonate **5.7** and benzyl alcohol **5.8** would be formed upon hydrolysis, it was not expected to produce dibenzyl phosphate **5.9**, benzyl phosphite **5.10**, benzyl benzyloxycarbonyl phosphonate **5.11** and dibenzyl phosphate **5.12**. The hydrolysis of the triester **5.6** to the diester **5.7** proceeds by P-O bond cleavage with neucleophilic attack of water at phosphorus. This contrasts with studies of dibenzyl methylphosphonate **5.13** (Hudson and Harper, 1958) and tetrabenzyl pyrophosphate **5.14** (Dudek and Westheimer, 1959) where these compounds lose a benzyl group with C-O cleavage.

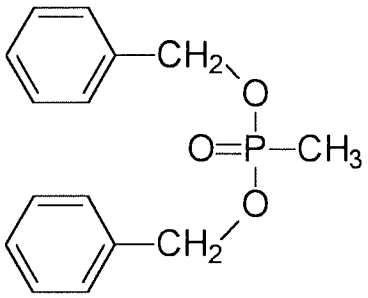

Dibenzyl methyl phosphonate (5.13)

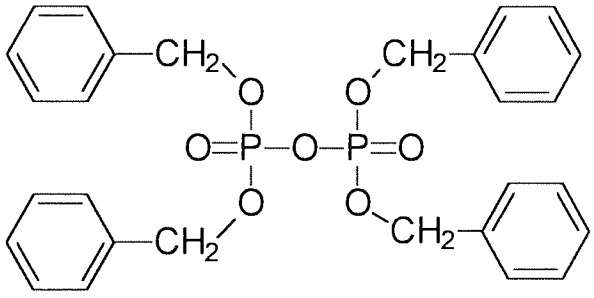

Tetra benzyl pyrophosphate (5.14)

The high reactivity and change in mechanism for the phosphonoformate triester **5.6** must be attributed to the electron-withdrawing effect of the methoxycarbonyl group making the phosphorus sensitive to nucleophilic attack. Most significantly, the hydrolysis proceeds in part *via* C-P bond cleavage to dibenzyl phosphite **5.9** and dibenzyl phosphate **5.12**, which destroys the parent compound. The rapid and complicated hydrolysis of dibenzyl methoxycarbonyl phosphonate, including competing pathways involving nucleophilic attack at both the phosphorus and carbonyl group, demonstrate that the preparation of triester prodrug analogues of phosphonoformate will be difficult.

In an attempt to direct the hydrolyses away from the destructive P-C bond cleavage and towards the objective of P-O bond cleavage, a series of *para*-substituted dibenzyl methoxycarbonyl phosphonates were synthesised (Figure 5.4) (Mitchell *et al.*, 1992a).

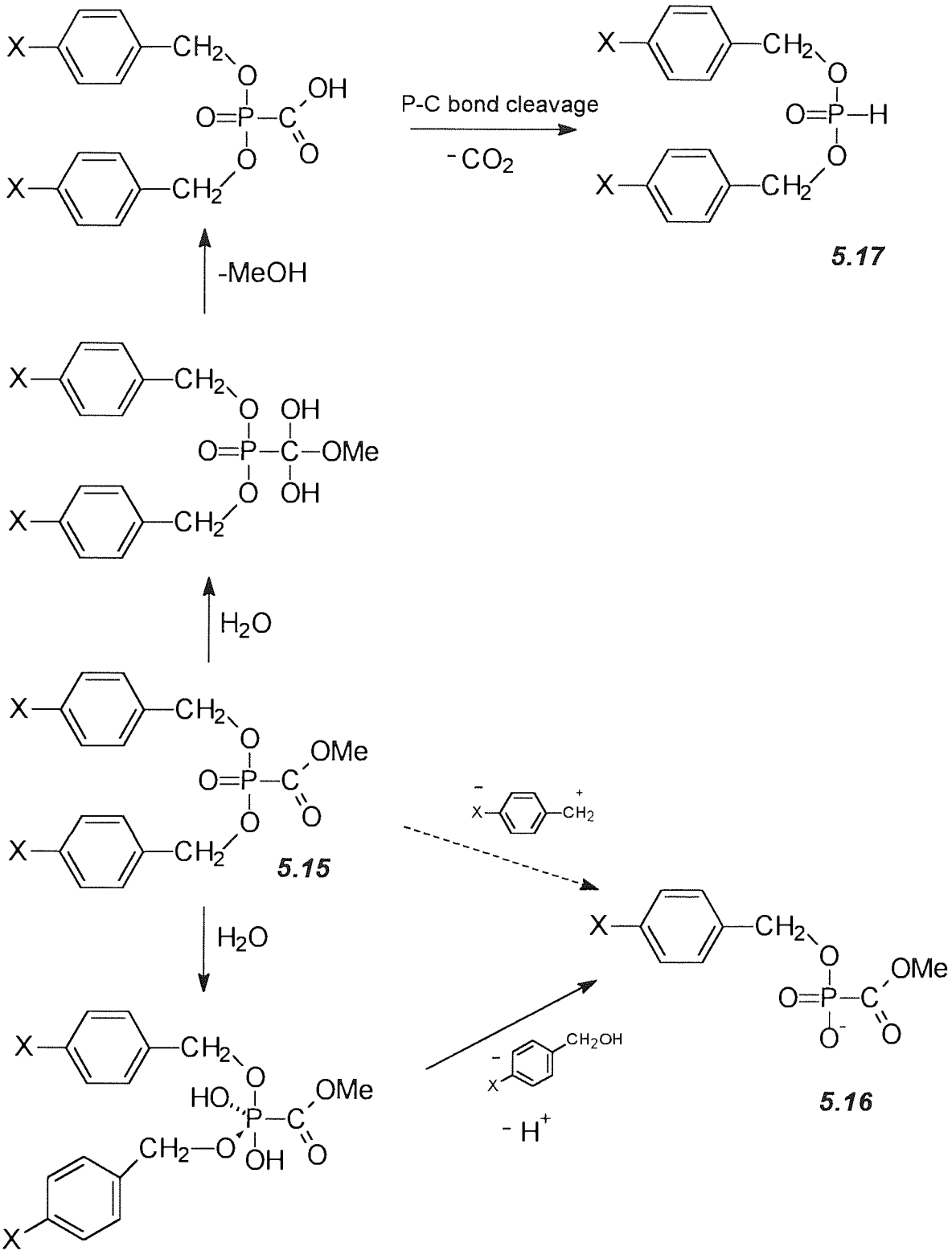

Figure 5.4 *Para*-substituted dibenzyl methoxycarbonyl phosphonates **5.15** (X = NO_2, CF_3, H, N_3)

The objective of designing compounds resistant to the P-C bond cleavage upon hydrolysis was partially achieved by these *para* substituted triesters. The hydrolysis of the electron-donating or electron-withdrawing *para* substituted dibenzyl methoxycarbonylphosphonates **5.15** (X=N_3

and NO_2) proceeds mainly *via* the benzyl methoxycarbonylphosphonate diesters **5.16** (X=N_3 and NO_2) with minimal dibenzyl phosphite **5.17** (X=N_3 and NO_2) formation. Unfortunately, these compounds still have limited prodrug use, as the para-substituted triesters (X=N_3 and NO_2) are unstable with half-lives of 2.5 and 5.6 minutes respectively (Mitchell *et al.*, 1992a).

The instability of the dibenzyl methoxycarbonyl phosphonates is possibly the result of the electron-withdrawing properties of the methoxycarbonyl group. The implication of this effect is that triesters of phosphonoformate may not be appropriate for use as prodrugs. More suitable compounds could be di(4-acyloxybenzyl) esters of phophonoacetate, where the phosphorus atom and the carbonyl function are separated by a methylene group, or the bis (4-acyloxybenzyl) esters of the 5' -monophosphate of AZT (Thomson *et al.*, 1993) .

Mitchell *et al.*, (1992b) monitored the chemical stability and metabolic conversion of the phosphonoacetate esters, di (4-acyloxybenzyl) triesters **5.18** (X=MeO_2C,R=Me, Et, Pr P_n, Bu or Bu^t) and di(4-acyloxybenzyl) diester **5.18** (X=H,R=Me). There was a significant improvement in chemical stability over the phosphonoformate derivatives. The hydrolysis of the diester **5.18** (X=H, R=Me) (5mmol dm^{-3}) in potassium phosphate buffer (0.1 mol dm^{-3}; D_2O, pD 8.0) - CD_3CN (9:1 v/v) at 36.4°C to the monoester potassium 4-acetoxybenzyl methylphosphonate **5.20** (X=H, R=Me) was slow with a half-life of 55.4 hours. The monoester decomposed further to dipotassium methylphosphonate **5.23** (X=H) with a half-life of 153.2 hours. The observed rate constants for these hydrolyses suggested that the compounds do not react by nucleophilic attack at phosphorus. 4-hydroxybenzyl alcohol **5.21** was formed with the monoester **5.20,** whereas acyloxybenzyl alcohols were not detected, suggesting that the reaction proceeded by hydrolysis of the acyloxybenzyl group to give the 4-hydroxybenzyl intermediates **5.19** and **5.22**. It was then proposed that the electron-donating 4-hydroxy group promotes cleavage of the benzyl-oxygen bond to give either the monoester **5.20** or methyl phosphonate **5.23** (Figure 5.5).

Triester **5.18** (X=MeO_2C) hydrolysis followed a similar breakdown cascade with all analogues demonstrating half-lives of in excess of 24 hours. The diester **5.20** degraded by typical first order reaction kinetics to methoxycarbonylphosphonate **5.23** (X=MeO_2C), 4-hydroxybenzyl alcohol and the acylate anion. The triesters **5.18** were approximately ten times more reactive

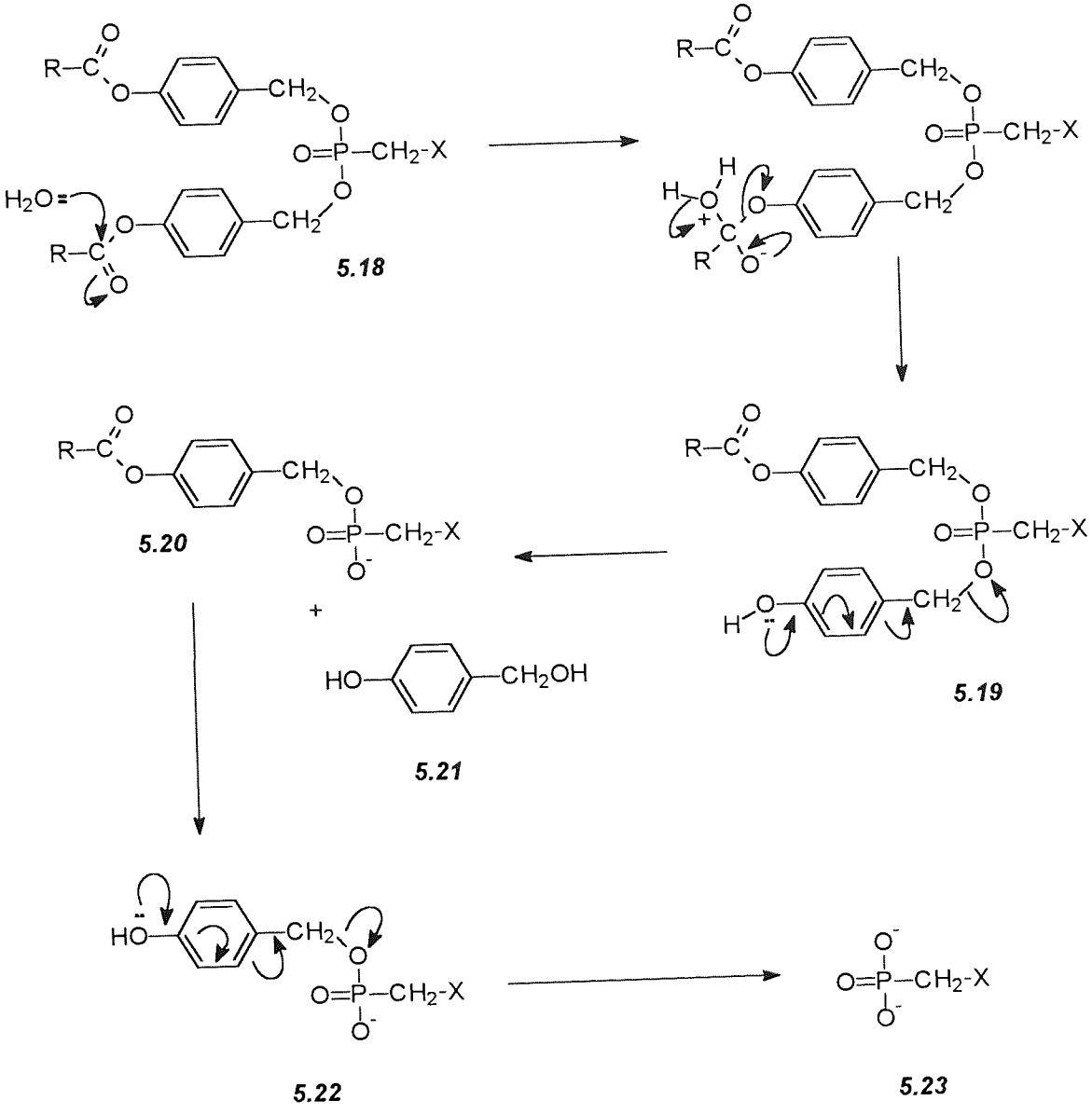

Figure 5.5 Mechanism of hydrolysis of 4-acyloxybenzyl triesters **5.18** (X=MeO_2C, R=Me, Et, Pr, Pr^i, Bu, or Bu^t) and diesters **5.18** (X=H, R=Me).

than the diesters **5.20** and the mechanism of degradation was assumed to be similar. The 4-acyloxybenzyl alcohols were not produced, which is again consistent with the hydrolysis proceeding *via* 4-hydroxybenzyl intermediates **5.19** and **5.22**.

For these compounds to have potential as prodrugs, they should be susceptible to bioconversion into the parent phospho compound as well as being moderately chemically stable. The 4-acetoxy group was shown to be susceptible to metabolic conversion by esterases to the electron-donating hydroxy group. In the presence of 50 units of porcine liver carboxyesterase (PLCE) the diester **5.18** (X=H,R=Me) decomposed to the monoester **5.20** in less than 3 minutes, which after 2 hours gave only methylphosphonate **5.23** (X=H) and in the presence of 100 units the monoester **5.20** was completely metabolised within 15.5 minutes. When incubated with PLCE, the phosphonoacetate triesters **5.18** (X=MeO_2C)(1 cm^3 of a 1 mmol dm^{-3} solution with 0.005units of esterase) demonstrated a similar breakdown profile and significant increase in decomposition rate compared with chemical hydrolysis. For example, the triester (R=Et) was converted to the diester **5.20** (X= MeO_2C, R=Et) with a half-life of 12 minutes and the diester to the monoester with a half-life of 8.7 minutes. Neither methanol or phosphonoacetic acid **5.1** were detected, showing that degradation beyond the monoester was not observed and complete bioactivation of the triester **5.18** to phosphonoacetate **5.1** has yet to be achieved. It was presumed that the monoester **5.22** was not a substitute for the esterase because of its dianionic nature.

Complete bioactivation to phosphonoacetate has not been observed in any of these compounds. The methoxycarbonyl group exhibits a high degree of stability towards chemical and enzymatic hydrolysis and further studies are required to investigate the removal of this carboxylate ester. The replacement of the methoxy group with a better leaving group such as phenoxy or the synthesis of a phosphonoacetate triester with all three negative charges masked by acyloxybenzyl groups **5.24** would be potential starting points for such investigations. A possible complication associated with the 4-acyloxybenzyl prodrug approach, is the release of the highly reactive 4-hydroxybenzyl carbonium ion which may react with cellular nucleophiles, such as DNA, or glutathione and cause toxicity. It is also important to determine the potential these compounds have to cross biological barriers such as the blood brain barrier.

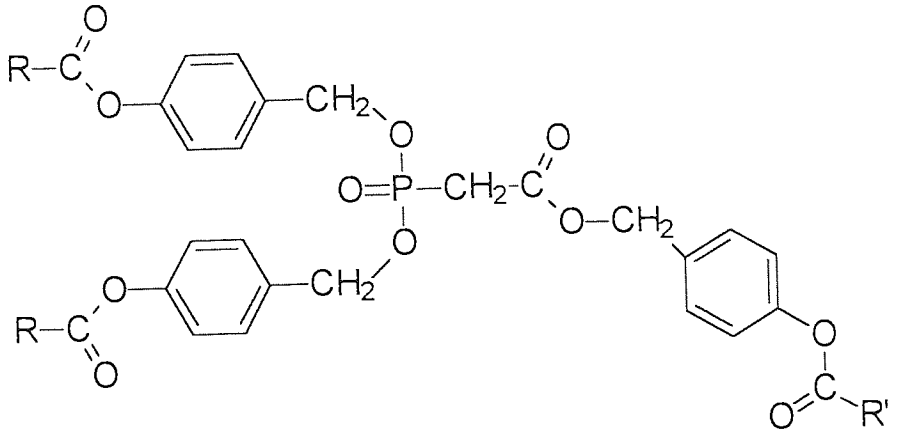

(5.24)

5.1.3 Aims and Objectives

The principal aim of this study was to investigate the transdermal permeation of ionic antiviral phosphonate agents and methods of enhancing this effect. The compounds were derived from phosphonoacetate; namely, the triester, dimethyl benzyloxycarbonylphosphonate **5.25**, the diester, lithium methyl benxyloxycarbonylmethyl phosphonate **5.26** and the monoester, di-monocyclohexylammonium benzyloxycarbonylmethyl phosphonate **5.27**. Excised human epidermis was selected as the *in vitro* membrane for this study due to its relative availability and the possible therapeutic benefits of active topical antiviral agents. Silastic rubber was not used in this study, because results from Chapter 3 showed it was an inappropriate model for absorption enhancers. IPM impregnated cellulose acetate filters were assessed as an alternative artificial membrane.

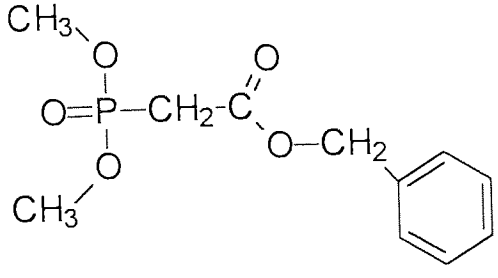

(5.25) Dimethyl benzyloxycarbonylmethyl phosphonate

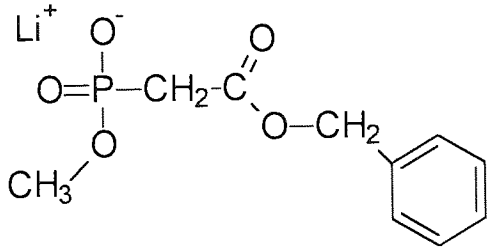

(2.26) Lithium methyl benzyloxycarbonylmethyl phosphonate

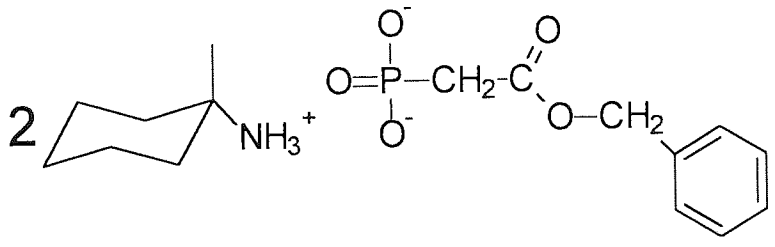

(5.27) Di-monocyclohexylammonium benzyloxycarbonylmethyl phosphonate

With the benzyloxycarbonyl group positioned at the carbonyl, this series of esters **5.25, 5.26, 5.27** should provide the opportunity to study options for novel antiviral prodrugs. If the ester groups are completely hydrolysed then the triester may provide a neutral compound that can be transported across biological membranes before being converted to the active phosphonoacetate.

The action plan to achieve the primary objective was:

- Monitor the hydrolysis of the tri-, di- and mono-esters to determine the reaction kinetics and potential breakdown pathways.

  In order to investigate the potential transdermal permeation of these compounds, it was necessary to determine their susceptibility to hydrolysis, the breakdown pathway and pH-stability profile. Using information from di(4-acyloxybenzyl) esters of methoxycarbonylmethyl phosphonate (Figure 5.5), the anticipated decomposition would be *via* P-O bond cleavage to the diester **5.26** and then to the monoester **5.27**. These compounds would all include the benzyloxycarbonyl group as a chromophore. This investigation sought to confirm the actual degradation pathway of the phosphonate esters and determine the reaction rates with respect to pH. Using this information pH-log rate profiles could be calculated for each compound to determine the pH at which the rate of hydrolysis is slowest (pH_{min}).

- Develop and validate an HPLC method to assay the esters **5.25, 5.26, 5.27**

  In order to monitor the hydrolysis pathway and transdermal permeation of the phosphonate esters (**5.25, 5.26, 5.27**) an assay method was required. The objective was to develop an HPLC assay that could resolve all of the esters and the potential degradent benzyl alcohol on one chromatogram. This would enable the breakdown pathway proposed above to be followed.

- Percutaneous absorption of phosphonoacetate ester prodrugs.

  Using Franz-type *in vitro* absorption cells a method was required that could determine the flux of the three phosphonate esters across human skin. Using this method the transdermal flux of the esters could be studied and the potential of chemical enhancer pretreatment of the absorption barrier to potentiate this permeation investigated.

5.2 Experimental

5.2.1 Hydrolysis Kinetics of the Phosphonoesters

Hydrolysis of the phosphonoacetate esters was performed over a pH range of 2 to 10 in McIlvaine buffers. The double-strength McIlvaine buffers were adjusted with potassium chloride to give an ionic strength in the final reaction solution of 1 M. The composition of the double strength-buffers are detailed in Table 5.1. The reaction solutions were prepared from stock solutions of the esters, these comprised 100 mg triester in 20 ml (50% acetonitrile in distilled water), 100 mg diester in 20 ml distilled water and 125 mg monoester in 20 ml distilled water. 2 ml of each of the above were added to 10 ml double-strength McIlvaine buffer and made up to 20 ml with distilled water.

The solutions were stirred in 20 ml universal vials and maintained at 40°C in an incubator. Replicates were performed in triplicate for the pH 9.98 profiles and in duplicate for all other pH profiles.

Theoretical pH	Sodium Phosphate (g) $Na_2HPO_4,12H_2O$	Citric Acid (g) $C_6H_8O_7,H_2O$	Potassium Chloride (g) KCl
2.28*	5.52	2.58	-
4	5.52	2.58	12.38
6	9.04	1.54	11.14
8	13.94	0.116	6.71
10+	13.94	0.116	6.51

* 16.6 ml 0.1M HCl used to adjust the pH.
\+ 2.7 ml 0.1M NaOH used to adjust the pH.

Table 5.1 Composition of double-strength McIlvaine's Buffers. (Adapted from Perrin and Dempsey, 1974)

Quantities are sufficient to product 100ml double-strength McIlvaine's buffer to give a final reaction solution ionic strength of 1M. Each double-strength solution contained 0.004% w/v phenylmercuric nitrate as an anti-microbial preservative.

Theoretical pH	Final Reaction Solution pH	Quenching Solution*
2.28	2.48	0.2M NaOH
4	3.80	0.1M NaOH
6	5.79	Distilled Water
8	7.95	0.1M HCl
10	9.98	0.1M HCl

* Each reaction sample was quenched with an equal volume of the stated solution.

Table 5.2 Final reaction pH and reaction quenching solutions for the phosphonoacetate ester hydrolysis

Samples were taken and adjusted to a pH of approximately 6 using a quenching solution (Table 5.2) before being injected onto the HPLC (section 2.2.2.1 and 5.3.2). The final reaction pH and the appropriate quenching solutions are detailed in Table 5.2.

5.2.2 Materials

The phosphonates dimethoxy (benzyloxycarbonylmethyl) phosphonate (triester), sodium cyclohexylamino methoxy (benzyloxycarbonylmethyl) phosphonate (diester) and disodium (benzyloxycarbonylmethyl) phosphonate (monoester), were supplied by Dr. S. Freeman Pharmaceutical Sciences Institute, Aston University; structures were confirmed by ^{1}H and ^{31}P NMR.

5.3 Methods of Analysis of the Phosphonates

5.3.1 Ultra-Violet Spectroscopy

Analysis was performed on a Perkin Elmer Lamba-5 UV/Vis spectrophotometer (2nm slit width; 0.05 second response; 0.02A peak threshold). The ultra-violet absorption spectra of the phosphonate triester **5.25**, diester **5.26** and monoester **5.27** were determined between 200-400 nm in 1 cm silica cells (Figure 5.6).

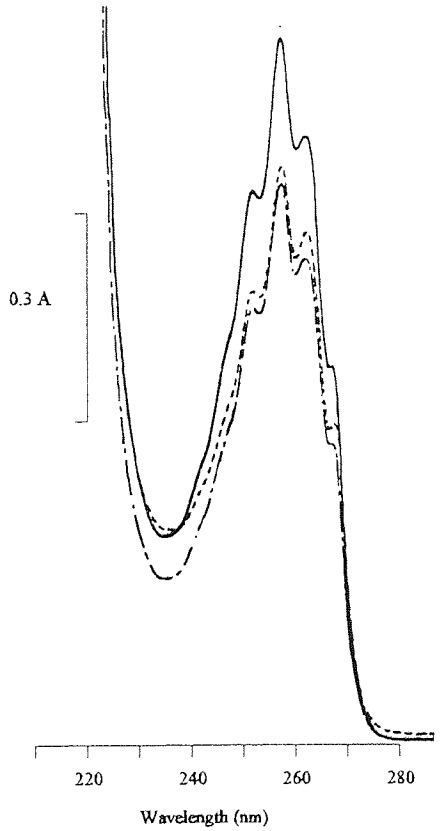

Figure 5.6 The ultra-violet absorption spectra of the phosphonoacetate triester, diester and monoester. (Monoester - solid ; diester - broken ; triester - dots)

Wavelength (nm)	251	256 (λ_{max})	261	266
Monoester	206.0	263.5	226.0	140.2
Diester	162.2	208.7	181.0	111.5
Triester	169.0	214.7	191.2	119.2

Table 5.3 Molar absorption coefficients ε_{max} (M^{-1} cm^{-1}) for the phosphonate esters **5.25,26,27** at various wavelenths.

5.3.2 HPLC Mobile Phase Development

The instrumentation used in this study is described in section 2.2.2.1. By manipulation of various parameters within an HPLC system, it is possible to achieve optimal detection and resolution of mixtures of compounds within a solution. The parameters that have the most significant influence upon analytical chromatography are choice of stationary phase, the selection of mobile phase and the wavelength of detection. There are detailed texts giving the theoretical principles of interactions between these variables and how they influence the chromatography of the analyte and of the practical aspects of HPLC. (Knox *et al*, 1978; Simpson 1978). The method of approach to the assay development for therapeutic compounds is also well documented (Moffat 1986, Tsuji & Morozowi 1978-79). To measure HPLC optimisation, there are several mathematical parameters that can define chromatographic performance in terms of resolution and retention (Irwin and Scott 1982; Li Wan Po and Irwin, 1980). These are summarised in Table 5.4.

The objective was to design a mobile phase that would resolve the three phosphonate esters **5.25, 5.26** and **5.27** and the possible degradation product benzyl alcohol on a single isocratic chromatogram. With HPLC mobile phase development, it is best practice to start with the simplest mobile phase possible and work through more complex combinations of organic modifiers, pH, ionic-strength and finally ion-pairs.

Ion-pair chromatography is a technique that is a versatile and efficient method for the separation of ionised and ionisable molecules by HPLC. Using mobile phases without ion-pairs, compounds of this type give broad and tailing peaks and have poor separation characteristics on most column types. With chemically bonded reversed-phase stationary phases on standard HPLC systems, the selectivity of the separation system can be easily altered by making all the changes to the composition of the mobile phase. An important advantage of ion-pair chromatography is its ability to simultaneously separate samples containing acids and bases or neutral and ionised molecules, such as the three esters of phosphonoacetate. **5.25, 5.26** and **5.27**. An ion-pair is a temporary or reversibly formed derivative of an ion from the solute molecule. It is generally considered that the analyte or solute ion forms a lipophilic complex with a counter ion of opposite charge delivered with the mobile phase. Tetrabutyl ammonium hydroxide is generally used as a counter-ion for anions and alkane sulphonic acid

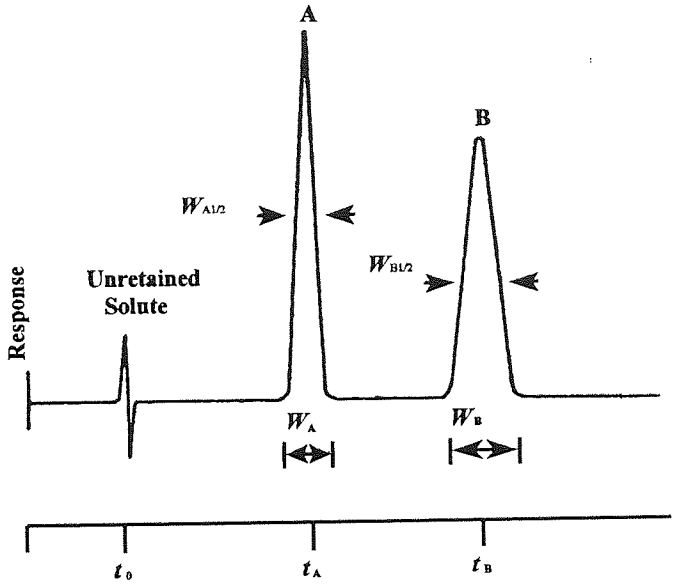

Definitions The mobile phase hold up time t_0 represents the dead or void volume of the system. t_A and t_B are the retentive times of compounds A and B. W_A and W_B are the base width of peaks A and B

Parameter	Formula	Comments
Retention Volumes	$V_0 = t_0 F$	V_0, V_A and V_B are calculated from the mobile phase flow rate F ml.min^{-1}
Capacity Factor for compound A	$k' = \dfrac{(t_A - t_0)}{t_0}$	k' is the number of column volumes needed to elute a given solute
Number of Theoretical Plates	$N = 16\ (t_A / W_A)^2$	N, gives a measure of the column efficiency for a particular analyte.
Resolution	$R_S = \dfrac{2\ (t_B - t_A)}{(W_A + W_B)}$	R_S, is a measure of the efficiency of the separation of different components

Table 5.4 Mathematical parameters used to define chromatographic performance.

for cations. The lipophilicity of the ion-pair can be adjusted by the relative chain-length of the alkyl groups upon either counter-ion. In reversed-phase mode, the mobile phase is considered the "aqueous phase" and the stationary phase the "organic phase". The ion-pair formation occurs in the aqueous phase and the net result is greater association of the ionic solute with the organic stationary phase. Chromatographic separations result principally from the dynamic exchange of the ionised solute between the mobile and stationary phases, either directly, as the ion-pair, or after dissociation into the ion-pair's constituent parts. This description is an over-simplification of the actual situation and the separation is more accurately described in terms of ionic interactions which do not require the formation of a formal ion-pair complex.

The pH of the mobile phase is usually chosen so that both the sample and the counter-ion are completely ionised. By adjusting the pH, the extent of dissociation of the sample, counter-ion and corresponding ion-pair may be varied. Hence, the system can be made very selective optimising the separation of compounds of interest. Ideal counter-ions should remain completely dissociated over a wide pH range to enable the utilisation of optimal pH for separation (Poole and Schnette, 1984). Strong acids, such as perchloric or alkylsulphonic, and salts of strong bases, such as quaternary ammonium salts, are usually used (Engelhardt, 1979).

The retention of a solute will increase with the ability of the counter-ion to form an ion-pair and with the size of the counter-ion. The optimum concentration of counter-ion for a particular separation is less predictable. For very low counter-ion concentrations, the solute retention usually increases rapidly with increasing counter-ion concentration. Eventually a plateau region is reached, at which point retention changes very slightly with further addition of counter-ion, although unpredictable changes can occur. For large counter-ions a mobile phase concentration of 0.005 M is fairly common. With small counter-ions, much higher concentrations are generally used, for example, 0.01 to 0.50 M. For any particular separation, the optimum concentration of the counter-ion can only be established by experiment.

It was anticipated that the most likely breakdown pathway for the triester would be hydrolysis of the methoxy groups on the phosphate atom or the hydrolysis at the carboxyl ester group with consequential appearance of benzyl alcohol. Therefore, the ability of the chromatographic profile to resolve benzyl alcohol and the three esters, **5.25, 5.26, 5.27**, on one chromatogram would be desirable. Tables 5.7 and 5.8 summarise the solvents tried and the mathematical

parameters of each. The compounds were assessed individually on separate chromatograms for retention time and theoretical plate number, then as a mixture for the resolution between compounds.

5.3.2.1 *Acetonitrile/Water Combinations (Table 5.5, mobile phases 1 & 2)*

Using the simple mobile phase of 65% acetonitrile, all the phosphonate esters eluted with the solvent front. As the acetonitrile concentration was reduced from 65% to 35%, the triester appeared on the chromatogram with a retention time of 3.4 minutes. The pK_a values for the hydroxyl groups on the phosphorus of phosphonoacetic acid are 2.30 and 8.60. The actual values for the esters are expected to be in this region, although they may be slightly lower (stronger acids) as the proton will be more easily removed from $(HO)_2PO.CH_2COOCH_2.C_6H_5$ than from $(HO)_2PO.CH_2\text{-}COO^-$. The mono- and di-esters would therefore be ionised in the unbuffered mobile phases and be expected to elute with the solvent front.

5.3.2.2 *pH Adjustment Acetonitrile/Water Combinations (Table 5.5, mobile phase 6)*

By adjusting the pH to 3.03 with orthophosphoric acid and using 35% acetonitrile, it was hoped to associate the diester and obtain a chromatogram of this compound. Unfortunately, the diester still eluted with the solvent front, as did the monoester. Again, a chromatogram of the triester was obtained with a retention time of 4.4 minutes.

5.3.2.3 *Changing the Organic Modifier to Methanol (Table 5.5, mobile phase 3)*

Using simple acetonitrile solutions, it appeared unlikely that all three esters were resolvable on one chromatogram. Before resorting to ion-pair chromatography, the organic modifier was changed to methanol. Using orthophosphoric acid to adjust the pH to 3, the mono- and di-ester were eluted on the chromatogram with retention times of 3.1 and 3.9 minutes respectively. However, the peak shapes were poor and these compounds were not resolved from each other. The triester eluted with a long retention time of 30.3 minutes. It was

assumed that to obtain a practical retention time for the triester by increasing the methanol content, the ionic compounds would elute with the solvent front as with mobile phases 1,2 and 6.

5.3.2.4 Ion-pair Chromatography

The conclusion was that all three phosphonate molecules would only appear on one chromatographic run with the aid of ion-pairing agents. The diester and monoester ionise to form anions so that the ion-pair agent chosen was tetrabutyl ammonium hydroxide (TBH). The concentration of TBH was set at 0.01M in the aqueous portion of the mobile phase, the actual concentration was dependent upon the proportion of organic modifier used. The triester is a neutral molecule and so its retention time should not be affected by the use of ion-pairing agents. Acetonitrile was chosen as the organic modifier.

5.3.2.5 Acetonitrile: 0.01M TBH (Table 5.5, mobile phase 3 & 4)

Using mobile phases of acetonitrile: 0.01M TBH (65:35) (0.0035M TBH in the final solution) all the compounds were eluted at the solvent front. It was quickly realised that the pH of these mobile phases was too high and that the mono- and di-esters were not sufficiently ionised to form ion-pairs. The pH of these mobile phases was above that recommended for use with HPLC columns and was probably damaging the column. Modifications of the acetonitrile concentration from 65% to 35% gave a peak corresponding to the triester at a retention time of 2.70 minutes.

5.3.2.6 Acetonitrile: 0.01M TBH, pH 3.03 (Table 5.5 mobile phase 7 & 8)

To assure the formation of ion-pairs, the mobile phase pH was adjusted to 3.03 with orthophosphoric acid. The use of this mobile phase, with 35% acetonitrile produced a chromatogram with all three compounds represented. The diester had a long retention time (8.3 minutes) and the triester and monoester were not resolved (Rs=0.31) with retention times

of 4.4 and 4.2 minutes respectively. By increasing the acetonitrile concentration from 35% to 40% and leaving all the other parameters the same, the diester retention time reduced to 4.1 minutes. The monoester and triester remained unresolved (Rs=0.50) with retention times of 3.2 and 3.0 minutes respectively.

5.3.2.7 Acetonitrile: 0.01M TBH (25:75), pH 5 (Table 5.6, mobile phase 9, Fig 5.7A)

Sodium phosphate 0.01M was added to the 0.01M TBH as a buffer to stabilise the pH of the mobile phase, any further pH adjustments were made with orthophosphoric acid. As the retention time of the triester should only be influenced by the concentration of the organic modifier and the triester and the monoester were interfering in mobile phase 7 and 8, the concentration of acetonitrile was reduced to 25%. The reduction in acetonitrile from 35% to 25% increased the retention time of the triester to 5.85 minutes from 4.2 minutes. Acetonitrile 25% has the added benefit that benzyl alcohol became resolved from the solvent front with a retention time of 2.53 minutes. The mobile phase pH was also adjusted to pH5 and although the reduction in organic modifier from 35% to 25% causing an increase in the retention time of the neutral triester, the retention time of the diester decreased from 9.3 to 6.29 minutes and the monoester from 4.40 to 3.74 minutes. This was because the ionisable hydroxyl group of these compounds at this pH has a pK_a in the region of 2 to 3. As the pH is increased, the degree of ionisation reduced with a consequential reduction in ion-pairing. With reversed-phase chromatography, the ion-pair will have a longer retention time relative to either of the parent compounds and so the retention time of these esters reduced with increasing pH. The retention time of the diester was longer than the monoester, due to the greater polarity of the monoester. Increasing polarity with reversed-phase chromatography lowers a compound's affinity for the stationary phase resulting in shorter retention times. Although the pH change from 3.03 to 5 resolved the monoester from the triester the diester was no longer resolved from the triester (Rs = 0.46).

5.3.2.8 Acetonitrile: 0.01M TBH (25:75) pH 6 & 7 (Table 5.6, mobile phases 10 & 11 Figure 5.7 B & C)

With mobile phases 10 and 11 the concentration of the organic modifier, acetonitrile, was

unchanged from mobile phase 9, at 25%. Therefore the retention times of the neutral triester and benzyl alcohol remained unchanged at approximately 5.9 and 2.6 minutes respectively. The increasing pH reduced the retention times of the monoester to 3.24 minutes at pH 6 and 2.60 at pH 7 and the diester to 4.70 minutes at pH 6 and 3.4 minutes at pH 7. At pH 6 an ideal chromatogram was produced where all compounds were resolved with Rs values greater than 1.5 and the number of theoretical plates per metre greater than 2500. The further increase in pH to 7 produced a chromatogram where the retention time of the monoester was reduced to 2.60 minutes. This peak was then superimposed upon the benzyl alcohol peak (Rt = 2.65 minutes Rs = 0.12).

Acetonitrile: sodium phosphate 0.01M, tetrabutyl ammonium hydroxide 0.01M (25:75) adjusted to pH 6 with orthophosphoric acid was chosen as the most suitable mobile phase to monitor the breakdown pathway and pH stability profile of the phosphonoacetate esters (Mobile phase 10, Table 5.6 indicated in bold type). Typical calibration plots for the phosphonate esters **5.25, 26, 27** and benzyl alcohol **5.20** using this mobile phase are shown in Figure 5.8 with the corresponding statistical parameters in Table 5.7. After assessment of the triester stability, the *in vitro* transdermal permeation of this compound was assayed by HPLC using acetonitrile:water (35:65) adjusted to pH 3 using orthophosphoric acid (mobile phase 6, Table 5.5). This mobile phase was used because the triester had a shorter retention time (4.4 minutes), it was also a simpler and less expensive mobile phase to produce, as it did not contain ion-pair agents, and the other esters eluted with the solvent front. A typical calibration plot for the triester **5.25** using mobile phase 6 (Table 5.5) is shown in Figure 5.9 with the corresponding statistical parameters in Table 5.8.

	MOBILE PHASE	MONOESTER			DIESTER			TRIESTER	
		Retention Time (min)	Theoretical Plates (m^{-1})	Resolution Monoester/ Diester	Retention Time (min)	Theoretical Plates (m^{-1})	Resolution Diester / Triester	Retention Time (min)	Theoretical Plates (m^{-1})
1	Acetonitrile : Water (65:35)	e/s			e/s			e/s	
2	Acetonitrile : Water (35:65)	e/s			e/s			3.4	2620
3	Acetonitrile : 0.01M Tetrabutyl Ammonium Hydroxide (65:35)	e/s			e/s			e/s	
4	Acetonitrile : 0.01M Tetrabutyl Ammonium Hydroxide (35:65)	e/s			e/s			2.7	2380
5	Methanol : Orthophosphoric Acid : Water (30:0.1:70)	3.1	1600	0.60	3.9	840	10.37	30.3	11360
6	Acetonitrile : Water (pH 3.03*) (35:65)	e/s			e/s			4.4	4840
7	Acetonitrile : 0.01M Tetrabutyl Ammonium Hydroxide (pH 3.03*) (35:65)	4.4	8604	0.31[a]	8.3	5623	3.90	4.2	5760
8	Acetonitrile : 0.01M Tetrabutyl Ammonium Hydroxide (pH 3.03*) (40:60)	3	9000	0.50[a]	4.1	5490	1.64	3.2	10240

Table 5.5 Mobile phases and HPLC mathematical parameters of phosphonates (Mobile phases delivered at a rate of 1ml per minute) {*, adjusted with orthophosphoric acid : e/s, eluted with solvent front : n/a, not applicable : a, triester / monoester)

MOBILE PHASE pH	BENZYL ALCOHOL			MONOESTER			DIESTER			TRIESTER	
	Retention Time (min)	Theoretical Plates (m^{-1})	Resolution Benzyl A/ Monoester	Retention Time (min)	Theoretical Plates (m^{-1})	Resolution Monoester /Diester	Retention Time (min)	Theoretical Plates (m^{-1})	Resolution Diester / Triester	Retention Time (min)	Theoretical Plates (m^{-1})
9 Adjusted to pH 5	2.53	4100	1.92	3.74	3870	2.89[a]	6.29	4400	0.46	5.85	11170
10 Adjusted to pH 6	**2.55**	**9000**	**1.53**	**3.24**	**5360**	**2.15**	**4.70**	**5520**	**1.57**	**5.83**	**13280**
11 Adjusted to pH 7	2.65	8670	0.12	2.60	4330	1.77	3.45	9000	4.64	5.91	15520

Table 5.6 Mobile phase pH and its effect upon the HPLC mathematical parameters for benzyl alcohol and the monoester, diester and triester phosphonates. The mobile phase was sodium phosphate 0.01M, tetra butyl ammonium hydroxide 0.01M: acetonitrile (75:25) adjusted to pH with orthophosphoric acid and delivered at a rate of 1 ml/minute. (a, monoester / triester).

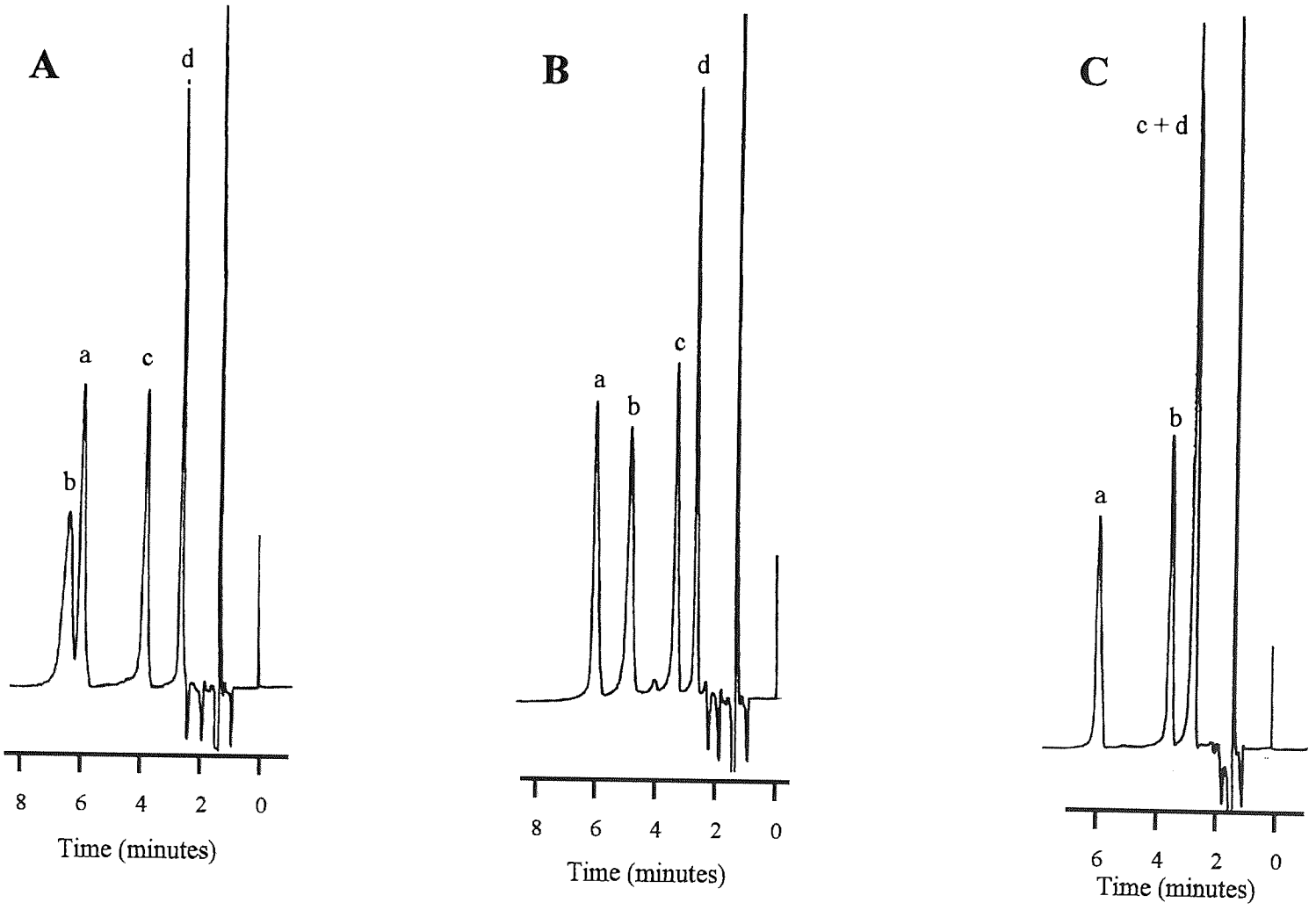

Figure 5.7 Example HPLC chromatograms demonstrating the effect of mobile phase pH upon the retention times of sample phosphonoacetate esters. Mobile phase -sodium phosphate 0.01M, tetra n-butyl ammonium hydroxide 0.01M: acetonitrile (75:25) adjusted to pH with orthophosphoric acid. A, pH5; B, pH6; C, pH7. (a, triester; b, diester; c, monoester; d, benzyl alcohol)

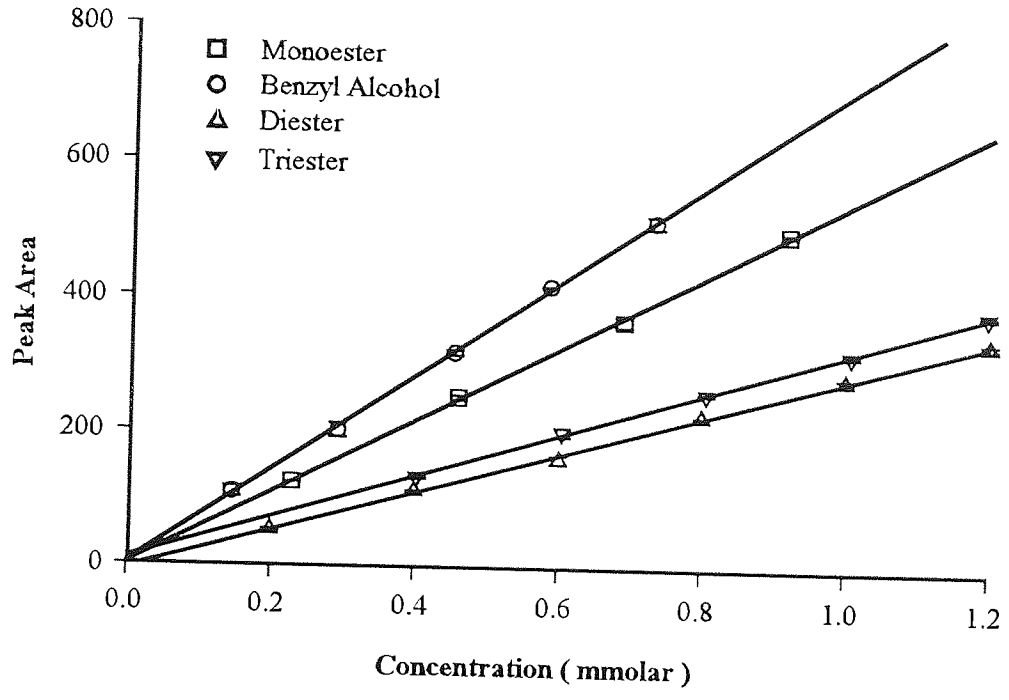

Figure 5.8 Typical calibration curves for the phosphonate esters **5.25,26,27** and benzyl alcohol **5.20** using HPLC mobile phase 10 Table 5.6. HPLC sensitivity 0.08 aufs. (Error bars represent range of two replicate samples)

	Intercept			Slope			Correl Coeff
	Value	± SE	± 95% CI	Value	± SE	± 95% CI	r
Benzyl Alcohol	540	9.72	41.82	1.5	6.10	26.27	0.9997
Monoester	702	10.65	33.90	3.0	5.19	16.51	0.9996
Diester	289	4.43	12.29	-5.3	3.44	9.57	0.9995
Triester	312	4.06	12.92	10.29	3.45	2.96	0.9997

Table 5.7 Statistics for the calibration curves of the phosphonate esters and benzyl alcohol in Figure 5.8. (SE, standard error ; CI confidence interval)

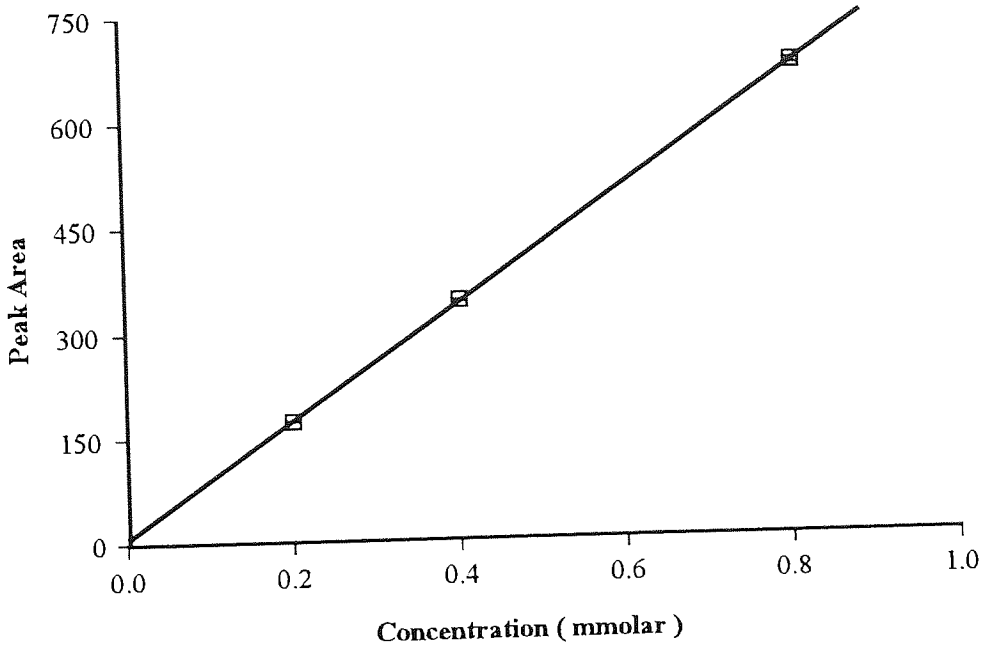

Figure 5.9 Typical calibration curve for the phosphonate triester **5.25** using HPLC mobile phase 6 Table 5.5. HPLC sensitivity 0.04 aufs. (Error bars represent the range of two replicate samples)

	Intercept		Slope		Correlation Coefficient
	Value	± SE	Value	± SE	r
Triester	7.4	2.71	826	5.09	0.9999

Table 5.8 Statistics for the calibration curve of the phosphonate triester **5.25** in Figure 5.9 (SE, standard error)

5.4 Results and Discussion

5.4.1 Triester Hydrolysis

HPLC chromatograms produced during hydrolysis of the phosphonate triester only revealed two discernible peaks, that of the original triester (retention time 7.5 minutes) and a peak corresponding to benzyl alcohol (retention time 3.3 minutes). Figure 5.10 shows an example chromatogram of the triester hydrolysis after 30 minutes at pH 9.98. The mobile phase was sodium phosphate 0.01M, tetra n-butyl ammonium hydroxide 0.01M : acetonitrile (75:25). The peak at 'a' represents benzyl alcohol and at 'b' the phosphonate triester **5.25**. The results show that the breakdown initially proceeds *via* loss of benzyl alcohol by hydrolysis at the carbonyl group. Loss of the chromophore prevents further analysis of degradation pathways. Figure 5.11A illustrates the breakdown profiles of the triester with varying pH. The logarithmic plot (Figure 5.11B) demonstrates a linear relationship between the natural logarithm of concentration and time implying that the reaction rate is first-order. The degradation rate constants (k_1) for the reduction and corresponding half-lives ($t_{½}$) were calculated from the slopes of the linear plots of natural logarithm of the concentration against time by linear regression. These are

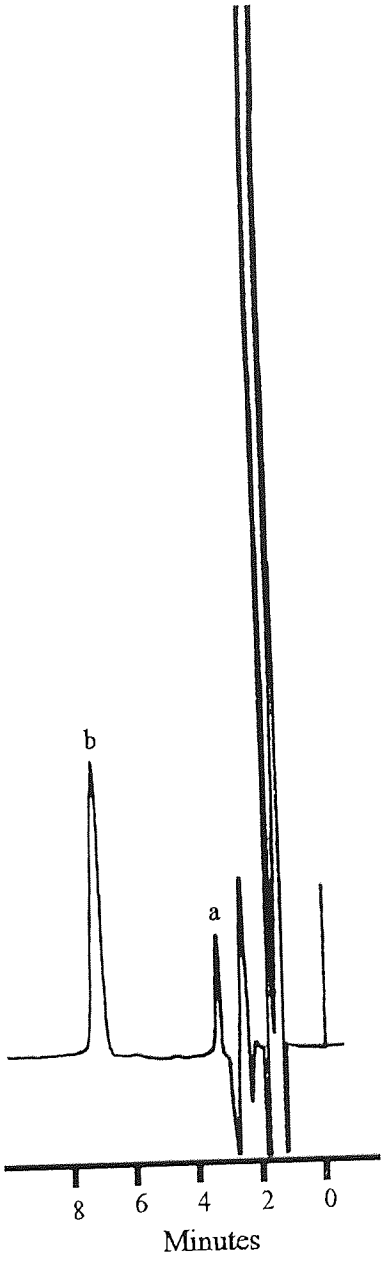

Figure 5.10 Example HPLC chromatogram showing the breakdown of the phosphonoacetate triester (a, benzyl alcohol; b, phosphonate triester **5.25**)

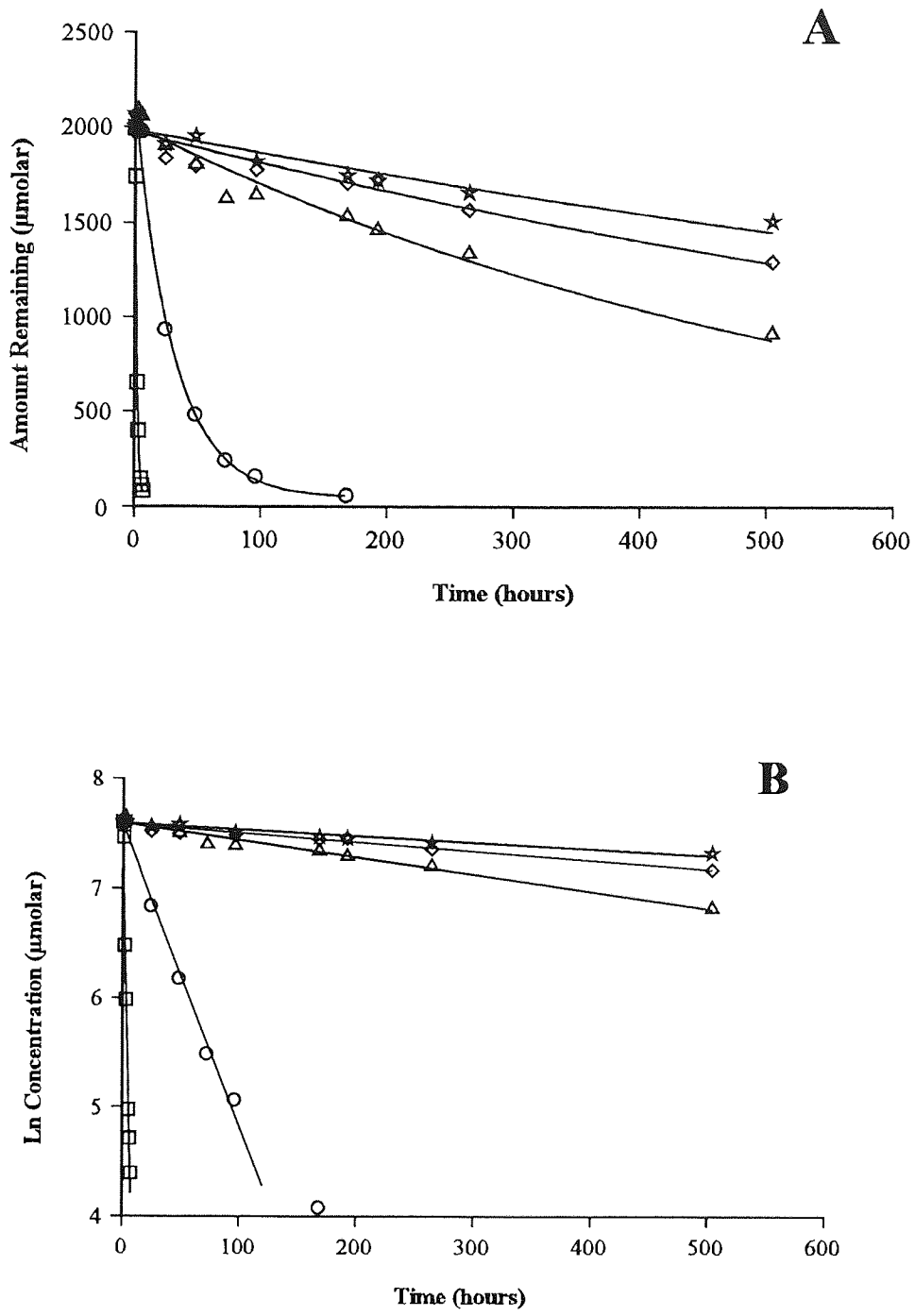

Figure 5.11 Plot of concentration versus time for the stability profile of the phosphonoacetate triester in relation to pH. (□, pH 9.98;○, pH 7.95;△, pH 5.79;◇, pH 3.80;☆, pH 2.48)

A Concentration versus time plot
B Ln concentration versus time plot

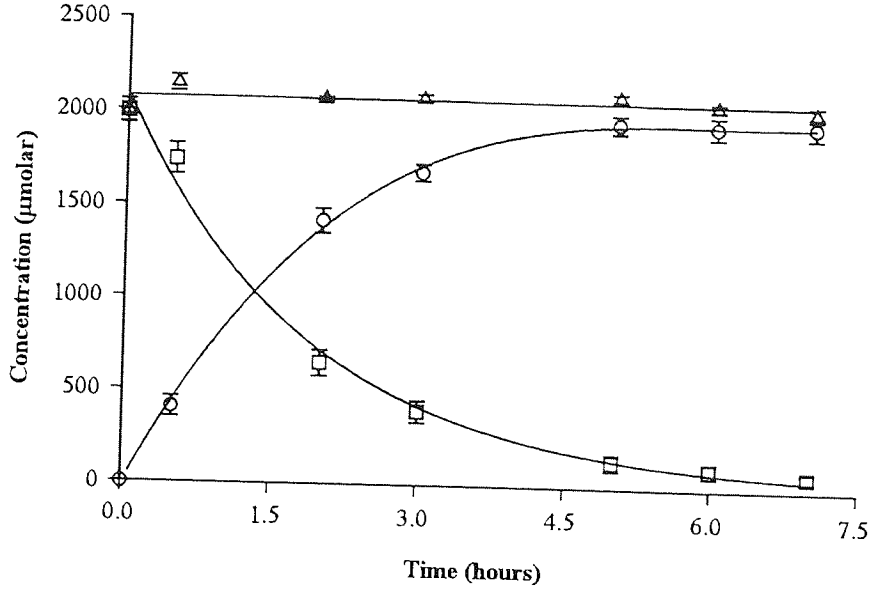

Figure 5.12 Time courses for triester (□), benzyl alcohol (○) and mass balance (△) during the triester hydrolysis at pH 9.98. (Error bars represent SEM).

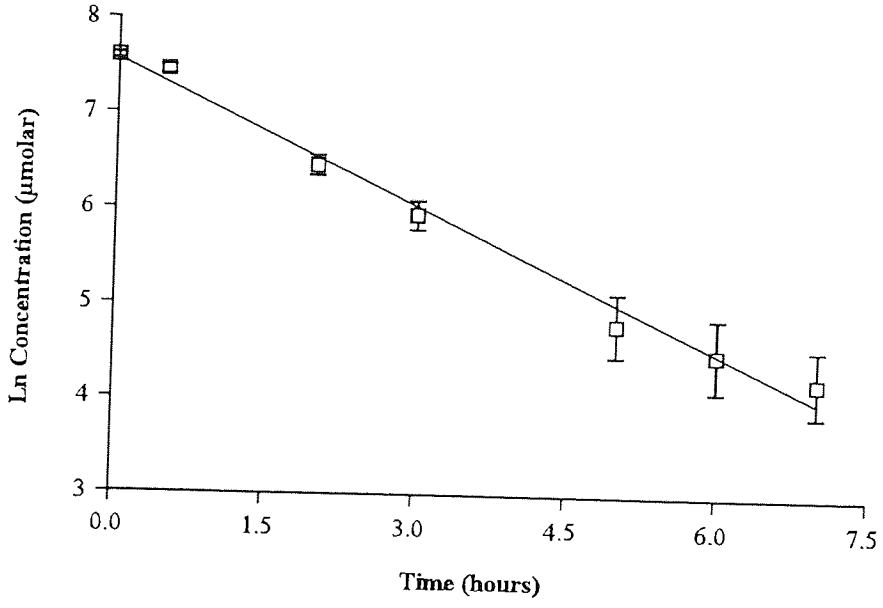

Figure 5.13 First-order reaction profile for the triester at pH 9.98. (Error bars represent SEM).

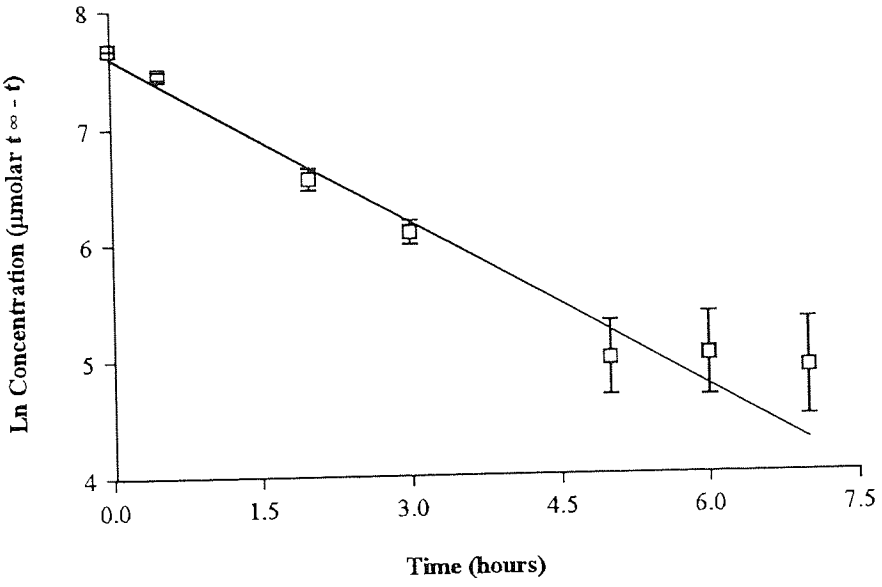

Figure 5.14 First-order plot for the appearance of benzyl alcohol during the hydrolysis of the triester at pH 9.98 (Error bars represent SEM).

summarised with respect to pH in Table 5.9. Figure 5.12 shows the breakdown of the triester **5.25** at pH 9.98 and the corresponding appearance benzyl alcohol in an equimolar ratio. The logarithmic plots are represented in Figures 5.13 and 5.14. The 6 and 7 hour time points in Figure 5.14 deviate from linearity, this is probably because the reaction was virtually complete and the concentration of benzyl alcohol was no longer increasing. From the gradient of these slopes the first-order rate of benzyl alcohol appearance is 0.475 hr^{-1} which compares to the rate of disappearance of the triester **5.25** of 0.508 hr^{-1} (SE=0.037). This confirms that the hydrolysis is limited to one reaction at the COOR group and hydrolysis at P-O is not observed. The reaction scheme for this hydrolysis is depicted in Figure 5.15.

pH	Rate (hr^{-1})	Rate ± SE	Rate ± 95% CI	Half Life (hr)	Ln Rate (hr^{-1})
9.98	5.08×10^{-1}	2.389×10^{-2}	6.164×10^{-2}	1.36	-0.294
7.95	2.75×10^{-2}	1.018×10^{-3}	2.617×10^{-3}	25.19	-1.560
5.79	1.55×10^{-3}	8.651×10^{-5}	1.957×10^{-4}	447.33	-2.809
3.80	8.35×10^{-4}	7.591×10^{-5}	1.750×10^{-4}	829.82	-3.078
2.48	5.94×10^{-4}	5.571×10^{-3}	1.284×10^{-4}	1167.11	-3.226

Table 5.9 Rate of breakdown for phosphonoacetate triester (k_1) with respect to pH (SE, standard error; CI, confidence interval).

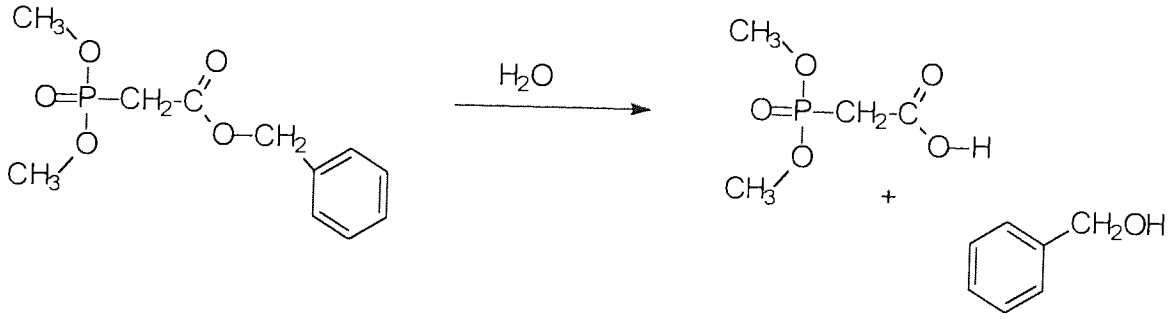

Figure 5.15 Mechanism of hydrolysis of dimethyl benzyloxycarbonylmethyl phosphonate **5.25**

5.4.2 Diester Hydrolysis

As with the triester, HPLC chromatograms produced during hydrolysis of the phosphonate diester **5.26** only contained two distinguishable peaks. That of the original diester (retention time 6.2 minutes) and a peak corresponding to benzyl alcohol (retention time 3.3 minutes). Figure 5.16 shows an example chromatogram of the diester hydrolysis after 19 hours at pH 9.98. The mobile phase was sodium phosphate 0.01M, tetra n-butyl ammonium hydroxide 0.01M : acetonitrile (75:25). The peak at 'a' represents benzyl alcohol and at 'b' the phosphonate diester. The results show that, here too the breakdown initially proceeds *via* the loss of benzyl alcohol and loss of the chromophore prevents further analysis of the degradation pathways. Figure 5.17A illustrates the linear breakdown profile of the diester with varying pH. The logarithmic plot (Figure 5.17B) demonstrates a linear relationship between the natural logarithm of concentration and time implying that the reaction rate is first-order. Figure 5.16 shows the linear breakdown of the diester at pH 9.98 and the corresponding appearance of benzyl alcohol in an equimolar ratio. The logarithmic plots are represented in Figures 5.19 and 5.20. From the gradient of these slopes the first-order rate of benzyl alcohol appearance is 7.12×10^{-2} hr^{-1} (SE=6.204×10^{-3}) which compares to the rate of disappearance of the diester **5.26** of 6.90×10^{-2} hr^{-1} (SE=9.470×10^{-4}).

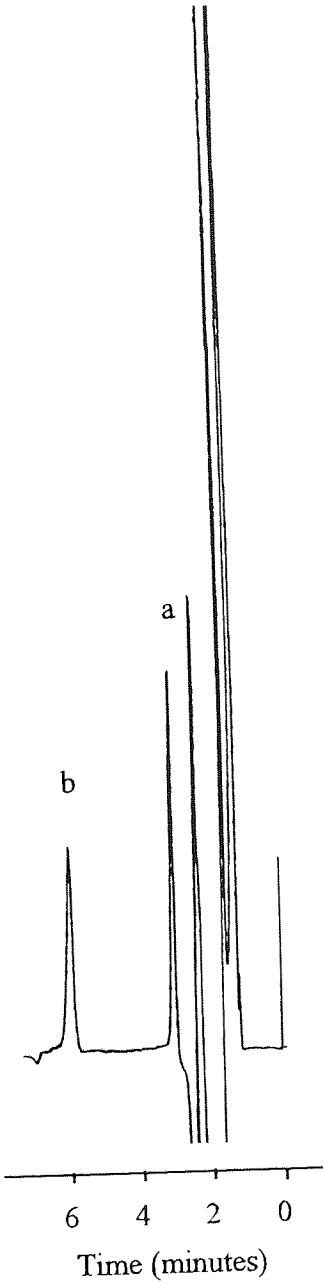

Figure 5.16 Example HPLC chromatogram showing the breakdown of the phosphonoacetate diester (a, benzyl alcohol; b, phosphonate diester **5.26**)

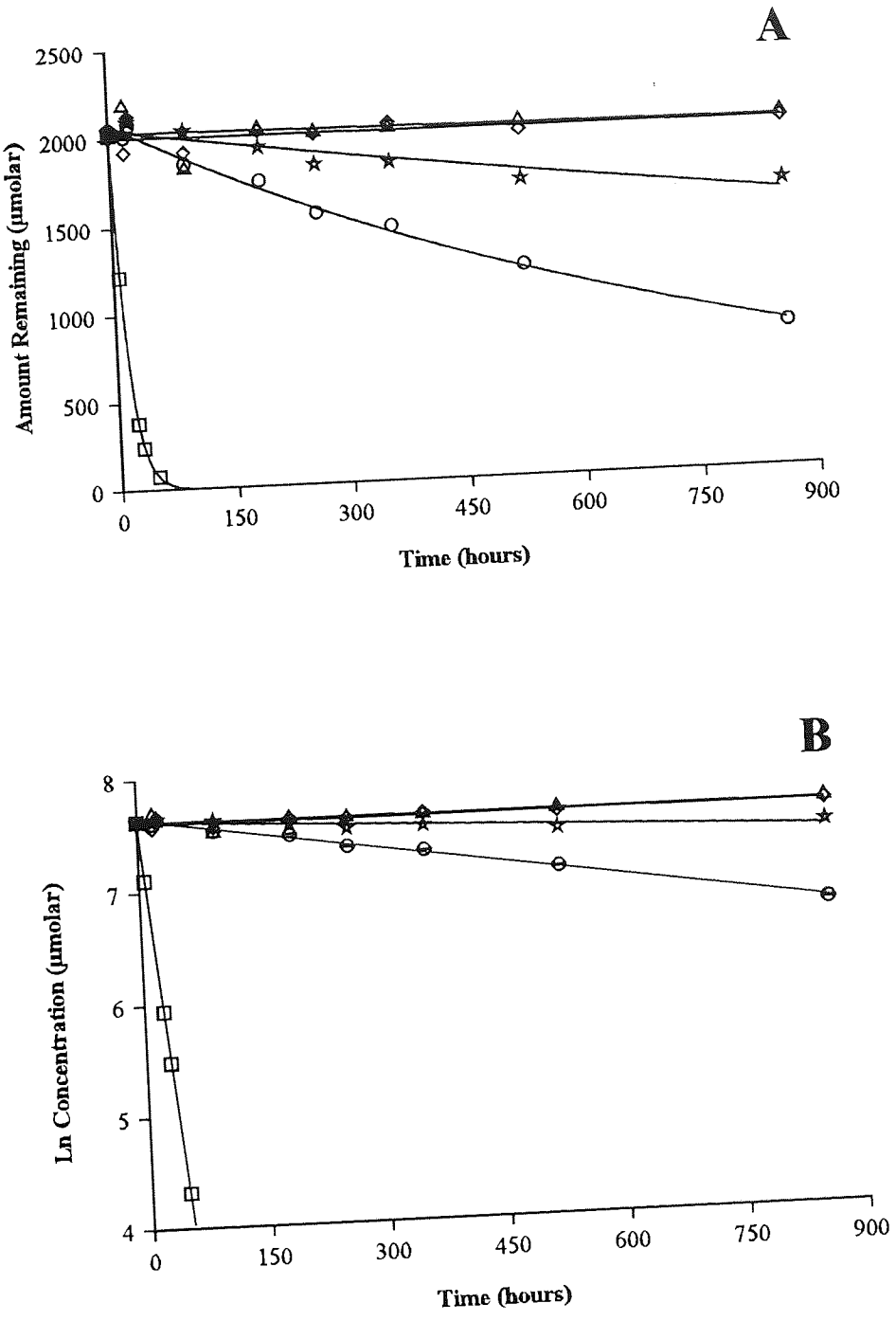

Figure 5.17 Plot of concentration versus time for the stability profile of the phosphonoacetate diester in relation to pH. (□, pH 9.98;○, pH 7.95;△, pH 5.79;◇, pH 3.80;☆, pH 2.48)

A Concentration versus time plot
B Ln concentration versus time plot

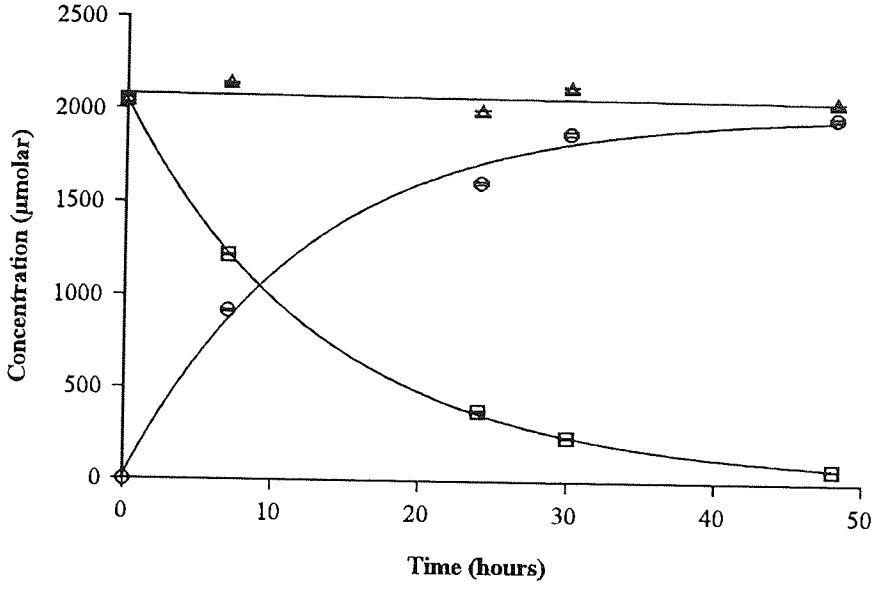

Figure 5.18 Time courses for diester (□), benzyl alcohol (○) and mass balance (△), during the diester hydrolysis at pH 9.98. (Error bars represent SEM)

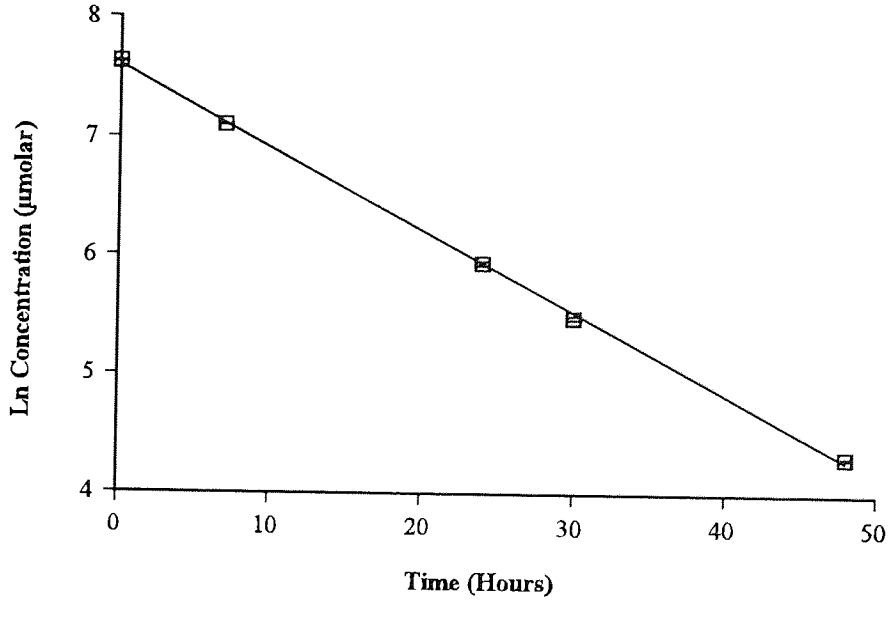

Figure 5.19 First-order reaction profile for the diester at pH 9.98. (Error bars represent SEM)

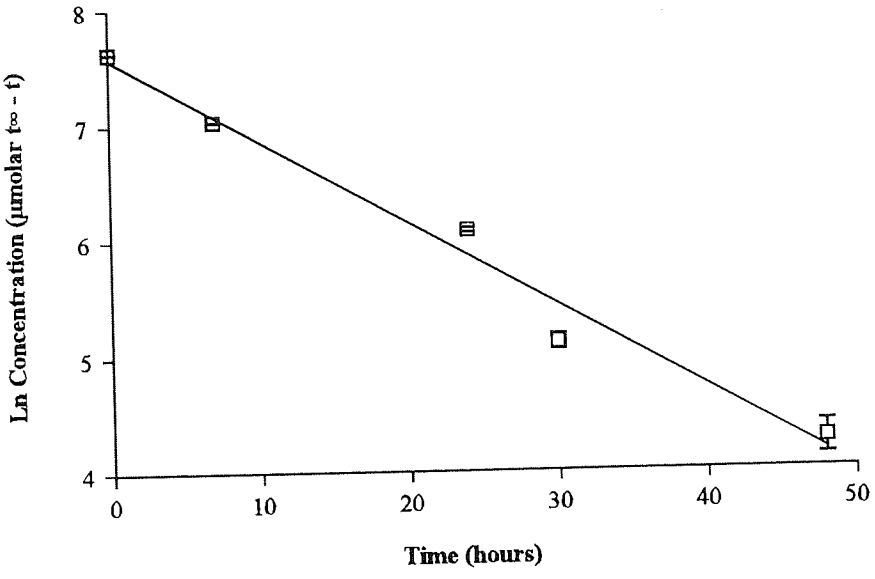

Figure 5.20 First-order plot for the appearance of benzyl alcohol during the hydrolysis of the diester at pH 9.98. (Error bars represent SEM)

This profile confirms the reaction scheme in Figure 5.21 where benzyl alcohol is produced on hydrolysis of the phosphonate at the carbonyl carbon. The degradation rate constants (k_1) for the reduction and corresponding half-lives ($t_{½}$) were calculated from the slopes of the natural logarithm of concentration against time graphs by linear regression. These are summarised with respect to pH in Table 5.10.

pH	Rate (hr^{-1})	Rate ± SE	Rate ± 95% CI	Half Life (hr)	Ln Rate (hr^{-1})
9.98	6.90×10^{-2}	9.470×10^{-4}	3.014×10^{-3}	10.05	-1.161
7.95	1.06×10^{-3}	2.530×10^{-5}	2.982×10^{-3}	655.77	-2.976
5.79	2.38×10^{-5}	6.356×10^{-5}	1.503×10^{-4}	29123.83	-4.623
3.80	9.65×10^{-6}	4.098×10^{-5}	9.691×10^{-5}	71806.40	-5.015
2.48	2.99×10^{-4}	3.393×10^{-5}	8.024×10^{-5}	2318.99	-3.524

Table 5.10 Rate of breakdown for phosphonoacetate diester (k_1) with respect to pH (SE, standard error; CI, confidence interval).

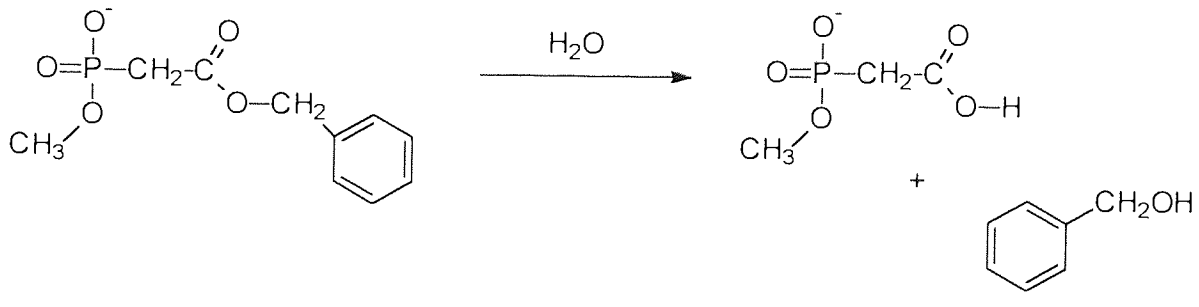

Figure 2.21 Mechanism of hydrolysis of methyl benzyloxycarbonylmethyl phosphonate **5.26**

5.4.3 Monoester Hydrolysis

Again, HPLC chromatograms produced during hydrolysis of the phosphonate monoester **5.27** only revealed two recognisable peaks, that of the original monoester (retention time 4.6minutes) and a peak corresponding to benzyl alcohol (retention time 3.3 minutes). Figure 5.22 shows an example chromatogram of the diester hydrolysis after 14 days at pH 9.98. The mobile phase was sodium phosphate 0.01M, tetra n-butyl ammonium hydroxide 0.01M : acetonitrile (75:25). The peak at 'a' represents benzyl alcohol and at 'b' the phosphonate monoester. In this compound too, the results show that the break down involves the loss of the sole remaining ester group through loss of benzyl alcohol. The breakdown profile of the monoester with varying pH is shown in Figure 5.23A. The logarithmic plot demonstrates a linear relationship between the natural logarithm of concentration and time, implying that the reaction rate is first-order (Figure 5.23B). The degradation rate constants (k_1) for the reduction and corresponding half-lives ($t_{½}$) were calculated from the slopes of the linear plots of natural logarithm of concentration against time by linear regression and are summarised with respect to pH in table 5.11.

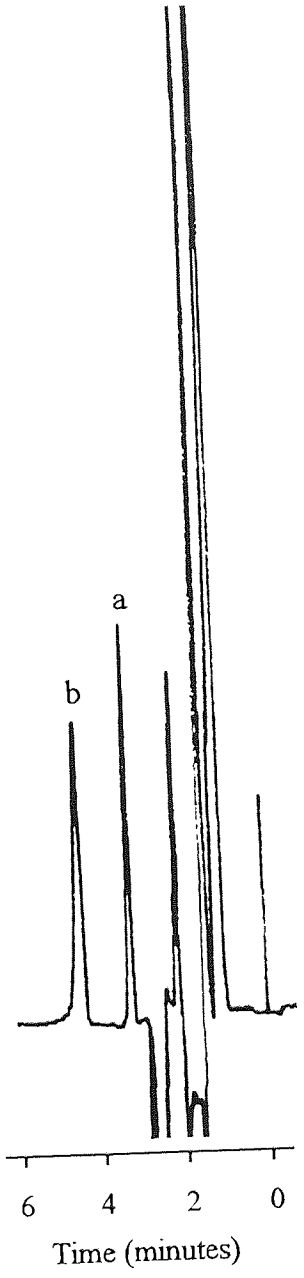

Figure 5.22 Example HPLC chromatogram showing the breakdown of the phosphonoacetate monoester (a, benzyl alcohol; b, phosphonate monoester **5.27**)

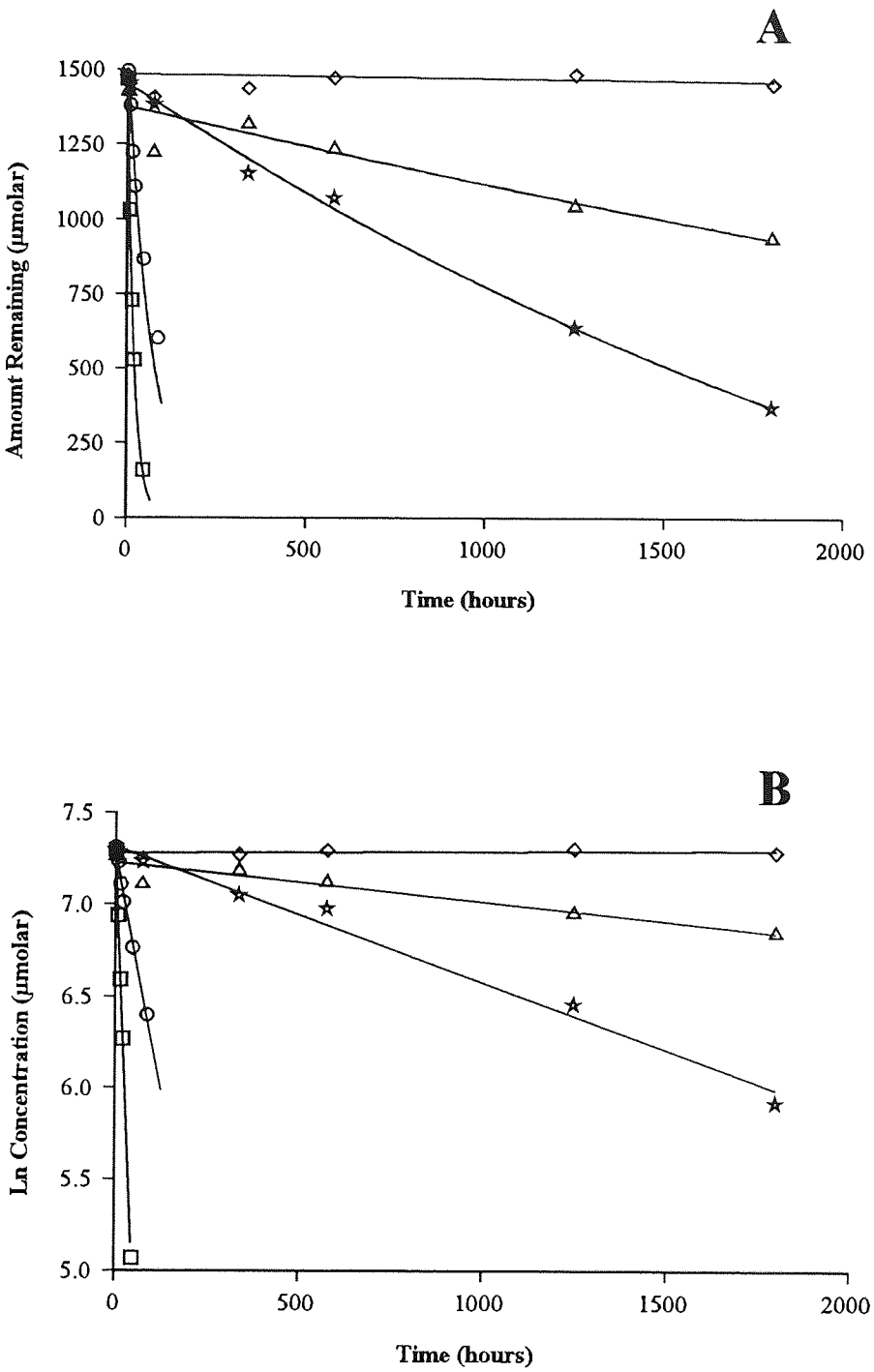

Figure 5.23 Plot of concentration versus time for the stability profile of the phosphonoacetate monoester in relation to pH. (□, pH 9.98;○, pH 7.95;△, pH 5.79;◇, pH 3.80;☆, pH 2.48)

A Concentration versus time plot
B Ln concentration versus time plot

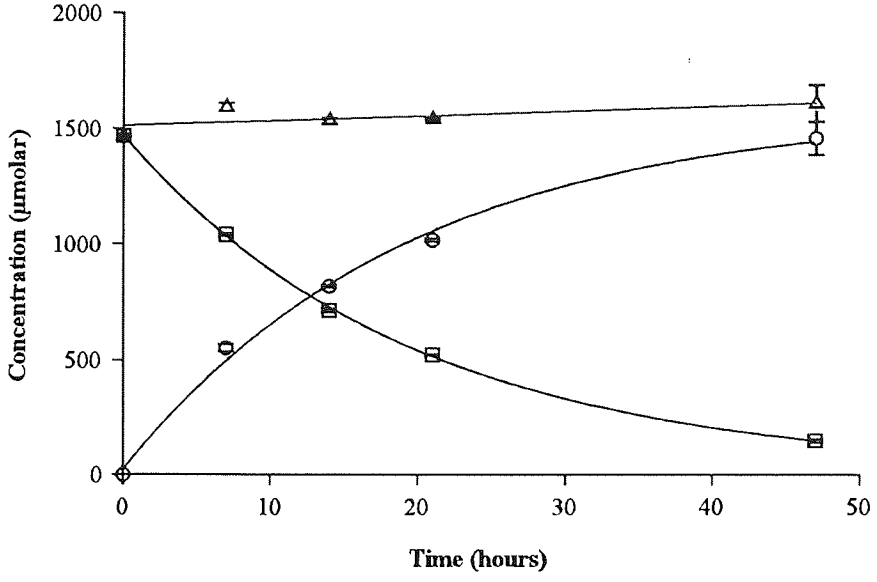

Figure 5.24 Time courses for monoester (□), benzyl alcohol (○) and mass balance (△), during the monoester hydrolysis at pH 9.98. (Error bars represent SEM)

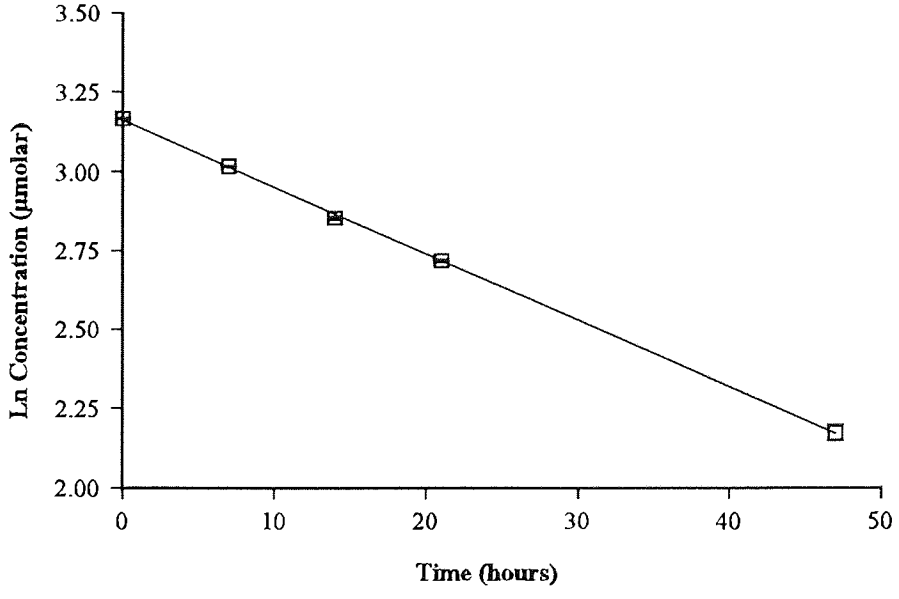

Figure 5.25 First-order reaction profile for the monoester at pH 9.98. (Error bars represent SEM)

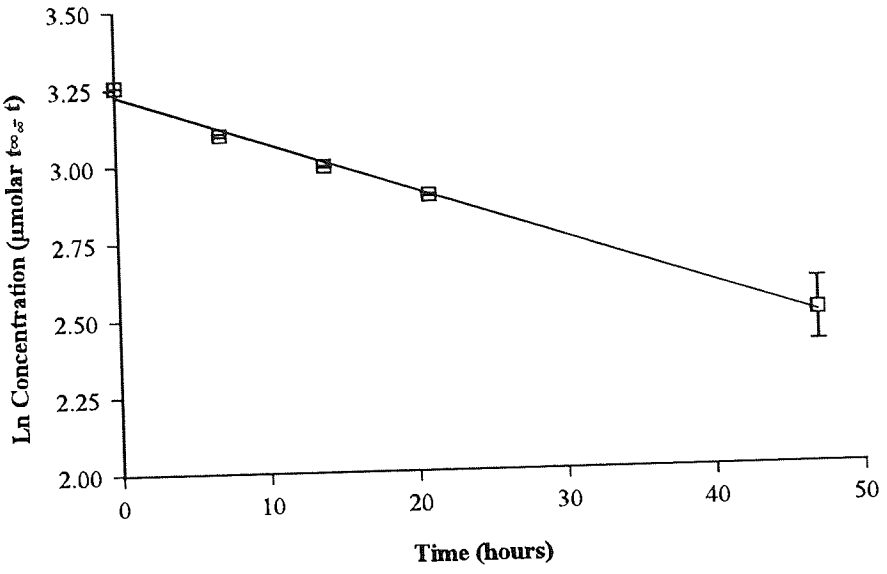

Figure 5.26 First-order plot for the appearance of benzyl alcohol during the hydrolysis of the monoester at pH 9.98. (Error bars represent SEM)

Figure 5.24 shows the breakdown of the monoester at pH 9.98 and the corresponding equimolar appearance of benzyl alcohol. The logarithmic plots are represented in Figures 5.25 and 5.26. From the gradient of these slopes the first-order rate of benzyl alcohol appearance is 3.61×10^{-2} hr^{-1} (SE=1.458×10^{-3}) which compares to the rate of disappearance of the monoester **5.27** of 4.85×10^{-2} (SE=5.060×10^{-4}). This profile confirms the reaction scheme depicted in Figure 5.27 where the hydrolysis is limited to one reaction at the COOR group and hydrolysis at P-O is not observed.

pH	Rate (hr^{-1})	Rate ± SE	Rate ± 95% CI	Half Life (hr)	In Rate (hr^{-1})
9.98	4.85×10^{-2}	5.060×10^{-4}	1.611×10^{-3}	14.28	-1.314
7.95	1.42×10^{-2}	3.120×10^{-4}	8.664×10^{-4}	48.88	-1.848
5.79	2.13×10^{-4}	3.139×10^{-5}	8.070×10^{-5}	3249.63	-3.671
3.80	8.14×10^{-6}	1.165×10^{-5}	2.996×10^{-5}	85153.22	-5.089
2.48	7.36×10^{-4}	3.607×10^{-4}	9.272×10^{-5}	941.78	-3.133

Table 5.11 Rate of breakdown for phosphonoacetate monoester (k_1) with respect to pH (SE- standard error; CI - confidence interval)

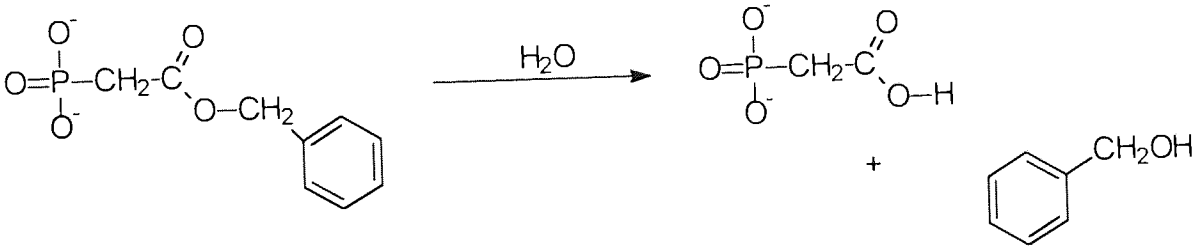

Figure 5.27 Mechanism of hydrolysis of benzyloxycarbonylmethyl phosphonate **5.27**

It was anticipated that the triester model of a potential prodrug form, would have followed a similar cascade reaction to the 4-alkanoyloxy benzyl triesters (Figure 5.5). These esters undergo cleavage of the phosphorous alkanoyloxybenzyl ester group (R', Figure 5.2) *via* 4-hydroxybenzyl intermediates (Figure 5.5) to the respective diester or monoester *via* C-O bond cleavage. The cleavage of the phosphorous methoxy ester groups with dimethyl (benzyloxy-carbonylmethyl) phosphonate could have been followed *via* the HPLC method developed in section 2.3.3. due to the benzyl chromophore on the carbonyl carbon (R, Figure 5.2). Unfortunately, the results in sections 5.4.1 to 3 show that this was not the preferred route of degradation and it was not possible to monitor the profile using the equipment available.

The pH-rate profile for the hydrolysis of the phosphate esters **5,25, 5.26** and **5.27** is shown in Figure 5.28. In the case of the diester and monoester, the profiles follow the characteristics 'V' shape curve for acid and base catalysis of an ionisable, anionic substrate. The triester is subject to base catalysis between pH 9.98 to pH 5.79 and then undergoes a period of pH-independent degradation between pH 5.79 and pH 2.48. The profile was not continued beyond pH 2.48, but either the hydrolysis of the triester would have remained independent of pH or a period of acid catalysis would have been observed at pHs lower than 2.48.

The observed rate constant, k_{obs} for the hydrolysis of an ionisable, anionic substrate may be represented by the following equation:

$$k_{obs} = \left(k_1.[H_3O^+] + k_2.[OH^-] + k_3.[H_2O]\right).\ \frac{[H_3O]}{K_a + [H_3O]} +$$

$$\left(k_4.[H_3O^+] + k_5.[OH^-] + k_6.[H_2O]\right).\ \frac{K_a}{K_a + [H_3O^+]}$$

Where, k_1, k_2 and k_3 refer to the rate constants for solvent, acid and base catalysis for the undissociated species. The terms k_4, k_5 and k_6 are the corresponding rate constants for the ionised species. K_a is the dissociation constant for the acid and the terms $[H_3O^+]/ (K_a + [H_3O^+])$ and $K_a/(K_a+[H_3O^+])$ refer to the concentration of the unionised, $[HA]$ or $(1-\alpha)$, and ionised, $[A^-]$ or α, species respectively.

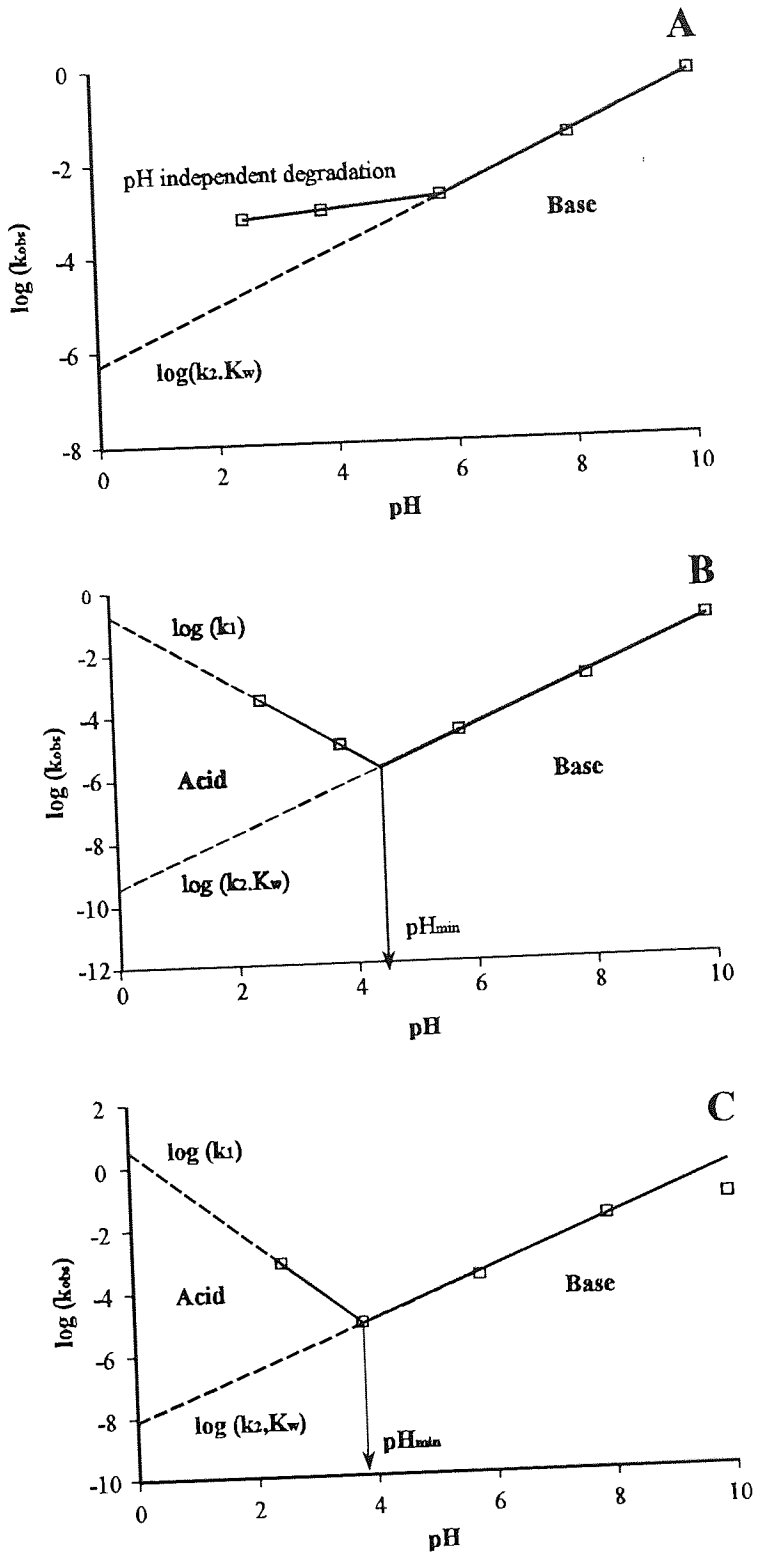

Figure 5.28 Log rate versus pH profile for the hydrolysis of the phosphonate triester **5.25** (A), diester **5.26** (B) and monoester **5.27** (C).

In the pH range where acid catalysis occurs, the reaction should proceed:-

$$\underset{Drug}{A} + H^{\cdot} \rightleftharpoons A\text{-}H^{\cdot} + H_2O \xrightarrow{k} \underset{Product}{B}$$

Where the equilibrium constant:

$$K_a = \frac{[AH^{\cdot}]}{[A].[H^{\cdot}]} \qquad \text{and} \qquad [AH^{\cdot}] = K_a.[A].[H^{\cdot}]$$

So the reaction rate in terms of change of product:-

$$\frac{dB}{dt} = k.[AH^{\cdot}].[H_2O] = k.K_a.[A].[H^{\cdot}].[H_2O]$$

and

$$\frac{dB}{dt} = k_1.[A].[H^{\cdot}] \qquad \text{where} \qquad k_1 = k.K_a.[H_2O]$$

At fixed pH

$$\frac{dB}{dt} = k_{obs}.[A] \qquad \text{where} \qquad k_{obs} = k_1.[H^{\cdot}]$$

Taking logs

$$\log(k_{obs}) = \log(k_1) - pH \qquad \text{(Eq 5.1)}$$

A plot of log k_{obs} against pH should therefore be linear with a negative slope equal to unity and acid intercept equal to the hydrogen ion catalytic rate constant. In solutions of higher pH where the base-catalysed reactions takes place, the reaction should proceed:

$$\underset{Drug}{A} + OH^{-} \xrightarrow{k_2} \underset{Product}{B}$$

The rate of reaction in terms of change of product:

$$\frac{dB}{dt} = k_2.[A].[OH^-] \qquad \text{and} \qquad [OH^-] = \frac{K_w}{[H^+]}$$

where K_w is the ionic product of water (1.0×10^{-14} mol dm^{-3}).

At fixed pH

$$\frac{dB}{dt} = k_{obs}.[A] \qquad \text{where} \qquad k_{obs} = k_2.[OH^-] = \frac{k_2.K_w}{[H^+]}$$

Taking logs

$$\log\ (k_{obs}) = \log\ (k_2.K_w) + pH \qquad \text{(Eq 5.2)}$$

Again a plot of log k_{obs} against pH should therefore be linear with a slope equal to unity and acid intercept equal to the product of the hydroxyl ion catalytic rate constant and K_w. The pH at which the rates of the acid and base-catalysed reactions are equal, pH represent the pH where the rate of hydrolysis is at its lowest, pH_{min}.

$$\log\ (k_{obs}) = \log\ (k_2.K_w) + pH = \log\ (k_1) - pH$$

Therefore

$$pH_{min} = \frac{\log\left(\frac{k_1}{k_2.K_w}\right)}{2} \qquad \text{(Eq 5.3)}$$

The values of log (k_1), log (k_2K_w) pH from Equations 5.1, 5.2 and 5.3 and the slopes from the plots of log k_{obs} against pH (Figure 5.28) for the three esters as detailed in Table 5.12. The values of the slope deviate from unity implying that hydroxyl or hydrogen ion catalysis is not the sole catalytic reaction influencing the reaction. Catalysis by other species such as buffer components may also be important. Phosphate ions are well known to complex with other organic and inorganic ions (Perrin and Dempsey, 1974). Significant errors are also likely to occur due to the number of points on the pH profile plots and further work is required to ascertain the absolute values of these plots.

	Triester **5.25**	Diester **5.26**	Monoester **5.27**
k_1 (hr^{-1})	-	0.189	3.483
k_2 (hr^{-1})	50.035	0.036	0.782
pH_{min}	< 5.79	4.36	3.78
Base catalysed slope	0.600	0.826	0.782
Acid catalysed slope	-	-1.129	-1.482

Table 5.12 Acid - base catalysis rate constants for the hydrolysis of the phosphonate esters.

Water alone does not generally hydrolyse esters as OR is a poor leaving group, therefore, the hydrolysis is usually catalysed by acids or bases. When bases catalyse the reaction, it is called saponification. The attacking species is the powerful nucleophile OH^- and the reaction product is the salt of the acid. Acid-catalysis makes the carbonyl carbon more positive and therefore more susceptible to attack by the nucleophile. The most likely route for both the acid- and base-catalysis of the phosphonate esters is *via* a tetrahedral mechanism (Ingold, 1969). These involve acyl-oxygen cleavage and their occurrence could be confirmed by hydrolysis with $H_2{}^{18}O$ which would result in the ^{18}O appearing in the acid and not in the alcohol. Under these circumstances, the base hydrolysis would proceed as detailed in Figure 5.29 and the acid hydrolysis *via* two molecules of water as detailed in Figure 5.30.

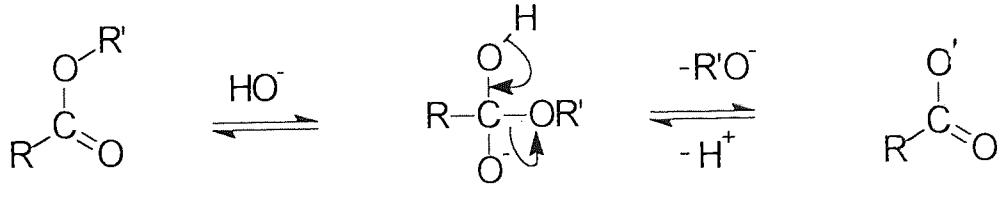

Figure 5.29 A possible tetrahedral, acyl cleavage for the base-catalysed hydrolysis of phosphonate esters. R=$(CH_3O)_2$ PO.CH_2; CH_3 O.O^-. $POCH_2$ or $(O^-)_2$. PO.CH_2 R'=$C_6H_5CH_2$.

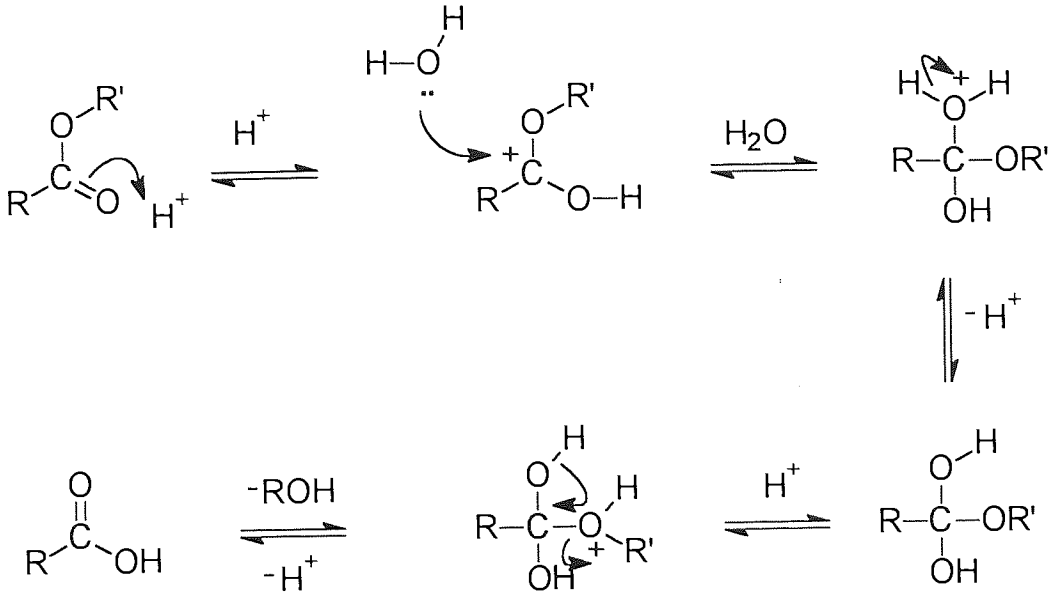

Figure 5.30 A possible tetrahedral, acyl cleavage for the acid-catalysed hydrolysis of phosphonate esters. R=$(CH_3O)_2$ PO.CH_2; CH_3 O.O^-. $POCH_2$ or $(O^-)_2$. PO.CH_2 R'=$C_6H_5CH_2$.

It was not anticipated that the electron-donating potential of the simple alkyl groups would stabilise the R' phosphate esters by reducing their susceptibility to nucleophilic attack. Conversely, the benzyl ester (R) becomes the preferred leaving group and the most vulnerable to attack. The unfortunate consequence of the particular degradation was that the molecule lost its chromophore as the primary breakdown step. This meant it was not possible to monitor the degradation further *via* the UV HPLC system. An interesting aspect of this work is that the R group is usually expected to be the least susceptible to nucleophilic or esterase attack. The ease with which this group is cleaved from the dimethyl (benzyloxycarbonyl-methyl) phosphonate warrants further investigation. For this to be studied *via* UV HPLC, an ideal molecule would have a chromophore on each of the ester radicals. Dibenzyl (benzyloxycarbonylmethyl) phosphonate **5.28** would be an ideal starting point, but was not available during this work.

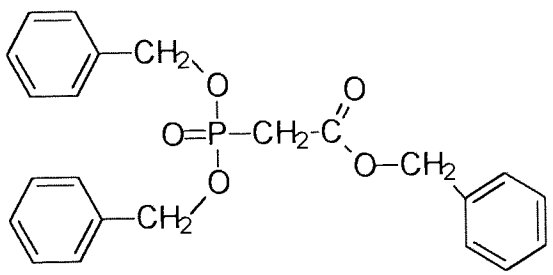

(5.28) Dibenzyl (benzyloxycarbonylmethyl) phosphonate

5.5 Percutaneous absorption of phosphonate esters

5.5.1 Materials

Chemicals used are as detailed in section 5.22 and the human skin samples were prepared as described in section 2.2.1. An artificial membrane was constructed from an 0.2μm pore size, 47 mm diameter Millipore cellulose acetate bacterial filter. This filter was impregnated by submerging the filter in isopropyl myristate for 10 minutes, then removing the filter and dabbing off the excess IPM with a soft tissue. Enhancers used were lauric acid N,N-dimethylamide, Azone® and oleic acid as 0.5M solutions in propylene glycol. Final pH values in Chapters 5 and 6 were measured using an Orion EA 940 2 decimal place pH meter.

5.5.2 Assay Procedure

All assays were carried out using HPLC as detailed in section 2.2.2.1. The mobile phase used for the mono- **5.25** and di-ester **5.26** permeation profiles was sodium phosphate 0.01M, TBH 0.01M: Acetonitrile (75.25) adjusted to pH 6 using orthophosphoric acid and for the triester profiles the mobile phase was sodium phosphate 0.01M: acetonitrile (35:65). The mathematical parameters for these mobile phases are detailed in section 5.3.2.

5.5.3 Permeation Procedure

Jacketed Franz-type diffusion cells were set up as described in section 3.4.6. The receiver solution for the mono- and di-esters was a 10% solution of the pH 7.2 McIlvaine buffer (Appendix 1) in distilled water and for the triester, the receiver was a 10 to 30% range of propylene glycol in a 10% pH 7.2 McIlvaine buffer. The esters were applied to the permeation barrier in a number of different presentations, the monoester was applied as a saturated solution in ethanol, the diester was applied as a saturated solution in ethanol and in pH 7.2 McIlvaine buffer (Appendix 1). The triester was applied either as a 10% solution in acetone, with the acetone being evaporated from the membrane surface before the permeation profile commenced or neat in its original liquid form. Permeation membranes were pretreated with enhancer solutions (section 5.5.1) as described in section 3.2.5.

5.6 Results and Discussion

5.6.1 *In Vitro* Skin Absorption Experiments

This study investigated the transdermal flux of the three phosphonate esters through human skin and the effect established penetration enhancers had upon this flux. These included oleic acid, LDA and Azone which were used as 0.5M solutions in propylene glycol. The barrier membrane was pretreated with the penetration enhancer formulation for a period of 12 hours prior to application of the phosphonate donor preparation. This pretreatment method avoids enhancer effects on the thermodynamic activity of the model drug. The transdermal absorption barrier used throughout this study was excised human epidermis. IPM-impregnated cellulose acetate filters (section 5.5.1) were tried as an artificial barrier, but although these were visually very promising, the rate of triester permeation was rapid and any further experiments using this membrane were abandoned.

Other than the supersaturated suspensions, saturated solutions give the greatest thermodynamic potential for transdermal flux. It was estimated that the solubility of the diester in McIlvaine buffer pH 7.2 (Appendix 1) was approximately 50 mg ml^{-1}. Unfortunately, when this suspension was applied to the skin surface as the donor phase, permeation could not be detected, even after 24 hours had lapsed. Pretreatment of the human skin with the enhancers Azone and oleic acid enabled some permeation of the diester, but this was only after 24 hours. This permeation was seen as a sudden increase in receiver phase diester concentration and was probably best explained as an artefact due to deterioration in the skin's integrity. During these experiments, the preparation of the skin, the 12-hour pretreatment and the 36-hour permeation profile, meant the skin sample had been at 20 to 32°C for in excess of 48 hours. Saturated suspensions of both the monoester and diester in 50% ethanol were investigated as skin permeation donor phases. Again, even pretreatment with N,N-lauric acid dimethylamide as an enhancer did not enable any detectable permeation.

Transdermal permeation was observed with the triester **5.25**, the results are shown in Figures 5.31 to 5.33. Due to the compounds insolubility in water, applying the donor as a solution in acetone and then evaporating the acetone was investigated. It was observed that following the evaporation, the triester did not cover the donor skin surface evenly and the resultant profiles were not reproducible. The larger donor surface area of approximately 2.5 cm^2 may well have

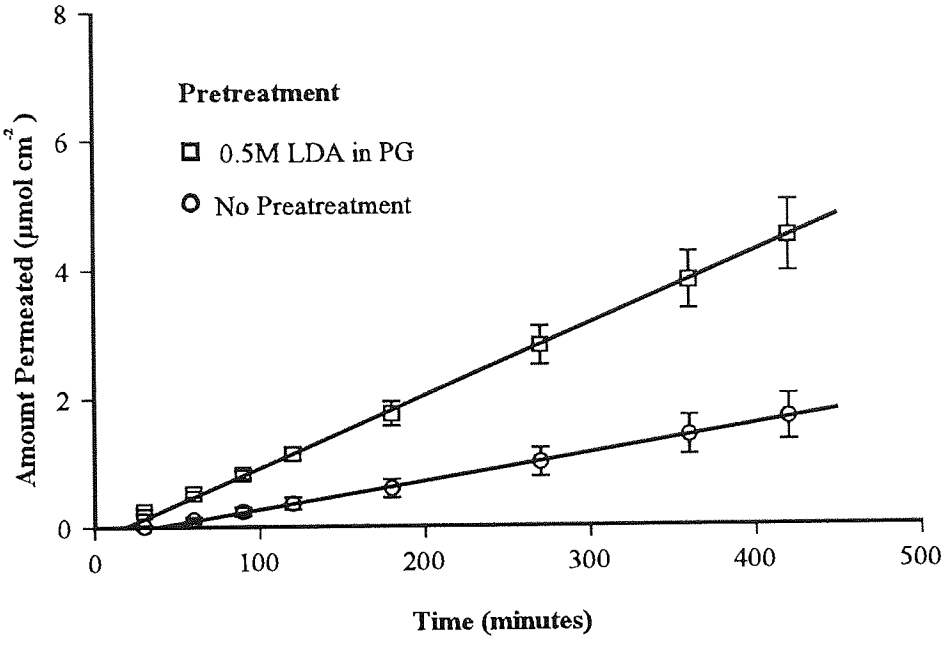

Figure 5.31 Permeation profile for the phosphonate triester **5.25** across human skin with and without a 12-hour pretreatment using 0.5M LDA in PG. The donor phase was 0.4ml of the triester and the receiver 10% PG in 10% McIlvaine's buffer at pH 7.2. (Error bars represent SEM)

Treatment	Initial Flux ($\mu mol.cm^{-2}.hr^{-1}$)	Lag Time (Minutes)	Enhancement Ratio
No Pretreatment	0.29 ± 0.048	46.1 ± 8.35	
			2.29
0.5M LDA in PG	0.67 ± 0.086	14.0 ± 7.62	

Table 5.13 Permeation data for the phosphonate triester **5.25** across human skin following 12-hour pretreatment using 0.5M LDA in PG.(Values presented as mean ± SEM)

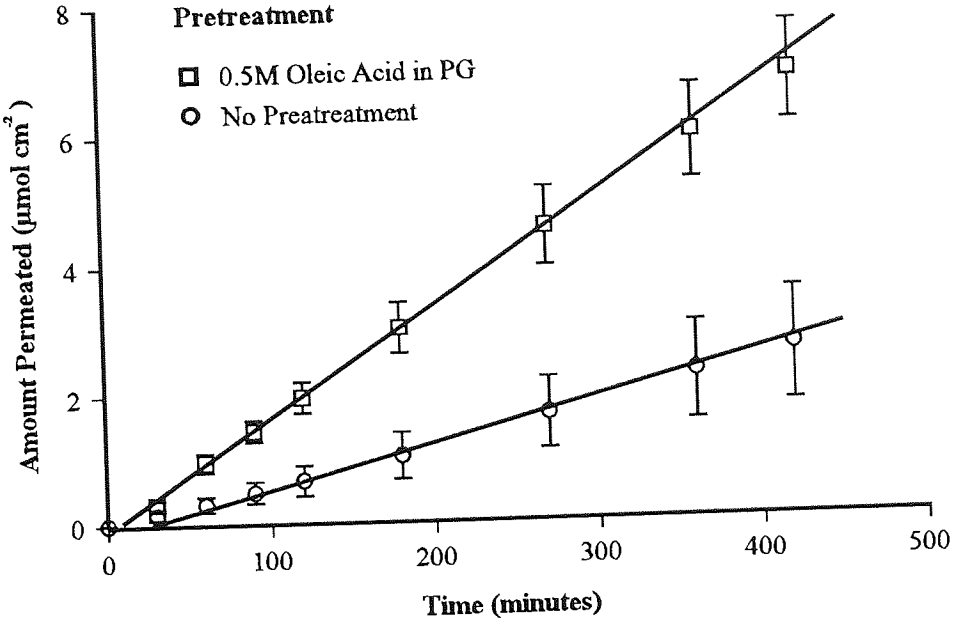

Figure 5.32 Permeation profile for the phosphonate triester **5.25** across human skin with and without a 12-hour pretreatment using 0.5M oleic acid in PG. The donor phase was 0.4ml of the triester and the receiver 10% PG in 10% McIlvaine's buffer at pH 7.2. (Error bars represent SEM)

Treatment	Initial Flux ($\mu mol.cm^{-2}.hr^{-1}$)	Lag Time (Minutes)	Enhancement Ratio
No Pretreatment	0.40 ± 0.132	25.9 ± 5.28	2.62
0.5M Oleic Acid in PG	1.04 ± 0.140	6.15 ± 2.86	

Table 5.14 Permeation data for the phosphonate triester **5.25** across human skin following 12-hour pretreatment using 0.5M oleic acid in PG. (Data presented as mean ± SEM)

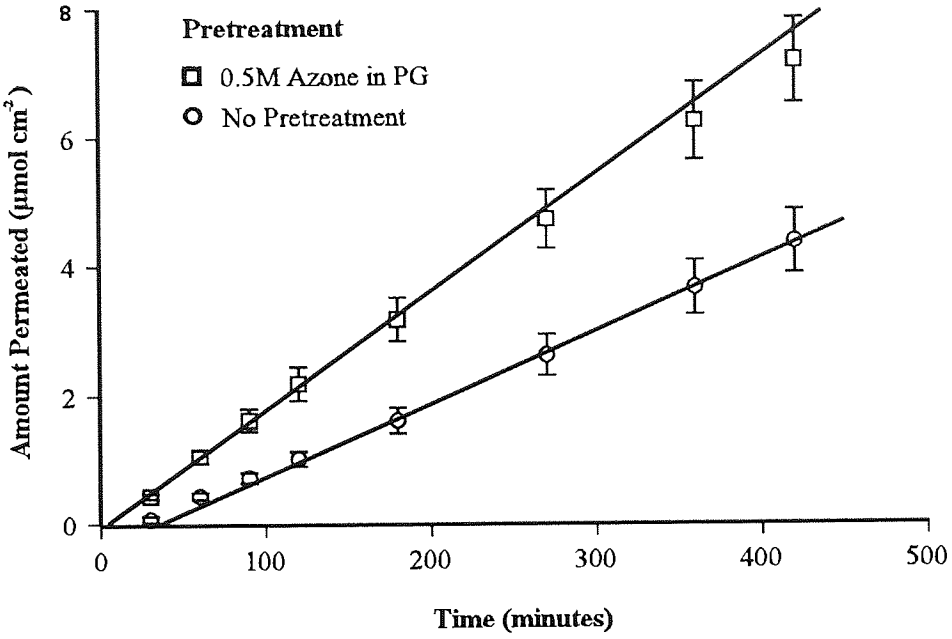

Figure 5.33 Permeation profile for the phosphonate triester **5.25** across human skin with and without a 12-hour pretreatment using 0.5M Azone in PG. The donor phase was 0.4ml of the triester and the receiver 10% PG in 10% McIlvaines buffer at pH 7.2. (Error bars represent SEM)

Treatment	Initial Flux (μmol cm^{-2} hr^{-1})	Lag Time (Minutes)	Enhancement Ratio
No Pretreatment	0.68 ± 0.077	35.8 ± 6.65	
			1.62
0.5M Azone in PG	1.10 ± 0.108	3.7 ± 0.90	

Table 5.15 Permeation data for the phosphonate triester **5.25** across human skin following 12-hour pretreatment using 0.5M Azone in PG. (Data presented as mean ± SEM)

	Enhancer		
	LDA	Oleic Acid	Azone
Mean	2.29	2.62	1.62
Standard Deviation	0.877	0.864	0.391
Variance	0.769	0.747	0.153
Standard Error of the Mean	0.292	0.353	0.160
*Correlation Data vs Model	0.9928	0.9613	0.9852
Number of Observations (n)	9	6	6

Table 5.16 Descriptive statistics of the enhancement ratios (ER) for the percutaneous absorption of the phosphonate triester **5.25**. (*The model is a normal cumulative frequency curve with the quoted mean and standard deviation)

	Comparative Groups		
	LDA / Oleic Acid	LDA / Azone	Azone / Oleic acid
t	-0.717	1.998	2.566
Degrees of Freedom	10	11	6
$P(t \leq t)$ one-tail	0.245	0.035	0.021
t critical one-tail ($P = 0.05$)	1.812	1.796	1.943
$P(t \leq t)$ two-tail	0.490	0.071	0.042
t critical two-tail ($P = 0.05$)	2.228	2.201	2.447

Table 5.17 t-test statistical analysis of enhancement ratios (ER) for the percutaneous absorption of the phosphonate triester **5.25**.

been responsible for this uneven coating, . The most successful method of applying the triester was as the neat liquid and in sufficient quantities to just cover the skin surface, 0.4 ml was generally used. Due to the triester's aqueous insolubility, propylene glycol was added to the receiver phase. An experiment was performed using 10%, 20% and 30% propylene glycol in 10% McIlvaine buffer pH 7.2 (Appendix 1). The permeation profiles from all three receivers were similar and the 20% propylene glycol was used as the receiver in all further experiments.

The data obtained from the triester *in vitro* transdermal flux through excised human skin was plotted as the cumulative amount of drug transported against time (Figures 5.31 to 5.33). The permeation profiles in these figures show the flux following membrane pretreatment with the appropriate enhancer relative to the triester flux through untreated human skin. The initial flux was calculated by regression analysis of the linear portion of the amount permeated versus time plot and the lag time estimated from the extrapolation of this line to the x-axis. The values of initial flux, lag time and enhancement ratio (section 3.3.4; Equation 3.3) are shown in Tables 5.16 to 5.18. Pretreating skin with compound in solvents such as propylene glycol (PG) has been accepted as an effective method of enhancing the transport of chemicals through the skin (Matheson *et al.*, 1979). Azone, for example, has been found to be more effective in increasing penetration of trifluorothymidine from PG if it is used to pretreat the skin, rather than incorporating it into the skin itself (Sheth *et.al.*, 1986). In this study, 0.5 M solutions of Azone, LDA and oleic acid in PG were used to pretreat human skin. These solutions were shown to be effective enhancers of the phosphonate triester with enhancement ratios over untreated skin was 1.62, 2.29 and 2.62 respectively (Tables 5.13 to 5.16). Table 5.16 shows the descriptive statistics of the enhancement ratios and Table 5.17 shows the t-test analysis for the probability of differences between the relative enhancement ratios. The mean, standard deviation and t-tests presented here assume that data being examined follows the normal (Gaussian) distribution. The correlation of data versus model expressed in Table 5.16 is an indication of the robustness of this model. It is the correlation coefficient, or goodness of fit of the data to a theoretical normal cumulative frequency line with a mean and standard deviation calculated from the data. If the data did not fit a normal distribution then statistical difference between the groups should be analysed by a non-parametric method, such as the Wilcoxon signed rank test. All the pretreatments produced increased absorption over the non-pretreated controls. Again oleic acid is the most effective enhancer at increasing the permeation of the triester from the donor to receiver phase. Although the mean extraction

ratio value for oleic acid is 2.62, which is greater than that for the LDA (2.29) there is no significant difference as determined by a two-sample heteroscedastic t-test (section 3.3.4; Equation 3.1). The enhancement ratio for Azone at 1.62 is significantly ($P<0.05$) different to that for oleic acid (see Tables 5.16 and 5.17). This series of experiments did not employ a pH-gradient from the donor to the receiver compartments of the *in vitro* absorption cell as the triester was a neutral compound. These factors may have prevented the occurrence of an ion-pair effect leaving Azone to exert its enhancing effect by other mechanisms, for example increased partition of diffusion of the permeate. This may explain the relatively small enhancing effect of pretreatment with this compound.

Significant increases of benzyl alcohol were not observed in the receiver phase, indicating that hydrolysis of the ester had not occurred either enzymatically or chemically. This may be partly due to non-viable skin being used with *in vitro* absorption cells. The validity of measuring skin metabolism *via* this technique has been questioned (Boehulein *et al.*, 1994), although hydrolysis of hydrocortisone acetate has been observed taking place in the skin during *in vitro* transdermal experiments using hairless mouse skin (Michniak *et al.*, 1994). Hairless mouse skin is known to possess relatively high amounts of esterase activity (Taüber, 1989) and it is now well established that esters undergo hydrolysis in the skin (Kao and Carver, 1990). Ester hydrolysis may also occur in the receiver, not only chemically, but enzymatically due to enzymes leached from the skin (Collier and Bronaugh, 1992).

This study only examined the amount of drug that was transported into the receiver compartment. It is being considered increasingly important to investigate the amount of drug that is retained in the skin (Reifenrath *et al.*, 1991, Borsadia *et al.*, 1992 and Sasaki *et al.*, 1991). This is because topical drug delivery can result in three possible outcomes: 1) transdermal penetration, where the drug crosses the skin and enters the systemic circulation, 2) enhanced skin concentrations of drug where the drug does not actually cross the skin, but is localised within it, 3) a combination of 1 and 2. This is why it is important to ascertain the concentrations of transported drug within both the skin and receiver solution before a full analysis of an enhancer's potential can be assessed. The results presented here show that to enhance systemic delivery of the triester, 0.5M oleic acid and LDA in PG are significantly superior to Azone.

5.7 Summary

In order to determine the potential hydrolysis and prodrug-to-parent breakdown of the phosphonate esters, it was essential to develop a stability-indicating assay. Using the isocratic HPLC system with a UV-detector described in section 2.2.2.1 and ion-pair agents, it was possible to resolve the three esters and the breakdown product benzyl alcohol on one chromatogram. The example hydrolysis of the 4-acyloxybenzyl triester **5.18** (Figure 5.5) suggested that the anticipated breakdown of the triester, dimethyl benzyloxycarbonyl methyl phosphonate **5.25** was initially *via* the methoxy groups at P-O giving the di- **5.26** and monoester **5.27**. The 4-acyloxybenzyl triester **5.18** did not degrade beyond the monoester **5.23** and as a consequence did not give the active parent phosphonoacetate. It was hoped that using benzyloxy, a better leaving group, at C-O, that this final step to phosphonoacetate might be achieved. The benzyloxy group was also the chromophore to enable the three phosphonate esters to be detected *via* UV-HPLC chromatography.

The breakdown study of the esters showed that the initial hydrolysis step was the loss of the benzyloxy group at C-O. This pathway was the same for the mono-, di- and tri-esters (**5.25**, **5.26** and **5.27**). Loss of the benzyloxy chromophore unfortunately prevented investigating the breakdown further by UV-HPLC which was the method of analysis available for this study. The pH-profiles for the ester hydrolysis were determined and the pH giving the lowest rate of hydrolysis (pH_{min}) calculated. The pH_{min} and corresponding rates were, for the triester, >5.79; 1.55×10^{-3} hr^{-1}, the diester, 4.36; 1.42×10^{-6} hr^{-1}, and for the monoester, 3.78; 7.04×10^{-6} hr^{-1}.

Transdermal permeation of the triester was achieved and could be potentiated by the three enhancers investigated. Enhancement of permeation was greatest using oleic acid, followed by LDA and least by Azone. With the experimental conditions in this study, including the use of absorption enhancers, transdermal permeation of the ionic mono- and di-esters was not achieved. The pH of the donor phase and the receiver phase was similar at pH 7.2. This may not have been ideal for the formation or delivery of these permeants *via* ion-pair facilitated transport and further experiments using a range of donor pHs may be useful.

Encouraging aspects of this work were that the phosphonate triester model of a prodrug has the potential to cross cellular membranes. The amount of compound transported is unlikely

to achieve therapeutic levels, but the principal of transporting an ester of phosphonoacetate across a biological membrane has been achieved. The objective of complete bioactivation of these compounds requires further investigation. The loss of the ester from the C-O was not observed with the 4-acyloxybenzyl triester **5.18**. As this was the initial breakdown pathway for dimethyl benzyloxycarbonyl methyl phosphate, it provides evidence that complete bioactivation to phosphonoacetate from ester prodrugs can be achieved.

The work undertaken here has given a useful insight into the potential of the triester phosphonate prodrug model. Future work would include partition work of the three esters into various organic phases, including octanol and IPM, and into skin. It may also give useful knowledge to study the amount of triester that is concentrated within the skin itself following permeation profiles.

CHAPTER SIX

THE EFFECT OF CYCLODEXTRINS ON THE STABILITY OF ESTERS IN ENZYMIC SYSTEMS

6.1 Introduction

6.1.1 Cyclodextrins

Cyclodextrins are crystalline, nonhygroscopic, cyclic oligosaccharides manufactured by the enzymatic degradation of starch using *Bacillus macerans*. β-Cyclodextrin is produced by the action of the enzyme cyclodextrin glucosyl transferase upon starch or a starch hydrolysate. Natural forms are α-, β- and γ-cyclodextrin, which have respectively 6,7 and 8 glucose units. (Figure 6.1). Modified derivatives of these compounds, such as hydroxyethyl or hydroxypropyl, are also available. These toroidal molecules are cone-like in shape with a rigid structure and a central cavity of differing size, dependant upon the cyclodextrin type (Table 6.1).

Figure 6.1 Structural formulae of various natural and derivatised cyclodextrins; Where R^1=H, R^2=CH_3, and R^3=$CHOHCH_3$, in α-, β-, and γ- n equals 0, 1, and 2 respectively (From Guttman *et al.*, 1996).

Due to the particular arrangements of the glucose units, the internal surface of the cyclodextrin is made up of two circles of C-H groups, and one of oxygen included in the glucosidic bonds. The free electrons of oxygen are directed into the interior of the cavity, giving it probable characteristics similar to ether. The hydroxyl groups situated on the sides of the ring mean that the external surface of the torus is hydrophilic (Duchêne and Wouessidjewe, 1990a), therefore cyclodextrins are soluble in water (Table 6.1).

Table 6.1 Physical characteristics of cyclodextrins (From Nash, 1993).

This ability, which is dependent upon steric hindrance and electrical charge requirements, can modify physicochemical properties of the guest molecule, for example, stability and solubility. (Duchêne *et al.*, 1991). Inclusion complexes have been investigated in the pharmaceutical field, primarily to improve dissolution and bioavailability (Jones *et al.*, 1984a; 1984b and Duchêne *et al.*, 1986). They can also mask secondary undesirable pharmaceutical properties such as irritation, unpleasant taste and phototoxicity (Irie and Uekama, 1985; Hoshino *et al.*, 1989).

Early reports suggested that orally administered cyclodextrins were toxic (French, 1957). This has since been considered to be due to toxic solvent residues. More recent animal studies have shown that cyclodextrins can be regarded as essentially non-toxic, non-irritant materials (Gergely *et al.*, 1982) and many countries have now approved their use in food products and orally administered pharmaceuticals. Orally administered cyclodextrin is metabolised by microflora in the colon forming the metabolites, maltodextrin, maltose and glucose, which are themselves further metabolised before being finally excreted as carbon dioxide and water. β-Cyclodextrin administered parenterally is not metabolised and accumulates in the kidneys as insoluble cholesterol complexes, resulting in severe nephrotoxicity (Frank *et al.*, 1976). Other cyclodextrin derivatives, for example 2-hydroxypropyl-β-cyclodextrin, have undergone extensive toxicological studies and are not associated with nephrotoxicity and are reported to be safe in parenteral preparations (Duchêne and Wouessidjewe, 1990b). Therefore,

formulations with cyclodextrins can provide stable and soluble aqueous parenteral products that would otherwise require a non-aqueous solvent. Cyclodextrins have also been used in the formulation of solutions (Prankerd *et al.*, 1992; Palmieri *et al.*, 1993), suppositories (Szente *et al.*, 1984: 1985) and cosmetics (Amann and Dressnaudt, 1993). There have been some interesting observations following administration of cyclodextrins suggesting that inclusion of toxic compounds or lipid mediators of pathological responses can affect their physicochemical characteristics and cause potentially toxic responses. Experimental evidence has shown that the potential bioavailability of environmental carcinogens can be increased by complex formation with cyclodextrins. Consequently, hydroxypropyl-β-cyclodextrins, when used in pharmaceutical formulations, have the potential to increase the absorption of carcinogens which enter the gastrointestinal tract either as food components, co-administration of cytotoxic drugs, or from air pollution through saliva (Horsky and Pitha, 1996). Parenteral administration of hydroxypropyl-β-cyclodextrin has caused agitation and pulmonary oedema in rabbits and dogs respectively. It is hypothesised that lipid mediators of pathological responses, such as prostaglandins, which normally have a brief and localised function, can couple with cyclodextrins which potentiates their influence and the host's response. (Carpenter *et al.*, 1995).

Cyclodextrins can form inclusion complexes with a variety of compounds. (Duchêne and Wouessidjewe, 1990b; Duchêne *et al.*, 1991). The single most important requirement being that the guest molecule fits, at least partially, into the cyclodextrin cavity. There are several forces attracting guest molecules into the cyclodextrin cavity. Although not accurately defined, they include van der Waal's forces (Matsui *et al.*, 1979, Otagiri *et al.*, 1971) and hydrophobic interactions (Matsui *et al.*, 1979; Rosanske and Connors, 1980; Thakkar and Demarco, 1971). Water molecules are located within the cavity and, in an aqueous solution, a guest molecule must displace these to enter the cyclodextrin. This is relatively easy, because water molecules inside the cavity are located in an unfavourable hydrophobic environment (Saenger, 1980; Linder and Saenger, 1978). The host-to-guest ratio is generally 1:1, although 1:2 or 2:1 has also been described. Their ratio depends upon the size of the guest molecule and the particular cyclodextrin cavity. For example, a relatively large molecule such as progesterone cannot penetrate entirely into the α-cyclodextrin cavity, but inclusion is feasible with β-cyclodextrin, although two molecules of β-cyclodextrin are required for each progesterone molecule (Uekama *et al.*, 1982). Inclusions form spontaneously in solution,

however pure solid inclusion compounds can be produced which may then be reformulated within a range of pharmaceuticals. These solid inclusion compounds have been prepared by co-precipitation (Kurozumi *et al.*, 1975), heating in sealed containers (Nakai *et al.*, 1987), kneading (Turuoka *et al.*, 1981), freeze-drying and co-grinding (Nakai *et al.*, 1978). The references quoted above give precise details for the preparation of the inclusions.

6.1.2 Uses of Cyclodextrins in Percutaneous Absorption

The objective of original studies with cyclodextrins was to improve oral bioavailability. Although the results were frequently successful, there have been few pharmaceutical dosage forms of this type to reach the market. This has not necessarily been for technical reasons, but from regulatory questions concerning pharmacokinetic and pharmacological problems. More recently, work on improving bioavailability by using cyclodextrin inclusions has focused on other administration routes, especially the dermal route (Okamoto *et al.*, 1986; Otagiri *et al.*, 1984; Uekama *et al.*, 1985).

The formulation of topical preparations using cyclodextrin complexes, must be undertaken with care to obtain an agent with optimal release characteristics. Earlier work using formulations based upon preformed inclusion compounds found that separate incorporation of the cyclodextrin and the active ingredient into a formulation did not result in an improvement in bioavailability (Glomot *et al.*, 1988; Shankland *et al.*, 1985). Other work contradicting these results (Orienti *et al.*, 1986; van Doorne *et al.*, 1988) led to the general assumption that when a significant effect from cyclodextrins is noted, it is because of the rapid formation of the inclusion within the ointment. For this to occur readily, the most appropriate bases are aqueous ointments, such as hydrogels, especially as cyclodextrins are usually used to improve the bioavailability of lipophilic ingredients. Excipients within oily bases will not only prevent the inclusions forming, explaining the earlier lack of enhancement, but they may also have a stronger affinity for the cyclodextrin cavity than the active ingredient. Consequently, the active drug is expelled from the cyclodextrin reducing the potential benefits in bioavailability. Therefore, the type of vehicle can have a significant effect upon the enhancing ability of cyclodextrin and better results can be obtained from an aqueous vehicle than from a lipophilic one (Uekama *et al.*, 1987b).

Cyclodextrins have been primarily associated with the enhancement of dermal bioavailability of the retinoids, dermocorticoids and non-steroidal anti-inflammatories. Retinoic acid (Vitamin A or Tretinoin) is primarily used to treat acne vulgaris in which comedones, papules and pustules predominate and is normally applied as a cream or ointment (Reynolds, 1996). Retinoic acid appears to stimulate the epithelium to produce horny cells at a faster rate and reduce their cohesion, possibly by altering the synthesis or quality of the intercellular cement which bind keratinocytes into impactions. Retinoids have been the focus of research into potential cyclodextrin inclusions as they are insoluble in aqueous media, they are chemically unstable in the presence of air and light, induce local irritation and have low cutaneous tolerance. Although there has been significant improvement in the aqueous solubility (Pitha, 1981; Pitha *et al.*, 1980) and irritation power of retinoids, results with respect to stability (Frömming *et al.*, 1988) and transdermal delivery (Duchêne *et al.*, 1991) are less encouraging. The poor transdermal results may be due to increased solubility and the subsequent thermodynamic effect this inclusion has upon the parent drug.

Topical bioavailability of well-known corticosteroids such as betamethasone (Otagiri *et al.*, 1984; Uekama *et al.*, 1985) and prednisolone (Uekama *et al.*, 1987a;1987b) can be significantly improved by cyclodextrins. *In vitro* diffusion tests on betamethasone showed that permeation from liquid, hydrophilic ointment and gel suspensions was greater with the inclusion complex than the parent drug. As with retinoic acid gels, the reverse effect is seen with solutions in that permeation of the parent drug is greater than the inclusion complex. This effect is presumably due to thermodynamic effects within solutions and the quantity of free drug (not included) that is available. Inclusion of prednisolone in β-, γ-, and dimethyl β-cyclodextrin improves the *in vitro* release and the *in vivo* bioavailability of the parent compound.

Use of novel parent steroids such as tixocortol 17-butyrate 21-propionate has limited market potential due to their extremely poor bioavailability, very low stability and very low water solubility. The incorporation of this dermocorticoid as a β-cyclodextrin inclusion compound within ointment bases increased the *in vitro* release rate by approximately two-fold (Glomot *et al.*, 1988). The inclusion also conferred a significant increase in solubility to the parent compound and an 8- to 10-fold increase in stability when incorporated into an ointment base.

Inclusion into cyclodextrins has similar benefits for the potential topical administration of indomethacin. This compound has poor aqueous solubility at physiological pH and is only soluble at pHs where the ionisation of the compound results in poor transdermal delivery. The use of β-cyclodextrin (Hamada *et al.*, 1975; Szejtli and Szente, 1981) and hydroxypropyl β-cyclodextrin (Backensfeld *et al.*, 1990) has lead to improvements in stability and solubility. Solid inclusion compounds of indomethacin have shown significant transdermal delivery both *in vitro* and *in vivo* (Poelman *et al.*, 1989)

The use of peptide and protein drugs is limited by the lack of appropriate delivery systems. These compounds are generally administered parenterally and more recently nasally, due to poor oral bioavailability resulting from enzymatic degradation in the gastro-intestinal tract and poor transport characteristics (Humphrey, 1986; Verhoef *et al.*, 1990). Treatment of chronic disease with long-term parenteral therapy is undesirable and the potential of reliable and reproducible intranasal delivery of peptide drugs is attractive. In order to overcome the disadvantages associated with the parentral administration of insulin, work has been performed to enable the nasal delivery of this peptide compound (Schipper *et al.*, 1993). However, due to high molecular weight and hydrophilicity, the intranasal bioavailability of peptide and protein compounds is low (Moses *et al.*, 1983). It can be improved by the co-administration of absorption enhancers, such as surfactants (Hirai *et al.*, 1981), bile salts (Gordon *et al.*, 1985) medium chain fatty acids (Mishima *et al.*, 1987) fusidate derivatives (Deurloo *et al.*, 1989; Longenecker *et al.*, 1987) and phospholipids (Illum *et al.*, 1989). Many of these compounds would be unsuitable for long-term therapy as they are harmful to the nasal epithelial membranes (Ennis *et al*, 1990) and interfere with the nasal ciliary movement (Hermens and Merkus, 1987). Evidence that dimethyl-β-cyclodextrin has only a small *in vitro* effect on ciliary movement (Schipper *et al.*, 1992; Merkus *et al.*, 1993), morphological studies, (Chandler *et al.*, 1991) and studies upon the release of marker compounds in the nasal cavity (Marttin *et al.*, 1995) have demonstrated that hydroxypropyl β-cyclodextrin and dimethyl cyclodextrin have low potential for damage to the epithelial membrane. Coupled with evidence that cyclodextrins appear to have significant ability as absorption enhancers, this research has generated a great deal of interest in cyclodextrins as nasal absorption enhancers of protein and peptide drugs (Verhoef *et al.*, 1994). Hence, there is now a wealth of data showing that cyclodextrins demonstrate a significant enhanced absorption of peptides and protein drugs such as buserelin (Matsubara *et al.*, 1995) and insulin (Schipper *et al.*, 1993; Merkus *et al.*, 1991;

Irie *et al.*, 1992). Even though the nasal mucosa can be used for transnasal delivery, it still remains an absorption barrier with specific constituents ensuring a protective function against the penetration of foreign material. The mucosal barrier is organised at three different levels: a physical barrier composed of the epithelial cells and mucus, a temporal barrier controlled by the mucociliary clearance, and an enzymatic barrier acting principally on peptides and proteins (Cornaz and Buri, 1994).

6.1.3 Mechanisms of Cyclodextrin Absorption Enhancement Activity.

The use of cyclodextrins and the formation of inclusions could increase the transdermal permeation of therapeutic agents by modifying a compounds solubility, increasing its stability and by a direct effect upon the barrier membrane.

Cyclodextrin inclusions complexes generally increase the aqueous solubility of lipophilic guest molecules with resulting improvement in bioavailability. The guest molecule and the inclusion complex are in constant equilibrium and gains in bioavailability are dependent upon the apparent stability constant of the inclusion. An increase in stability and solubility is dependent upon a high inclusion stability constant, but the stability constant must be low to enable the guest molecule to leave the host cavity for absorption through a barrier membrane. Therefore a compromise between these two requirements must be sought (Duchêne and Wouessidjewe, 1990). Inclusion can also modify the dissolution kinetics of the guest molecule and in order to improve bioavailability an increase in a drug's apparent solubility and dissolution is generally required. Although, if a guest molecule is highly water-soluble, an inclusion can result in slower dissolution kinetics which could be used usefully to formulate sustained-release preparations.

Cyclodextrin inclusions have enabled the increased stability of compounds against a number of degradation pathways. These include dehydration (mitomycin, prostaglandins), hydrolysis (aspirin, atropine, digoxin, procaine), oxidation (aldehydes, epinephrine, phenothiazines), photodecomposition (phenothiazines, ubiquinones) (Nash, 1994). The significance of this stabilisation to dermal absorption is that pharmaceuticals can be formulated with practical shelf-lives and the active ingredients can have a longer residence time at their site of action. This increased residence time provides the opportunity for enhanced transdermal absorption.

The role of the skin to protect the body from the ingress of foreign chemical is often regarded as a physical barrier created by the keratinocytes within the stratum corneum. There is increasing evidence that this barrier function may not only be a passive process, but also an active one (Ando *et al.*, 1977; Rawlin *et al.*, 1980). Exogenous and endogenous substances can be metabolised within the skin (Pannatier *et al.*, 1978; Vainio and Hietanen, 1980; Täuber, 1989) and biotransformations comprise functionalisation (phase 1) and conjugation (phase II) reactions. The spectrum of reactions in the skin seems similar to that observed in the liver. This elimination by biotransformation in the skin may be an alternative mechanism to protect the body against lipophilic substances which have passed the horny layer barrier. In addition to skin, the nasal mucosa is also recognised as a site of metabolism (Sarkar, 1992). Significant peptidase activity has been demonstrated both *in vivo* (Hussain, *et al.*, 1985) and *in vitro* (Hirai, *et al.*, 1981a) and both endopeptidases and exopeptidases are present (Stratford and Lee, 1986; Dodda Kashi and Lee, 1986). Cyclodextrins can protect peptides from enzymic attack and it was proposed that, given the appropriate conditions for guest molecule to cyclodextrin affinity and substrate concentration with relation to K_m, cyclodextrins could protect molecules sufficiently from enzymic attack to potentiate transdermal permeation (Irwin *et al.*, 1994).

Cyclodextrins have also been shown to have a direct absorption enhancement effect on permeation barriers. They are capable of extracting specific membrane lipids such as cholesterol and phospholipids from the nasal mucosa through rapid and reversible formation of inclusion complexes. This selective solubilisation of the membrane lipids may reduce the barrier function of the nasal epithelium (Corbo *et al.*, 1990).

6.1.4 Theoretical Treatment of Results

In Chapter 5, the use of ester prodrugs was investigated to enhance the absorption of ionic compounds. Where prodrugs are applied topically for systemic action, they must cross the skin or mucosal barrier intact. The intact molecule would then be available for bioactivation at its site of action. This study investigated the ability of cyclodextrins to protect model compounds, alkyl parabens, from enzyme hydrolysis. If protection from ester hydrolysis was observed then this may become a method of stabilising prodrugs prior to transport across biological membranes.

The model enzyme used throughout this study was porcine liver carboxyesterase. There is increasing evidence that cyclodextrins have an enhancing effect on the transdermal absorption of a variety of compounds. The mechanism of this enhancement has still to be fully elucidated. If cyclodextrins can protect compounds from enzymatic degradation, then this would increase the potential residence time of the compound in the absorption barrier. This may, at least in part, be an explanation to an aspect of the cyclodextrins transdermal enhancement mechanism.

The ability of the cyclodextrins to form inclusion compounds with guest molecules is an equilibrium which, in effect, reduces the concentration of free guest molecules in solution. This may be described by the following equilibrium, assuming that only one guest molecule interacts with each cyclodextrin molecule.

$$P + CD \rightleftharpoons P\text{-}CD \qquad \text{(Eq 6.1)}$$

Where *CD* represents the cyclodextrin, *P*, the guest molecule and *P-CD*, the inclusion complex. The equilibrium position may be quantified using the association constant (K_s) where:-

$$K_s = \frac{[P\text{-}CD]}{[P]\ [CD]} \qquad \text{(Eq 6.2)}$$

Taking the total concentration of guest molecule [P_0] and the total concentration of cyclodextrin [CD_0] the concentration of free guest drug can be expressed as (Irwin *et al.*, 1994):-

$$[P] = \frac{\sqrt{(K_s\ ([CD_0] - [P_0]) + 1)^2 + 4\ K_s\ [P_0]} - (K_s\ ([CD_0]\ \ [P_0]) + 1)}{2K_s} \qquad \text{(Eq 6.3)}$$

For special cases when the initial concentrations are equal ([CD_0]=[P_0]) as for example when a 1:1 complex is dissolved, this yields

$$[P] = \frac{\sqrt{1 + 4K_s\ [P_0]} - 1}{2K_s} \qquad \text{(Eq 6.4)}$$

Using β-cyclodextrin, a small but measurable protection of peptides has been achieved against enzymic degradation (Irwin *et al.*, 1994). This work concluded that the effect's magnitude was insufficient to account for large increases in bioavailability and was unlikely to be a major enhancement mechanism. Although it was possible to deduce pointers appropriate to enhancing the protective potential of cyclodextrins. Possible explanations for the limited effect were the low affinity of the peptide for the cyclodextrin inclusion (low K_s) and the relatively small peptide-cyclodextrin ratio utilised (25:1). This meant that there was still a relatively high concentration of free peptide available for enzymatic degradation. The cyclodextrin-peptide ratio was limited by the relative insolubility of β-cyclodextrin, the cyclodextrin used in all experiments. It was hypothesised that using more soluble cyclodextrins, such as hydroxypropyl or dimethyl-β-cyclodextrins, greater cyclodextrin:peptide ratios could be tested which gave a significantly lower free peptide ratio and had greater protection from enzymatic degradation.

Enzymes are protein catalysts that increase the velocity of a chemical reaction and are not consumed during the reaction they catalyze. Michaelis and Menten proposed a model that accounts for most of the kinetic features of enzyme catalysed reactions. In this model, the enzyme reversibly combines with its substrate to form a complex that subsequently breaks down to product, regenerating the free enzyme. The model, involving one substrate molecule is represented below:

$$E + S \underset{k_{-1}}{\overset{k_1}{\rightleftharpoons}} ES \xrightarrow{k_2} E + P \qquad \text{(Eq 6.5)}$$

Where S is the substrate, E is the enzyme, ES is the enzyme-substrate complex and k_1, k_{-1} and k_2 are rate constants. The Michaelis-Menten equation describes how reaction velocity varies with substrate concentration:

$$V_o = \frac{V_{max}\,[S]}{K_m + [S]} \qquad \text{(Eq 6.6)}$$

Where V_o is initial reaction velocity, V_{max} is the maximum reaction velocity. K_m is the Michaelis constant $((k_{-1} + k_2)/k_1)$ which is equal to the substrate concentration at which the reaction rate is half its maximum value and [S] is the substrate concentration. The derivation

of the Michaelis-Menten rate equation makes various assumptions: the concentration of the substrate [S] is much greater than the concentration of the enzyme [E] so that the amount of substrate bound by the enzyme at any one time is small: there is a steady-state assumption that [ES] does not change with time: only initial reaction velocities are used in the analysis of enzyme reaction (This is so that the concentration of product is very small and the rate of any reverse reaction of *P* to *S* can be ignored).

The Michaelis constant is characteristic of an enzyme and a particular substrate. It reflects the affinity of the enzyme for that substrate whereby a low K_m demonstrates a high affinity of an enzyme for a substrate and *vice versa*. The initial reaction rate is directly proportional to the enzyme concentration at all substrate concentrations. The K_m is numerically equal to the substrate concentration at which the reaction velocity is equal to $\frac{1}{2}V_{max}$ and does not vary with enzyme concentration. It was important to determine the substrate concentration equivalent to the K_m for the cyclodextrin protection experiments. This was because when the [S] is much less than K_m, the velocity of the reaction is roughly proportional to the substrate concentration and the overall reaction rate is first-order with a rate constant of V_{max} / K_m. When [S] is much greater than K_m, the velocity is constant and equal to V_{max}. The reaction rate is then independent of substrate concentrations and the overall reaction rate is zero-order. If the experiments using cyclodextrin to include and protect the paraben were conducted at substrate concentrations much greater than K_m, the protective effect is likely to go unobserved. This is because the concentration of free paraben would still exceed the K_m by greater than 10 times and a reduction in rate would not be seen because zero- order kinetics would still apply.

The direct linear plot of the Michaelis-Menten equation shows a curve of rectangular hyperbolic nature. Due to the gradual upward slope of the hyperbolic curve at high substrate concentrations, it is not always possible to determine when V_{max} has been achieved. However, if $1/V_o$ is plotted against $1/[S]$, a straight line is achieved. This is called the Lineweaver-Burk or double reciprocal plot and can be used to ascertain the mechanism of action of enzyme inhibitors. The equation that describes the Lineweaver-Burk plot is:

$$\frac{1}{V_o} = \frac{K_m}{V_{max}[S]} + \frac{1}{V_{max}} \qquad \text{(Eq 6.7)}$$

It is arguably the worst transformation of the Michaelis-Menten plot and is very poor for least

squares linear regression analysis. Other linear plots to determine the parameters of enzyme kinetics are the Hanes-Woolf and the Eadie-Hofstee plots (Rodwell, 1996; Davidson and Sittman, 1994).

Once the appropriate substrate and esterase concentrations have been established, cyclodextrins can be added to the reaction solution in various substrate : cyclodextrin ratios. Initial reaction rates can then be determined and related to the levels of protection observed. With regard to the magnitude of this protection, the potential of cyclodextrins to enhance the trans-membrane absorption of intact ester prodrugs and the likelihood of this protection contributing to the absorption enhancer action of cyclodextrins can then be discussed.

6.1.5 Aims and Objectives

This present study was conducted to determine whether using compounds with significant affinity for forming inclusions (methyl, propyl and butyl paraben) and higher ratios of cyclodextrins (1:50 to 1:2500) would afford an increased guest molecule protection from enzyme hydrolysis. Using this series of parabens, it would be possible to observe if there was any relationship between the association constant (K_s), the Michaelis-Menten constant (K_m), the maximum reaction velocity (V_{max}), the initial reaction velocities and the resultant levels of protection afforded by the cyclodextrins. If the cyclodextrins protected these compounds from esterase hydrolysis, this may provide a potential explanation of the transdermal permeation enhancement by cyclodextrins.

The action plan to achieve this objective was:

- Develop and validate an experimental system for monitoring esterase hydrolysis of alkylparabens.
- Determine the substrate concentration of paraben that provides a reaction rate numerically equal to the K_m of the esterase.
- Determine the level of paraben stabilisation from esterase hydrolysis that can be obtained with cyclodextrins. Relate any observed protection to physicochemical characteristics between the parabens, cyclodextrin and esterase.

6.2 Experimental

6.2.1 Materials

The methyl, propyl and butyl paraben were obtained as sodium salts and were gifts from Nipa Laboratories. The hydroxypropyl-β-cyclodextrin, β-cyclodextrin and porcine liver carboxy-esterase were purchased from Sigma chemicals. All other chemicals used were of the appropriate laboratory grade.

6.2.2 Assay Procedures

The HPLC system was used as described in Chapter 2 section 2.2.2 and the mobile phases for the individual paraben are detailed in Table 6.2 and delivered at a rate of 1 ml min^{-1}. Reversed-phase HPLC was employed for the quantification of all parabens. UV detection of the elute was performed at 256 mm and a sensitivity of 0.04 Aufs was used for all analyses. Examples of an assay validation calibration curve for butyl paraben is shown in Figure 6.2 with the respective statistical parameters for the plot given in Tables 6.3 and 6.4. Typical calibration curves are shown in Figure 6.3 for each of the parabens and their respective statistical parameters are given in Table 6.5.

Paraben	Methyl	Propyl	Butyl
Concentration Range (μmolar)	3.71 - 37.26	3.70 - 18.52	3.70 - 18.52
Mobile phase (methanol:water ratio)	50:50	65:35	65:35
Retention Time (minutes)	2.86	2.13	2.77

Table 6.2 Summary of HPLC conditions employed for the quantification of the parabens

6.2.3 Preparation of Ester-Esterase Solutions

The required amount of ester and esterase (1 unit ml^{-1} for butyl and propyl paraben and 2 units ml^{-1} for methyl paraben) were prepared in 0.1 M phosphate buffer (adjusted to pH 7.4 with potassium hydroxide). 1 ml of the esterase solution was added to 18 ml 0.1M phosphate

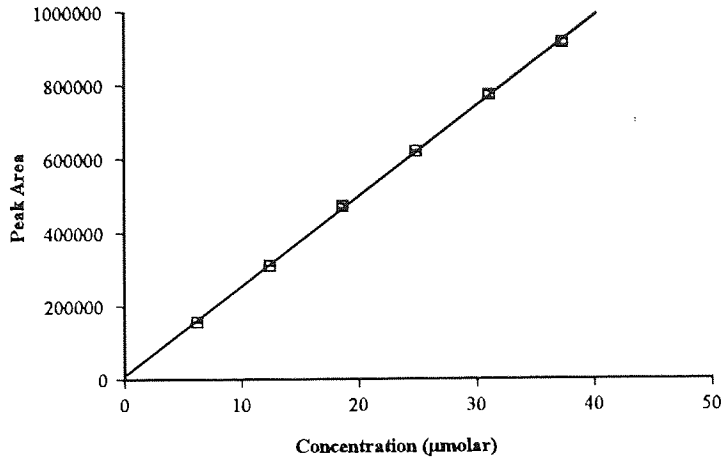

Figure 6.2 Assay validation calibration curve for butyl paraben. Mobile phase methanol:Water 65:35 delivered at 1ml min^{-1}, HPLC sensitivity 0.04 aufs. (Error bars represent SEM)

	Calibrators					
Calibrator Conc (µmolar)	6.210	12.421	18.631	24.841	31.052	37.262
Number of Samples	5	5	5	5	5	5
Mean Peak Area	157003	310814	472587	680040	772736	914988
Standard Deviation of Peak Area	2919.2	952.4	11317.6	8530.8	1824.6	13824.3
Coefficient of Variation (CV%)	1.859	0.306	2.395	1.254	0.236	1.511

Table 6.3 Parameters for reproducibility of butyl paraben validation calibration curve.

	Intercept			Slope			Correl Coeff
	Value	± SE	± 95% CI	Value	± SE	± 95% CI	r
Butyl Paraben	9049.9	4734.0	9697.2	24489.7	195.73	400.95	0.9997

Table 6.4 Statistics for the assay validation calibration curve for butyl paraben in Figure 6.2 (SE, standard error: CI, confidence interval).

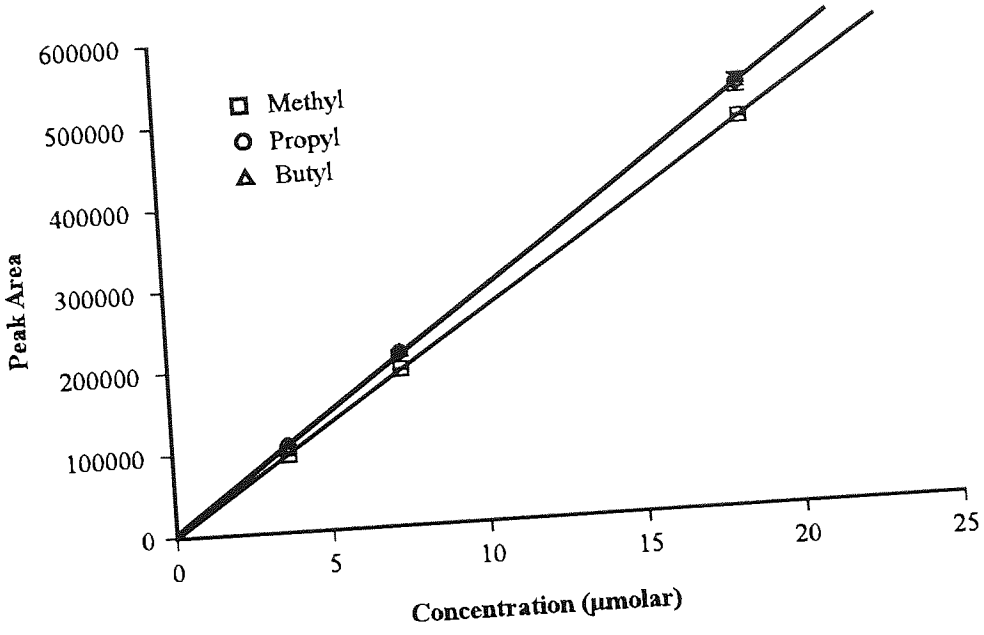

Figure 6.3 Typical calibration curves for methyl, propyl and butyl paraben using the mobile phases as described in Table 6.3. HPLC sensitivity 0.04 aufs. (Error bars represent the range of two replicate samples)

	Intercept			Slope			Correl Coeff
	Value	± SE	± 95% CI	Value	± SE	± 95% CI	r
Methyl	-43.28	947.09	2704.50	25562.5	83.01	230.49	0.9999
Propyl	5171.74	1421.95	3947.98	27545.0	121.42	337.12	0.9999
Butyl	2448.73	6562.59	18220.7	2768.37	560.28	1555.60	0.9999

Table 6.5 Statistics for the typical calibration curves of methyl, propyl and butyl paraben in Figure 6.3 (SE, standard error; CI, confidence interval)

buffer (pH 7.4) and incubated for 30 minutes in a water bath at 37°C. The degradation was initiated by the addition of 1 ml of the ester solution, which had also been incubated at 37°C for 30 minutes. At appropriate time intervals, 0.5 ml samples were taken using an autopipette and the reactions quenched in 0.5 ml 0.2M citric acid, then plunged into ice water. Samples were stored at 0°C for assay the same day, or frozen at -20°C, if overnight storage was required. Samples were injected directly onto the HPLC without pre-treatment. Standards were prepared in 0.1M phosphate buffer (adjusted to pH 7.4), quenched in 0.2M citric acid and cooled in the same way as the analytical samples.

6.2.4 Preparation of Ester-Esterase-Cyclodextrin Solutions

Solutions containing cyclodextrin:ester ratios of up to 500:1 were prepared by dissolving the appropriate amount of β-cyclodextrin in 0.1M phosphate buffer (pH 7.4) and incubating multiples of 9 ml with 1 ml of the ester solution prepared as in section 6.2.3 (Solution A, Table 6.6). These solutions were stirred overnight at room temperature. Then 1 ml of the esterase solution prepared as in section 6.2.3 was added to 9 ml 0.1M phosphate buffer (pH 7.4) and incubated for 30 minutes in a water bath at 37°C (Solution B, Table 6.6). The degradation was initiated by the addition of 10 ml of the ester/cyclodextrin solution which had also been incubated at 37°C for 30 minutes to avoid any potential temperature change. Samples were taken and quenched as section 6.2.3. Controls were prepared by replacing the cyclodextrin solution with 0.1M phosphate buffer (pH 7.4).

The 1000:1 ratio of β-cyclodextrin to ester solutions had to be prepared differently due to the solubility limitations of the β-cyclodextrin. This ratio was only used with an ester initial substrate concentration of 18.5 μmolar. Solution A (Table 6.6) was prepared by dissolving and diluting an ester to produce a solution with a final concentration of 370 μmol ml^{-1} (for example 100 mg butyl paraben dissolved in 100 ml and diluted 4 ml to 50 ml with 0.1M phosphate buffer). Multiples of 1 ml of this solution was stirred overnight with 18 ml cyclodextrin solution. This cyclodextrin solution was prepared by dissolving 370 μmol (0.499g) β-cyclodextrin in 18 ml 0.1M phosphate buffer (pH 7.4). After stirring overnight this solution A (19 ml) was incubated at 37°C for 30 minutes. The degradation was initiated by the addition of 1 ml of the esterase solution which had also been incubated at 37°C. Control solutions were prepared by replacing the cyclodextrin solution with 0.1M phosphate buffer (pH

	Volumes of Solutions in Cyclodextrin:Ester Reaction Mixtures				
	Solution A			Solution B	
CD-Ester Ratios	β-CD Solution	HPβ-CD Solution	Ester Soln (370μM)	Phosphate Buffer 0.1M	Esterase* (Units ml^{-1})
1:10	9ml 0.41mM	-	1ml	9ml	1ml
1:50	9ml 2.05mM	-	1ml	9ml	1ml
1:100	9ml 4.11mM	-	1ml	9ml	1ml
1:200	9ml 8.22mM	-	1ml	9ml	1ml
1:500	9ml 20.55 mM	-	1ml	9ml	1ml
1:1000	18ml 20.55 mM	-	1ml	-	1ml
1:2500	-	4.5ml 102.77 mM	0.5ml	4.5ml	0.5ml

Table 6.6 Component volumes and concentrations used in the cyclodextrin:ester reaction mixtures. (*, An esterase concentration of 1 unit ml^{-1} was used for propyl and butyl paraben and 2 unit ml^{-1} for methyl paraben).

7.4). The 2500:1 ratio of hydroxypropyl β-cyclodextrin was again only used with an initial ester substrate concentration of 18.5 μmolar. The ester solution was prepared as the 1000:1 β-cyclodextrin ratios. Multiples of 0.5 ml of the ester solution were mixed overnight with 4.5ml cyclodextrin solution which contained 462.5 μmol (0.6382g) hydroxypropyl β-cyclodextrin (Solution A, Table 6.6). 0.5 ml esterase solution was incubated in a water bath at 37°C for 30 minutes with 4.5 ml 0.1M phosphate buffer (pH 7.4). The degradation was initiated by the addition of 5 ml of the cyclodextrin/ester mixture previously incubated at 37°C for 30 minutes. Controls were prepared as for the ratios used above.

6.2.5 Validation of Reaction Quenching

In order to validate the quenching process, 20 ml tubes containing an initial substrate

concentration of sodium butyl paraben 27.75 μmolar (120 μg in 20 ml) and 1 unit of esterase in 0.1M phosphate buffer (pH 7.4), were incubated as section 6.2.3 at 37°C. Samples were taken at 30 minutes, quenched, stored at 0°C for 3 hours, frozen at -20°C for 3 days and then re-assayed. Five replicates were performed.

6.2.6 Shelf-life of Reconstituted Esterase

The esterase was reconstituted from the concentrate as supplied by Sigma and diluted with 0.1M phosphate buffer (pH 7.4) to a final concentration of 1 unit ml^{-1}. Three tubes were prepared as described in section 6.2.3 using 18.5 μmolar (80 μg in 20 ml) sodium butyl paraben in 0.1M phosphate buffer (pH 7.4). The initial rate was calculated following samples at time intervals of 4.5, 10, 20, 30 and 40 minutes. This experiment was repeated following storage of the reconstituted esterase solution in a refrigerator at 2 to 8°C for 7 days. This stability test was repeated using esterase reconstituted to a strength of 2 units ml^{-1} and 18.5 mmolar (64.56 μg in 20 ml) sodium methyl paraben. Sampling time intervals were 20, 40, 80 and 120 minutes.

6.2.7 Effect of Esterase Concentration on Initial Reaction Velocities

A series of 20 ml reaction tubes were prepared at pH 7.4 containing a 55.13 μmolar initial substrate concentration of sodium butyl paraben. A range of esterase concentrations were added to each tube (1 to 5 units in 20 ml) and the reaction profile monitored. Each esterase concentration was performed in triplicate.

6.2.8 Determination of the Michaelis-Menten Kinetic Parameters for the Esterase Hydrolysis of Methyl and Butyl Paraben

A series of reaction tubes were prepared at pH 7.4 as described in section 6.2.3 with the initial substrate concentration of paraben in the range of 4.65 μmolar (16.14 μg sodium methyl paraben; 20 μg sodium butyl paraben in 20 ml) to 46.5 μmolar (161.4 μg sodium methyl paraben; 200 μg sodium butyl paraben in 20 ml). These reaction profiles were monitored at 20, 40, 80 and 120 minutes for the methyl and 10, 20, 30, 40 minutes for the butyl paraben.

6.2.9 The Effect of Cyclodextrins Upon the Esterase Hydrolysis of Methyl and Butyl Paraben

Using initial paraben concentrations of 18.5 μmolar, reaction tubes were prepared at pH 7.4 and pH 6.0 as detailed in section 6.2.4. A control series of reaction tubes without cyclodextrin, prepared as section 6.2.3, were used to compare each hydrolysis run. Sampling times were as section 6.2.8 and as detailed in the results. 1 unit of esterase in 20 ml was used for the propyl and butyl parabens and 2 units in 20 ml for the methyl paraben.

Solution Components	Volumes of Solutions in Reaction Mixtures for the CD:Ester Ratios				
	Control	1:1000[a]	1:1000[b]	1:2500[a]	1:2500[b]
Solution A					
Ester (18.5 μM)	1ml	1ml	-	0.5ml	-
Phosphate Buffer (0.1M)	9ml	-	-	-	-
β-CD (20.55 mM)	-	18ml	18ml	-	-
HPβ-CD (102.8 mM)	-	-	-	4.5ml	4.5ml
Esterase (1or2 units ml^{-1})	-	-	1ml	-	0.5ml
Solution B					
Ester (18.5 μM)	-	-	1ml	-	0.5ml
Phosphate Buffer (0.1M)	9ml	-	-	4.5ml	4.5ml
Esterase (1or2 units ml^{-1})	1ml	1ml	-	0.5ml	-

Table 6.7 Component volumes and concentrations for the reaction mixtures used in the cyclodextrin:ester:esterase overnight incubation experiments. (The cyclodextrin used in the 1:2500 CD:ester ratios was hydroxypropyl β-cyclodextrin (HP β-CD) and β-cyclodextrin (β-CD) was used in the 1:1000 ratios. [a], cyclodextrin mixed with ester overnight; [b], cyclodextrin mixed with esterase overnight).

6.2.10 The Effect of Overnight Mixing of Cyclodextrins with Either Esterase or Ester

These reaction profiles were designed similar to those described in section 6.2.4. Three reaction tubes were set up as controls, three were pre-mixed overnight with cyclodextrin and esterase solutions and three pre-mixed overnight with cyclodextrin and ester solutions.

Solution compositions for these experiments are detailed in Table 6.7. Solution A was pre-mixed overnight. The following day both solution A and B were incubated at 37°C for 30 minutes before the reaction was initiated by adding solution B to solution A. Samples were taken and the reaction quenched as detailed in section 6.2.3.

6.2.11 The Effect of Cyclodextrins on K_m and V_{max} of the Esterase Hydrolysis of Methyl Paraben

A series of reaction tubes were prepared to monitor the Michaelis-Menten kinetics of the esterase hydrolysis of sodium methyl paraben over the initial substrate concentration range of 4.6 to 58.0 μmolar. The profile was carried out as described in section 6.2.4. An identical series of tubes were prepared, except that each of the ester solutions (1 ml of 180 to 930 μmolar) was incubated overnight with 74 μmol of β-cyclodextrin (9 ml of 8.22 mmolar). Table 6.8 details the concentrations of ingredients contained in the 20 ml reaction tubes to enable to determination of the K_m and V_{max} of the esterase hydrolysis of methyl paraben in the presence of cyclodextrin.

Flask	Ester Conc. μmolar	CD Conc μmolar	Ester / CD Ratio	Esterase Units / 20ml	Free Ester μmolar
1	4.55	3700	800 : 1	2	0.98
2	9.29	3700	400 : 1	2	2.01
3	13.87	3700	267 : 1	2	3.01
4	18.63	3700	200 : 1	2	4.04
5	23.37	3700	160 : 1	2	5.07
6	27.86	3700	133 : 1	2	6.05
7	37.19	3700	100 : 1	2	8.09
8	46.44	3700	80 : 1	2	10.12
9	58.00	3700	64 : 1	2	12.66

Table 6.8 Concentrations of ester, cyclodextrin and esterase used to determine the K_m and V_{max} of esterase hydrolysis of methyl paraben in the presence of cyclodextrin (Each reaction tube contained a total of 20 ml).

6.3 Results and Discussion

Validation of the quenching process (section 6.2.5) showed that there was no statistical difference (P = 0.8562) between the original assay (Mean = 17.830 µmolar ; Standard deviation = 1.1886 µmolar) and the stored samples (Mean = 17.991 µmolar ; Standard deviation = 1.2321 µmolar). The conclusion of this result is two-fold. It shows that the quenching was sufficient to halt the enzymatic hydrolysis and was not so severe that it caused a chemical breakdown of the esters. This quenching process was therefore used throughout the remainder of this study. The rate of enzymatic hydrolysis of butyl and methyl paraben using freshly reconstituted esterase was not significantly different to that of esterase which had been diluted to 1 or 2 units ml^{-1} with 0.1M phosphate buffer (pH 7.4) and stored for 7 days at 2 to 8°C. Therefore, 1 or 2 units ml^{-1} solutions of esterase in 0.1M phosphate buffer (pH 7.4) were used for 7 days if stored at 2 to 8°C. In order to counteract any potential variation during storage or inter-batch variation associated with esterase samples, control reaction profiles, for example without cyclodextrin, were run in order to compare, and if necessary, normalise results.

Figures 6.4 and 6.5 show that there is a linear relationship between esterase concentration and the initial reaction velocity for the hydrolysis of butyl paraben ($y = 0.6564x - 0.1307$; $r = 0.9993$). The initial rate velocities throughout this study were assessed by polynomial curve fitting of the data points versus time and solving the differentiated equation of the curve at $t = 0$. Plots of the amount remaining versus time for esterase hydrolysis of methyl and butyl paraben are shown in Figures 6.6 and 6.8. The appropriate Michaelis-Menten plots are shown in Figures 6.7 and 6.9. Values of K_m and V_{max} obtained from the Michaelis-Menten plots and its various linear derivations for methyl and butyl paraben are given in Tables 6.9 and 6.10 respectively. To study the effect of cyclodextrins upon the stabilisation of esters in enzymic systems, a substrate concentration of 18.5 µmolar was selected for all of the parabens. A similar molar concentration was chosen to enable a direct comparison of the cyclodextrin:ester ratios between each of the methyl, propyl and butyl esters. A value of 18.5 µmolar was used as it was similar in value to the K_m for butyl paraben (18.3 µmolar) and methyl paraben (28.7 µmolar) and enabled Michaelis-Menten kinetics to apply is defined in Equation 6.6.

For the majority of experiments, β-cyclodextrin was used to study the stabilisation of the

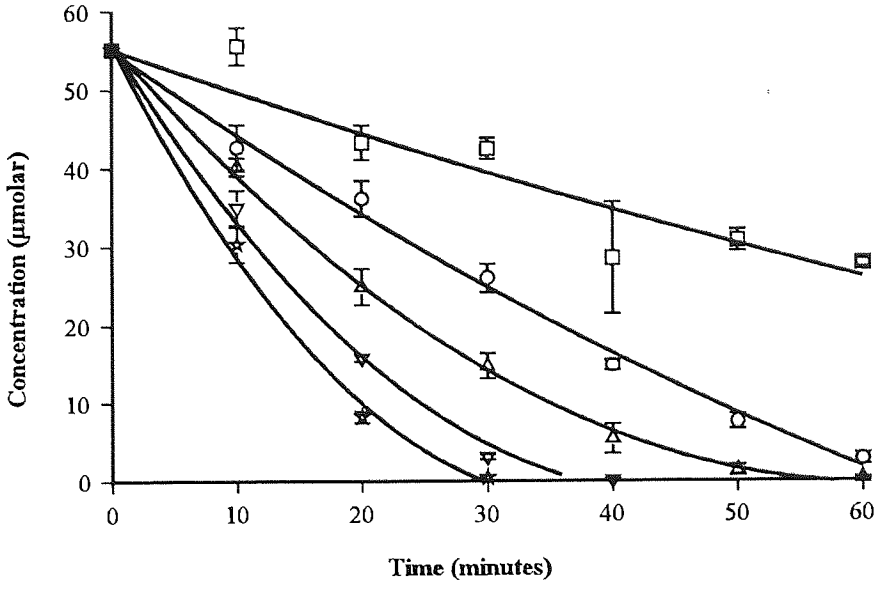

Figure 6.4 Plot of concentration versus time for the esterase hydrolysis of butyl paraben showing the effect of esterase concentration (□, 1 unit/20ml;○, 2 units/20 ml; △, 3 units/20ml; ▽, 4 units/20ml;☆, 5units/20ml). (Error bars represent SEM)

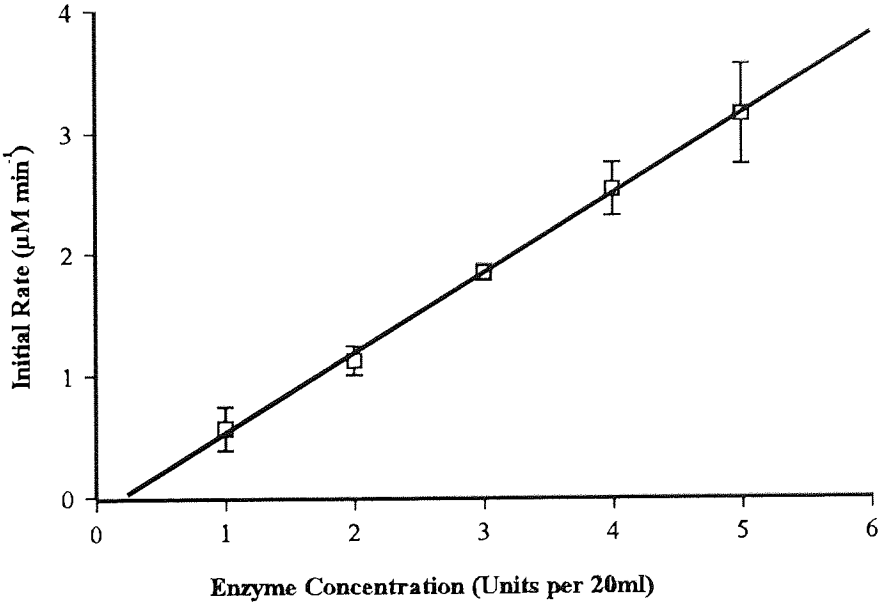

Figure 6.5 Plot of initial rate versus enzyme concentration for the esterase hydrolysis of butyl paraben (error bars represent standard error).

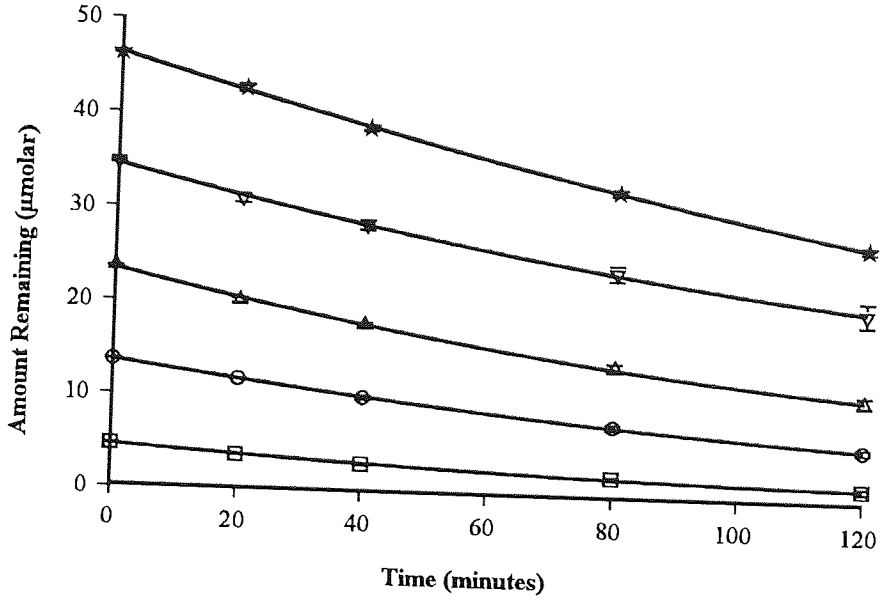

Figure 6.6 Plot of amount remaining versus time for the esterase hydrolysis of methyl paraben showing the effect of initial substrate concentration (□, 4.63 µmolar; ○, 13.90 µmolar;△, 23.17 µmolar;▽, 34.76 µmolar;☆, 46.34 µmolar)(Error bars represent the standard error of the mean).

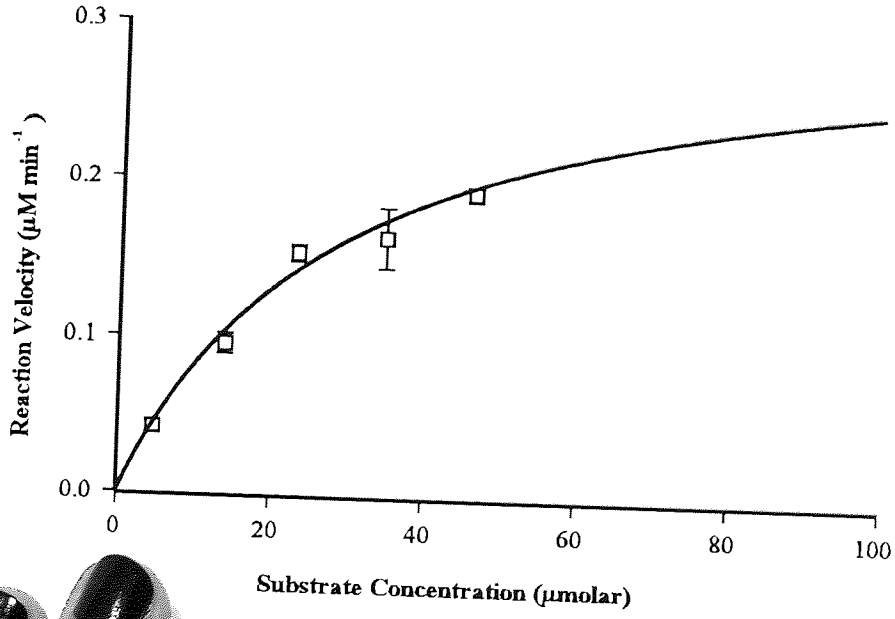

Figur …n plot for the esterase hydrolysis of methyl paraben (Error bars …ard error of the mean) (See Table 6.9 for analysis of K_m and

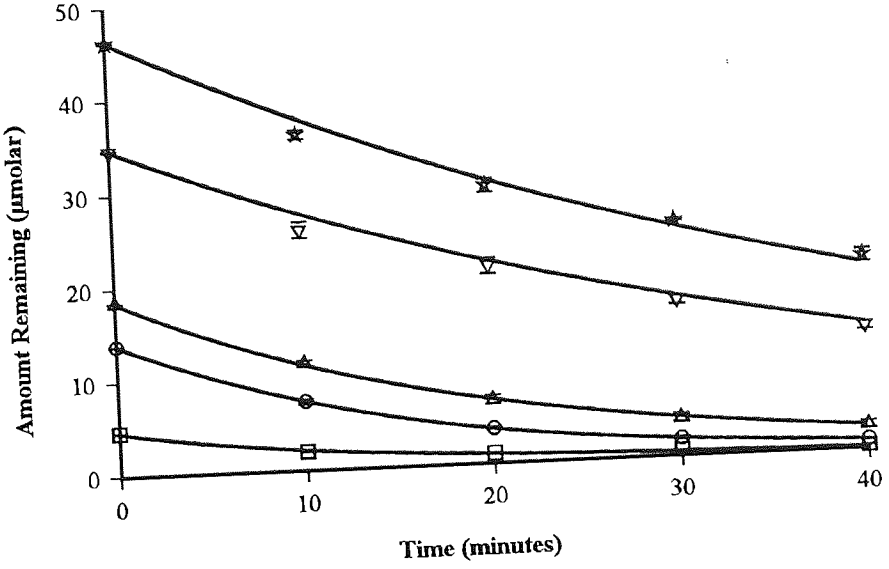

Figure 6.8 Plot of amount remaining versus time for the esterase hydrolysis of butyl paraben showing the effect of initial substrate concentration (□, 4.62 µmolar; ○, 13.87 µmolar;△, 18.5 µmolar;▽, 34.68 µmolar;☆, 46.25 µmolar)(Error bars represent standard error of the mean)

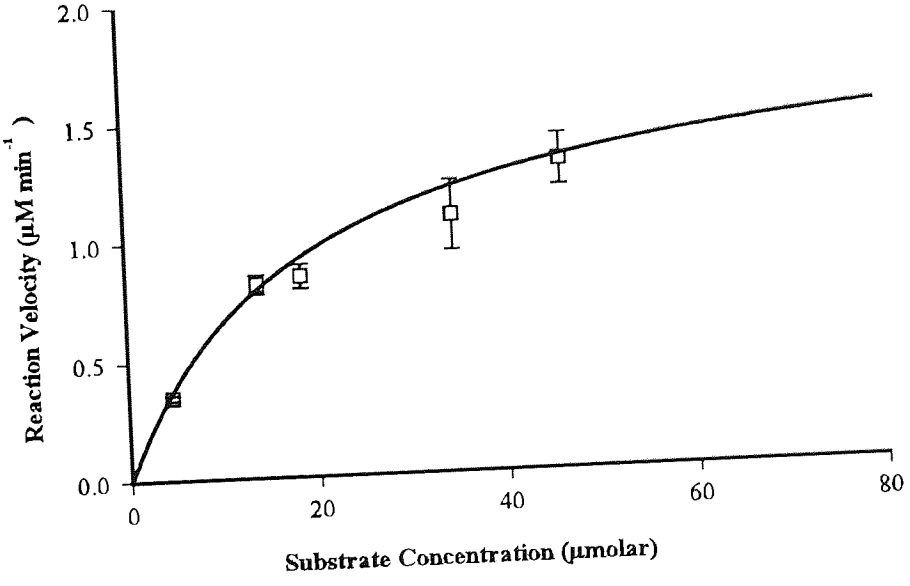

Figure 6.9 Michaelis-Menten plot for the esterase hydrolysis of butyl paraben (error bars represent standard error of the mean) (See Table 6.10 for analysis of K_m and V_{max})

	K_m (μM)	V_{max} (μM min^{-1})
From DIRECT LINEAR:	28.7	0.318
68% Confidence limits:	25.5-33.2	0.296 - 0.355
From LINEWEAVER-BURK plot:	31.6	0.325
Correlation coefficient = 0.97		
From HANES-WOOLF plot:	30.2	0.315
Correlation coefficient = 0.896		
From EADIE-HOFSTEE plot:	22.8	0.273
Correlation coefficient = 0.777		
From method of WILKINSON:	27.9	0.309
Standard errors:	7.97	0.0426

Table 6.9 Michaelis-Menten parameters for the esterase hydrolysis of methyl paraben.

	K_m (μM)	V_{max} (μM min^{-1})
From DIRECT LINEAR:	18.4	1.85
68% Confidence limits:	13.8 - 21.6	1.37 - 1.99
From LINEWEAVER-BURK plot:	18.2	1.73
Correlation coefficient = 0.986		
From HANES-WOOLF plot:	17.9	1.71
Correlation coefficient = 0.925		
From EADIE-HOFSTEE plot:	15.0	1.60
Correlation coefficient = 0.807		
From method of WILKINSON:	18.0	1.74
Standard errors:	5.36	0.223

Table 6.10 Michaelis-Menten parameters for the esterase hydrolysis of butyl paraben.

parabens against attack by porcine carboxyesterase. Hydroxypropyl β-cyclodextrin was used for the highest cyclodextrin:ester ratio (2500:1) due to its greater aqueous solubility. The effect of various cyclodextrin:ester ratios upon amount remaining versus time are shown for the methyl (Figure 6.10), propyl (Figure 6.12) and the butyl paraben (Figure 6.14). The initial reaction velocities calculated from the polynomial regression analysis are given in Tables 6.11, 13 and 15 for methyl, propyl and butyl parabens respectively with the corresponding overall apparent first-order reaction rates shown in Tables 6.12, 14 and 16. The relationship between the apparent first-order half-life and the cyclodextrin:ester ratio is shown for each of these compounds in Figures 6.11, 13 and 15. The effect of cyclodextrin addition to the reaction mixture has a significant effect upon the apparent first-order rate constants (Tables 6.12, 14 and 16) and in the presence of a 1000:1 μmolar ratio of β-cyclodextrin the $t_{½}$ for methyl paraben hydrolysis increases by a factor of 10 over the control.

The protection of the parabens from esterase hydrolysis by cyclodextrins is not as significant when the initial velocity is used as a measure of reaction rate. In Tables 6.11, 13 and 15, the degree of stabilisation and protection afforded by the cyclodextrins is represented by the protection factor. This is calculated from:

$$\text{Protection fraction} = \frac{\text{Initial velocity in presence of cyclodextrin}}{\text{Initial velocity in absence of cyclodextrin}} \qquad \text{(Eq 6.8)}$$

The lower cyclodextrin:ester ratios demonstrate very little protective effect for the esters and it was not unusual for an increase in initial velocity to be seen. For the propyl paraben an increase in initial velocity was observed for the 50:1 and 100:1 ratios and the butyl paraben an increase was observed for the 50 to 200:1 ratios.The degree of protection does not become significant until ratios of 200 to 500:1 are achieved and even at these levels the degree of protection was less than 2.3 (Tables 6.11, 13 and 15), rather than orders of magnitude. In the presence of a 1000:1 μmolar ratio of β-cyclodextrin the protection factor for methyl paraben was only 2.33.

Using Equation 6.3 it is possible to calculate a theoretical amount of free ester that is not

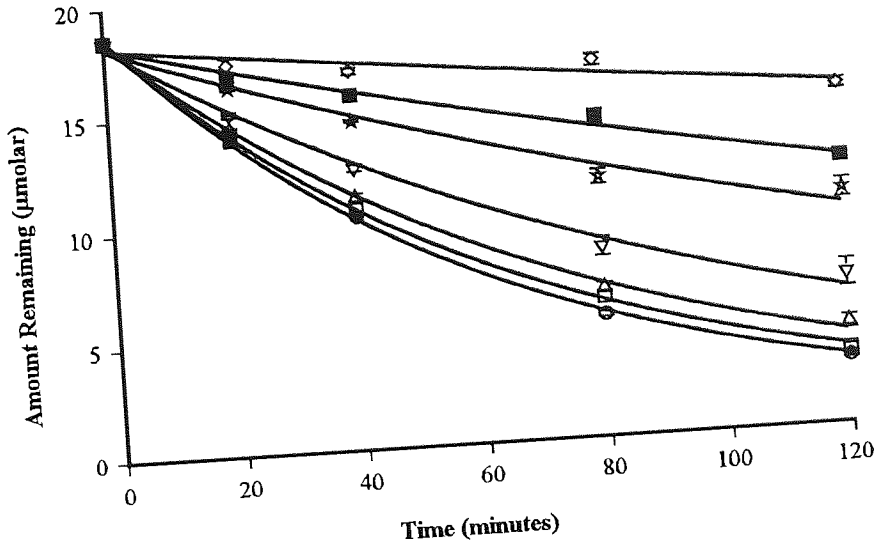

Figure 6.10 Plot of amount remaining versus time for the esterase hydrolysis of methyl paraben showing the effect of differing ester:cyclodextrin ratios (□, No cyclodextrin; ○, 1:50; △, 1:100; ▽, 1:200; ☆, 1:500; ■, 1:1000; ◇, 1:2500) [Error bars represent the standard error of the mean].

Ester:CD Ratio	Initial Rates (min^{-1}) Value	± SE	± 95% CI	Protection Ratio
Zero	0.256	0.0147	0.0302	-
1:50	0.255	7.98×10^{-3}	0.0176	1.00
1:100	0.226	0.0144	0.0316	1.13
1:200	0.185	0.0267	0.0587	1.38
1:500	0.113	0.0191	0.0420	2.26
1:1000	0.110	0.0146	0.0321	2.33
1:2500	0.093	0.0164	0.0362	2.75

Table 6.11 Initial rates for the esterase hydrolysis of methyl paraben in the presence of cyclodextrin (The cyclodextrin used in the 1:2500 ratio was hydroxypropyl β-cyclodextrin, β-cyclodextrin was used with all other ratios).

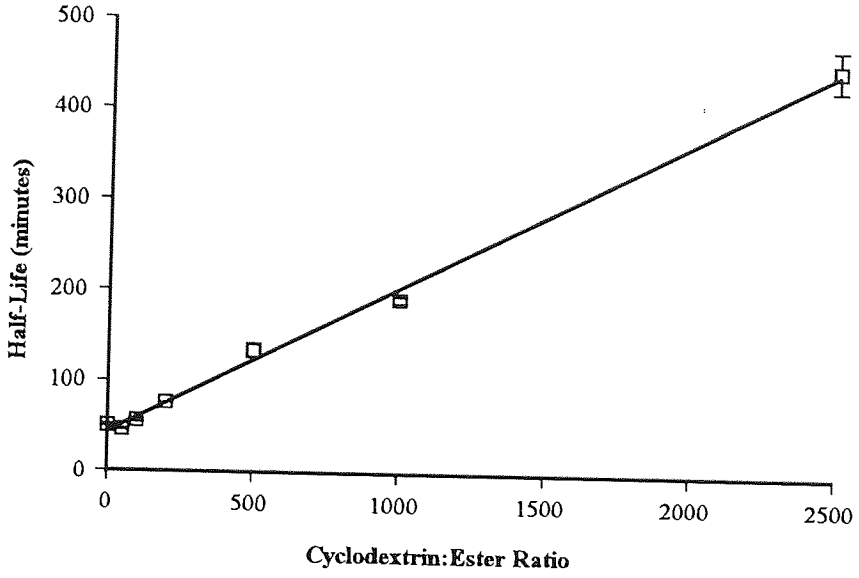

Figure 6.11 Plot of the half-life of methyl paraben due to esterase hydrolysis versus cyclodextrin:ester ratio (Error bars represent the standard error of the mean)

	Overall Apparent 1st Order Reaction Rate (min^{-1})			
Ester:CD Ratio	Value	± SE	± 95% CI	$t_{½}$
Zero	1.39×10^{-2}	2.649×10^{-4}	5.428×10^{-4}	49.7
1:50	1.51×10^{-2}	1.904×10^{-3}	4.114×10^{-4}	45.9
1:100	1.25×10^{-2}	2.669×10^{-3}	5.767×10^{-3}	55.6
1:200	9.19×10^{-3}	4.031×10^{-3}	8.710×10^{-3}	75.4
1:500	5.22×10^{-3}	2.774×10^{-3}	5.993×10^{-3}	132.8
1:1000	3.62×10^{-3}	1.674×10^{-3}	3.618×10^{-4}	191.3
1:2500	1.55×10^{-3}	1.899×10^{-3}	4.104×10^{-3}	446.0

Table 6.12 Overall apparent reaction rates for the esterase hydrolysis of methyl paraben in the presence of cyclodextrin (The cyclodextrin used in the 1:2500 ratio was hydroxypropyl β-cyclodextrin, β-cyclodextrin was used with all other ratios).

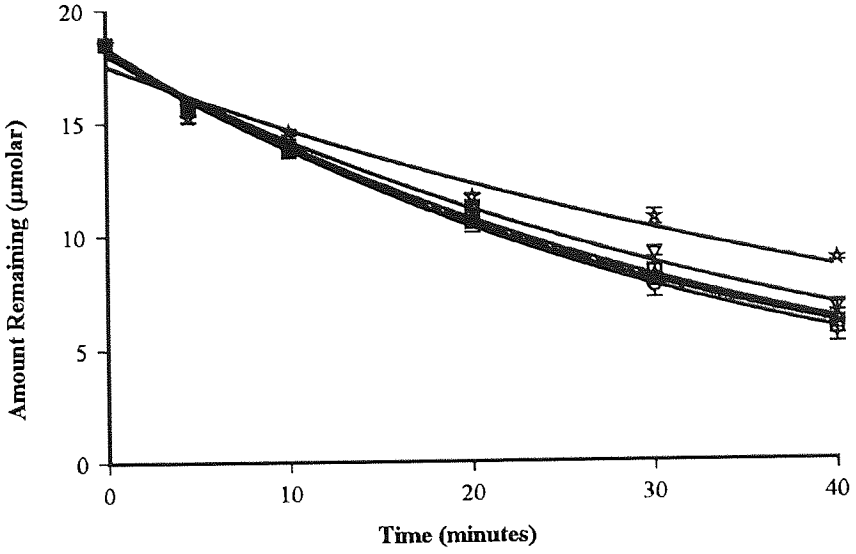

Figure 6.12 Plot of amount remaining versus time for the esterase hydrolysis of propyl paraben showing the effect of differing ester:cyclodextrin ratios (□, No cyclodextrin; ○, 1:50; △, 1:100; ▽, 1:200; ☆, 1:500). (Error bars represent the standard error of the mean)

	Initial Rates (min^{-1})			Protection Ratio
Ester:CD Ratio	Value	± SE	± 95% CI	
Zero	0.426	0.0329	0.0702	-
1:50	0.473	0.0382	0.0814	0.90
1:100	0.484	0.0412	0.0879	0.88
1:200	0.417	0.0318	0.0677	1.02
1:500	0.384	0.0432	0.0921	1.11

Table 6.13 Initial rates for the esterase hydrolysis of propyl paraben in the presence of β-cyclodextrin.

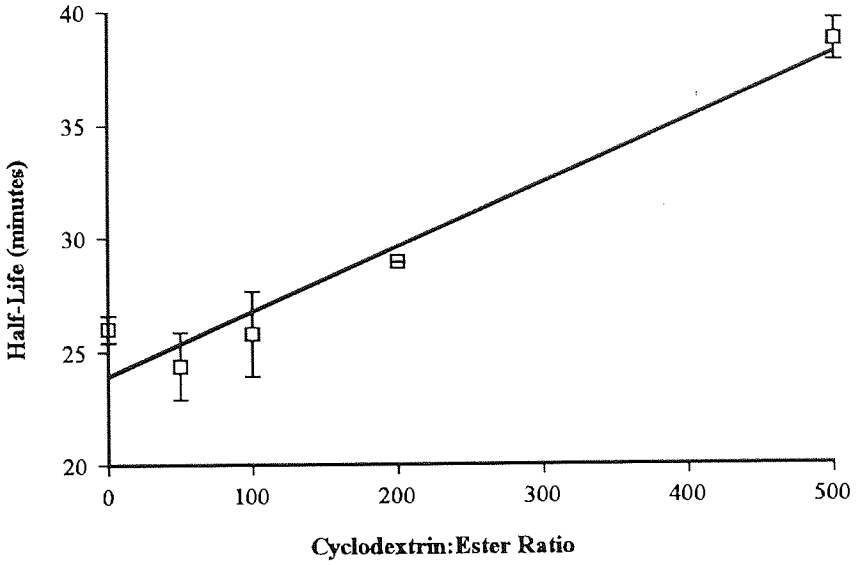

Figure 6.13 Plot of the half-life of propyl paraben during esterase hydrolysis versus cyclodextrin:ester ratio (Error bars represent the standard error of the mean)

	Overall Apparent 1st Order Reaction Rate (min^{-1})			$t_{½}$
Ester:CD Ratio	Value	± SE	± 95% CI	
Zero	0.027	8.42×10^{-4}	1.79×10^{-3}	26.0
1:50	0.029	1.03×10^{-3}	2.18×10^{-3}	24.2
1:100	0.027	1.10×10^{-3}	2.32×10^{-3}	25.5
1:200	0.024	7.42×10^{-4}	1.57×10^{-3}	28.9
1:500	0.018	1.07×10^{-3}	2.28×10^{-3}	38.6

Table 6.14 Overall apparent reaction rates for the esterase hydrolysis of propyl paraben in the presence of β-cyclodextrin.

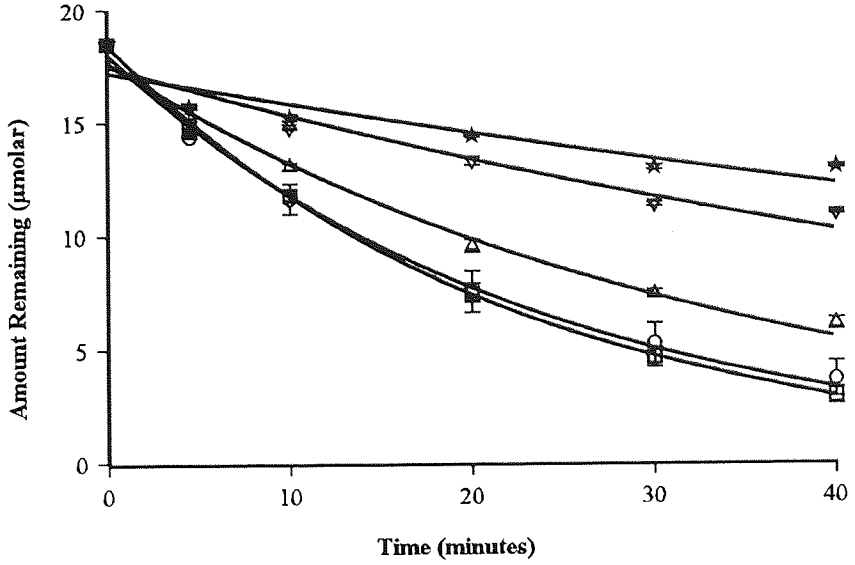

Figure 6.14 Plot of amount remaining versus time for the esterase hydrolysis of butyl paraben showing the effect of differing ester:cyclodextrin ratios (□, No cyclodextrin; ○, 1:100; △, 1:500; ▽, 1:1000; ☆, 1:2500). (Error bars represent standard error of the mean.)

	Initial Rates (min^{-1})			
Ester:CD Ratio	Value	± SE	± 95% CI	Protection Ratio
Zero	0.807	0.0739	0.147	-
1:10	0.908	0.0421	0.093	0.89
1:50	0.931	0.0596	0.128	0. 87
1:100	0.888	0.1605	0.327	0.91
1:200	1.037	0.0599	0.128	0.78
1:500	0.702	0.0606	0.123	1.15
1:1000	0.472	0.0708	0.152	1.71
1:2500	0.43	0.0767	0.164	1.88

Table 6.15 Initial rates for the esterase hydrolysis of butyl paraben in the presence of cyclodextrin (The cyclodextrin used in the 1:2500 ratio was hydroxypropyl β-cyclodextrin, β-cyclodextrin was used with all other ratios).

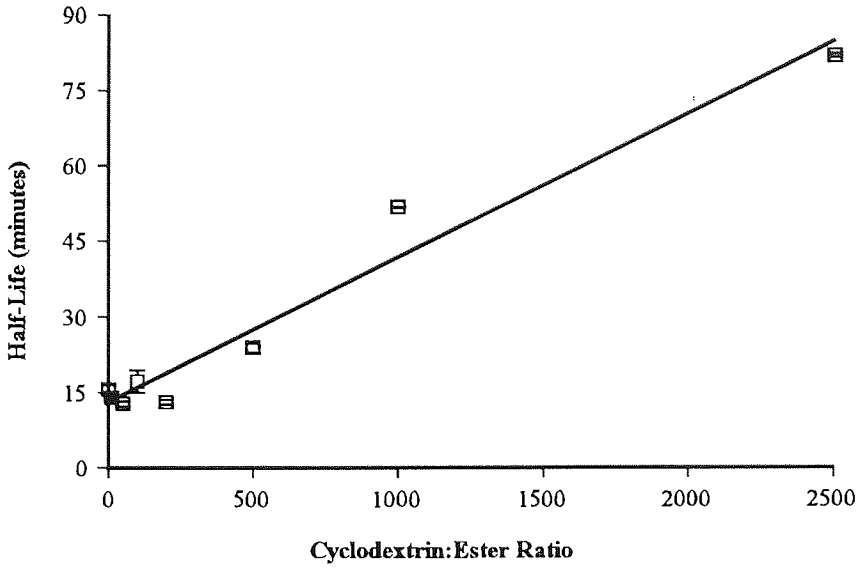

Figure 6.15 Plot of the half-life of butyl paraben during esterase hydrolysis versus cyclodextrin:ester ratio (Error bars represent the standard error of the mean)

	Overall Apparent 1st Order Reaction Rate (min^{-1})			$t_{½}$
Ester:CD Ratio	Value	± SE	± 95% CI	
Zero	4.57×10^{-2}	1.34×10^{-3}	2.67×10^{-3}	15.1
1:10	4.97×10^{-2}	7.87×10^{-4}	1.70×10^{-3}	13.9
1:50	5.47×10^{-2}	1.30×10^{-3}	2.75×10^{-3}	12.6
1:100	4.25×10^{-2}	2.78×10^{-3}	5.65×10^{-3}	16.5
1:200	5.30×10^{-2}	1.40×10^{-3}	2.97×10^{-3}	13.1
1:500	2.92×10^{-2}	9.61×10^{-4}	1.95×10^{-3}	23.9
1:1000	1.34×10^{-2}	9.49×10^{-4}	2.01×10^{-3}	53.3
1:2500	8.48×10^{-3}	9.51×10^{-4}	2.02×10^{-3}	86.6

Table 6.16 Overall apparent reaction rates for the esterase hydrolysis of butyl paraben in the presence of cyclodextrin (The cyclodextrin used in the 1:2500 ratio was hydroxypropyl β-cyclodextrin, β-cyclodextrin was used with all other ratios).

included within the cyclodextrin. By assuming that only the free ester is available for enzyme hydrolysis there should be a relationship between the initial reaction velocity and the free ester concentration. This relationship is shown in Figure 6.16 where the initial rate is plotted against the percentage of free ester available for hydrolysis. The data appear to follow a Michaelis-Menten plot, but cannot strictly follow such kinetics as the V_{max} is limited by a substrate concentration of approximately the K_m of the enzyme for a particular substrate (18.5 mmolar). The apparent V_{max} in these plots is equivalent to approximately $V_{max}/2$ and

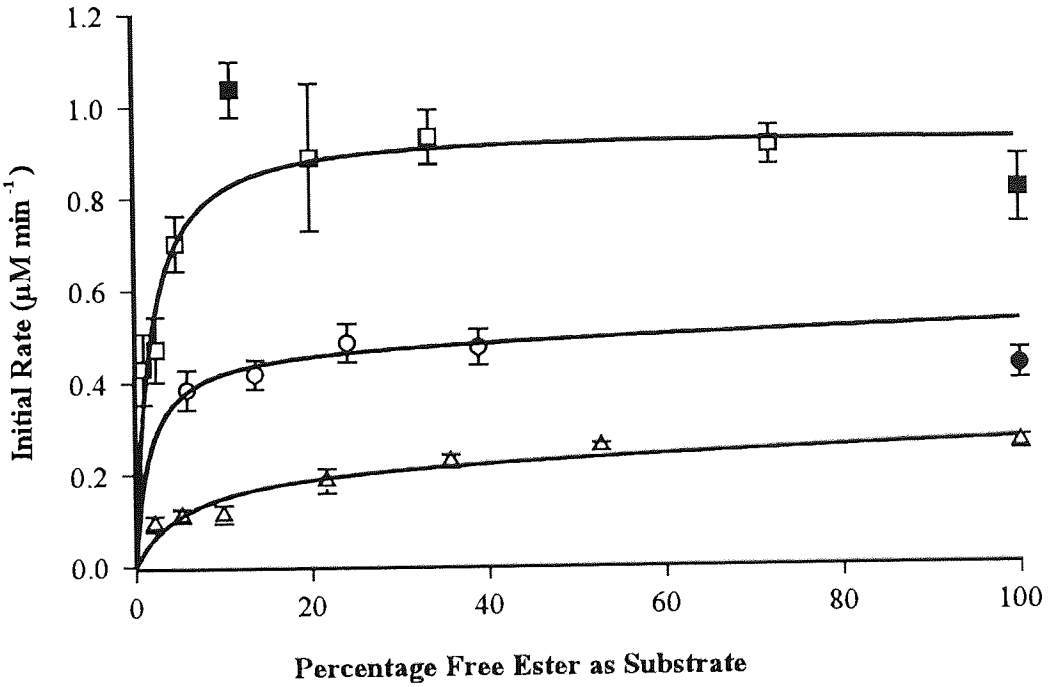

Figure 6.16 Initial rate of paraben hydrolysis by esterase versus the calculated percentage available free ester. (□, methyl; ○, propyl; △, butyl paraben; lines generated by best fit Michaelis-Menten curves)

K_m which correspond to V_{max} /4, which has values of 0.31 μmolar for butyl paraben and 1.72 μmolar for the methyl paraben. These results do not equate to the K_m for the corresponding ester in Tables 6.9 and 6.10. Therefore either the affinity of the enzyme for the free ester is not the same as the ester without cyclodextrin or that this is not an appropriate model. Figure 6.16 does show that a considerable proportion, approximately 90%, of ester must be included within the cyclodextrin before a significant effect upon initial rate is observed. As the 100%

free ester equates to the K_m of the enzyme, any reduction in the substrate concentration would be expected to have a significant corresponding reduction in initial reaction velocity. As this does not occur questions must be asked of the initial model which supposed that included ester is not available for enzyme hydrolysis. A possible explanation for this phenomenon is that the ester has a considerably greater affinity for the enzyme (K_m) than the cyclodextrin (K_s) pushing the equilibrium in Equation 6.9 to the left.

$$\text{Product} \leftarrow ES \overset{K_m}{\rightleftharpoons} E + S + CD \overset{K_s}{\rightleftharpoons} CD.S$$

(Eq 6.9)

Where E is the enzyme, S is the substrate, CD the cyclodextrin, ES the enzyme substrate complex and CD.S the cyclodextrin substrate complex. This difference in affinity may be sufficient to draw the included ester from the cyclodextrin torus, therefore the included quest compound is not completely protected from enzymatic hydrolysis. Another possible explanation for the deviation from the original model is that the ester group of the paraben molecule may protrude from the cyclodextrin torus. This protruding group may still remain available for hydrolysis despite the paraben molecule being included within the cyclodextrin.

The protective effect observed could be the result of the enzyme being inhibited by the cyclodextrin. Experiments were performed with the methyl and the butyl paraben to compare the effect of incubating either the enzyme or the ester overnight with the cyclodextrin (section 6.2.10). The 1000:1 and 2500:1 cyclodextrin:ester ratios were selected for the experiment as they had shown the most effective protection in the previous experiments. The results of these experiments are shown in Figure 6.17 and Table 6.17 for the methyl and Figure 6.18 and Table 6.18 for the butyl paraben. The 2500:1 ratios showed very little difference in protection irrespective of whether the ester or esterase was stirred overnight. This may well have been due to the excess of cyclodextrin available, pushing the equilibrium so far in favour of whichever complex was forming that any preference observed during the overnight stirring was negated. A difference was observed with the 1000:1 ratios. The overall apparent first-order rate constant is significantly different with both the methyl (Table 6.17) and butyl paraben (Table 6.18). The first-order rate constants are lower when the cyclodextrin has been

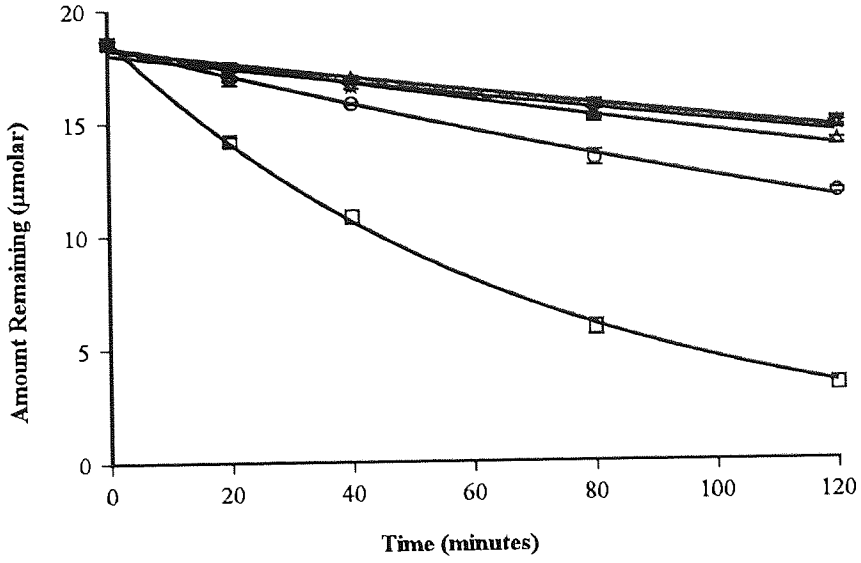

Figure 6.17 Plot of amount remaining versus time for the esterase hydrolysis of methyl paraben showing the effect of differing ester:cyclodextrin ratios and overnight incubation of cyclodextrin with either ester or esterase (□, No cyclodextrin; ○, 1:1000 Ester incubation; △, 1:1000 Esterase incubation; ▽, 1:2500 Ester incubation; ☆, 1:2500 Esterase incubation) [Error bars represent the standard error of the mean].

	Overall Apparent 1st Order Reaction Rate (min^{-1})			t-test probability (two-tail)
Ester:CD Ratio	Value	± SE	± 95% CI	
Zero	1.413×10^{-2}	3.634×10^{-4}	7.846×10^{-4}	-
1:1000[a]	3.846×10^{-3}	1.295×10^{-4}	2.797×10^{-4}	0.0008
1:1000[b]	2.327×10^{-3}	1.041×10^{-4}	2.249×10^{-4}	
1:2500[a]	1.758×10^{-3}	1.348×10^{-4}	2.912×10^{-4}	0.4736
1:2500[b]	1.892×10^{-3}	1.602×10^{-4}	3.461×10^{-4}	

Table 6.17 Apparent first-order rates for the esterase hydrolysis of methyl paraben in the presence of cyclodextrin. The cyclodextrin used in the 1:2500 ratio was hydroxypropyl β-cyclodextrin and β-cyclodextrin for the 1:1000 ratio ([a] cyclodextrin incubated with ester overnight; [b] cyclodextrin incubated with esterase overnight).

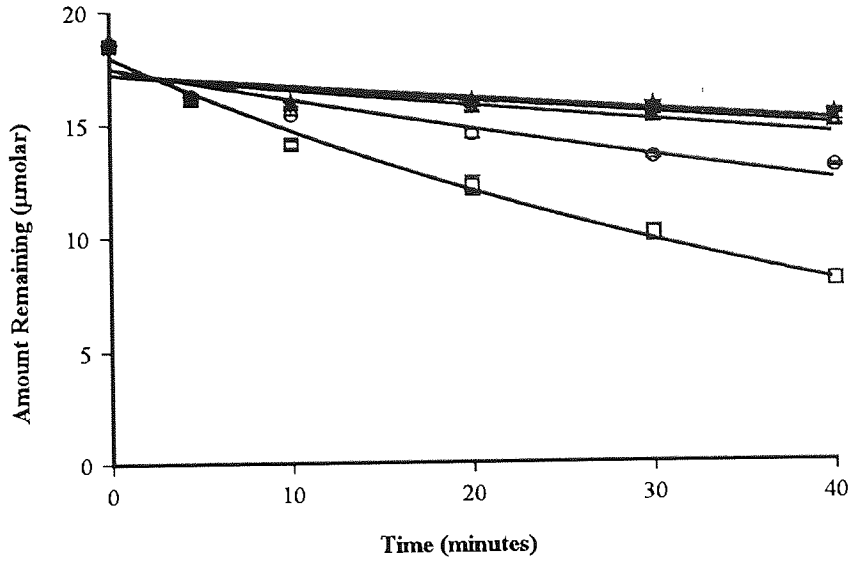

Figure 6.18 Plot of amount remaining versus time for the esterase hydrolysis of butyl paraben showing the effect of differing ester:cyclodextrin ratios and overnight incubation of cyclodextrin with either ester or esterase (□, No cyclodextrin; ○, 1:1000 Ester incubation; △, 1:1000 Esterase incubation; ▽, 1:2500 Ester incubation; ☆, 1:2500 Esterase incubation) (Error bars represent the standard error of the mean).

	Overall Apparent 1st Order Reaction Rate (min^{-1})			t-test probability (Two-tail)
Ester:CD Ratio	Value	± SE	± 95% CI	
Zero	2.014×10^{-2}	8.333×10^{-4}	1.767×10^{-3}	-
1:1000[a]	8.518×10^{-3}	7.857×10^{-4}	1.666×10^{-3}	0.0010
1:1000[b]	4.334×10^{-3}	8.252×10^{-4}	1.749×10^{-3}	
1:2500[a]	3.618×10^{-3}	7.920×10^{-4}	1.679×10^{-3}	0.5565
1:2500[b]	3.488×10^{-3}	7.650×10^{-4}	1.622×10^{-3}	

Table 6.18 Apparent first-order rates for the esterase hydrolysis of butyl paraben in the presence of cyclodextrin. The cyclodextrin used in the 1:2500 ratio was hydroxypropyl β-cyclodextrin and β-cyclodextrin for the 1:1000 ratio ([a] cyclodextrin incubated with ester overnight; [b] cyclodextrin incubated with esterase overnight).

incubated overnight with the esterase rather than the ester. This would imply that the cyclodextrin is having a more pronounced effect interfering with the enzyme than incorporating the ester into an inclusion complex. These results contrast with work on peptides (Irwin *et al.*, 1994), where the stability increase was assumed unlikely to be due to a direct effect on the enzyme. Irwin *et al* (1994) based this supposition upon evidence using carboxypeptidase and a 1:25 substrate to cyclodextrin ratio. Under these conditions, using the same enzyme some protection was observed for leucine enkephalin, but not for phenylalanylglycylglycine. When comparing these sets of results it must be taken into account that different enzymes and substrates were used to give these contrasting results.

To further investigate this action mechanism, the K_m and V_{max} of the esterase hydrolysis of methyl paraben was determined in the presence and absence of cyclodextrin. The experiment was conducted using a technique similar to that used in classical enzyme inhibition experiments (section 6.2.11). The rationale behind this model is that if the kinetics demonstrate a reduction in V_{max}, while K_m remains the same, the cyclodextrin is complexing the ester. This is because the effective substrate concentration is reduced, therefore the V_{max} will be lower, while the affinity of the enzyme for the ester remains the same and therefore the apparent K_m will remain the same. If the kinetics demonstrated a reduction in K_m, while V_{max} remains the same, then the assumption is that the cyclodextrin was interfering with the enzyme. This is because when the effective substrate concentration remains the same, V_{max} will be similar, but the substrate:enzyme affinity will change reducing the apparent K_m. A possible source of error in the experimentation is that there are three variables, the ester concentration, the cyclodextrin concentration and the esterase concentration. It is not possible to keep the ratio between all three variables constant. The esterase concentration must remain the same and the ester concentration varied to obtain the K_m and V_{max}. Therefore, if the cyclodextrin concentration is held constant the esterase:cyclodextrin ratio will be constant, but the ester:cyclodextrin ratio will change (Table 6.8).

The effect of adding cyclodextrin on the K_m and V_{max} of the esterase hydrolysis of methyl paraben was an increase in the K_m from 48.71 to 62.24 μmolar and a decrease in the V_{max} from 61.00 to 53.46 μM hr^{-1} (Table 6.19). This would mean that from the above argument cyclodextrin included or affected both the ester and the esterase. Further evidence for this hypothesis is obtained by the presumption that the enzyme can only hydrolyse "free" or non-

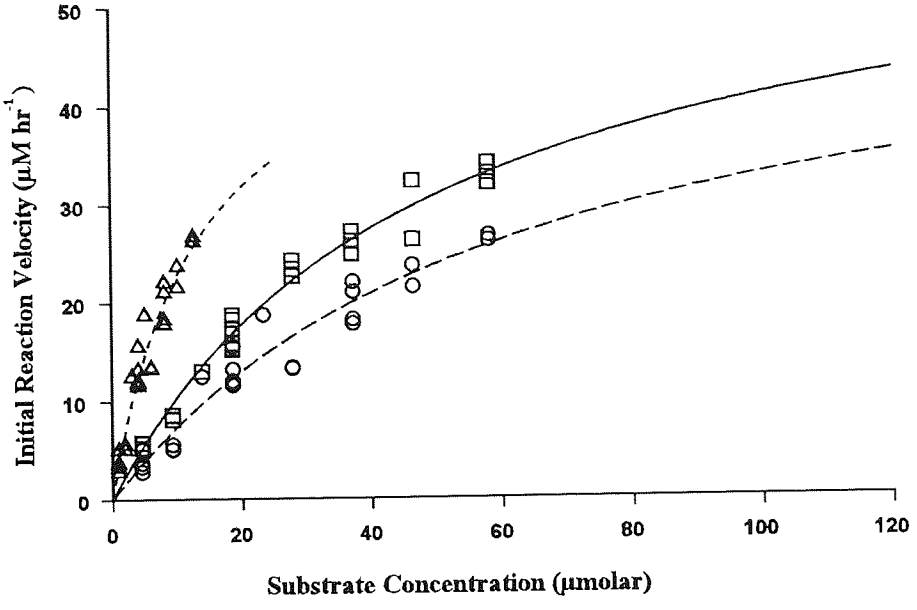

Figure 6.19 Michaelis-Menten plot for the esterase hydrolysis of methyl paraben. (□, control - no cyclodextrin; ○, with cyclodextrin; △, with cyclodextrin - substrate concentration determined as free ester).

	K_m (μmolar)			V_{max} (μM hr^{-1})		
	Value	± SE	± 95% CI	Value	± SE	± 95% CI
Control- No cyclodextrin	48.71	6.38	13.27	61.00	4.63	9.63
With cyclodextrin	62.24	16.15	33.49	53.46	8.89	18.43
With cyclodextrin - substrate concentration as free ester	13.31	3.42	7.08	52.89	8.65	17.94

Table 6.19 Michaelis-Menten constants for the esterase hydrolysis of methyl paraben in the presence of cyclodextrin (SE, standard error; CI, confidence interval).

included ester. Therefore, if the cyclodextrin only interacted with the ester, recalculation of the initial reaction velocities for the results with cyclodextrin (○, Figure 6.19) with respect to free ester using Equation 6.3 should superimpose these results onto the control. Figure 6.19 shows that this does not occur and that the calculated free ester (△) results produce a K_m of 13.31 which is significantly lower than the control of 48.71. An explanation of this is that Equation 6.3 under estimates the levels of free ester, which would occur if a proportion of the cyclodextrin was bound to the esterase rather than including the ester.

6.4 Summary

The epidermis and nasal mucosa are becoming recognised as sites of enzymic activity. It may be possible to include topically applied vulnerable ester prodrugs in the cyclodextrin torus to protect them from enzymic hydrolysis.

A system was developed to investigate the esterase hydrolysis of alkyl parabens, the model ester compounds. The K_m (28.7 μM) and V_{max} (0.318 μM min^{-1}) of methyl and the K_m (18.4 μM) and V_{max} (1.85 μM min^{-1}) of butyl paraben hydrolysis by porcine liver carboxyesterase were determined using this system. Cyclodextrins were incubated overnight with an 18.5 μM paraben substrate solution. Cyclodextrin protection of the paraben from esterase hydrolysis was investigated and the substrate : cyclodextrin concentration ratio at which any effect become significant was determined. Cyclodextrin : substrate ratios greater than 200 : 1 were required to provide a significant protection from hydrolysis. The level of protection did not appear to be related directly to the quantity of non-included or "free" ester available for hydrolysis There is evidence that the small amount of protection observed could be due to an interaction of the cyclodextrin with both the ester and esterase. Additional work is required to confirm these results.

The level of protection observed would not be expected to provide a major protection of ester prodrugs from enzymic hydrolysis, but it may be a mechanism that contributes, at least to some extent, to the overall transdermal absorption enhancement of compounds by cyclodextrin.

Chapter Seven

General Summary

7.1 General Summary

The topical delivery of drugs is presently receiving interest as an administration route for both locally and systemically active compounds. It has the potential advantages of avoiding first-pass intestinal and hepatic metabolism, reducing the side-effects of systemically administered compounds and providing a relatively easy method of administration termination. The use of transdermal drug delivery is limited for many compounds by the impervious nature of the stratum corneum. This is especially so for ionogenic compounds presented in their ionised form, because according to the pH-partition hypothesis it is only unionised compounds that pass through lipoidal membranes. The phospholipid bilayer composition of the stratum corneum cannot only pose a comprehensive physical obstruction but there is increasing evidence that enzymes within the skin can metabolise absorbed compounds. To enhance the often limited transdermal absorption of ionogenic compounds, a variety of processes can be used. These include the modification of vehicle parameters such as solubility or pH and the use of chemical enhancers that disrupt or modify the physical skin barrier. The active enzyme aspect of the stratum corneum barrier can be overcome by either protecting the permeating species from enzyme deactivation or utilising the enzyme's ability to activate prodrugs. With prodrugs more easily penetrating compounds are biotransformed within the skin to the pharmacologically active parent compound. To optimise the use of the topical delivery route, it is essential to understand the process of absorption and the mechanisms of enhancing this effect. This study has set out to investigate aspects of the transdermal absorption of ionogenic compounds and methods of enhancing this absorption.

The pH-partition hypothesis states that flux is proportional to the concentration of the unionised species. Therefore only unionised drug forms pass through lipoidal membranes and that these membranes are impervious to the ionised form. There is some evidence that ionised species can penetrate biological membranes *via* various shunt routes. Although, it is generally accepted that when a drug exists as both ionised and unionised forms, it is the unionised species that penetrates the skin most rapidly (Touitou and Donbrow, 1982; Swarbrick *et al.*, 1984). Loftsson (1985) provided an exception to this generalisation and showed that under certain conditions, increased ionisation can promote the topical delivery of salicylic acid. This was based upon the observation of increasing flux with higher donor pH through excised mouse skin. Experiments in Chapter 2 were performed using Franz-type *in vitro* penetration

cells to investigate the correlation between pH and salicylic acid flux across excised human skin and silastic rubber. The results contrast with those of Loftsson (1985) and show that the topical delivery of salicylic acid, the model ionogenic permeant, is essentially due to the unionised species. The flux of the ionised species is insignificant and under these conditions does not contribute to transdermal delivery.

Following optimisation of vehicle pH and solute concentration, the transdermal drug penetration still may not be sufficient to achieve appropriate therapeutic levels. One approach is to introduce chemicals that increase the driving force for drug diffusion or reduce the diffusional resistance of the skin. The precise mechanism of action of these chemicals or absorption enhancers is still under investigation. The work undertaken in Chapters 3 and 4 provided information about these mechanisms. Results in Chapter 3 showed that chemical enhancers can increase the permeation of salicylic acid across human skin, with LDA in IPM providing the greatest level of enhancement with flux ratios of 5.496 and 8.684 into the pH 7.22 and 3.40 receivers respectively. LDA, Azone and oleic acid in PG gave flux ratios of 3.529, 2.522 and 3.192 into the pH 7.22 receiver and 2.932, 1.653 and 3.037 into the pH 3.40 receiver respectively. Experiments with and without a trans-membrane pH-gradient provided data on the potential for compounds to demonstrate ion-pair facilitated transport. The rationale for these experiments being that a trans-membrane pH-gradient is required for ion-paired facilitated transport. Any enhancement without a pH-gradient was due to alternative mechanisms, such as partition effects. LDA, Azone and oleic acid in PG did not show a significant difference ($P = 0.357$, 0.091 and 0.668 respectively) in enhancing effect with and without a pH-gradient.

Ratios of salicylic acid extraction coefficients from aqueous buffers into IPM phases with and without Azone can be plotted against pH and shows a maximum of about pH 5.5. Hadgraft (1985) stated that this maximum represented an optimum pH for ion-pair formation between Azone and salicylic acid. The conclusion of this work was that Azone could be used to enhance the percutaneous absorption of anionic entities by a similar ion-pair facilitated transport mechanism. In Chapter 4, evidence is presented using ratios of extraction coefficients of salicylic acid into IPM phases. These IPM phases contain various putative enhancer compounds. The maximum in the extraction ratio against pH plot was, in certain circumstances explained without recourse to ion-pair facilitated transport.

Chemical modification of ionic molecules to neutral prodrug compounds with, for example esters, may provide another mechanism to transport ionogenic compounds across the stratum corneum. Phosphonoacetate, a model topical ionogenic compound is ionised at physiological pH and therefore does not easily cross the stratum corneum. Ester prodrugs of this compound were synthesised within the Pharmaceutical Sciences Institute at Aston University and assessed for their *in vitro* transdermal penetration. Transdermal absorption of the triester, dimethyl benzyloxycarbonylmethyl phosphonate was achieved and this could be further enhanced by absorption enhancers such as oleic acid and Azone.

The skin is an active biological barrier where exogenous and endogenous substances can be metabolised (Ando *et al.*, 1972; Rawlin *et al.*, 1980). It may be assumed that transdermal absorption of drugs can be reduced by this metabolism. Cyclodextrin inclusions have increased the stability of various compounds (Nash, 1994), including peptides, where a small but measurable protection was achieved against enzymic attack (Irwin, *et al.*, 1994). The work in Chapter 6 shows that using model ester compounds (alkyl parabens) with significant guest molecule to cyclodextrin affinity, a cyclodextrin ester ratio of greater than 200:1 was required before significant protection from enzymic attack can be achieved. It was concluded that this level of protection could not be expected to provide major defence of ester prodrugs from enzymic hydrolysis. Although it may be a mechanism that contributes, at least to some extent, to the overall transdermal absorption enhancement of compounds by cyclodextrin.

Due to the physical nature of ionisable compounds, the transdermal absorption of their ionised forms is likely to be limited. This work was undertaken to investigate four methods of enhancing this absorption, vehicle composition, chemical absorption enhancers, prodrug formation and protection from enzymic degradation. Using these techniques either individually or in combination it should be possible to achieve, with appropriate formulation, significant enhancement in transdermal penetration of ionisable compounds.

REFERENCES

ABPI, Data sheet compendium. Datapharm Publication Ltd (1996).

Ackerman, C. and Flynn, G.L., Ether-water partitioning and permeability through nude mouse skin *in vitro*. I. Urea, thiourea, glycerol and glucose. *Int. J. Pharm.*, 36 (1987) 61-66.

Ackerman, C., Flynn, G.L. and Van Wyk, C.J., Percutaneous absorption of urea. *Int. J. Cosmet. Sci.*, 7 (1985) 251-264.

Ackerman, C., Flynn, G.L. and Smith, W.M., Ether-water partitioning and permeability through nude mouse skin *in vitro*. II. Hydrocortisone-n-alkyl esters, alkanols and hydrophobic compounds. *Int. J. Pharm.*, 36 (1987) 67-71.

Adelman, R.L., Base Strengths of N,N-disubstituted amides. *J. Org. Chem.*, 29 (4) (1964) 1837-1844.

Aguiar, A.J. and Weiner, M.A., Percutaneous absorption studies of chloramphenicol solutions. *J. Pharm. Sci.*, 58 (1969) 210-215.

Akerman, B., Haegerstam, G., Pring, B.G. and Sandberg, R., Penetration enhancers and other factors governing percutaneous local anaesthesia with lidocaine. *Acta. Pharmacol. Toxicol.*, 45 (1979) 58-65.

Akhter, S.A. and Barry, B.W., Absorption through human skin of ibuprofen and flurbiprofen; effect of dose variation, deposited drug films, occlusion and the penetration enhancer N-methyl-2-pyrrolidone. *J. Pharm. Pharmacol.*, 37 (1985) 27-37.

Albery, W.J., Burke, J.F., Leffler, E.B., and Hadgraft, J., Interfacial transfer studied with a rotating diffusion cell. *J. Chem. Soc., Faraday Trans.* 1, 72 (7) (1976) 1618-1626.

Albery, W.J. and Hadgraft, J., Percutaneous absorption: *in vivo* experiments. *J. Pharm. Pharmacol.*, 31 (1979) 140-147)

Amey, R.L. and Chapman, D., Infrared spectroscopic studies of model and natural membranes. In *Biomembrane Structure and Function.* Edited by Chapman, D. Verlag Chemie, Weinheim, (1984), 199-256.

Albert, A. and Serjeant, E., The Determination of Ionisation Constants. *A Laboratory Manual, Chapman and Hall,* London, 3rd Edn, (1984).

Albert, A., "Selective Toxicity" Chapman & Hall London (1951).

Albert, A., Chemical aspects of selective toxicity. *Nature* (London) 182 (1958) 421-423.

Allenby, A.H., Creasey, N.H., Edginton, J.A.G., Fletcher, J.A. and Schock, C., Mechanism of action of accelerants on skin penetration., *Br. J. Dermatol.*, 81 (suppl 4) (1969) 47-55.

Al-Saidan, S.M.H., Selkirk, A.B. and Winfield, A.J., Effect of dimethylsulphoxide concentration on the permeability of neonatal rat stratum corneum to alkanols., *J. Invest. Dermatol.*, 89 (1987) 426-429.

Amann, M. and Dressnaudt, G., Solving problems with cyclodextrins in cosmetics. *Cosmet. Toilet.*, 108 (11): 90, (1993) 92-95.

Ando, H.Y., Ho, N.F.H. and Higuchi, W. I., Skin as an active metabolising barrier 1: Theoretical analysis of topical bioavailability. *J. Pharm. Sci.*, 66 (1977) 1525-1528.

Anon, FDC Reports: Astra EMLA cream launch to follow completion of 8000-patient study. *Prescription and OTC pharmaceuticals - The Pink Sheet.* (1993) ,55 : T&G-1.

Arita, T., Hori, R., Anmo, T., Washitake, M. Akatsu, M. and Yajima, T., Studies on percutaneous absorption of drugs. I. *Chem. Pharm. Bull.*, 18 (1970) 1045-1049.

Ashton, P., Hadgraft, J. and Walters, K.A., Effects of surfactants in percutaneous absorption *Pharm. Acta. Helv.*, 61 (8) (1986) 228-235.

Aungst, B.J., Rogers, N.J. and Shefter, E., Enhancement of naloxone penetration through human skin *in vitro* using fatty acids, fatty alcohols, surfactants, sulphoxides and amides. *Int. J. Pharm.*, 33 (1986) 225-234.

Bach, D., Calorimetric studies of model and natural membranes. In *Biomembrane Structure and Function.* Edited by Chapman D . Verlag Chemie, Weinheim, (1984), 1-41.

Backensfeld, T., Müller, B.W., Wiese, M. and Seydel, J.K., Effect of cyclodextrin derivatives on indomethacin stability in aqueous solution. *Pharm. Res.*, 7 (1990) 484-490.

Baker, N.D., Griffin, R.J. and Irwin, W.J., The percutaneous absorption of m-azido-pyrimethamine: a soft antifolate for topical use. *Int. J. Phar.*, 64 (1990) 115-125.

Barditch-Crovo, P., Petty, B.J., Gambertoglio, J., *et al.*, The effect of increasing gastric pH upon the bioavailibility of orally administered phosphonoformic acid (Foscarnet) (abstr W.B. 2115), In *Proceedings of the VII International Conference on AIDS.*, (1991) Florence, Italy :210

Barker, N., Hadgraft, J. and Wotton, P.K., Facilitated transport across liquid-liquid interfaces and its relevance to drug diffusion across biological membranes. *J. Chem. Soc., Faraday Disc.*, 77 (1984) 97-104.

Barker, N. and Hadgraft, J., Facilitated percutaneous absorption : A model system. *Int. J. Pharm.*, 8 (1981) 193-202.

Barry, B.W., Dermatological Formulations: Percutaneous Absorption, Marcel Dekker Inc., New York (1983).

Barry, B.W., Optimizing percutaneous absorption. In *Percutaneous Absorption: Mechanisms, Methodology, Drug Delivery.* Edited by Bronaugh. R.L., Maibach, H.I. Marcel Dekker New York (1985) 489-511.

Barry, B.W., The transdermal route for the delivery of peptides and proteins. NATO ASI Ser., Ser. A, 125 (1986) 265-275.

Barry, B.W., Mode of action of penetration enhancers in human skin. *J.Controlled Release,* 6 (1987a) 85-97.

Barry, B.W., Penetration enhancers; mode of action in human skin, *Pharmacol. Skin,* 1 (1987b) 121-137.

Barry, B.W., Topical Preparations, In *Pharmaceutics; the science of dosage form design.* Edited by Sutton, M.E., Churchill Livingston (1988a) 381-411.

Barry, B.W., Action of skin penetration enhancers - the lipid-protein-partitioning theory. *Int.J.Cosmet. Sci.*, 10 (1988a) 281-293.

Barry, B.W., Lipid-Protein-Partitioning theory of skin penetration enhancement. *J. Controlled Release,* 15 (1991a) 237-248.

Barry, B.W., The LLP theory of skin penetration. In *in vitro Percutaneous Absorption: Principles, Fundamentals and Applications.* Edited by Bronaugh, R.L. and Maibach, H.I. CRC Press, Boca Raton, (1991b) p165.

Barry, B.W. and Bennett, S.L., Effect of penetration enhancers on the permeation of mannitol, hydrocortisone and progesterone through human skin. *J. Pharm. Pharmacol.*, 39 (1987) 535-546.

Barry, B.W.and Brace,A.R., Permeation of oestrone,oestradiol,esteriol and dexamethasone across cellulose acetate membrane. *J.Pharm. Pharmacol.*, 29 (1977) 397-400.

Barry, B.W. and Eleini, D.I.D., Influence of non-ionic surfactants on permeation of hydrocortisone, dexamethasone, testosterone and progesterone, across cellulose acetate membrane. *J. Pharm. Pharmacol.*, 28 (1976) 219-227.

Baumberger, J.P., Suntzeff, V. and Cowdry, E.V., Methods for the separation of epidermis and some physiological and chemical properties of the isolated epidermis., *J. Nat. Cancer. Ind.* 2 (1942) 413-423.

Beastall, J.C., Hadgraft, J. and Washington, C., Mechanism of action of Azone as a percutaneous penetration enhancer : lipid bilayer fluidity and transition temperature effects. *Int. J. Pharm.*, 43 (1988) 207-213.

Beastall, J.C., Hadgraft, J., Palin, K.J. and Washinton, C., Interaction of Azone with lipid bilayers and its significance in percutaneous absorption. *J. Pharm. Pharmacol.*, 39 (1987) 23p.

Behl, C.R., Kreuter, J., Flynn, G.L., Walters, K.A. and Higuchi, W.I., Mechanisms of surfactant effects on percutaneous absorption. I: Effects of polysorbate 80 on permeation of methanol and n-octanol through hairless mouse skin. *A. Ph. A. Abst.*, 10 (1): (1980) 98.

Bel'skii, V., Kinetics of the hydrolysis of phosphoric acid esters. *Russ. Chem. Rev.*, 46 (9) (1977) 1578-1603.

Benet, L.Z., Kroetz, D.L. and Sheiner, L.B., Pharmacokinetics : The dynamics of drug absorption, distribution, and elimination. In *The pharmacological basis of theraputics*, Ninth edition. Consultant Editor Goodman Gilman, A.,. McGraw-Hill. (1995) 3-32.

Benezra, C., Structure activity relationships of skin haptens with a closer look at the compounds used in transdermal devices. *J. Controlled Release*, 15 (1991) 267-270.

Bennett, S.L. and Barry, B.W., Effectiveness of skin penetration enhancers propylene glycol, Azone, Decylmethylsulphoxide and oleic acid with model polar (mannital) and non-polar (hydrocortisone) penetrants. *J. Pharm. Pharmacol.*, 37 (1985) 84P.

Bennett, S.L., Barry, B.W. and Woodford, R., Optimisation of bioavailability of topical steriods: non-occluded penetration enhancers under thermodynamic control. *J.Pharm. Pharmacol.*, 37 (1985) 298-304.

Berner, B., Mazzenga, G.C., Otte, J.H., Steffens, R.J., Juang, H. and Ebert, C.D., Ethanol: water mutually enhanced transdermal therapeutic system II: skin permeation of ethanol and nitroglycerin. *J.Pharm. Sci.*, 78 (1989) 402-407.

Bettly, F.R., The influence of detergents and surfactants on epidermal permeability., *Br. J. Dermatol.*, 77 (1965) 98-100.

Blake-Haskins, J.C., Scala, D., Rhein, L.D. and Robbins, C.R., Predicting surfactant irritation from the swelling response of a collagen film. *J. Soc. Cosmet. Chem.*, 37 (1986) 199-210.

Blank, I.H., Penetration of low-molecular weight alcohols into the skin. I. The effect of concentration of alcohol and type of vehicle. *J. Invest. Dermatol.*, 43 (1964) 415-420.

Blank, I.H. and Miller, O.G., A method for the separation of the epidermis from the dermis. *J. Invest. Dermatol.* 15 (1950) 9-10.

Bodor, N., Physiological means of enhancing transdermal delivery of drugs. *International Patent* PCT/US85/01951, (1986).

Boehulein, J., Saler, Adel, Lichtin, J.L. and Bronaugh R.L. Characterization of esterase and alcohol dehydrogenase activity in skin. Metabolism of retinyl palmitate to retinol (Vitamin A) during percutaneous absorption. *Pharm. Res.* 11(8) (1994) 1155-1159.

Boezi, J.A., The antiherpes virus action of phosphonoacetate. *Pharmac. Ther.*, 4 (1979) 231-243.

Brain, K.R. and Walters, K.A. Molecular modeling of skin permeation enhancement by chemical agents. In *Pharmaceutical Skin Penetration Enhancement*. Edited by Walters, K.A. and Hadgraft, J. Marcel Dekker Inc. New York. (1993) 389-416.

Bonina, F.P. and Montenegro, L., Penetration enhancer effects on *in vitro* percutaneous absorption of heparin sodium salt. *Int. J. Pharm.*, 82 (1992) 171-177.

Bopp, B.A., Estep, C.B. and Andersson, D.J., Deposition of disodium phosphonoacetate in rat, rabbit, dog and monkey. *Fedn. Proc.*, 36 (1977) 939.

Borodkin, S. and Tucker, F.E. Drug release from hydroxypropyl-cellulose-polyvinyl acetate films. *J. Pharm. Sci.*, 63 (1974) 1359-1364.

Borsadia, S., Ghanem, A.H., Seta, Y., Higuchi, W.I., Flynn, C.L., Behl, C.R. and Shah, V.P., Factors to be considered in the evaluation of bioavailability and bioequivalence of topical formulations. *Skin Pharmacol S.* (1992) 129-145.

Bottari, F., Dicolo, G., Nannipieri, E., Saettone, M.F. and Serafini, M.F. Influence of drug concentration on *in vitro* release of salicylic acid from ointment bases. *J.Pharm. Sci.*, 63 (1974) 1779-1783.

Bouwstra, J.A, de Vries, M.A., Gooris, G.S., Bras, W., Brussee, J. and Ponec, M., Thermodymamic and structural aspects of the skin barrier. *J. Controlled Release*, 15 (1991) 209-220.

Bristow, P.A., Liquid chromatography in practice, Handforth, Hetp (1976) 181-185.

Broberg, F., Brodin. A., Aakerman, B. and Frank, S.G., *In vitro* and *in vivo* studies of lidocaine formulated in an o/w cream and in a polyethylene glycol ointment. *Acta. Pharm.Suec.*, 19 (1982) 229-240.

Bronaugh, R.L., Congdon, E.R. and Scheuplein, R.J., The effect of cosmetic vehicles on the penetration of N-nitrosodiethanolamine through excised human skin. *J. Invest. Dermatol.*, 76 (1981) 94-96.

Bronaugh, R.L. and Maibach, H.I., *In vitro* models for percutaneous absorption, In *Models in Dermatology.* Edited by Maibach, H.I. and Lowe, N.J. Karger. Volume 2 (1985) 178-188.

Bronaugh, R.L. and Maibach, H.I., Percutaneous Absorption. *Methods-Mechanisms-Drug Delivery,* 2nd Edition, Marcel Dekker, New York, (1989).

Bronaugh, R.L. and Stewart, R.F. and Congdon, E.R., Methods for *in vitro* percutaneous absorption studies. II. Animal models for human skin, *Toxicol. Appl. Pharmacol.*, 62 (1982) 481-488.

Bronaugh, R.L. and Stewart, R.F., Methods for *in vitro* percutaneous absorption studies. III. Hydrophobic compounds. *J.Pharm. Sci.*, 73 (1984) 1255-1258.

Bronaugh, R.L. and Stewart, R.F., Methods for *in vitro* percutaneous absorption studies. IV. The flow though diffusion cell. *J. Pharm. Sci.*, 74 (1985a) 64-67.

Bronaugh, R.L. and Stewart, R.F., Methods for *in vitro* percutaneous absorption studies. V. Permeation through damaged skin. *J. Pharm. Sci.*, 74 (1985b) 1062-1066.

Bronaugh, R.L. and Stewart, R.F., Methods for *in vitro* percutaneous absorption studies. VI. Preparation of the barrier layer. *J. Pharm. Sci.*, 75 (1986) 487-491.

Bronaugh, R.L., Stewart, R.F. and Simon, M., Methods for *in vitro* percutaneous absorption studies. VII. Use of excised human skin. *J. Pharm. Sci.*, 75 (1986) 1094-1097.

Budavari, S. (editor) The Merck Index. 12th Edition (1996).

Bundgaard, H., Design of prodrugs: Bioreversible derivatives for various functional groups and chemical entities. In *Design of Prodrugs.* Edited by Bundgaard, H., Elsever, Amsterdam (1985) 70-74.

Burnette, R.R., Iontophoresis In *Transdermal Drug Delivery.* Edited by Hadgraft, J. and Guy, R.H. Marcel Dekker, New York (1989) p247-292.

Carpenter, T.O., Gerloczy, A. and Pitha, J., Safety of parenteral hydroxypropyl β-cyclodextrin. *J. Pharm. Sci.*, 84 (2) (1995) 222-225.

Chanderasekaran, S.K. and Shaw, J.E., Factors influencing the percutaneous absorption of drugs. *Curr. Probl. Dermatol.*, 7 (1978) 142-155.

Chandler, S.G., Illum, L. and Thomas, N.W., Nasal absorption in rats. II. Effects of enhancers on insulin absorption and nasal histology. *Int. J. Pharm.*, 76 (1991) 61-70.

Chiang, C.M., Flynn, G.L., Weiner, N.D. and Szunar, G. J. Bioavailability assessment of topical delivery systems: Effect of vehicle evaporation upon *in vitro* delivery of minoxidil from solution formulation. *Int. J. Pharm.*, 55 (1989) 229-236.

Chien, Y.W., Keshary, P.R., Huang, Y.C. and Sarpotdar, P.P., Comparative controlled skin permeation of nitroglycerin from marketed transdermal delivery systems. *J. Pharm. Sci.*, 72 (1983) 968-970.

Chien, Y.W. and Valia, K.H., Development of a dynamic skin permeation system for long term permeation studies. *Drug. Dev. Ind. Pharm.*, 10 (1984) 575-599.

Choman, B.R., Detemination of the response of skin to chemical agents by an *in vitro* procedure, II. Effects of aqueous anionic, cationic, and non-ionic surfactant solutions., *J. Invest. Dermatol.*, 40 (1963) 177-182.

Chowhan, Z.T. and Pritchard, R., Effect of surfactants on percutaneous absorption of naproxen I: Comparisons of rabbit, rat and human excised skin. *J. Pharm. Sci.*, 67 (1978) 1272-1274.

Chrisp. P. and Clissold, S.P., Foscarnet : A review of its antiviral activity, pharmacokinetic properties and theraputic use in immunocompromised patients with cytomegalovirus retinitis. *Drugs*, 41 (1991) 104-129.

Cohen, S.S., A strategy for the chemotherapy of infectious diseases. *Science*, 197 (1977) 431-432.

Coldman, M.F., Poulsen, B.J., and Higuchi, T., Enhancement of percutaneous absorption by use of volatile :non-volatile systems as vehicles. *J. Pharm. Sci.*, 58 (1969) 1098-1102.

Collier, S.W. and Bronaugh, R.L., Cutaneous metabolism during percutaneous absorption. In *Pharmacology of the skin.* Edited by Mukhtar, H., CRC Press Boca Raton FL. (1992) 111-129.

Cooper, E.R., Effect of decylmethyl sulphoxide on skin penetration. In *Solution Behaviour of Surfactants.* Vol 2. Edited by Mittal, K.L. and Fendler E.J. Plenum Press. New York (1982) 1505-1516.

Cooper, E.R., Increased skin permeability for lipophilic molecules. *J.Pharm. Sci.*, 73 (1984a) 1153-1156.

Cooper, E.R., Effect of substituents on benzoic acid transport across human skin. *J.Controlled Release*, 1 (1984b) 153-156.

Cooper, E.R. and Berner, B., Skin Permeability, In *Methods in Skin Research.*, Edited by Skerrow, D. and Skerrow, C.J., John Wiley & Sons Ltd (1985).

Cooper, E.R., Merritt, E.W. and Smith, R.L., Effect of fatty acids and alcohols on the penetration of acyclovir across human skin *in vitro*. *J. Pharm. Sci.*, 74 (1985) 688-689.

Corbo, D.C., Liu, J.C., Chien, Y.W.,Characterization of the barrier properties of mucosal membranes. *J. Pharm. Sci.*, 79 (1990) 202-206.

Cornaz, A.L. and Buri, P., Nasal mucosa as an absorption barrier. *Eur. J. Pharm. Biopharm.*, 40(5) (1994) 261-270.

Cornwell, P.A., Barry, B.W., Bouwstra, J.A. and Gooris, G.S., Modes of action of terpene penetration enhancers in human skin; differential scanning calorimetry, small-angle X-ray diffraction and enhancer uptake studies. *Int. J. Pharm.*, 127 (1996) 9-26.

Cramer, M.B. and Cates, L.A., Effect of dimethyl sulphoxide and trimethylphosphine cortco-steroids in the rat. *J. Pharm. Sci.*, 63 (1974) 793-794.

Croda Chemicals Ltd, Healthcare product guide. (1995).

Croda Chemicals Ltd, Crodamol emollient esters. (1996).

Crumpacker. C.S., Mechanism of action of Foscarnet against viral polymerase. *Am. J. Med.*, 92 (Suppl 2A) (1992) 3S-7S.

Curatolo, W., The lipoidal permeability barriers of the skin and alimentary tract. *Pharm. Res.*, 4 (1987) 271-277.

Dallas, P., Sideman, M.B., Polak, J. and Plakogiannis, F.M., Medicament release from ointment bases : IV: Piroxicam: *in vitro* release and *in vivo* absorption in rabbits. *Drug Dev. Indus. Pharm.*, 13 (1987) 1371-1369.

Datta, A.K. and Hood, R.E., Mechanism of inhibition of Epstein-Barr virus replication by phosphonoformic acid. *Virology*. 114 (1981) 52-59.

Davidson, G.W.R., Yu, D., Sanders, L.M. and Ling, T., Effect of vehicle composition on percutaneous absorption of nicardipine and ketorolac in rhesus monkeys. *Proc. 13th Int. Symp. on Contr. Release of Bioactive Materials*, (1986) 113-114.

Davidson, V. L. and Sittman, D. B., Enzymes. In *Biochemistry*. Third Edition, Edited by Davidson, V.L. and Sittman, D.B. Harwel Publishing (1994) 85-104.

Davis, A.F., United States Patent, 4, 940,701, 1990.

Davis, A.F. and Hadgraft, J., Effect of supersaturation on membrane transport: I Hydrocortisone acetate. *Int. J. Pharm.*, 76 (1991) 1-8.

De Clercq, E., Chemotheraputic approaches to the treatment of the aquired immune deficiency syndrome (AIDS). *J. Med. Chem,*. 29 (1986) 1561-1569

DeNoble, L.J., Knutson, K., and Kurihara-Bergstrom, T., Enhanced skin permeation by ethanol: Mechanistic studies of human stratum corneum measured by DSC and FTIR. *Pharm. Res.*, 4 (1987) 59s.

Derse, D., Bastow, K.F., Cheng, Y-C., Characterisation of the DNA polymerase included by a group of herpes simplex virus type 1 variants selected for growth in the presence of phosphonoformic acid, *J. Biol. Chem.*, 257 (1982) 10251-10260.

Deurloo, M.J.M., Hermens, W.A.J.J., Romeyn, S.G., Verhoef, J. and Merkus, F.W.H.M., Absorption enhancement of intranasally administered insulin by sodium taurodihydrofusidate (STDHF) in rabbits and rats. *Pharm. Res.* 6 (1989) 853-856.

Diez-Sales, O., Pérez-Sayas, A., Martín-Villodre and Herráez-Domínguez, M., The prediction of percutaneous absorption: I. Influence of the dermis on *in vitro* permeation models., *Int. J. Pharm.*, 100 (1993) 1-7.

Diez-Sales, O., Watkinson, A.C., Herràez-Dominguez, C., Javaloyes, C. and Hadgraft, J. A., mechanistic investigation of the *in vitro* human skin permeation enhancing effect of Azone®. *Int. J. Pharm.*, 129 (1996) 33-40.

Dodda Kashi, S. and Lee, V.H.L., Enkephalin hydrolysis in homogenates of various absorptive mucosae of the albino rabbit: similarities in rates and involvement of aminopeptidases. *Life Sci.* 38 (1986) 2019-2028

Donbrow, M. and Samuelov, Y., Zero-order drug delivery from double layered porous films: Release rate profiles from ethyl cellulose, hydroxypropyl cellulose and polyethylene glycol mixtures. *J. Pharm. Pharmacol.*, 32 (1980) 463-467.

Duchêne, I.D., and Wouessidjewe, D., The current state of ß-cyclodextrin in pharmaceutics. *Acta. Pharm. Technol.*, 36 (1) (1990a) 1-6.

Duchêne, I. D. and Wouessidjewe, D., Physicochemical characteristics and pharmaceutical uses of cyclodextrin derivatives. Part 1. *Pharmaceuti. Technol.*, 14 (6) (1990b) 26-34.

Duchêne, D., Wouessidjewe, D., and Poelman, M.-C., Dermal uses of cyclodextrins and derivatives. In *New trends in cyclodextrins and derivatives*. Edited by Duchêne, D. Copédith (1991) Chapter 13.

Duchêne, D. Vaution, C., Glonedt, F., Cyclodextrins, their value in pharmaceutical technology. *Drug Devel. Ind. Pharm.*, 12 (1986) 2193-2215.

Dudek, G.O. and Westheimer, F.H., Solvolysis of tetrabenzyl pyrophosphate. *J. Am. Chem. Soc.*, 81 (1959) 2641-2946.

Durrheim, H., Flynn, G.L., Higuchi, W.I. and Behl, C.R., Permeation of hairless mouse skin. I. Experimental methods and comparison with human epidermal permeation by alkanols. *J. Pharm. Sci.*, 69 (1980) 781-786.

Edwards, D.A. and Langer, R. A., linear theory of transdermal transport phenomena. *J. Pharm. Sci.*, 83 (1994) 1315-1334.

Elder, G.A., and Sever, J.L., Neurologic disorders associated with aids retroviral infection. *Rev. Inf. Diseases*, 10(2) (1988) 286-302.

Elfbaum, S.G. and Laden, K., The effect of dimethylsulphoxide on percutaneous absorption: a mechanistic study, Part III. *J. Soc. Cosmet. Chem.*, 19 (1968) 841-847.

Elias, P.M., Epidermal lipids, membranes and keratinization. *Int. J. Dermatol.*, 20 (1981) 1-19.

Elias, P.M., Epidermal lipids, barrier function, and desquamation. *J. Invest. Dermatol.*, 80 (1983) 44S-49S.

Elias, P.M., Goerke,J. and Friend, D.S., Mammalian epidermal barrier layer lipids: composition and influence on structure. *J. Invest. Dermatol.*, 69 (1977b) 535-546.

Elias, P.M., Mittermayer, H., Fritsch, P., Tappeiner, G. and Wolff, K., Experimental staphylococcal toxic epidermal necrolysis in adult humans and mice. *J. Lab. Clin. Med.*, 84 (1974) 414-424.

Elias, P.M., McNutt, N. S. and Friend, D. S., Membrane alterations during cornification of mammalian squamous epithelia: A freeze-fracture, tracer and thin-section study. *Anat. Rec.*, 189 (1977a) 577-594.

Embery, G. and Dugard, P.H., The isolation of dimethyl sulphoxide soluble components from human epidermal preparations: A possible mechanism of action of dimethyl sulphoxide in effecting percutaneous migration phenomena., *J. Invest. Dermatol.*, 57 (1971) 308-311.

Engelhardt, H., High performance liquid chromatography: chemical laboratory practice. *Springer-Verlag* (1979) 183-187.

Ennis, R.D., Bordeu, L. and Lee, W.A., The effects of permeation enhancers on the surface morphology of the rat nasal mucosa: a scanning electron microscopy study. *Pharm. Res.*, 7 (1990) 468-475.

Eriksson, B.F.H., Larsson, A., Helgstrand, E., Johansson, N-G., Öberg, B., Pyrophosphate analogues as inhibitors of herpes simplex virus type 1, DNA Polymerase, *Biochem. Biophys. Acta.*, 607 (1980) 53-64.

Eriksson, B.F.H., Öberg, B., Wahren, B., Pyrophosphate analogues as inhibitors of DNA polymerases of cytomegalovirus, herpes simplex virus and cellular origin, *Biochem. Biophys. Acta.*, 696 (1982) 115-123.

Eriksson, B.F.H., Öberg, B., Characteristics of herpes virus mutants resistant to phosphonoformate and phosphonoacetate, *Antimicrob. Agents Chemother.*, 15 (1979) 758-762

Evers, H., Von Dardel, O., Juhlin, L., Ohlsen, L. and Vinnars. E., Dermal effects of compositions based on the eutectic mixture of lignocaine and prilocaine (EMLA). *Br. J. Anaesth.*, 57 (10) (1985) 997-1005.

Fan, J., Epidermal separation with purified trypsin. *J. Invest. Dermatol.* 30 (1958) 271-276.

Farbman, A I., Plasma membrane changes during keratinization. *Anat. Rec.*, 156 (1966) 269-282.

Feldman, R.J. and Maibach, H.I., Regional variation in percutaneous penetration of [^{14}C] cortisol in man., *J. Invest. Dermatol.*, 60 (1973) 262-269.

Feldman, R.J. and Maibach, H.I., Percutaneous absorption of hydrocortisone with urea. *Arch. Dermatol.*, 109 (1974) 58-59.

Felsher, Z., Studies on the adherence of the epidermis to the corium., *J. Invest. Dermatol.*, 8 (1947) 35-37.

Ferguson, J.A., A method to facilitate the isolation and handling of stratum corneum. *B.J. Dermatol.*, 96 (1977) 21-23.

Finkel, M.J.,Dimethyl sulphoxide. In *Questions and Answers, J. Am. Med. Ass.*, 244 (24) (1980) 2767-2768.

Fisher, A.A., Dermatitis due to transdermal theraputic systems. *Cutis.*, 34 (1984) 526-532.

Fisher, L.B. *In vitro* studies on the permeability of infant skin. In *Percutaneous Absorption. Mechanisms-methods-Drug Delivery.* Edited by Bronaugh, R.L. and Maibach, H.I. Mercel Dekker, New York (1985) 213-222.

Florence, A.T. and Gillan, J.M.N., Biological implications of the use of surfactants in medicines: and the biphasic effects of surfactants in biological systems. *Pestic. Sci.*, 6 (1975) 429-439.

Flynn, G.L., Mechanism of percutaneous absorption from physicochemical evidence. In *Percutaneous Absorption. Mechanisms-methods-Drug Delivery.* Edited by Bronaugh, R.L. and Maibach, H.I. Mercel Dekker, New York (1985) 17.

Flynn, G.L. and Smith, E.W., Membrane diffusion. I. Design and testing of a new multi-featured diffusion cell. *J. Pharm. Sci.*, 60 (1971) 1713-1717.

Flynn, G.L., Yalkowsky, S.H. and Roseman, T.J., Mass transport phenomena and models: theoretical concepts. *J. Pharm. Sci.*, 63 (1974) 479-510.

Foreman, M.I., Kelly, I. and Lukowiecki., A method for the measurement of diffusion constants suitable for studies of non-occluded skin. *J. Pharm. Pharmacol.*, 29 (1977) 108-109.

Foreman, M.I., Clanachan, I. and Kelly, I.P., The diffusion of nandrolone through occluded and non-occluded human skin. *J. Pharm. Pharmacol.*, 30 (1978) 152-157.

Frank, D.W., Gray, J.E., and Weaver, R.N., Cyclodextrin nephrosis in the rat. *Am. J. Pathol.*, 83 (1976) 367-382.

Franz, T.J., Percutaneous Absorption, On the relevance of *in vitro* data., *J. Invest. Dermatol.*, 64 (1975) 190-195.

Franz, T.J., The finite dose technique as a valid *in vitro* model for the study of percutaneous absorption. *Curr. Probl. Dermatol.*, 7 (1978) 58-68.

Frei, J. V. and Sheldon H., A small granular component of the cytoplasm of keratinizing epithelia. *J. Biophys. Biochem. Cytol.*, 11 (1961) 719-724.

French, D., The Schardinger dextrins. *Adv. Carbohydrate Chem.*, 12 (1957) 189-260.

Friend, D.R., Catz, P. and Heller, J., Transdermal permeation enhancers for drugs. *Proc. Int. Symp. Controlled Release Bioactive Mater.*, 15 (1988a) 152.

Friend, D.R., Catz, P. Heller, J., Reid, J. and Baker, R.D., Transdermal delivery of levonorgestrel. II: Effect of prodrug structure on skin permeability *in vitro*. *J. Control. Rel.*, 7 (3) (1988b) 251-261.

Frömming, K-H., Geider, T. and Mehnert, W., Inclusion compound of cyclodextrin and vitamin A acetate. *Acta Pharm. Technol.*, 34 (1988) 152-155.

Galey, W.R., Lonsdale, H.K. and Nacht, S. The *in vitro* permeability of skin and buccal mucosa to selected drugs and tritiated water. *J. Invest. Dermatol.*, 67 (1976) 713-717.

Gergely, V., Sebestyén, G., Virag, S. *Proc. 1st Int. Symp. Cyclodextrins* edited by Szejtli Reidel, Dordrecht (1982) p109.

Gerstein, D.D., Dawson, C.R. and Oh, J.O., Phosphonoacetic acid in the treatment of experimental herpes simplex keratitis. *Antimicrob. Agents Chemother.*, 7 (1975) 285-288.

Ghanem, A.H., Mahmoud, H., Higuchi, W.I., Rohr, U.D., Borsadia, S., Liu, P., Fox, J.L. and Good, W.R., The effects of ethanol on the transport of β-estradiol and other permeants in hairless mouse skin. II. A new quantitative approach. *J. Controlled Release,* 6 (1987a) 75-83.

Ghanem, A., Mahmoud, H., Rohr, U.D., Higuchi, W.I., Liu, P., Bursadia, S. and Fox, J.L., Quantification of lipid pathway and pore transport enhancing effects of ethanol in hairless mouse stratum corneum. *Pharm. Res.*, 4 (suppl.) (1987b) S70.

Gibson, W.T. and Teall, M.R., Interactions of C12 surfactants with the skin: Studies on enzyme release and percutaneous absorption *in vitro*. *Food Chem. Toxicol.*, 21 (1983) 581-586.

Glomot, F., Benkerrour, L., Duchêne, D., and Poelman, M.-C., Improvement in availability and stability of a dermacorticoid by inclusion in ß-cyclodextrin. *Int. J. Pharm.*, 46 (1988) 49-55.

Golden, G.M., Guzek, D.B., Harris, R.R, McKie, J.E. and Potts R.O., Lipid thermotropic transitions in human stratum corneum. *J. Invest. Dermatol.*, 86 (1986) 255-259.

Golden, G.M., McKie, J.E. and Potts, R.O., The role of stratum corneum lipid fluidity in transdermal flux. *J.Pharm. Sci.*, 76 (1987) 25-28.

Good, W.R., Powers, M.S., Campbell, P. and Schenkel, L., A new transdermal delivery system for estradiol. *J. Controlled Release,* 2 (1985) 89-87.

Goodman, M. and Barry, B.M., Differential scanning calorimetry of human stratum corneum: Effect of azone. *J. Pharm. Pharmacol.*, 37 (suppl.) (1985) 80P.

Goodman, M. and Barry, B.M., Action of skin permeation enhancers azone, oleic acid and decylmethyl sulphoxide : permeation and DSC studies. *J.Pharm. Pharmacol.*, 38 (suppl.) (1986) 71P.

Goodman, M. and Barry, B.M., Action of penetration enhancers on human stratum corneum as assessed by differential scanning calorimetry. In *Percutaneous Absorption Mechanisms - Methodology, Drug Delivery,* 2nd Edition. Edited by Bronaugh, R.L.and Maibach, H.I. Marcel Dekker Inc. New York (1989a) 567-593.

Goodman, M. and Barry, B.W., Lipid-protein-partitioning (LLP) theory of skin enhancer activity: finite dose technique. *Int.J. Pharm.*, 57 (1989b) 29-40.

Gordon, G.S., Moses, A.C., Silver, R.D., Flier, J.S., and Carey, M.C. Nasal absorption of insulin: enhancement of hydrophobic bile salts. *Proc. Natt. Acad. Sci.* USA. 82 (1985) 7419-7423.

Green, P.G., Flanagen, M., Short, B. and Guy, R.H., Iontophoretic drug delivery. In *Pharmaceutical skin penetration enhancement.* Edited by Walters K.A. and Hadgraft, J. Marcel Dekker (1993) 311-333.

Green, P.G., Guy, R.H. and Hadgraft, J., *In vitro* and *in vivo* enhancement of skin permeation with oleic acid and lauric acids. *Int. J. Pharm.*, 48 (1988) 103-111.

Green, P.G. and Hadgraft, J., Facilitated transfer of cationic drugs across a lipoidal membrane by oleic acid and lauric acid. *Int. J. Pharm.*, 37 (1987) 251-255.

Griesmer, R.D. and Gould, E., A method for the study of the intermediary carbohydrate metabolism of epidermis: Oxidation of acids of citric acid cycle. *J. Invest. Dermatol.*, 22 (1954) 299-315.

Griffin, R.J., Evers, E., Davison, R., Gibson, E., Layton, D. and Irwin, W.J., The 4-azido-benzyloxycarbonyl function: application as a novel protecting group and potential prodrug modification for amines, *J. Chem. Soc., Perkin Trans. 1,* (1996) 1205-1211

Gummer, C.L., The *in vitro* evaluation of transdermal delivery. In *Transdermal Drug Delivery: Developmental Issues and Research.* Edited by Hadgraft, J. and Guy, R.H. Marcel Dekker. New York. (1989) 177-196.

Gummer, C.L., Hinz, R.S. and Maibach, H.I., The skin penetration cell: A design update. *Int. J. Pharm.*, 40 (1987) 101-104.

Guttman, A., Brunet, and Cooke, N., Capillary electophoresis separation of enantiomers using cyclodextrin array chiral analysis. *LC-GC Int.*, 9(2) (1996) 88-100.

Guy, R.H., Carlstrom, E.H., Bucks, D.A.W., Hinz, R.S. and Maibach, H.I., Percutaneous penetration of nicotinates: *In vivo* and *in vitro* measurements. *J. Pharm. Sci.*, 75 (1986) 968-972.

Guy, R.H. and Fleming, R., The estimation of diffusion coefficients using the rotating diffusion cell. *Int. J. Pharm.*, 3 (1979) 143-149.

Guy, R.H. and Hadgraft, J., Transdermal drug delivery: The ground rules are emerging. *Pharm.Int.*, 6 (1985) 112-116.

Guy, R.H. and Hadgraft, J., Physicochemical aspects of percutaneous penetration and its enhancement. *Pharm. Res.*, 5 (1988) 753-758.

Guy, R.H. and Hadgraft, J., Selection of drug candidates for transdermal drug delivery. In *Transdermal Drug Delivery.* Edited by Hadgraft,J. and Guy, H.R., Dekker (1989a) 59-81.

Guy, R.H. and Hadgraft, J., Mathematical models of percutaneous absorption. In *Percutaneous Absorption.* Edited by Bronaugh, R.L. and Maibach, H.I., Dekker (1989b) 13-27.

Guy, R.H. and Hadgraft, J., Structure activity correlations in percutaneous absorption. In *Percutaneous Absorption.* Edited by Bronaugh, R.L. and Maibach, H.I., Dekker (1989c) 95-109.

Guy, R.H. and Hadgraft, J., Percutaneous penetration enhancement: Physicochemical considerations and implications for prodrug design. In *Prodrugs: Topical and ocular drug delivery.* Edited by Sloan, K.B., Marcel Dekker Inc. New York (1992) 1-16.

Hadgraft, J., Calculations of drug release rates from controlled release devices. The slab. *Int. J. Pharm.*, 2 (1979) 117-114.

Hadgraft, J., Percutaneous absorption: possibilities and problems. *Int. J. Pharm.*, 16 (1983) 255-270.

Hadgraft, J., Penetration enhancers in percutaneous absorption. *Pharm. Int.*, 5 (1984) 252-254.

Hadgraft, J., Structure activity relationships and percutaneous absorption. *J. Controlled Release,* 15 (1991) 221-226.

Hadgraft, J., Green, P.G. and Wotton, P.K., Facilitated absorption of charged drugs. In *Percutaneous Absorption.* Edited by Bronaugh, R. and Maibach, H.I. Marcel Dekker Inc., New York Second Edition. (1989) 555-565.

Hadgraft, J. and Ridout, G., Development of model membranes for percutaneous absorption measurements. I. Isopropyl myristate. *Int. J. Pharm.*, 39 (1987) 149-156.

Hadgraft, J. and Ridout, G. Development of model membranes for percutaneous absorption measurements. II. Dipalmitoyl phosphatidycholine, linoleic acid and tetradecane. *Int. J. Pharm.*, 42 (1988) 97-104.

Hadgraft, J. and Guy, R.H., *Transdermal Drug Delivery. Developmental; Issues and Research Initiatives,* Dekker, New York (1989).

Hadgraft, J., Walters, K.A. and Wotton, P.K., Facilitated transport of sodium salicylate across an artificial lipid membrane by Azone. *J. Pharm. Pharmacol.*, 37 (1985) 725-727.

Hadgraft, J., Walters, K.A. and Wotton, P.K., Facilitated percutaneous absorption: A comparison and evaluation of two *in vitro* models. *Int.J. Pharm.*, 32 (1986) 257-263.

Hadgraft, J., Williams, D.G. and Allan, G., Azone : Mechanisms of action and clinical effect. In *Pharmaceutical Skin Penetration Enhancement.* Edited by Walters, K.A. and Hadgraft. J., Marcel Dekker Inc. New York. (1993) 175-197.

Hamada, Y., Namba, N., and Nagai, T., Interactions of α and β-cyclodextrin with several non-steroidal anti-inflammatory drugs in solution. *Chem. Pharm. Bull.*, 23 (1975) 1205-1211.

Harper Bellantone, N., Rim. S., Francoeur, M.L. and Rasadi, B. Enhanced percutaneous absorption via iontophoresis. I. Evaluation of an *in vitro* system and transport of model compounds. *Int. J. Pharm.*, 30 (1986) 63-72.

Harrison, J.E., Watkinson, A.C., Green, D.M., Hadgraft, J. and Brain, K. The relative effect of azone and transcutol on permeant diffusivity and solubility in human stratum corneum. *Pharm. Res.*, 13 (4) (1996) 542-546.

Harrison, S.M., Barry, B.W. and Dugard, P.H. Effects of freezing on human skin permeability. *J. Pharm. Pharmacol.*, 36 (1984) 261-262.

Hawkins, G.S. and Reifenrath, W.G., Influence of skin source, penetration cell fluid, and partition coefficient on *in vitro* skin penetration. *J. Pharm. Sci.*, 75 (1986) 378-381.

Hay, J., Brown, S.M., Jamieson, A.T., Rixon, F.J., Moss, H., Dargan, D.A. and Subak-Sharpe, J.H. The effect of phosphonoacetic acid on herpes virus. *J. Antimicrob. Chemother.* 3 (Suppl. A) (1977) 63-70.

Hayward, A. F., Membrane coating granules. *Int. Rev. Cytol.*, 59 (1979) 97-127.

Helgstrand, E., Eriksson, B., Johansson, N.G., Lannerö, B., Larson, A., Misiorny, A., Norén, J.O., Sjöberg, B., Stenberg, K., Stening,G., Stridh,S., Öberg, B., Alenius, S. and Phillipson, L., Trisodium phosphonoformate, a new antiviral compound. *Science*. 201 (1978) 819-821.

Hermens, W.A.J.J. and Merkus, F.W.M.H., The influence of drugs on nasal ciliary movement. *Pharm. Res.*, 4 (1987) 445-449.

Higuchi, T.,Physical chemical analysis of percutaneous absorption process for creams and ointments. *J. Soc. Cosmetic Chemists*, 11 (1960) 85-97.

Higuchi, T., Design of biopharmaceutical properties through prodrugs and analogues. Edited by Roche,E.D *Amer. Pharm. Association*, Washington (1977) p 409.

Higuchi, T., Design of chemical structure for optimal dermal delivery. *Curr. Probl. Dermatol.*, 7 (1978) 121-131.

Higuchi, T., Barnstein, C.H., Ghassemi, H. and Perez, W.E., Evaluation of amides and other very weak bases in acetic acid. *Anal. Chem.*, 34 (1962) 400-403.

Higuchi, W., Rohr, U.D., Burton, S.A., Liu, P., Fox, J.L., Ghanem, A.H., Mahmoud, H., Borsadia, S. and Good, W.R., Effect of ethanol on the transport of β-estradiol in hairless mouse skin. In *Controlled Release Technology: Pharmaceutical Applications*, Edited by Lee, P.I. and Good, W.R., ACS Symposium Series 248, American Chemical Society, Washington, D.C. (1987) Chapter 17.

Hirai, S., Yashiki, Matsuzawa, T. and Mima, H., Absorption of drugs from the nasal mucosa of the rat. *Int. J. Pharm.*, 7 (1981a) 317-325

Hirai, S., Yashiki, T. and Mima, H., Effects of surfactants on the absorption of insulin in rats. *Int. J. Pharm.*, 9 (1981b) 165-172.

Holdiness, M.R., A review of contact dematitis associated with transdermal theraputic systems. *Contact Dermatitis*, 20 (1989) 3-9.

Hopkins, C.S., Buckley. C.J. and Bush, G.H., Pain-free injection in infants. *Anaesthesia*, 43 (1988) 198-201.

Horsky, J. and Pitha, J., Hydroxypropyl cyclodextrins: potential synergism with carcinogens. *J. Pharm. Sci.*, 85(1) (1996) 96-100.

Hoshino, T., Ishida, K., Irie, T., Uekama, K. and Ono, T., An attempt to reduce the photo-sensitivity potential of chlorpromazine with the simultaneous use of ß- and dimethyl ß-cyclo-dextrins in the guinea-pig. *Arch. Dermatol. Res.*, 281 (1989) 60-65.

Houk, J. and Guy, R.H., Membrane models for skin penetration studies. *Chem. Rev.*, 88 (1988) 455-57.

Hsieh, D.S., Understanding permeation enhancement technologies. In *Drug permeation enhancement : Theory and applications.* Edited by Hsieh, D.S. Marcel Dekker (1994).

Hsu, L.R., Tsai, Y.H. and Huang, U.B., The effect of pretreatment by penetration enhancers on the *in vivo* percutaneous absorption of piroxicam from its gel form in rabbits. *Int. J. Pharm.*, 71 (1991) 193-200.

Huang, E-S., Human Cytomegalovirus. IV specific inhibition of virus-induced DNA polymerase activity and viral DNA replication by phosphonoacetic acid. *J. Virol.*, 16 (1975) 1560-65.

Hudson, R.F., and Harper D.C., The reactivity of esters of quinquevalent phosphorous towards anions. *J. Chem, Soc.*, (1958) 1356-60.

Humphrey, M.J. The oral bioavailability of peptides and related drugs. In *Delivery systems for peptide drugs.* Edited by Davis, S.S., Illum, L. and Tomlinson, E., Plenum Press, New York. 1986 pp 139-151.

Humphries, W.T. and Wildnauer, R.H., Thermomechanical analysis of stratum corneum., *J. Invest. Dermatol.*, 57 (1971) 32.

Hussain, A.A., Faraj, J., Aramaki, Y. and Truelove, J.E., Hydrolysis of leucine enkephalin in the nasal cavity of the rat-a possible factor in the low bioavailability of nasally administered peptides. *Biochem. Biophys. Res. Comm.*, 133 (1985) 923-928.

Hwang, C.C. and Danti, A.G., Percutaneous absorption of flufenamic acid in rabbits : Effect of dimethyl sulphoxide and various nonionic surface active agents. *J.Pharm. Sci.*, 72 (1983) 857-860.

Idson, B., Percutaneous absorption. *J. Pharm. Sci.*, 64 (1975) 901-924.

Illel, B., Schaefer, H., Wepierre, J. and Doucet, O., Follicles play an important role in percutaneous absorption. *J. Pharm. Sci.*, 80 (1991) 424-427.

Illum, L., Farraj, N.F., Titchley, H., Johansen, B.R. and Davis S.S., Enhanced nasal absorption of insulin in rats using lysophosphatidylcholine. *Int. J. Pharm.*, 57 (1989) 49-54.

Ingold, C.K., Structure and mechanism in organic chemistry, Cornell University Press, Ithaca, NY. Second Edition (1969) 1129-1131

Imokawa, G., Kuno, H., and Kawai, M., Stratum corneum lipids serve as a bound-water modulator. *J. Invest. Dermatol.*, 96 (1991) 845-851.

Irie, T. and Uekama, K., Protection against the photosensitized skin irritancy of chlorpromazine by cyclodextrin complexation. *J. Pharmacobio-Dyn.*, 8 (1985) 788-791.

Irie, T., Wakamatsu, K., Arima, H., Aritomi, H. and Uekama, K., Enhancing effects of cyclodextrins on nasal absorption of insulin in rats. *Int. J Pharm.*, 84 (1992) 129-139.

Irwin, W.J., *Kinetics of Drug Decomposition: BASIC Computer Solutions,* Elsevier, Amsterdam, 1990, pp. 175-181.

Irwin, W.J., Dwivedi, A.K., Holbrook, P A. and Dey. M.J., The effect of cyclodextrins on the stability of peptides in nasal enzymic systems. *Pharm. Res.*, 11 (12) (1994) 1698-1703.

Irwin, W.J. and Li Wan Po, A., The dependence of amitriptyline partition coefficients on lipid phase, *Int. J. Pharm.* 4 (1979) 47-56.

Irwin, W.J., Sanderson, F.D. and Li Wan Po, A., Percutaneous absorption of ibuprofen: Vehicle effects on transport through rat skin. *Int. J. Pharm.*, 66 (1990a) 193-200.

Irwin, W.J., Sanderson, F.D. and Li Wan Po, A., Percutaneous absorption of ibuprofen and naproxen: Effect of amide enhancers on transport through rat skin. *Int. J. Pharm.*, 66 (1990b) 243-252.

Irwin, W.J. and Scott, D.K., HPLC in pharmacy. *Chemistry in Britain* 18 (1982) 708-718.

Irwin, W.J. and Smith, J.C., Extraction coefficients and facilitated transport: The effect of absorption enhancers. *Int. J. Pharm.*, 76 (1991) 151-159.

Iyer, R.P., Phillips, L.R., Biddle, J.A., Thakker, D.R., Egan, W., Aoki, A. and Mitsuya, H., Synthesis of acyloxyalkyl acylphosphonates as potential prodrugs of the antiviral, trisodium phosphonoformate (forscarnet sodium). *Tetrahedron Lett.*, 30 (51) (1989) 7141-7144.

Jacobson. M.A., Crowe, S., Levy, J., Aweeka, F., Gambertoglio, J., McManns, N. and Mills, J., Effects of Foscarnet therapy on infection with human immunodeficiency virus in patients with AIDS. *J. Infect. Dis.*, 158(40) (1988) 862-865.

Jones, S.P., Grant, D.J.W., Hadgraft, J. and Parr, G.D., Cyclodextrins in the pharmaceutical sciences. Part I: Preparation, structure and properties of cyclodextrin and cyclodextrin inclusion compounds. *Acta Pharm. Technol.*, 30 (1984a) 213-223.

Jones, S.P., Grant, D.J.W., Hadgraft, J. and Parr, G.D., Cyclodextrins in the pharmaceutical sciences. Part II: Pharmaceutical, biopharmaceutical, biological and analytical aspects, and applications of cyclodextrin and its inclusion compounds. *Acta Pharm. Technol.*, 30 (1984b) 263-277.

Kadir, R., Stempler, D., Liron, Z. and Cohen, S., The delivery of theophylline into excised human skin from alkanoic acids in solution : a "push-pull" mechanism. *J. Pharm. Sci.*, 76 (1987) 774-779.

Kadir, R., Stempler, D., Liron, Z. and Cohen, S., Penetration of adenosine into excised human skin from binary vehicles: the enhancement factor. *J.Pharm. Sci.*, 77 (1988) 409-413.

Kadir, R., Tiemessen, H.L.G.M., Ponec, M., Junginger, H.E. and Boddé, H.E., Oleyl surfactants as skin penetration enhancers : Effects on human stratum corneum permeability and *in vitro* toxicity to cultured human skin cells. In *Pharmaceutical Skin Penetration Enhancement.* Edited by Walters, K.A. and Hadgraft, J. Marcel Dekker Inc. New York (1993) 215-227.

Kao, J. and Carver, M.P., Cutaneous metabolism of xenobiotics. *Drug Metab. Rev.*, 22 (1990) 363-410.

Katz, M. and Poulson, B.J., Absorption of drugs through the skin. In *Handbook of Experimental Pharmacology.* Edited by Brodie, B.B. and Gillette, J.R. Springer - Verlag 28 (1971) 103-174.

Kemken, J., Ziegler, A. and Muller, B.W., Influence of super saturation on the pharmacodynamic effect of bupranolol after dermal administration using microemulsions as vehicle. *Pharm. Res.*, 9 (4) (1992) 554-558.

Keshary, P.R. and Chien, Y.W., Mechanisms of controlled nitroglycerin administration. I. Development of a finite-dosing skin permeation system. *Drug. Dev. Ind. Pharm.*, 10 (1984) 883-913.

Klausner, R.D., Kleinfeld, A.M., Hoover, R.L., and Karnovsky, M.J., Lipid domains in membranes: Evidence derived from structural perturbations induced induced induced by free fatty acids and lifetimeheterogeneity analysis. *J. Biol. Chem.*, (1980) 255:1286-1295.

Klein, R.J. and Friedman-Kien, A.E., Phosphonoacetic acid in the treatment of experimental herpes simplex keratitis. *Antimicrob. Agents Chemother.*, 7 (1975) 289-293.

Kligman, A.M., In *The Epidermis.* Edited by Montagu, M. and Lobitz, W.C., Academic Press, New York, (1964) 387.

Kligman, A.M., Topical pharmacology and toxicology of dimethyl sulfoxide., *J. Am. Med. Assoc.*, 193 (1965) 796-804.

Kligman, A.M., A biological brief on percutaneous penetration., *Drug. Devel. Indust. Pharm.*, 9(4) (1983) 521-560.

Kligman, A.M. and Christophers, E., Preparation of isolated sheets of human stratum corneum., *Arch. Dermatol.*, 88 (1963) 702-705.

Knox, J.H., Done, J.N., Fell, A.F., Gilbert, M.T., Pryde, A. and Wall, R.A., High performance liquid chromatography. Edinburgh University Press, Edinburgh (1978).

Kondo, S., Yamanaka, C., and Sugimoto, I., Enhancement of transdermal delivery by superfluous thermodynamic potential. I. Thermodynamic analysis of nifedipine transport across the lipoidal barrier. *J. Pharmacobio-Dyn.*, 10 (1987a) 587-594.

Kondo, S., Yamanaka, C., and Sugimoto, I. Enhancement of transdermal delivery by superfluous thermodynamic potential. II *in vitro-in vivo* correlation of percutaneous nifedipine transport. *J. Pharmacobio-Dyn.* 10 (1987b) 662-668.

Kondo, S., Yamanaka, C., and Sugimoto, I. Enhancement of transdermal delivery by superfluous thermodynamic potential.III Percutaneous absorption of nifedipine in rats. *J. Pharmacobio -Dyn.*, 10 (1987c) 743-749.

Kraak, J.C., Ion-Exchange and ion-pair chromatography. In *Techniques in liquid chromatography* Edited by Simpson C.F. Wiley Heyden (1982) 303-335.

Kupchan, S.M., Casey, A.F., and Swintosky, J.V., Synthesis and Preliminary evaluation of testosterone derivatives.*J. Pharm. Sci.*, 54 (4) (1965) 514-424

Kurihara-Bergstrom, T., Flynn, G.L. and Higuchi, W.I., Physicochemical study of percutaneous absorption enhancement by dimethyl sulphoxide: Kinetic and thermodynamic determinants of dimethyl sulphoxide mediated mass transfer of alkanols., *J.Pharm. Sci.*, 75 (1986) 479-486.

Kurihara-Bergstrom, T., Flynn, G.L. and Higuchi, W.I., Physicochemical study of percutaneous absorption enhancement by dimethyl sulphoxide: dimethyl sulphoxide mediation of vidarabine (Ara-A) permeation of hairless mouse skin. *J. Invest. Dermatol.*, 89 (1987) 274-280.

Kurihara-Bergstrom, T., Good, W.R., Feisullin, S. and Signor, C., Skin compatibility of transdermal drug delivery systems. *J. Control. Rel.*, 15 (1991) 271-277.

Kurihara-Bergstrom, T., Knutson, K., DeNoble, L.J. and Goates, C.Y., Percutaneous absorption enhancement of an ionic molecule by ethanol-water systems in human skin., *Pharm. Res.*, 7 (1990) 762-766.

Kurozumi, M., Nambu, N. and Nagai, T., Pharmaceutical interactions in dosage forms and processing. Part IV Inclusion compounds of non-steroidal anti-inflammatory and other slightly water-soluble drugs with α- and β- cyclodextrins in powdered form. *Chem. Pharm. bull.*, 23 (12) (1975) 3062-3068.

Kushida, K., Masaki, K., Matsumura, V., Ohshima, T., Yoshikawa, K., Takada, K. and Musanishi, S., Application of calcium thioglycolate to improve transdermal delivery of theophylline in rats. *Chem. Pharm. Bul.*, 321 (1984) 268-274.

Lampe, M.A., Burligame, A.L., Whitney, J., Williams, M.L., Brown, B.E., Roitman, E., and Elias, P.M., Human stratum corneum lipids: Characterisation and regional variations. *J. Lipid Res.*, 24 (1983) 120-130.

Landmann, L., Lamellar granules in mammalian, avian, and reptilian epidermis. *J. Ultrastr. Res.*, 72 (1980) 245-263.

Langguth, P., Sphan, H., Mutscher, E. and Hubner, K., An approach to reduce the number of skin samples in testing the transdermal permeation of drugs. *J. Pharm. Pharmacol.*, 38 (1986) 726-730.

Laurence, D.R., Poisoning: Chelating agents: Poisons. In *Clinical Pharmacology.* 4th Edition Churchill Livingstone (1973) Chapter 31.

Lee, G., Swarbrick, J., Kryohara, G. and Payling, D.W., Drug permeation through human skin. III. Effect of pH on the partitioning behaviour of a chromone -2- carboxylic acid. *Int. J. Pharm.*, 23 (1985) 43-54.

Lee, S.J., Kurihara-Bergstrom, T. and Kim, S.W., Ion-paired drug diffusion through polymer membranes. *Int. J. Pharm.*, 39 (1987) 59-73.

Leinbach, S.S.,Reno, J.M., Lee L.F., Isbell, A.F.and Boezi, J.A., Mechanism of phosphono-acetate inhibition of herpesvirus-induced DNA polymerase. *Biochemistry,* 15(2) (1976) 426-430.

Lewis, D. and Hadgraft, J., Mixed monolayers of dipalmitoylphosphatidylcholine with azone or oleic acid at the air-water interface. *Int. J. Pharm.*, 65 (1990) 211-218.

Lien, E.J. and Tong, G.L., Physicochemical properties and percutaneous absorption of drugs. *J. Soc. Cosmet. Chem.*, 24 (1973) 371-384.

Lietman, P.S., Clinical pharmacology: Foscarnet. *Am.J. Med.* 92 (Suppl. 2A) (1992) 2A-11 S.

Lindner, K and Saenger, W., β-cyclodextrin dodecahydrate: Accumulation of water molecules in a hydrophobic cavity. *Angew. Chem.Int., Ed Engl.* 17 (1978) 694-696.

Liron, Z. and Cohen, S., Percutaneous absorption of alkanoic acids. II. Application of regular solution theory. *J. Pharm. Sci.*, 73 (4) (1984) 538-542.

Liu, J.C., Tojo, S.K. and Chien, Y.W., Membrane permeation kinetics of nortestosterone: effect of methyl groups on thermodynamics. *Int. J. Pharm.*, 25 (1985) 265-274.

Li Wan Po, A. and Irwin, W.J., High-performance liquid chromatography. Techniques and applications. *J. Clin. Hosp. Pharm.* 5 (1980) 107-144.

Loftsson, T., Experimental and theoretical model for studying simultaneous transport and metabolism of drugs in excised skin. *Arch. Pharm. Chemi. Sci.*, 10 (1982) 63-66.

Loftsson, T., The effect of ionisation on partition coefficients and topical delivery, *Acta. Pharm. Suec.*, 22 (1985) 209-214.

Long, S.A., Wertz, P.W., Strauss, J.S. and Downing, D.T., Human stratum corneum polar lipids and desquamation. *Arch. Dermatol Res.*, 277 (1985) 284-287.

Longenecker, J.P., Moses, A.C., Silver, R.D., Carey, M.C., Dubovi, E.J., Effects of sodium taurodihydrofusidate on nasal absorption of insulin in sheep. *J. Pharm. Sci.*, 76 (1987) 351-355.

Lorenzetti, O.J., Propylene glycol gel vehicles. *Cos. Dermatol.*, 23 (1979) 747-750.

Lovering, E.G. and Black, D.B., Diffusion layer effects on permeation of phenylbutazone through polydimethylsiloxane. *J.Pharm. Sci.*, 63 (1974) 1399-1402.

Luis, A.D., Heaphy, M.R., Caluanico, N.J., Thomasi, T.B. and Jordan, M.D., Separation of epidermis from dermis with sodium thiocyanate. *J. Invest. Dermatol.*, 68 (1977) 36-38.

Lynch, D.H., Roberts, L.K. and Daynes, P.A., Skin immunology : the achilles heel to trans-dermal delivery. *J. Controlled Release*, 6 (1987) 39-50.

Maibach, H.I., Oral substitution in patients sensitised by transdermal clonidine treatment. *Contact Dermatitis,* 16 (1987) 1-8.

Mak, V.H.W., Potts, R.O. and Guy, R.H., Oleic acid concentration and effect in human stratum corneum: non-invasive determination by attenuated total reflectance infrared spectroscopy *in vivo*. *J.Controlled Release,* 12 (1990) 67-75.

Makowski, L. and Li, J., X-ray diffraction and electron microscope studies of the molecular structure of biological membranes. In *Biomembrane Structure and Function.* Edited by Chapman, D. Verlag Chemie, Weinheim, (1984) 43-166.

Malkinson, F.D.,In *The Epidermis.* Edited by Montagu, M. and Lobitz, W.C., Academic Press, New York, (1964) 435.

Manschel, H., Kolloidchemie und pharmakologie der keratinzubstanzen unde menschlichen, Haut. *Arch. Exp. Path. Pharmacol.*, 110 (1925) 1045.

Mao, J.C-H and Robishaw, E., Mode of inhibition of herpes simplex virus DNA polymerase by phosphonoacetate, *Biochemistry*, 14 (1975) 5475-5479.

Mao, J.C-H, Robishaw, E.E., Overley, L.R., Inhibition of DNA polymerase actrivity from herpes simplex infected W.I. 38 cells by phosphonoacetic acid, *J. Virol* 15 (1975) 1281-1283.

Marttin, E., Verhoef. J.C., Romeijn S.G. and Merkus, F.W.H.M., Effects of absorption enhancers on rat nasal epithelium in vivo: Release of marker compounds in the nasal cavity. *Pharm. Res.*, 12 (8) (1995) 1151-1157.

Marzulli, F.N., Brown, D.W.C. and Maibach, H.I., Techniques for studing skin penetration. Toxicol. *Appl. Pharmacol., Suppl.* 3 (1969) 79-83.

Matoltsy, A.G., Keratinization. *J.Invest.Dermatol.*, 67 (1976) 20-25.

Matoltsy, A.G., Structure and function of the mammalian epidermis. In *Biology of the Integument*. Vol. II. Edited by Bereiter-Hahn, J., Matoltsy, A.G. and Richards, K.S. Springer-Verlag, Berlin, (1986) 255-271.

Matusbara, K., Abe, K., Irie, T. and Uekama, K., Inprovement of nasal bioavailability of luteinizing hormone-releasing agonist, buserelin, by cyclodextrin derevatives in rats. *J. Pharm. Sci.*, 84 (11) (1995) 1295-1300.

Matsui, Y., and Mochida, K., Binding forces contributing to the association of cyclodextrin with alcohol in an aqueous solution. *Bull. Chem. Sol. Jap.*, 52 (10) (1979) 2808-2814.

Matheson, L.E., Wurster, D.E. and Ostreuga, J.A., Sarin transport across excised human skin II: effect of solvent pretreatment on permeability. *J. Pharm. Sci.*, 68 (1979) 1410-1413.

McBurney, E.M., Noel, S.B. and Collins, J.L., Contact dermatitis to transdermal estradiol systems. *J. Am. Acad. Dermatol.*, 20 (1989) 508-510.

Medawar, P.B., Sheets of pure epidermal epithelium from human skin, (letters to the editor) *Nature*, 148 (1941) 783.

Megrab, N.A., Williams, A.C. and Barry, B.W. Oestradiol permeation through human skin and silastic membrane: effects of propylene glycol and supersaturation. *J.Controlled Release*, 36 (3) (1995) 277-294.

Menczel, E. and Goldberg, S., pH effect on the percutaneous penetration of lignocaine hydrochloride. *Dermatologica.*, 156 (1978) 8-14.

Merkus, F.W.H.M., Schipper, N.G.M., Hermens, W.A.J.J., Romeijn, S.G. and Verhoef, J.C., Absorption enhancers in nasal drug delivery: efficacy and safety. *J. Controlled Release*, 24 (1993) 201-208.

Merkus, F.W.H.M., Verhoef, J.C., Romeijn, S.G. and Schipper N.G.M. Absorption enhancing effect of cyclodextrin on intranasally administered insulin in rats. *Pharm. Res.*, 8(5) (1991) 588-592.

Metzler, C.M. and Weiner, D.L., PCNONLIN, Statistical Consultants Inc., Lexington, Kentucky, U.S.A., 1986.

Meyer, R.F., Varnell, E.D. and Kaufman H.E., Phosphonoacetic Acid in the treatment of experimental ocular herpes simplex infections. *Antimicrob. Agents Chemother.*, 9 (2) (1976) 308-311.

Mezei, M. and Ryan, K.J., Effect of surfactants on epidermal permeability in rabbits. *J.Pharm. Sci.*, 61 (1972) 1329-1331.

Michaels, A.S., Chanderasekaran, S.K. and Shaw, J.E., Drug permeation through human skin, theory and *in vitro* experimental measurement., *Am. Inst. Chem. Eng. J.*, 21 (1975) 895-996.

Michniak, B.B., Player, M.R., Chapman, Jr., J.M. and Sowell, Sr., J.W., Azone analogues as penetration enhancers: effect of different vehicles on hydrocortisone acetate skin permeation and retention. *J. Controlled Release*, 32 (1994) 147-154

Mishima, M., Wakita, Y and Nakano, M. Studies on the promoting effect of medium chain fatty acid salts on the nasal absorption of insulin in rats. *J. Pharmacobio-Dyn.*, 10 (1987) 624-631.

Mitchell, A.G., Nicholls, D., Walker, I., Irwin, W.J., and Freeman, S., Prodrugs of phosphonoformate: products, kinetics and mechanisms of hydrolysis of dibenzyl (methoxycarbonyl) phosphonate. *J. Chem. Soc. Perkin. Trans* 2, (1991) 1297-1303.

Mitchell, A.G., Nicholls, D., Irwin, W.J. and Freeman, S., Prodrugs of phosphonoformate: the effect of para-substituents on the products, kinetics and mechanism of hydrolysis of dibenzyl methoxycarbonylphosphonate. *J. Chem.Soc. Perkin Trans* 2, (1992a) 1145-1150.

Mitchell, A.G, Thomson, W., Nicholls, D., Irwin, W.J. and Freeman, S., Bioreversible protection for the phospho group: Bioactivation of the di(4-acyloxybenzyl) and Mono(4-acyloxybenzyl) phosphoesters of methylphosphonate and phosphonoacetate. *J. Chem. Soc. Perkin. Trans.* 1, (1992b) 2345-2353.

Mitsuya, H., and Broder, S., Stategies for antiviral therapy in AIDS. *Nature*, 325(6107) (1987) 773-778.

Møllgaard, B., Synergistic effects in percutaneous enhancement. In *Pharmaceutical Skin Penetration Enhancement.* Edited by Walters, K.A. and Hadgraft, J. Marcel Dekker Inc. New York. (1993) 229-242.

Møllgaard, B. and Hoelgaard, A., Permeation of estradiol through the skin - effect of vehicles., *Int. J. Pharm.*, 15 (1983a) 185-197.

Møllgaard, B. and Hoelgaard, A., Vehicle effects on topical drug delivery. I. Influence of glycols and drug concentration on skin transport. *Acta. Pharm. Suec.*, 20 (1983b) 433-442.

Møllgaard, B. and Hoelgaard, A., Vehicle effects on topical drug delivery. II. Concurrent skin transport of drugs and vehicle components. *Acta. Pharm. Suec.*, 20 (1983c) 443-450.

Møllgaard, B. and Hoelgaard, A., Enhancement of cutaneous estradiol permeation by propylene glycol and dimethylsulphoxide. *Arch. Pharm. Chem. Soc. Ed.*, 12 (1985) 71-78.

Morita, M., and Horita, S., Effect of crystallinity on the percutaneous absorption of corticosteroid. II. Chemical activity and biological activity. *Chem. Pharm. Bull.*, 33 (1985) 2091-2097.

Moses, A.C., Gordon, G.S., Carey,M.C. and Flier, J.S., Insulin administered intranasally as an insulin-bile salt aerosol: effectiveness and reproducibility in normal and diabetic subjects. *Diabetics*, 32 (1983) 1040-1047.

Muktadair, A., Babar, A., Cutie, A.J. and Plakogiannis, F.M., Medicament release from ointment bases: III Ibuprofen: *in vitro* release and *in vivo* absorption in rabbits. *Drug Dev. Indus. Pharm.*, 12 (1986) 2521-2540.

Munro, D.D., Relation between percutaneous absorption and stratum corneum retention. *Br. J. Dermatol.*, 81 (Suppl.) (1969) 92-97.

Munro, D.D. and Stoughton, R.B., Dimethylacetamide (DMAC) and dimethylformamide (DMFA) effect on percutaneous absorption. *Arch. Dermatol.*, 92 (1965) 585-586.

Nacht, S. and Yeung, D. Artificial membranes and skin permeability. In *Percutaneous Absorption;Mechanisms-Methodology-Drug Delivery.* Edited by Bronaugh, R.L. and Maibach, H.I. Marcel Dekker. New York. (1985) 373.

Naik, A., Azidoprofen as a soft anti-inflammatory agent for the topical treatment of psoriasis, PhD thesis Aston University. (1990)

Naik, A., Irwin, W.J. and Griffin, R.J., Percutaneous absorption of azidoprofen, a model for a soft anti-inflammatory drug for topical application. *Int. J. Pharm.*, 90 (1993) 129-140.

Nakai, Y., Nakajima, S., Yamamoto, K., Terada, K. and Konno, T., Effects of grinding on the physical and chemical properties of crystalline medicinals with microcrystalline cellulose.III. Infrared spectra of medicinals in ground mixtures., *Chem. Pharm. Bull.*, 26 (11) (1978) 3419-3425.

Nakai.Y., Yamamoto, K., Terada, K. and Watanabe, D., New methods for preparing cyclodextrin inclusion compounds. I Heating in a sealed container. *Chem. Pharm. Bull.*, 35 (11) (1987) 4609-4615.

Nash. R.A., Cyclodextrins, In *Pharmaceutical Excipients*. Edited by Wade, A. and Weller, P.J. Second Edition. The Pharmaceutical Press. London (1994) 145-148.

Neubert, R., Ion pair transport across membranes. *Pharm. Res.*, 6 (1989) 743-747.

Norén, J.O., Helgstrand, I.E., Johansson, N.G., Misiarny, A. and Stewning, G., Synthesis of esters of phosphonoformic acid and their anti-herpes activity. *Med. Chem.*, 26 (1983) 264-270.

Novac, E. and Francom, S.F., Inflammatory response to sodium lauryl sulphate in aqueous solutions applied to the skin in normal human volunteers., *Contact Dermatitis*, 10 (1984) 101-104.

Nunberg. J.H., Schleif. W.A., Boots. E.J., Obrien, J.A.,Quintero, J.C., Hoffman. J.M., Emini, E.A and Goldberg, M.E.,Viral resistance to human immunodeficiency virus type 1 - specific pyridinone reverse transcriptase inhibitors. *J. Virol.*, 65 (9) (1991) 4887-4892.

Oakley, D.M. and Swarbrick, J., Thermodynamics of the partitioning of nicotine in organic liquids and stratum corneum. *Pharm. Res.*, 3(5) (1986) 49.

Oakley, D.M. and Swarbrick, J., Effects of ionisation on the percutaneous absorption of drugs: partitioning of nicotine into organic liquids and hydrated stratum corneum. *J. Pharm. Sci.*, 76 (1987) 866-871.

Öberg, B., Molecular basis of foscarnet action. In *Human herpes virus infections*. Edited by Lopez, C. and Roizman. B., (1986) 141-151.

Öberg, B., Antiviral effects of phosphonoformate. *Pharmac. Ther.*, 40(2) (1989) 213-285.

Odland, G.F., A submicroscopic granular component in human epidermis. *J. Invest. Dermatol.*, 34 (1960) 11-15.

Oguia, R., Knox, J.M. and Griffen, A.C., Separation of epidermis for the study of epidermal sulphydryl. *J. Invest. Dermatol.*, 35 (1960) 239-243.

Okamoto, H., Komatsu, H., Hashida, M. and Sezaki, H., Effects of ß-cyclodextrin and di-o-methyl ß-cyclodextrin on the percutaneous absorption of butyl paraben indothethacin and sulphanilic acid. *Int. J. Pharm.*, 30 (1986) 35-45.

Ongpipattanakul, B., Burnette, R. and Potts, R.O., Evidence that oleic acid exists as a separate phase within stratum corneum. *Pharm. Res.*, 8 (1991) 350-354.

Orienti, I., Zecchi, V., Bertasi, V., and Fini, A. Control of the released dose of NSAID by cyclodextrin complex formation, ketoprofen in topical systems. *Minutes of the 5th Int. Symp. on Cyclodextrins*, Edited by Duchêne, D., Editions de Santé Paris 1990 pp 381-385.

Ostrander, M., Cheng, Y-C., Properties of herpes simplex virus type 1 and type 2 DNA polymerase. *Biochem. Biophys. Acta.*, 609 (2) (1980) 232-245.

Ostrenga, J.A., Steinmetz, C. and Poulsen, B.J., Significance of vehicle composition. I: Relation between topical vehicle composition , skin penetrability, and clinical efficacy. *J. Pharm. Sci.*, 60 (8) (1971) 1175-1179.

Otagiri, M., Fujinaga, T., Sakai, A. and Uekama, K., Effects of β-and γ-cyclodextrins on release of betamethasone from ointment bases. *Chem. Pharm. Bull.*, 32 (1984) 2401-2405.

Otagiri, M., Perrin, J.H., Uekama, K., Ikeda, K. and Takeo, K., The interaction of some N-phenylanthranilic acid derivatives with cyclodextrins in phosphate buffers. *Pharm. Acta. Helv. Si* (11) (1976) 343-347.

Overby, L.R., Duff, R.G. and Mao, J.C-H., Antiviral potential of phosphonoacetic acid. *Ann. N.Y.Acad. Sci.*, 284 (1977) 310-320.

Palmieri, G.F., Wehrlé, P. and Stamm, A., Inclusion of vitamin D2 in ß-cyclodextrin. Evaluation of different complexation methods. *Drug Dev. Ind. Pharm.*, 19 (1993) 875-885.

Panchagnula, R. and Ritschel, W.A., Development and evaluation of an intracutaneous depot formulation of corticosteriods using transcutol as a cosolvent: *in vitro*, *ex vitro* and *in vivo* rat studies. *J. Pharm. Pharmacol.*, 43 (1991) 609-614.

Pannatier, A., Jenner, P., Testa, B., and Etter, J.C., The skin as a drug metabolising organ. *Drug. Metab. Rev.*, 8 (1978) 319-343.

Pellett, M.A., Davis, A.F., Hadgraft, J. and Brain, K.R. The stability of supersaturated solutions for topical drug delivery. In *Prediction of Percutaneous Penetration*, Edited by Brain, K R., James,V.J.and Walters, K.A.STS Publishing, Cardiff, (1993), Vol. 3b, 292-298.

Pershing, L.K., Lambert, L.D. and Knutson, K., Mechanism of ethanol-enhanced estradiol permeation across human skin *in vivo*. *Pharm. Res.*, 7 (1990) 170-175.

Perrin, D.D. and Dempsey, B., Buffers for pH and metal ion control. Chapman and Hall, London (1974).

Pitha, J., Enhanced water solubility of vitamins A,D,E and K by substituted cycloamyloses. *Life Sci.*, 29 (1981) 307-311.

Pitha, J., Zawadzki, S., Chytil, F., Lotan, D. and Lotan R., Water solubile, dextran linked retinal preparation, Vitamin A-like activity in rats, and effects on melanoma cells. *JNCL.*, 65 (1980) 1001-1015.

Poelman, M-C., Piot, B., Guyon, F., Deroni, M. and Lévégue, J.L., Assessment of topical non-steroidal anti-inflammatory drugs. *J. Pharm. Pharmacol.*, 41 (1989) 720-722.

Poole, C.F. and Schnette, S.A., Contemporary practice of chromatography. Elsevier (1984) 526-537.

Potts, R.O., Physical characterisation of the stratum corneum: the relationship of mechanical and barrier properties to lipid and protein structure, In *Transdermal Drug Delivery; Developmental Issues and Research Initiatives*, Edited by Hadgraft, J. and Guy, R.H. Marcel Dekker, New York (1989) Chapter 2.

Poulsen, B.J., Diffusion of drugs from topical vehicles : An analysis of vehicle effects. *Adv. Biol. Skin.*, 12 (1972) 495-509.

Poulsen, B.J., Young. E., Coquilla, V. and Katz. M., Effect of topical vehicle composition on the *in vitro* release of fluocinolone acetonide and its acetate ester. *J. Pharm. Sci.*, 57 (1968) 928-933.

Prankerd, R.J., Stone, H.W., Sloan, K.B., and Perrini, J.H., Degradation of aspartamine in acidic aqueous media and its stabilisation by complexation with cyclodextrins or modified cyclodextrins. *Int. J.Pharm.*, 88 (1992) 189-199.

Rapoport. S.I., Blood brain barrier. In *Physiology and medicine.* Raven, New York (1976).
Rawlins, M.D., Shuster, S., Chapman, P.H., Shaw, J. and O'Neill, V.A., Drug Metabolism in Skin in *Clinical Pharmacology and Therapeutics.* Edited by Turner P. Macmillan, London (1980) 410-414.
Reifenrath, W.G., Hawkins, G.S., and Kartz, M.S., Percutaneous penetration and skin retention of topically applied compounds: an *in vitro* study. *J. Pharm. Sci.*, 80 (1991) 526-532.
Reifenrath, W.G., Lee, B., Wilson, D.R. and Spencer, T.S., A comparison of *in vitro* skin-penetration cells. *J. Pharm. Sci.*, 83 (1994) 1229-1233.
Reynolds, J.E.F. Editor, Martindale, The Extra Pharmacopoeia. The Royal Pharmaceutical Society, Thirty First Edition (1996) 1097-1098.
Rhein, L.D., Robbins, C.R. Fernee, K. and Cantore, R., Surfactant structure effects on swelling of isolated human stratum corneum. *J. Soc. Cosmet. Chem.*, 37 (1986) 125-139.
Roberts, D.V., Simple enzyme-catalysed reactions, In *Enzyme kinetics.* Cambridge Chemistry Texts. (1977) 23-47.
Robinson, A., Evers, E.L., Griffin, R.J. and Irwin, W.J., Azidobenzyl carbamates as potential prodrugs for amines: synthesis and kinetic evaluation. *J. Pharm. Pharmacol.*, 40 (1988) 61P.
Rodgers, W.A., Buritz, R.S. and Alpert, D., The diffusion coefficient, solubility and permeability of helium in glass. *J. Appl.Physiol.*, 25 (1954) 868-875.
Rodwell, V.M., Enzymes: Kinetics. In Harper's Biochemistry 24th Edition. Edited by Murray, R.K., Granner, D.K., Mayes, P.A., and Rodwell, V.M. Appleton and Lange. (1996) 75-90.
Rosanske, T.W., and Connors, K.A., Stoichiometric model of α-cyclodextrin complex formation. *J.Pharm. Sci.*, 69 (1980) 564-567.
Roxburgh's Common Skin Diseases, Revised by John D. Kirby., Fifteenth Edition. H.K. Lewis & Co Ltd., 1986.
Ruland, A. and Kreuter. J., Influence of various penetration enhancers in the *in vitro* permeation of amino acids across hairless mouse skin. *Int. J. Pharm.*, 85 (1992) 7-17.
Ryan, K.J. and Mezei, M. In vivo method for monitoring polysorbate 85 effect on epidermal permeabiltiy. *J. Pharm. Sci.*, 64 (1975) 671-673.
Saenger, W. Cyclodextrin inclusion compounds in research. *Angew. Chem. Int., Ed. Engl.* 19 (1980) 344-360.
Safrin, S. Crumpacker, C.S., Chatis, P.A., Davis, R., Hafner, R., Rush, J., Kessler, H.A., Landry, B. and Mills, J., A controlled trial comparing foscarnet with vidarabine for acyclovir-resistant mucocutaneous herpes-simplex in the aquired-immunodeficiency-syndrome. *New Engl. J. Med.*, 325 (1991) 551-555.
Samuelov, Y., Donbrow, M. and Frieman, N., Effect of pH on salicylic acid permeation through ethyl cellulose-PEG 4000 films. *J. Pharm. Sci.*, 31 (1979) 120-124.
Sandström, E.G., Byington, R.E., Kaplan, J.C. and Hirsch, M.S., Inhibition of human T-cell lymphotropic virus type III *in vitro* by phosphonophormate. *Lancet i* (1985) 1480-1482
Sarkar, M.A., Drug metabolism in nasal mucosa. *Pharm. Res.*, 9 (1992) 1-9
Sarin, P.S., Tagudni, Y., Sun, D., Thornton, A., Galla, R.C. and Öberg, B., Inhibition of HTLV-III ILAV replication by Coscarnet. *Biochem. Pharmac.* 34 (1985) 4075-4079.
Sariti, P., Catellani, P.L., Colombo, P., Ringard-Lefebvre, C., Barthiélémy, C. and Guyot-Herman, A.M., Partition and transport of verapamil and nicotine through artificial membranes. *Int. J. Pharm.*, 68 (1991) 43-49.

Sarpotdar, P.P. and Zatz, J.L., Percutaneous absorption enhancement by non-ionic surfactants. *Drug Devel. Ind. Pharm.*, 12 (1986a) 1625-1647.

Sarpotdar, P.P. and Zatz, J.L., Percutaneous absorption enhancement by non-ionic surfactants. *Drug, Dev. Ind. Pharm.*, 12 (1986a) 1625-1647.

Sarpotdar, P.P. and Zatz, J.L., Evaluation of penetration enhancement of lidocaine by non-ionic surfactants through hairless mouse skin *in vitro*. *J.Pharm. Sci.*, 75 (1986b) 176-181.

Sasaki, H., Kojima, M., Mori., Y., Nakamura, J. and Shibasaki, J., Enhancing effect of pyrrolidone derivatives as transdermal penetration of 5-fluorouracil, triancinolone acetonide, indomethacin, and flubiprofen. *J. Pharm. Sci.*, 80 (1991) 533-538.

Sato, S. and Wan Kim, S. Macromolecular diffusion through polymer membranes. *Int. J. Pharm.*, 22 (1984) 229-255.

Sato, K., Sugibayashi, K. and Morimoto, Y., Effect and mode of action of aliphatic esters on the *in vitro* skin permeation of nicorandil. *Int. J. Pharm.*, 43 (1988) 31-40.

Scheuplein, R.J., Mechanisms of percutaneous absorption. II. Transient diffusion and the relative importance of various routes of skin penetration. *J. Invest. Dermatol.*, 45 (1967) 334-346.

Scheuplein, R.J. Properties of the skin as a membrane. *Adv. Biol. Skin.*, 12 (1972) 125-152.

Scheuplein, R.J., In *The Physiology and Pathophysiology of the Skin,* Volume 5. Edited by Jarratt, A. Academic Press, New York. (1978) 1692-1730.

Scheuplein, R.J. and Blank, I.H., Permeability of the skin. *Physiol. Rev.*, 51 (4) (1971) 702-747.

Scheuplein, R.J. and Blank, I.H., Mechanisms of percutaneous absorption. IV: Penetration of non electrolytes (alcohols) from aqueous solutions and from pure liquids., *J. Invest. Dermatol.*, 60 (5) (1973) 286-296.

Scheuplein, R.J. and Ross, L., Effects of surfactants and solvents on the permeability of the epidermis. *J. Soc. Cosmet. Chem.*, 21 (1970) 853-873.

Schipper, N.G.M., Romeijn, S.G., Verhoef, J.C. and Merkus F.W.H.M., Nasal Insulin Delivery with dimethyl-β-cyclodextrin as an absorption enhancer in rabbits: powder more effective than liquid formulations. *Pharm. Res.*, 10(5) (1993) 682-686.

Schipper, N.G.M., Verhoef, S.G., Romeijn and Merkus, F.W.H.M., Absorption enhancers in nasal insulin delivery and their influence on nasal ciliary functioning. *J. Control. Rel.* 21 (1992) 173-186.

Schuhmann, R. and Touibert, H.D., Long-term application of steroids enclosed in dimethyl-polysiloxane (silastic): *in vitro* and *in vivo* experiments. *Acta. Biol. Med. Germ.*, 24 (1970) 897-910.

Scott, R.C., Walker, M. and Dugard, P.H., *In vitro* percutaneous absorption experiments. A technique for the production of intact epidermal membranes from rat skin., *J. Soc. Cosmet. Chem.*, 37 (1986) 35-37.

Sekura, D.L. and Scala, J., The percutaneous absorption of alkyl methyl sulfoxides. *Adv. Biol. Skin.*, 12 (1972) 257-269.

Shankland, N., Pearson,, A., Johnson, J.R. and Salole, E.G., The influence of ß-cyclodextrin on the release of hydrocortisone from a topical cream base. *J. Pharm. Pharmacol.* 37 supp. (1985) 107P.

Shahi, V. and Katz, J.L., Effect of formulation factors on penetration of hydrocortisone through mouse skin. *J. Pharm. Sci.*, 67 (1978) 789-792.

Sharata, H.H. and Burnette, R.R., Effect of dipolar aprotic permeability enhancers on the basal stratum corneum. *J. Pharm. Sci.*, 77 (1988) 27-32.

Shaw, J.E. and Urquhart, J., Transdermal drug administration - a nuisance becomes an opportunity. *Br. Med. J.*, 283 (1981) 875-876.

Shelley, W.B. and Melton, F.M., Factors accelerating the penetration of histamine through normal intact human skin. *J. Invest. Dermatol.*, 13 (1949) 61-71.

Sheth, N.V., Freeman, D.J., Higuchi, W.I. and Spruance, S.L., The influence of azone, propylene glycol and polyethylene glycol : On *in vitro* skin penetration of trifluorothymidine. *Int. J. Pharm.*, 28 (1986) 201-209.

Shipkowitz, N.L., Bower, R.R, Appell, R.N., Nardeen, C.W., Overby, L.R., Roderick, U.R., Cleicher, J.B., and von Esch A.M., Suppression of herpes simplex infection by phosphono-acetic acid. *Applied Mircobiology*, 27 (1973) 264-267.

Short, P.M., Abbs, E.T. and Rhodes, C.T., The effect of nonionic surfactants on the transport of testosterone across a cellulose acetate membrane. *J. Pharm. Sci.*, 59 (1970) 995-998.

Siddiqi, M. and Ritschel, W.A., pH effects on salicylate absorption through the intact rat skin. *Sci. Pharm.*, 40 (1972) 181-189.

Silverman, R.Z., Prodrugs and drug delivery systems. In *The organic chemistry of drug design and drug action.* Academic Press Ltd (1992).

Simpson, C.F., Practical high performance liquid chromatography. Heyden, London (1978).

Sjovall, J., Karlsson, A., Ogenstad, S., Sandström, E. and Saarimaki, M., Pharmacokinetics and absorption of forscarnet after intravenous and oral administration to patients with human immunodeficiency virus. *Clin. Pharmacol. Ther.*, 44 (1988) 65-73.

Sloan, K.B., Functional group considerations in the development of prodrug approaches to solving topical delivery problems. In *Prodrugs: Topical and Ocular drug delivery.* Edited by Sloan, K.B. Marcel Dekker Inc New York (1992).

Sloan, K.B., Kock, S.A.M., Siver, K.G. and Flowers, F.P., Use of solubility parameters of drug and vehicle to predict flux through the skin. *J. Invest. Dermatol.*, 87 (2) (1986) 244-252.

Smith, E.W. and Haigh, J.H., *In vitro* systems for assessment of drug release from topical formulations and transmembrane permeation. In *Percutaneous Absorption.* Edited by Bronaugh, R.L. and Maibach, H.I. Marcel Dekker (1989) 2nd Edition 465-507.

Smith, H.W. and White, T.A., Distribution ratios of some organic acids. *J. Phys. Chem.*, 33 (1929) 1953-1974.

Smith, W.P., Yeung, D. and Nacht, S., Stratum corneum isolation: Effect on physical properties. *J. Invest. Dermatol.*, 78 (1982) 341.

Southwell, D. and Barry, B.W., The accelerant activity of 2-pyrrolidone in human stratum corneum, steady-state diffusion of model penetrants, methanol and N-octanol. *J. Pharm. Pharmacol.*, 33 (Suppl.) (1981) 1p.

Southwell, D. and Barry, B.W., Penetration enhancers for human skin: mode of action of 2-pyrrolidone and dimethylformamide on partition and diffusion of model compounds water, n-alcohols and caffeine. *J. Invest. Dermatol.*, 80 (1983) 507-514.

Southwell, D. and Barry, B.W., Penetration enhancement in human skin; effect of 2-pyrrolidone, dimethylformamide and increased hydration on finite dose permeation of aspirin and caffeine. *Int. J. Pharm.*, 22 (1984) 291-298.

Southwell, D., Barry, B.W. and Woodford, R., Variations in permeability of human skin within and between specimens. *Int. J. Pharm.*, 18 (1984) 299-309.

Staros, J.V.,Bayley, H., Standring ,D.N. and Knowles, J.R., Reduction of aryl azides by thiols:implications for the use of photoaffinity reagents. *Biochem. Res. Comm.*, 80(3) (1978) 568-572.

Stehle, R.G. and Higuchi, W.I., *In vitro* model for transport of solutes in three-phase system II: experimental concideration. *J.Pharm. Sci.*, 61 (1972) 1931-1935.

Stelzer, J.M., Colaizzi, J.L. and Wurdack, P.J., Influence of dimethyl sulphoxide (DMSO) on the percutaneous absorption of salicylic acid sodium salicylate from ointments. *J. Pharm. Sci.*, 57 (1968) 1732-1737.

Stratford, R.E., and Lee, V.H.L., Aminopeptidase activity in homogenates of various absorptive mucosae in the albino rabbit: implications in peptide delivery. *Int. J. Pharm.* 30 (1986) 73-82.

Stoughton, R.B., Enhanced percutaneous penetration with 1-dodecylazacycloheptan-2-one. *Arc. Dermatol.*, 118 (1982) 474-477.

Stoughton, R.B., Percutaneous absorption of drugs. *Annu. Rev. Pharmacol. Toxicol.*, 29 (1989) 55-69.

Stoughton, R.B. and McClure, W.O., Azone: a new non-toxic enhancer of cutaneous penetration. *Drug Dev. Ind. Pharm.*, 9 (1983) 725-744.

Stoughton, R.B. and Cleveland, W.F., Influence of dimethylsulphoxide (DMSO). *Arch. Dermatol.*, 90 (1964) 512-517.

Sugibayashi, K., Nakayama, S., Seki, T., Hosoya, K-I, and Morimoto, Y., Mechanism of skin penetration - enhancing effect by laurocapram. *J. Pharm. Sci.*, 81 (1) (1992) 58-64.

Swarbrick, J., Lee, G., Brom, J. and Gensmantel, N.P., Drug permeation through human skin II: permeability of ionizable compounds. *J.Pharm. Sci.*, 73 (1984) 1352-1355.

Szente, L., Apostol, I., and Szejtli, J., Suppositories containing ß-cyclodextrin complexes, part 1: Stability studies. *Pharmazie*, 39 (1984) 697-699.

Szente, L., Apostol, I., Gerloczy, A. and Szejtli, J., Suppositories containing ß-cyclodextrin complexes, part 2: dissolution and absorption studies. *Pharmazie*, 40 (1985) 406-407.

Szejtli, J., and Szente, L., Interaction between indomethacin and β-cyclodextrin. *Pharmazie*, 36 (1981) 694-698.

Tanaka, S., Takashima, Y., Murayama, H. and Tsuchika, S., Studies on drug release from ointments. V. Release of hydrocortisone butyrate propionate from topical dosage forms to silicone rubber. *Int. J. Pharm.*, 27 (1985) 29-38.

Tanojo, H., Bos-van Geest, A., Junginger, H.E. and Boddé, H.E., Mechanism of skin barrier perturbation by oleic acid: A new perspective. *Proceed. Intern. Symp. Control. Rel. Bioact. Mater.*, 22 (1995) 692-693.

Tateishi, K., Toh, J., Minagawa, H. and Tashiro, H., Detection of herpes-simplex virus (HSV) in the saliva from 1,000 oral surgery outpatients by the polymerase chain-reaction (PCR) and virus isolation. *J. Oral Path. Med.* 23 (2) (1994) 80-84.

Täuber, U., Drug metabolism in the skin: advantages and disadvantages. In *Transdermal Drug Delivery* Edited by Hadgraft, J. and Guy, R.H., Marcel Dekker New York (1989) 99-112.

Thakkar, A.L. and Demarco, P.V., Cycloheptaamylose inclusion complexes of barbiturates: Correleation between proton magnetic resonance and solubility studies. *J.Pharm.Sci.*, 60 (1971) 652-653.

Theeuwes, F., Gale, R.M. and Baker, R. W., Transference: a comprehensive parameter governing permeation of solutes through membranes. *J. Membr. Sci.*, 1 (1976). 3-6.

Thomson, W. Nicholls, D. Irwin, W.J., Al-Mushadani, J.S., Freeman, S., Karpas, A., Petrik, J., Mahmood, N. and Hay, A.J., Synthesis, bioactivation and anti-HIV activity of the bis(4-acyloxybenzyl) and mono(4-acyloxybenzyl) esters of the 5'-monophosphate of AZT. *J. Chem. Soc. Perkin Trans. 1*, (1993) 1239-1245.

Touitou, E. and Abed, L,. The permeation behaviour of several membranes with potential use in the design of transdermal devices. *Pharm. Acta. Helv.*, 60 (1985) 193-198.

Touitou, E and Donbrow,M., Drug release from non-disintegrating hydrophilic matrices: sodium salicylate as a model drug. *Int. J. Pharm.*, 11 (1982) 355-364.

Tsuji, A., Kubo, O., Miyamoto, E. and Yamana, T., Physico-chemical properties of β-lactam antibiotics: oil-water distribution. *J. Pharm. Sci.*, 66 (1977) 1675-1679.

Tsuji, K. and Morozwich, W., GLC and HPLC determination of therapeutic agents. Parts 1-3. Marcel Dekker, New York (1978-79).

Turnbull, B.C. and MacGregor, I., The enhancing effects of dimethylsulphoxide vehicle upon the antiviral actions of 5-iododeoxyuridine., *N. Z. Med. J.*, 70 (1969) 317-320.

Turro, N.J., Okubo, T. and Chung, C.J., Analysis of static and dynamic host-guest associations of detergents with cyclodextrins via photo-luminesence methods. *J.Am. Chem. Soc.*, 104 (7) (1982) 1789-1794.

Tsuruoka, M., Hashimoto, T., Seo, H., Ichimasa, S., Ueno, O., Fujinaga, T., Otagiri, M. and Uekama, K., Enhanced bioavailability of phenytoin by β-cyclodextrin complexation. *Yakugaku Zasshi* 101 (4) (1981) 360-367.

Tyle, P. and Kari, B., Iontophoretic devices. In *Drug Delivery Devices: Fundamentals and Applications.* Edited by Tyle, P., Dekker, New York (1988) 421-454.

Uekama, K., Arimori, K., Sakai, A., Masaki, K., Irie, T. and Otagiri, M., Improvement in the percutaeneous absorption of prednisolone by β- and γ-cyclodextrin complexation. *Chem. Pharm. Bull.*, 35 (1987a) 2910-2913.

Uekama, K., Fujinaga, T., Hirayama, F., Otagiri, M. and Yamasaki, M., Inclusion complexes of steroid-hormones with cyclodextrins in water and in solid state. *Int. J. Pharm.*, 10 (1) (1982) 1- 15.

Uekama, K., Masaki, K., Arimori, K., Irie, T. and Hirayama, F. Effects of β-cyclodextrins on release and percutaneous absorption behaviours of prednisolone from ointment bases. *Yakugoku Zasshi*, 107 (1987b) 449-456

Uekama, K., Otagiri, M., Sakai, A., Irie, T., Matsuo, N. and Matsuoka, Y. Improvement in the percutaneous absorption of bectomethasone dipropionate by γ-cyclodextrin complexation. *J. Pharm. Pharmacol.*, 37 (1985) 532-535.

Vaidyanathan, R., Chaubal, M.G. and Vasauada, R.C., Effect of pH and solubility on *in vitro* skin penetration of methotrexate from a 50% v/v propylene glycol-water vehicle. *Int.J.Pharm.*, 25 (1985) 85-93.

Vainio, H. and Hietanen, E. Role of extrahepatic metabolism. In *Concepts in Drug Matabolism Part A.* Edited by Jenner, P. and Testa, B. Marcel Dekker, New York (1980) 251-284.

Valia, K.H. and Chien, Y.W., Long-term skin permeation kinetics of estradiol: I. Effect of drug solubiliser - polyethylene glycol 400. *Drug Dev. Ind. Pharm.*, 10 (1984a) 951-981.

Valia, K.H. and Chien, Y.W., Long-term skin permeation kinetics of estradiol. II. Kinetics of skin uptake, binding, and metabolism. *Drug Dev. Ind. Pharm.*, 10 (1984b) 991-1015.

Van Scott, E.J., Mechanical separation of the epidermis from the corium. *J. Invest. Dermatol.*, 18 (1952) 377-379.

Van-Doone, H., Bosch, E.H. and Lerk, C.F., Formation and antimicrobial activity of complexes of ß-cyclodextrin and some antimycotic imidazole derivatives. *Pharm. Weekbl.*, 10 (1988) 80-85.

Verhoef, J.C., Boddé, H.E. de Boer, A.G., Bonwstra, J.A., Junginger, H.E., Merkos, F.W.H.M. and Breimer, D.D. Transport of peptide and protein drugs across biological membranes. *Eur. J. Drug Metab. Pharmacokin.*, 15 (1990) 83-93.

Verhoef, J.C., Schipper, N.G.M., Romeijn, S.G. and Merkus, F.W.H.M. The potential of cyclodextrins as absorption enhancers in nasal delivery of peptide drugs. *J. Controlled Release*, 29(3) (1994) 351-360.

Vermeer, B.J., Skin irritation and sensitization. *J. Controlled Release*, 15 (1991) 261-266.
Wahren, B. and Oberg, B. Inhibition of cytomegalovirus late antigens by phosphonoformate . *Intervirology*. 12(6) (1979) 335-339.
Wahren, B. and Oberg, B., Reversible inhibition of cytomegalovirus replication by phosphonoformate. *Intervirology* 14 (1) (1980) 7-15.
Walker, M. and Hadgraft, J., Oleic acid - a membrane "fluidiser" or fluid within the membrane? *Int. J. Pharm.*, 71 (1991) R1-R4.
Walker, G.K., Sachs, L., Sibrack, L.A., Ball, R.D. and Bernstein, I.A., Separation of epidermal layers of the new born rat *J. Invest. Dermatol.*, 68 (1977) 105-107.
Walkow, J.C. and McGinity, J.W. The effect of physicochemical properties on the *in vitro* diffusion of drug through synthetic membranes and pigskin. I. Methyl salicylate. *Int. J. Pharm.*, 35 (1987a) 91-102.
Walkow, J.C. and McGinity, J.W. The effect of physicochemical properties on the *in vitro* diffusion of drug through synthetic membranes and pigskin. I. Salicylic acid. *Int.J.Pharm.*, 35 (1987b) 103-109.
Wallace, S.M., Runikis, J.O. and Stewart, W.D., The effect of pH on *in vitro* percutaneous penetration of methotrexate. *Canadian J. Pharm. Sci.*, 13 (1978) 66-68.
Walters, K.A., Penetration enhancers and their use in transdermal therapeutic systems. In *Transdermal Drug Delivery*. Edited by Hadgraft, J. and Guy, R.H., Marcel Dekker, New York (1989) 197-246.
Walters, K.A., Florence, A.T. and Dugard, P.H., Interactions of polyoxyethylene alkyl ethers with colesterol monolayers. *J. Colloid. Interface. Sci.*, 89 (1982) 584-587.
Walters, K.A. and Hadgraft, J., Pharmaceutical Skin Penetration Enhancement, Marcel Dekker, New York, 1993
Warren, S. and Williams, M.R., The acid-catalysed decarboxylation of phosphonoformic acid. *J. Chem. Soc. (B)* (1971) 618-621.
Watkinson,A.C., Hadgraft, J. and Bye, A., Aspects of the transdermal delivery of prostaglandins. *Int.J.Pharm.*, 74 (1991) 229-236.
Watkinson, A.C., Joubin, H., Green, D.M., Brain, K.R. and Hadgraft, J., The Influence of vehicle on permeation from saturated solutions. *Int. J. Pharm.*, 121 (1) (1995) 27-36.
Wertz, P.M. and Downing, D.T., Stratum Corneum: Biological and Biochemical Considerations. In *Transdermal Drug Delivery* edited by Jonathan Hadgraft, Richard H Guy, Dekker (1989) p10.
Wertz, P.M., Madison, K.C. and Downing, D.T, Covalently bound lipids of human stratum corneum. *J. Invest. Dermatol.*, 92 (1989) 109-111.
Wester, R.C., In *Animal models in dermatology*, Edited by Maibach, H.I. Churchill Livingstone, London (1975) p133.
Wester, R.C. and Maibach, H.I., Individual and regional variation with *in vitro* percutaneous absorption. In *in vitro percutaneous absorption: Principles, fundamentals, and applications*. Edited by Bronaugh, R.L. and Maibach, H.I. CRC Press, Boca, Raton FL (1991) pp 25-30.
Wester, R.C. and Noonan, P.K., Relevance of animal models for percutaneous absorption. *Int.J. Pharm.*, 7 (1980) 99-110.
Wiechers, J.W., the barrier function of the skin in relation to percutaneous absorption of drugs. *Pharm. Weekbl [Sci]*, 11 (1989) 171-187.
Wiles, J.S. and Narcisse, J.K., The acute toxicity of dimethylamides in several animal species. *Amer. Indus. Hygiene Assoc. J.*, 32 (1971) 539-545.
Williams, A.C. and Barry, B.W., Essential oils as novel human skin penetration enhancers . *Int. J. Pharm.*, 57 (1989) R7.

Williams, A.C. and Barry, B.W., Skin absorption enhancers. *Crit. Rev. Ther. Drug Carr. Syst.*, 9(3,4) (1992) 305-353.

Williams, M.L. and Elias P.M., The extracellular matrix of stratum corneum: role of lipids in normal and pathological function. *CRC Crit. Rev. Ther. Drug Carr. Syst.*, 3(2) (1987) 95-122.

Windheuser, J.J., Haslam, J.L., Cadwell, L.J. and Shaffer, R.D., The use of N,N-diethyl-m-toluamide to enhance dermal and transdermal delivery of drugs. *J.Pharm. Sci.*, 71 (1982) 1211-1213.

Woodford, R. and Barry, B.W., Penetration enhancers and the percutaneous absorption of drugs: An update. *J.Toxicol. Cutaneous. Ocul. Toxicol.*, 5 (1986) 167-177.

Wondrak, E.M., Loewer, J. and Kurth, R., Inhibition of HIV-1 RNA-dependent DNA polymerase and cellular DNA polymerases α, β and γ by phosphonoformic acid and other drugs. *J. Antimicrob. Chemother.* 21 (2) (1988) 151-161.

Wotton, P.K., Møllgaard, B., Hadgraft, J. and Høelgaard, A., Vehicle effect on topical delivery. III Effect of Azone on the cutaneous permeability of metronidazole and propylene glycol. *Int. J. Pharm.*, 24 (1985) 19-26.

Xu, P. and Chien, Y.W., Enhanced skin permeability for transdermal drug delivery: Physio-pathological and physicochemical considerations. *Crit. Rev. Ther. Drug Carr. Syst.*, 8(3) (1991) 211-236.

Yamahara, J., Kashiwa, H., Kishi, K. and Fujimura, H., Dermal penetration enhancement by crude drugs: *in vitro* skin penetration of prednisolone enhanced by active constituents in cardamon seed. *Chem. Pharm. Bull.*, 37 (3) (1989) 855-856.

Yamane, M.A., Williams, A.C. and Barry, B.W., Effects of terpenes and oleic acid as skin penetration enhancers towards 5-fluorouracil as assessed with time, permeation, partitioning and differential scanning calorimetry. *Int. J. Pharm.*, 116 (1995a) 237-251.

Yamane, M.A., Williams, A.C. and Barry, B.W., Terpene penetration enhancers in propylene glycol/water co-solvent systems: Effectiveness and mechanism of action. *J. Pharm. Pharmacol.*, 47 (1995b) 978-989.

Yardley, H.J. Epidermal Lipids. In *Biochemistry and Physiology of the skin* vol 1. Edited by Goldsmith, L.A. Oxford University Press, New York (1983) 365-381.

Yardley, H.J. and Summerly, R., Lipid composition and metabolism in normal and diseased epidermis. *Pharmacol. Ther.*, 13 (1981) 357-383.

APPENDIX 1 Composition of McIlvaine Buffers (From Perrin and Dempsey, 1974).